CORA Cork Open Research Archive
Cartlann Taighde Oscailte Chorcaí

Title	Application of mesoporous silica for the oral delivery of poorly water-soluble drugs
Authors	Ahern, Robert J.
Publication date	2014
Original Citation	Ahern, R. J. 2014. Application of mesoporous silica for the oral delivery of poorly water-soluble drugs. PhD Thesis, University College Cork.
Type of publication	Doctoral thesis
Rights	© 2014, Robert J. Ahern - http://creativecommons.org/licenses/by-nc-nd/3.0/
Download date	2023-05-07 18:34:12
Item downloaded from	http://hdl.handle.net/10468/1381

UCC
University College Cork, Ireland
Coláiste na hOllscoile Corcaigh

APPLICATION OF MESOPOROUS SILICA FOR THE ORAL DELIVERY OF POORLY WATER – SOLUBLE DRUGS

A thesis submitted in fulfilment of the requirements for the degree

of

DOCTOR OF PHILOSOPHY

in

Pharmacy – Pharmaceutics

at

THE NATIONAL UNIVERSITY OF IRELAND

UNIVERSITY COLLEGE CORK

by

Robert J. Ahern, B.Eng (Hons) AMIChemE

under the direction and supervision of

Dr. Abina M. Crean, B.Sc. (Pharm.), Ph. D., M.P.S.I.

and

Dr. Katie B. Ryan, B.Sc. (Pharm.), Ph. D., M.P.S.I.

Head of School

Professor Catriona M. O'Driscoll B.Sc. (Pharm.), M.A., Ph. D., M.P.S.I.

Declaration

This thesis is submitted to the National University of Ireland, University College Cork by Robert Ahern for examination in the degree of Doctor of Philosophy (Pharmacy – Pharmaceutics). This thesis has not been submitted for any other purpose or degree offered by this or any other university. The material presented in this thesis is entirely the author's own original work, except where duly noted and acknowledged. This thesis was authored by Robert Ahern with supervision and editorial advice from my PhD supervisors, Dr. Abina Crean and Dr. Katie Ryan.

Signature: **Date**

Acknowledgements

I wish to acknowledge all the help, support and guidance of my supervisors, Dr. Abina Crean and Dr. Katie Ryan throughout my PhD. I am eternally grateful that you gave me the opportunity to pursue the PhD and for the continuous encouragement throughout it.

I want to thank Dr. John Hanrahan and Dr. Joe Tobin of Glantreo Ltd. for supplying the mesoporous silica which I have used in my research.

I want to thank the technical staff of the school; Dr. Michael Cronin, Dr. Ken Devine, Dr. Tom O'Mahony and Ms. Aine Healy for ensuring that all equipment required for my research was in working order and for their help with particular techniques like the TGA, DSC, HPLC and BET where necessary.

The administrative staff; Ms. Noreen Moynihan, Ms. Kathleen Murphy, Ms. Aisha Murphy and Ms. Debbie Curran have ensured that the paperwork has flowed smoothly throughout my research. I want to particularly acknowledge Aisha for ensuring that the team room club was maintained, which has ensured that I have had my cups of tea when desired.

I want to thank Ms. Nuala Maguire of the ABCRF for running my samples on the pXRD and Ms. Suzanne Crotty for her help with the SEM.

My colleagues in the Pharmaceutics lab have continuously provided mirth, companionship and encouragement.

Finally, I want to thank my family for all their support throughout these long four years.

Table of Contents

Table of Figures

Table of Tables

1

Table of Equations

Abbreviations

API	active pharmaceutical ingredient
BCS	biopharmaceutics classification system
BET	Brunauer, Emmett and Teller
BJH	Barrett-Joyner-Halenda
CO_2	carbon dioxide
C_p	heat capacity
DSC	differential scanning calorimetry
FaSSIF	fasted state, simulated intestinal fluid
FDA	food and drug administration
FT-IR	fourier transform – infrared spectroscopy
g	gram
GIT	gastrointestinal tract
H.R.	Hausner Ratio
h	hour
kg	kilogram
l	litre
MCM	mobil-crystalline-material
MDSC	modulated differential scanning calorimetry
ml	millilitre
mm	millimetre
min	minute
MPa	megapascal
MS	mesoporous silica
N/A	not applicable

NCE	new chemical entity
N/D	not detected
nm	nanometer
N/P	not present
N/R	not reported
N_2	nitrogen
O_2	oxygen
p	pressure
P.A.	pore area (m^2/g)
psi	pounds per square inch
P.V.	pore volume (cm^3/g)
pXRD	powder x-ray diffraction
HCl	hydrochloric acid
HPLC	high performance liquid chromatography
RH	relative humidity
RPM	revolutions per minute
s	second
SBA-15	Santa Barbara amorphous type-15
SCF	supercritical fluid
SC-CO_2	supercritical carbon dioxide
SD	standard deviation
SDS	sodium dodecyl sulphate
SEM	scanning electron microscopy
SGF	simulated gastric fluid
SLS	sodium lauryl sulphate

SIF	simulated intestinal fluid
SiO_2	silicon dioxide
S.S.A.	specific surface area (m^2/g)
T_c	recrystallization temperature
T_g	glass transition temperature
T_m	melting temperature
T_r	reduced temperature
TEM	transmission electron microscopy
TGA	thermogravimetric analysis
UV-Vis	ultraviolet-visible
µm	micron/micrometer
% v/v	% volume/volume
% w/v	% weight/volume
% w/w	% weight/weight

Abstract

The objective of this thesis was to improve the dissolution rate of the poorly water – soluble drug, fenofibrate by processing it with a high surface area carrier, mesoporous silica. The subsequent properties of the drug – silica composite were studied in terms of drug distribution within the silica matrix, solid state and release.

Prior to commencing any experimental work, the properties of unprocessed mesoporous silica and fenofibrate were characterised (chapter 3), which allowed for comparison with the processed samples studied in later chapters. Fenofibrate was a highly stable, crystalline drug that did not adsorb moisture, even under long term accelerated storage conditions (75% RH, 40 ^{o}C). It maintained its crystallinity even after SC-CO_2 processing. Its dissolution rate was limited and dependent on the characteristics of the particular *in vitro* media studied. Mesoporous silica had a large surface area and mesopore volume and readily picked up moisture when stored under long term accelerated storage conditions. It maintained its mesopore character after SC-CO_2 processing.

A variety of methods were employed to process fenofibrate with mesoporous silica including physical mixing, melt method, solvent impregnation and novel methods such as liquid and supercritical carbon dioxide (SC-CO_2) (chapter 4). It was found that it was important to break down the fenofibrate particulate structure to a molecular state to enable drug molecules enter into the silica mesopores. While all processing methods led to some increase in fenofibrate release properties, the impregnation, liquid and SC-CO_2 methods produced the most rapid release rates.

SC-CO_2 processing was further studied with a view to optimising the processing parameters to achieve the highest drug-loading efficiency possible (chapter 5). In this thesis, it was observed that SC-CO_2 processing pressure had a bearing on drug-

loading efficiency. Neither SC-CO_2 pressure nor duration time or CO_2 depressurisation rate affected drug solid state or release properties.

The amount of drug that could be loaded onto to the mesoporous silica successfully was also investigated at different ratios of drug mass to silica surface area under constant SC-CO_2 conditions; as the drug – silica ratio increased, the drug-loading efficiency decreased, while there was no effect on drug solid state or release properties.

The influence of the number of drug-loading steps was investigated (chapter 6) with a view to increasing the drug-loading efficiency. A multiple step approach did not yield an increase in drug-loading efficiency compared to the single step approach. It was also an objective in this chapter to understand how much drug could be loaded into silica mesopores; a method based on the known volume of the mesopores and true density of drug was investigated. However, this approach led to serious repercussions in terms of the subsequent solid state nature of the drug and its release performance; there was significant drug crystallinity and reduced release extent.

The impact of *in vitro* release media on fenofibrate release was also studied (chapter 6). Here it was seen that media containing HCl led to reduced drug release over time compared to equivalent media not containing HCl.

The key findings of this thesis are discussed in chapter 7 and included:

1. Drug – silica processing method strongly influenced drug distribution within the silica matrix, drug solid state and release.
2. The silica surface area and mesopore volume also influenced how much drug could be loaded.

3. It was shown that SC-CO_2 processing variables such as processing pressure (13.79 – 41.37 MPa), duration time (4 – 24 h) and CO_2 depressurisation rate (rapid or controlled) did not influence the drug distribution within the SBA-15 matrix, drug solid state form or release.

Possible avenues of research to be considered going forward include the development and application of high resolution imaging techniques to visualise drug molecules within the silica mesopores. Also, the issues surrounding SBA-15 usage in a pharmaceutical manufacturing environment should be addressed.

1 Introduction to this thesis: The exploitation of silicon dioxide (SiO_2) for oral drug delivery

1.1 Introduction

Oral drug delivery is the most convenient method of drug administration for patients. In oral drug delivery, the administered drug normally needs to be dissolved in the gastrointestinal tract (GIT) in order to be absorbed into systemic circulation. Therefore, there are two issues that need to be considered for when assessing a drug candidate for oral delivery; its water solubility (hydrophobic or hydrophilic) and permeability into the bloodstream from the GIT (lipophobic or lipophilic). The ideal drug candidate for oral delivery should have high water solubility and permeability. The Biopharmaceutics classification system (BCS) was developed in order to classify drugs according to their water solubility and permeability. Four classes were proposed: BCS Class I drugs have high water solubility and high permeability (the ideal drug for oral delivery), BCS Class II drugs have poor water solubility and high permeability, BCS Class III drugs have high water solubility and low permeability and BCS Class IV drugs have low water solubility and low permeability (Amidon et al., 1995). Oral pharmaceutical products that have poor water solubility are said to be dissolution-rate limited which in turn limits their oral bioavailability. For these drugs to have enhanced oral bioavailability, considerable formulation and process development is required, which can be a significant challenge. It has been estimated that the cost of developing a new chemical entity (NCE) and bringing it to market as a new pharmaceutical drug product lies in the region of approximately $1.8 billion United States dollars (USD) (Paul et al., 2010); previously the cost was estimated to

be approximately $802 million USD (DiMasi et al., 2003). Many NCE's developed through high-throughput screening and combinatorial chemistry exhibit poor water solubility because these methods tend to produce drugs that are more lipophilic than hydrophilic (Lipinski et al., 1997). In fact, it has been estimated that 40% of drugs developed through these methods exhibit poor water solubility (Merisko-Liversidge and Liversidge, 2008) . Drug dissolution rate can be expressed as Eq.1.1:

Equation 1.1: $$\frac{dC}{dt} = \frac{DS}{vh}(Cs - C)$$

where $\frac{dC}{dt}$, the rate of drug dissolution is dependent upon: D, the diffusion coefficient (m^2/s), S, the surface area (m^2), h, the thickness of the diffusion layer (m), v, the volume of dissolution medium (ml), Cs, the saturation solubility of a specific drug in a specific medium (mg/ml) and C, the solubility of specific drug in a specific medium at a specific time (mg/ml) (Bruner, 1904, Nernst, 1904).

If the drug dissolution rate can be improved, drug oral bioavailability can also be improved (Amidon et al., 1995). A well established method for improving the dissolution rate of a BCS Class II drug is to increase its effective surface area (Equation 1.1); this can be achieved by loading the drug onto a high surface area carrier like porous silica (Vallet-Regi et al., 2001). Porous silicas are attractive for drug dissolution rate enhancement because of their high surface areas, high mesopore volumes and ordered mesopore networks (Kresge et al., 1992) which permit homogeneous and reproducible drug-loading and release (Vallet-Regi, 2006). In this introductory chapter several aspects will be reviewed. Firstly the aim of this chapter was to understand of the key properties of amorphous, hydrophilic silicas

(SiO_2) that affect drug-loading, drug solid state and dissolution rate enhancement. Mesoporous silica was employed in this thesis as the host matrix for the poorly water – soluble drug fenofibrate and therefore, it was important to understand its properties prior to any research being carried out. Secondly this chapter aimed to understand the influence of drug-loading method on subsequent drug physicochemical properties. The work that will be outlined later in this thesis was focused on investigating methods of loading and the subsequent properties of the drug-silica systems. Finally, the *in vivo* performance of silica based oral drug delivery systems was also reviewed in this chapter.

1.2 Silica

Silicon dioxide (silica) describes materials with a wide range of properties. They can be crystalline or amorphous, hydrophilic or hydrophobic and porous or non-porous. Crystalline silicas are found mainly in quartz and sand and have melting points of 1710 ^{o}C (Lewis, 2013), have densities of 2.6 g/cm^3 (Lewis, 2013) and are non-combustible materials (Daubert and Danner, 1989), bulk densities are generally low. Silicon dioxide is composed of the elements silicon (Si) and oxygen (O) bonded together via tetrahedral bonding (Zheng et al., 2001). There is cross-linking of the Si-O-Si, which makes amorphous, hydrophilic, colloidal silica very stable; its glass transition temperature (T_g) is very high at 1202 ^{o}C (Ojovan, 2004).

The main application of silica in the pharmaceutical industry has been as a glidant for improved powder flow and compression (York, 1975) and in powder tabletting processes (Lerk et al., 1977, Lerk and Bolhuis, 1977, Jonat et al., 2005). Hydrophobic colloidal silicas are similar to hydrophilic colloidal silicas except that it has been treated with hydrophobic moieties (Rowe et al., 2012). In this thesis, there

will be a focus on amorphous hydrophilic silica for oral drug delivery. Amorphous hydrophilic silica can be divided into two broad categories (1) non-porous silica and (2) porous silica; the surface (and porosity) properties of a range of silicas are presented in Table 1.1.

Table 1.1: Surface and mesopore properties of a range of amorphous, hydrophilic silica materials.

Silica	Type	Surface area (m^2/g)	Mesopore volume (cm^3/g)	Mesopore size (nm)	Reference
Colloidal SiO_2	Aerosil®	50 – 300	N/A	N/A	(Rowe et al., 2012)
Colloidal SiO_2	Cab-O-Sil®	90 – 380	N/A	N/A	(Rowe et al., 2012)
Colloidal SiO_2	HDK®	150 – 200	N/A	N/A	(Rowe et al., 2012)
Mesoporous	MCM-41	800 – 1000	0.50 – 1.5	1.5 – 10	(Kresge et al., 1992)
Mesoporous	MCM-48	1000	1.048	1.5 – 10	(Izquierdo-Barba et al., 2005) (Kim et al., 1998)
Mesoporous	SBA-15	400 – 800	0.50 –0. 65	5 – 8	(Zhao et al., 1998)
Mesoporous	KIT-1	1000	Not reported	3.4	(Ryoo et al., 1996)
Mesoporous	FSM-16	680 – 1000	0.28 – 0.83	1.5 – 4	(Inagaki et al., 1996)
Mesoporous	BMM	1005	1.59	2.71, 23.8	(Gao et al., 2012)
Mesoporous	TUD-1	400 – 1000	0.50 – 1.7	4 – 18	(Jansen et al., 2001)
Mesoporous	HMS	1210	1.04	2.67	(Zhu et al., 2005a)
Mesoporous	COK-12	429 – 547	0.45 – 0.88	5.8 – 9.4	(Jammaer et al., 2009)

The differences across the mesoporous silicas discussed in this introduction in terms of mesopore array, order and direction, whether unidirectional, or 2 or 3 directional (2 or 3-D) are shown in Table 1.2.

Table 1.2: Description of the mesoporous array, order, shape and structure.

Material	Mesopore array	Ordered	Mesopore description	Reference
MCM-41	Hexagonal	Ordered	Long unidirectional mesopores through the particle	(Kresge et al., 1992)
MCM-48	Cubic	Ordered	Long 3-directional mesopores through the particle	(Izquierdo-Barba et al., 2005) (Kim et al., 1998)
SBA-15	Hexagonal	Ordered	Long unidirectional mesopores through the particle	(Zhao et al., 1998)
KIT-1	Worm-like	Disordered	Short 3-directional mesopores	(Ryoo et al., 1996)
FSM-16	Honeycomb	Ordered	Long unidirectional mesopores through the particle	(Inagaki et al., 1996)
BMM	Random	Disordered	Short randomly connected mesopores through the particle	(Gao et al., 2012)
TUD-1	Foam-like	Disordered	Randomly connected mesopores through the particle	(Jansen et al., 2001)
HMS	Hexagonal	Ordered	Short mesopores running into a hollow core	(Zhu et al., 2005a)
COK-12	Hexagonal	Ordered	2-directional mesopores through the particle	(Jammaer et al., 2009)

1.2.1 Non-porous amorphous hydrophilic silica

The most common non-porous fumed silica is colloidal silicon dioxide (hydrophilic fumed silica). Cab-O-Sil® (Cabot Corporation), Aerosil® (Evonik Industries) and HDK® (Wacker) are commercial varieties of colloidal silicon dioxide. The manufacturing process involves the hydrolysis of silicon tetrachloride vapour in a flame of hydrogen and oxygen at temperatures greater than 1000 ^{o}C, giving rise to the term fumed silica (Katz and Milewski, 1987). Aerosil® has a specific surface area from 50 – 300 m^2/g (Table 1.1), depending on the particular grade (Rowe et al., 2012). CAB-O-SIL® has specific surface areas from 90 – 380 m^2/g (Table 1.1). When discussing non-porous silica, the specific surface area is the most important parameter to consider as this determines how much drug can be loaded onto the silica.

1.2.2 Porous amorphous hydrophilic silica

Porous silica can be divided into macroporous (> 50 nm), mesoporous (2 – 50 nm) and microporous (< 2 nm) silica. Porous silica has been widely employed to improve the dissolution rate of poorly water – soluble drugs. Due to the porous nature, drug molecules can be confined and stabilised within the silica mesopores in a non-crystalline form (Azais et al., 2006, Mellaerts et al., 2008a, Shen et al., 2010), with re-crystallisation prevented by nano-confinement because the ratio of drug molecule size to mesopore width is insufficient to permit drug re-crystallisation (Sliwinska-Bartkowiak et al., 2001). There are many varieties of amorphous mesoporous silica. The Mobil composition of matter (MCM) range of mesoporous silicas were developed by researchers at the Mobil Corporation in 1992 and are part of the M41S family of molecular sieves. MCM-41 was synthesised by adding catapal aluminium,

tetramethylammonium silicate and precipitated silica (HiSil) to a solution of hexadecyltrimethylammonium, which was then autoclaved at 150 ^{o}C for 48 h (Kresge et al., 1992). MCM-41 has a well ordered, stable, hexagonal, unidirectional mesopore network. It has a large specific surface area that ranges from 800 – 1000 m^2/g, mesopore volumes from 0.5 – 1 .5 cm^3/g, and mesopore sizes ranging from 1.5 – 10 nm (Kresge et al., 1992).

MCM-48 is a modification of MCM-41 where the mesopores are arranged in a cubic instead of hexagonal array (Fig.1.1) (Kim et al., 1998). It has been reported that a cubic mesopore array would increase molecular accessibility and transport (Izquierdo-Barba et al., 2005).

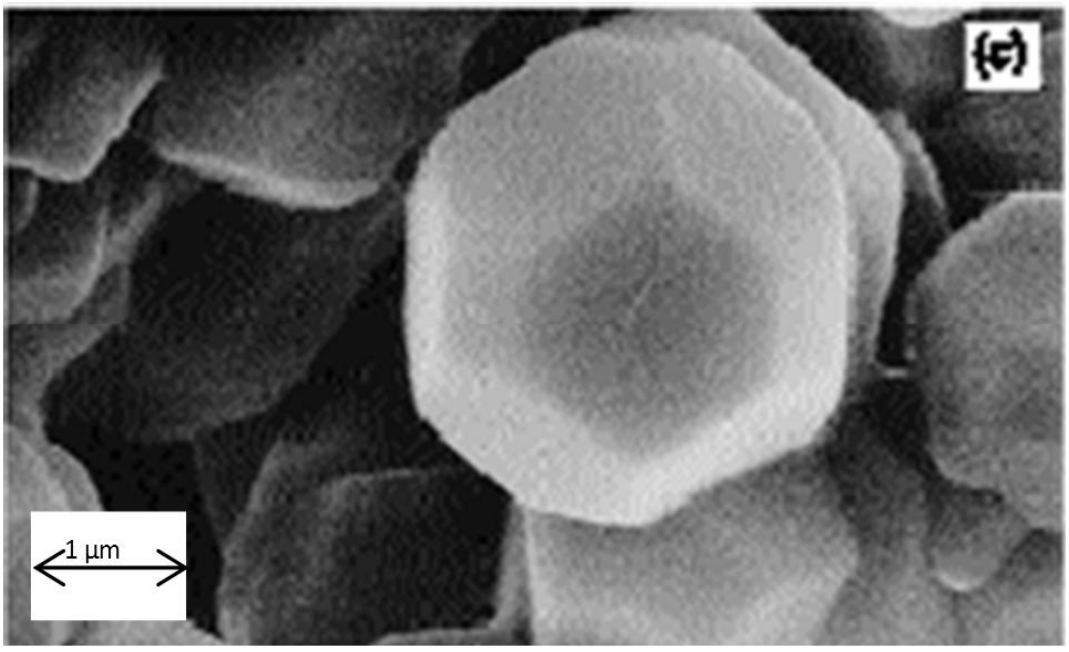

Figure 1.1: Field emission SEM image for MCM-48 synthesised at 413 K (Kim et al., 1998).

The Santa Barbara Amorphous type mesoporous silica (SBA-15) was developed by researchers at the University of California, Santa Barbara in 1998. Using an

amphiphilic block co-polymer (Pluronic P123) dissolved in acidic aqueous conditions (pH 1) and tetraethyl orthosilicate (TEOS) as the silica source, Zhao and co-workers were able to produce a hexagonal mesopore structure with thick mesopore walls (3.1 – 6.4 nm) (Zhao et al., 1998). These mesopore walls are thicker than those of MCM-41 and ensure SBA-15 has higher hydrothermal stability compared to MCM-41 (Fulvio et al., 2005). SBA-15 has a large surface area (> 600 m^2/g) and mesopore volume (> 0.50 cm^3/g) and a well ordered, stable, unidirectional mesopore network connected by micropores (Fulvio et al., 2005, Zhao et al., 1998). The ordered hexagonal pore array of SBA-15 can be seen below (Fig.1.2).

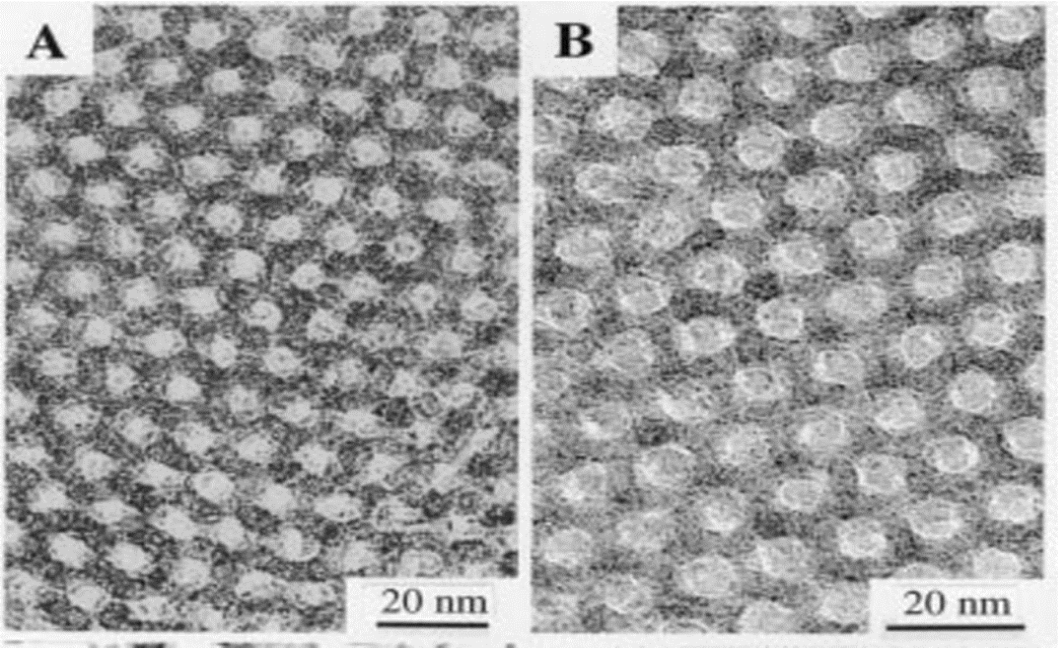

Figure 1.2: TEM images of calcined hexagonal SBA-15 mesoporous silica with different average mesopore sizes (**A**) 60 Å, (**B**) 89 Å (Zhao et al., 1998).

The mesopore sizes of SBA-15 tend to be larger than MCM-41 (Galarneau et al., 2007); this property should facilitate faster release from SBA-15 than MCM-41 as it

has been previously reported that faster drug release is obtained from larger mesopore sizes (Horcajada et al., 2004).

Researchers in Korea developed the Korea Advanced Institute of Science and Technology (KIT) range of mesoporous silicas. KIT-1 was synthesised by an electrostatic templating route using sodium silicate, hexadecyltrimethylammonium chloride and ethylenediaminetetraacetic acid tetrasodium salt. The silicate was hydrothermally polymerised at 97 ^{o}C (Ryoo et al., 1996). These mesoporous silicas contained short worm-like mesoporous channels, connected in a 3-directional, disordered manner through many branches. There was no evidence of any hexagonal structure in the TEM images of KIT-1. It was reported that the thermal and hydrothermal stabilities of KIT-1 were higher than MCM-41 (Ryoo et al., 1996). The disordered nature of KIT-1 mesoporous silica can be seen below (Fig.1.3).

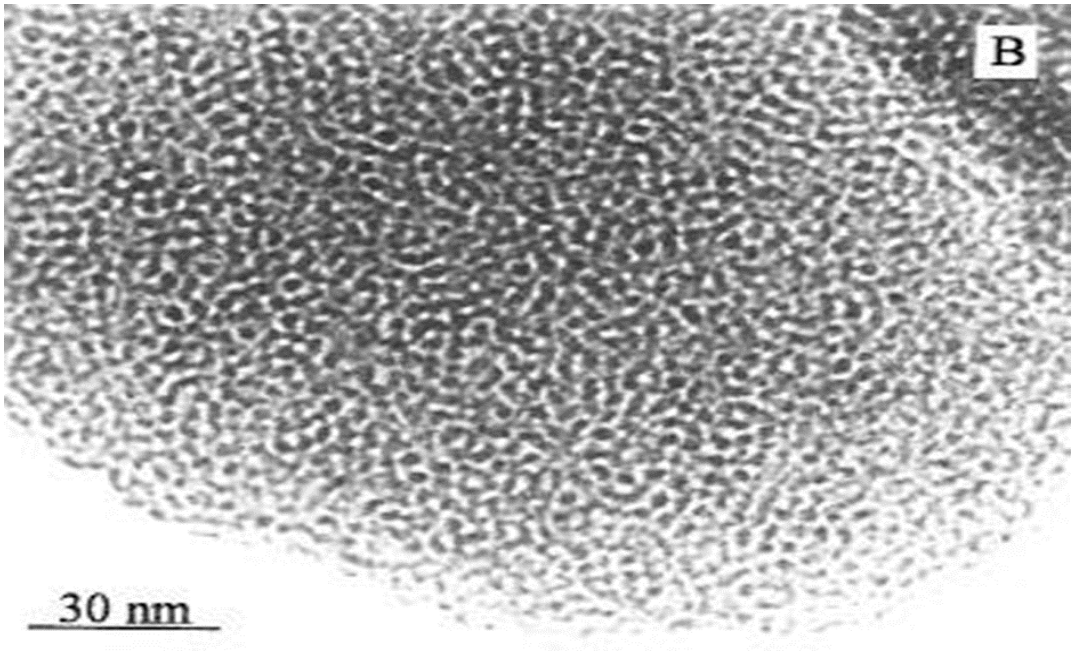

Figure 1.3: TEM of disordered molecular sieve, KIT-1 (Ryoo et al., 1996).

Folded sheet mesoporous silica (FSM-16) was first synthesised in the 1990's with specific surface areas from 680 – 1000 m^2/g, mesopore volumes from 0.28 – 0.83 cm^3/g and mesopore sizes up to 4 nm, depending on the surfactant chain length used in the synthesis step. It can be prepared by the intercalation of sodium silicate (Kanemite) followed by calcination (Inagaki et al., 1996, Tozuka et al., 2005). FSM-16 has a highly uniform, mesopore structure with honeycomb one-dimensional straight channels (Inaki et al., 2000, Nishiwaki et al., 2009).

Researchers at the Technische Universiteit Delft, Holland developed the TUD-1 range of mesoporous materials. The TUD-1 materials were prepared with a range of surface areas (400 – 1000 m^2/g), mesopore volumes (0.5 – 1.7 cm^3/g) and tuneable mesopore diameters depending on the heating rate employed during hydrothermal treatment. The mesopore structure is described by a foam-like network, with random connections between the mesopores (Fig.1.4) (Jansen et al., 2001).

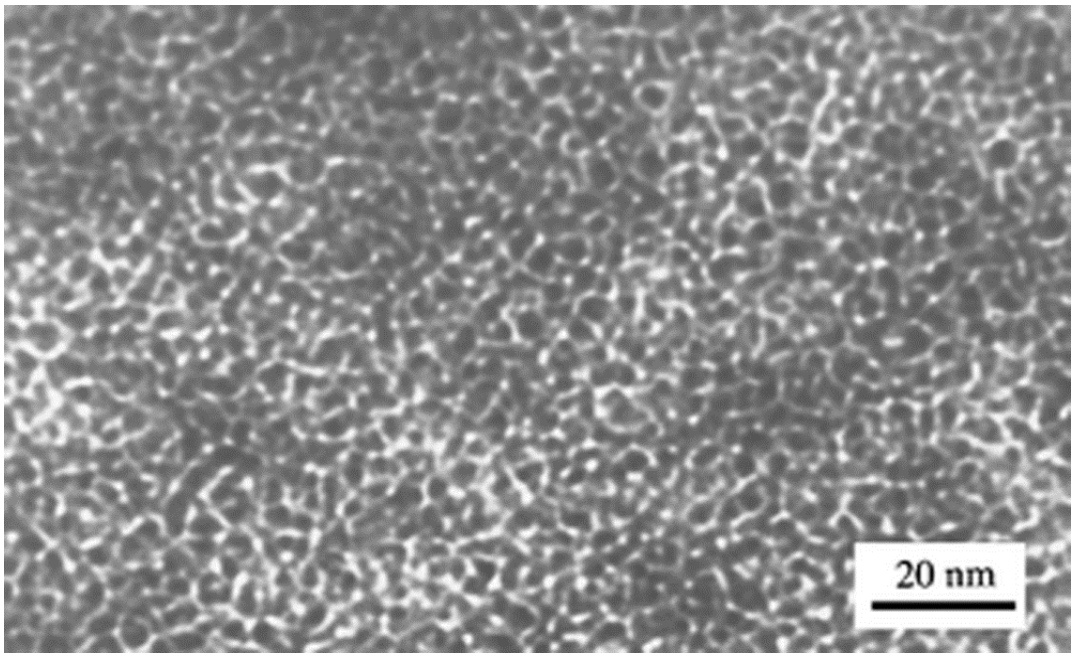

Figure 1.4: High resolution TEM image of the foam-like mesoporous structure of TUD-1 (Jansen et al., 2001).

Hollow mesoporous silica spheres (HMS) are another type of mesoporous silica that contain a hollow structure, with uniform, well-defined hexagonal and straight mesopore channels of about 2 – 3 nm length. The specific surface area of HMS can be up to 1000 m^2/g, with mesopore volumes of 1 cm^3/g. HMS are synthesised by the dissolution of polyvinylpyrrolidone (PVP) and sodium hydroxide in water. Cetyltrimethyllammonioum bromide was subsequently added to the solution, followed by TEOS. The solution was stirred and autoclaved at 80 ^oC for 48 h, the recovered product was then calcined (Zhu et al., 2005a). The spherical nature of HMS particles can be clearly observed (Fig.1.5).

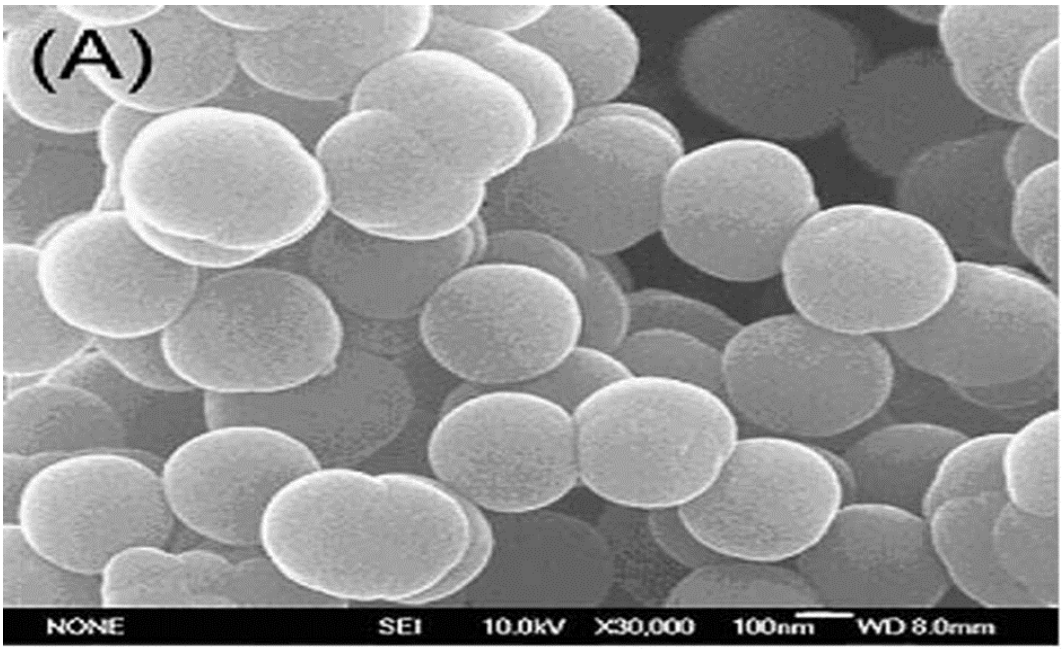

Figure 1.5: Field emission SEM micrograph of the calcined HMS (Zhu et al., 2005a).

COK-12 is a type of ordered mesoporous silica developed by researchers in Katholieke Universiteit de Leuven, Belgium. It was synthesised by dissolving Pluronic P123 is an aqueous solution of citric acid and trisodium citrate. The silica was manufactured at various temperatures and pH values, increasing the temperature

resulted in larger mesopore sizes. The specific surface areas were in the range 429 – 547 m^2/g, the mesopore volumes were 0.45 – 0.88 cm^3/g with the mesopore sizes from 5.8 – 9.4 nm (Figs.1.6&1.7) (Jammaer et al., 2009).

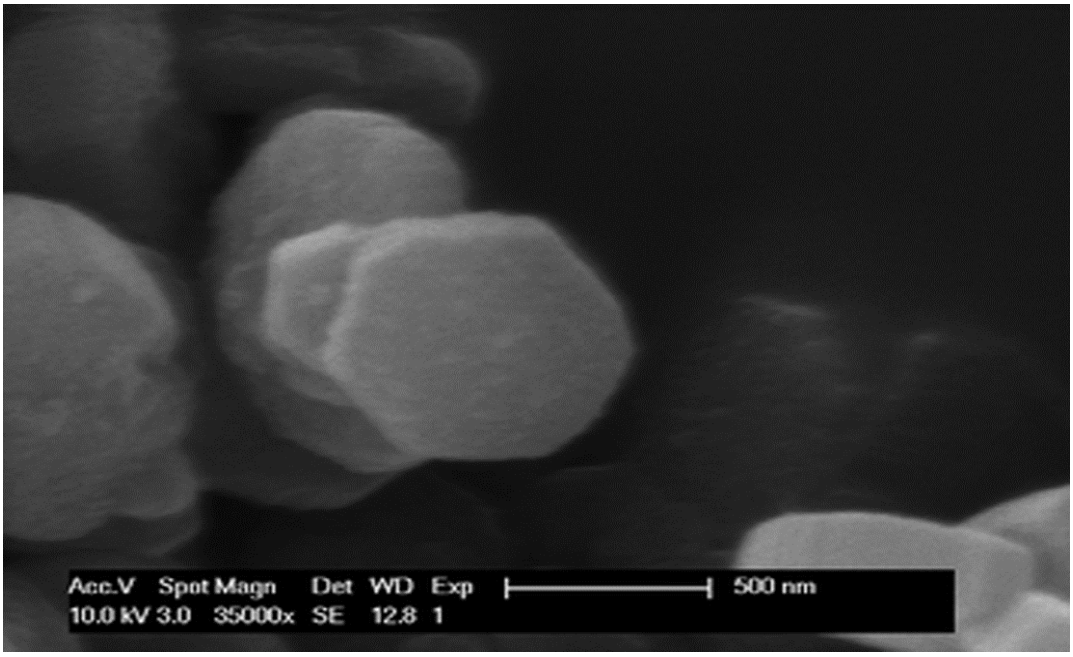

Figure 1.6: SEM of COK-12 (Jammaer et al., 2009).

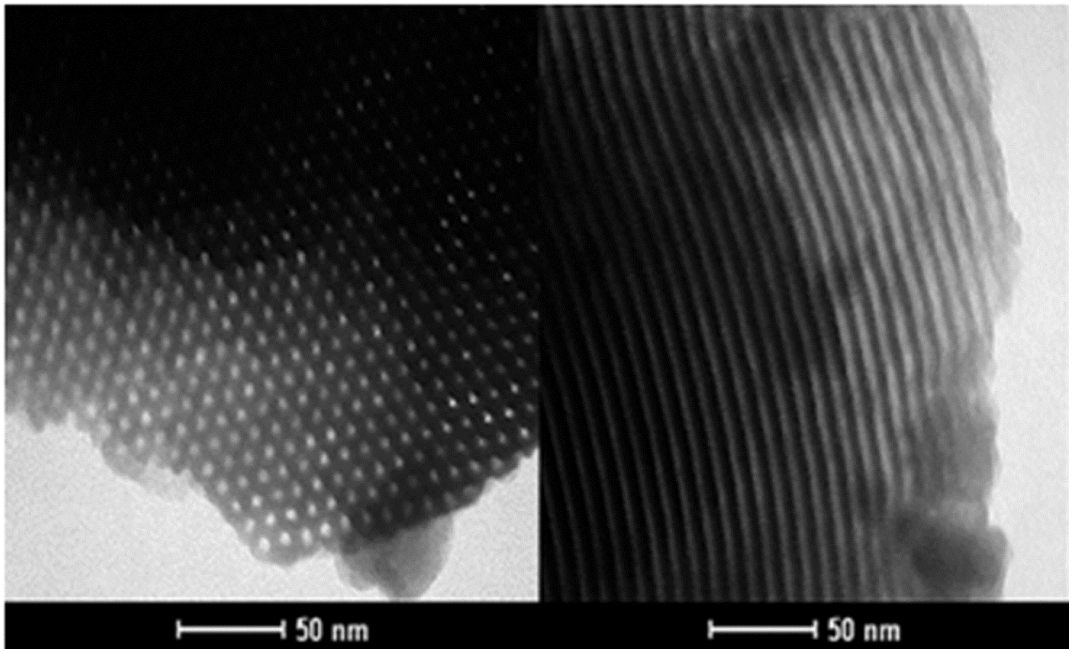

Figure 1.7: TEM of calcined COK-12) with the orientation perpendicular to the mesopores (left) and parallel to the mesopores (right) (Jammaer et al., 2009).

1.3 The influence of drug-loading process on drug physicochemical properties

In this section, the influence of drug-loading process on drug physicochemical properties will be discussed. There have been many loading methods proposed to load drugs onto silica materials. These include physical processes, melting processes, various organic solvent processes and alternative processes such as supercritical fluid (SCF) technology.

1.3.1 Physical processes

The simplest physical loading method published involved grinding 1 g of SBA-15 and 1g ibuprofen in a mortar and pestle for 5 min, the drug remained crystalline post grinding (Shen et al., 2010). Another physical method reported in the literature

involved blending a mixture of flurbiprofen and FSM-16 in a glass vial for 1 min. Once more, the drug remained crystalline post blending and was only weakly adsorbed onto the silica surface, despite the range of FSM-16 properties investigated (surface areas: 700, 1250 and 1040 m^2/g and pore widths: 1.6, 2.16 and 4.5 nm). Also prepared were sealed – heated, physical mixtures of flurbiprofen and FSM-16 which were heated to 100 ^oC for 6 h (Tozuka et al., 2005); this temperature was below the melting point of flurbiprofen which was 115 ^oC (Knox et al., 2011). In a previous publication, these researchers had reported that the sealed – heated method could reduce the crystallinity of drug in a drug – silica physical mixture (Tozuka et al., 2003). The drug was amorphous in the systems containing FSM-16 with mesopore widths of 2.16 and 4.5 nm but crystalline for the FSM-16 with the smallest pore width (1.6 nm) (Tozuka et al., 2005). This work showed the effect of loading process and silica properties on loaded drug physicochemical properties.

There have been interesting reports of physically mixing crystalline compounds with mesoporous silica gels where the crystalline compounds subsequently transitioned to the amorphous state after storage with the silica gel, when stored in 0% RH environment. Qian and Bogner studied the interaction of naphthalene and ibuprofen with mesoporous silica gel. They found that crystalline naphthalene stored under conditions of 0% RH and 40 ^oC became amorphous after 2 weeks while ibuprofen was fully amorphous after 5 weeks. The vapour pressure of naphthalene was 45 Pa at 40 ^oC while the vapour pressure of ibuprofen was 1.7×10^{-2} Pa at 40 ^oC. This phenomenon was attributed to compound sublimation through the vapour phase followed by adsorption onto the silica (Qian and Bogner, 2011). This amorphisation process was not dependent upon silica surface area or mesopore volume. Instead, they reported that the surface curvature/mesopore diameter determined the silica

amorphisation capacity, with smaller mesopore sizes leading to greater amorphisation capacity (Qian et al., 2011). The amorphisation process was reversible in the presence of moisture (Qian et al., 2012). This work highlighted that compounds with relatively high vapour pressures would readily convert to the amorphous phase after physical mixing with mesoporous silica, as long as there was no moisture present.

1.3.2 Melt processes

Melt processes involve the melting of a drug onto the mesoporous silica followed by cooling below the drug's melting point. Mellaerts and co-workers utilised a melt method to load ibuprofen and itraconazole onto SBA-15. The mixture was heated above each of the drugs melting point for 5 min, vortexed and heated back up above the melting point for a further 5 min. The mixtures were then stored under vacuum at 40 ^{o}C for 48 h (Mellaerts et al., 2008a). Itraconazole was not successfully loaded into the SBA-15 mesopores at any of the drug loads investigated, nor was it homogeneously distributed throughout the silica surface and it was still somewhat crystalline. Ibuprofen was successfully loaded into the SBA-15 mesopores, was in a non-crystalline state and achieved rapid *in vitro* release (Mellaerts et al., 2008a). This work highlighted that the melt method was highly dependent on drug molten viscosity for mesopore penetration.

Another melt method reported was melt-quenching. Here, 50% w/w ibuprofen was mixed with SBA-15 and heated above 120 ^{o}C to melt the drug and subsequently quench cooled using liquid nitrogen. In this method some of the drug was located outside the SBA-15 mesopores in the crystalline state (Shen et al., 2010).

1.3.3 Solvent processes

Organic solvent drug-loading methods have been extensively reported in the literature by several research groups. The first report of mesoporous silica (MCM-41) for drug delivery was by Vallet-Regi and co-workers in 2001. They prepared a solution of ibuprofen in hexane (33 mg/ml) and added MCM-41 to the solution. The MCM-41 had a surface area of 1157 m^2/g and a mean mesopore size of 2.5 nm. Loading of drug resulted in a lower surface area of 688 m^2/g and reduced mean pore size of 1.9 nm. The drug-load was 30% w/w and the maximum *in vitro* drug release was 100% after 3 days (Vallet-Regi et al., 2001).

Charnay and co-workers studied the loading of ibuprofen onto MCM-41 and Aerosil® by preparing 2.5 ml solutions of drug in various solvents including dimethyl sulphoxide (DMSO), dimethyl acetamide (DMA), dimethyl formamide (DMF), ethanol and hexane at a concentration of 65 mg/ml; 0.05g of silica was then added to the 2.5 ml solution. Suspensions of silica and drug were stirred for 24 h and then filtered to recover the drug-loaded silica. The strongly polar solvents such as DMA failed to load any drug onto the either MCM-41 or Aerosil®, while DMSO and DMF also loaded low amounts of drug (<4.7% w/w). The less polar solvent ethanol and the non-polar solvent hexane loaded the greatest quantity of drug onto both silicas: hexane loaded 59% w/w onto MCM-41 and 10.4% w/w onto Aerosil® while ethanol loaded 18.4% and 4.2% respectively (Charnay et al., 2004). This study highlighted very clearly that both the choice of solvent and silica material (porous or non-porous) are crucial factors for maximising drug-loading.

Tozuka and co-workers loaded FSM-16 with flurbiprofen by dissolving the drug in ethanol, adding the FSM-16 to the solution, sonicating the suspension for 3 min and

then allowing the ethanol to evaporate at room temperature. They reported that the drug was deposited in the mesopores in the amorphous form (Tozuka et al., 2005).

Mellaerts and co-workers loaded ibuprofen and itraconazole onto SBA-15 using dichloromethane (DCM) as the solvent. Physical mixtures of 7, 20 and 30% w/w drug to SBA-15 were first prepared, to which were added 6 ml of DCM. The suspensions were sonicated for 1 min and then agitated for 24 h using a rotary mixer at 20 rpm. The solvent was removed by drying at 35 ^{o}C, the mixtures were then vortexed for 20 sec and stored under vacuum for 48 h at 40 ^{o}C. The authors reported that this solvent method preferentially loaded the drug into the SBA-15 mesopores because this solvent method resulted in slow drug-loading as the drug had to diffuse out of solution and adsorb onto the SBA-15, which allowed the drug molecules to rearrange and aggregate themselves in the SBA-15 mesopores and not the micropores (Mellaerts et al., 2008a).

A very interesting solvent based drug-loading method which involved the application of spray drying technology was reported by Shen and co-workers. A 100 ml solution of ibuprofen dissolved in ethanol (10 mg/ml) was stirred with 1 g of SBA-15 overnight prior to spray-drying using a BUCHI B-290 spray-dryer with an inlet temperature of 81 ^{o}C, a feed rate of 4 ml/min and outlet temperature of 50 – 55 ^{o}C. The drug-loads achieved were 25, 50 and 75% w/w, although above 50% w/w the drug displayed evidence of crystallinity. At 50% w/w drug, there was no evidence of crystallinity while the drug release rate from this sample was 100% after 20 min (Shen et al., 2010).

Limnell and co-workers studied the loading of indomethacin onto MCM-41 by a solvent method, with different solvent removal processes post loading. In the immersion method, a drug – ethanol solution (17 mg/ml) was prepared, to which was

added the MCM-41. The suspension was stirred for 1.5 h, vacuum filtered through 0.45 µm filter with the solid residue subsequently oven dried for 4.5 h at 60 ^{o}C. In the rotavapor method, a drug – ethanol solution (9 mg/ml) was prepared with MCM-41 added to it; the resulting suspension was shaken for 1.5 h. The solvent was evaporated using a Hei-VAP Advantage rotavapor under reduced pressure in a water bath set at 45 – 50 ^{o}C for 15 min. The recovered powder was subsequently dried at room temperature for 5 days. In the fluidized-bed method, MCM-41 was again added to a drug – ethanol solution (9 mg/ml) and suspended for 1.5 h. The solvent was removed through a MINI-Glatt fluidized bed. The indomethacin load was approximately 27% w/w by the rotavapor, 24.4% w/w by the fluidized bed and 1.7% by immersion method. Post drug-loading, the drug was mainly in the amorphous form. The drug release from the samples prepared by the fluidised bed and rotavapor methods was approximately 50% after 60 min, while the release from the immersion samples was over 70% after 60 min. It was considered that the drug was not diffused deeply into the MCM-41 mesopores in the immersion method, hence the more rapid release (Limnell et al., 2011).

1.3.4 Impregnation processes

Several impregnation processes have been reported in the literature. A solvent impregnation process is based on the principle of preparing a concentrated solution of drug and adding this solution to the silica, whereas in the solvent method, there is a large volume of solvent used and the silica is added to it to form a suspension.

Charney and co-workers loaded MCM-41 using an impregnation method over multiple steps with an ibuprofen – ethanol solution (65 mg/ml); the rationale was to completely fill the mesopores. The solvent was evaporated at 50 ^{o}C after each

impregnation step and there was also washing step to remove any drug from the MCM-41 surface after the highest loading. The drug load increased with each step from 30 mg of drug per gram of MCM-41 to 1350 mg/g; at the highest drug load there was evidence of drug crystallinity ascribed to the presence of drug crystals outside the mesopores. After the washing step to remove surface drug, there was no evidence of drug crystallinity observed. It was suggested that the drug molecules were packed inside the mesopores but not uniformly distributed on the inner surfaces because while the mesopore volume was greatly decreased by drug-loading, the mesopore size distribution did not dramatically decrease until saturation of the mesopores by the drug. In other words, the mesopores had to be filled up before the mesopore size was greatly affected. The drug release of the amorphous drug from the MCM-41 was rapid (Charnay et al., 2004).

A commonly reported single step incipient wetness impregnation involves preparing a concentrated solution of drug in solvent followed by its dropwise addition to the mesoporous silica. Depending on the drug, the wetted silica is stirred with a spatula or mortar and pestle. The powder is subsequently dried using air for 24 h and then placed under vacuum for 48 h at 40 ^{o}C (Mellaerts et al., 2010, Mellaerts et al., 2008a, Mellaerts et al., 2008b, Van Speybroeck et al., 2011, Van Speybroeck et al., 2010b, Van-Speybroeck et al., 2009). Mellaerts and co-workers employed the incipient wetness method to preferentially load itraconazole into SBA-15 micropores rather than the mesopores. It was suggested that the rapid solvent evaporation encountered in the incipient wetness method may have preferentially loaded the drug into the SBA-15 micropores, compared to solvent loading. However there was no difference in drug release between the impregnation and solvent methods (Mellaerts et al., 2008a), which could have conclusively proved this point.

1.3.5 Supercritical drug-loading processes

Drug-loading processes employing supercritical fluids (SCF) have recently been reported in the literature (Cha et al., 2012, Miura et al., 2010, Sanganwar and Gupta, 2008). An SCF is a fluid that possesses the properties of the liquid and gaseous state; it has liquid-like density and gas-like viscosity and diffusivity (Pasquali and Bettini, 2008). Carbon dioxide (CO_2) is the most commonly used SCF because it has a low critical point (7.4 MPa, 31.2 ^{o}C), is non-flammable, recyclable, environmentally benign and inexpensive (Pasquali and Bettini, 2008). The supercritical region of CO_2 can be seen in the CO_2 pressure – temperature diagram (Fig.1.8).

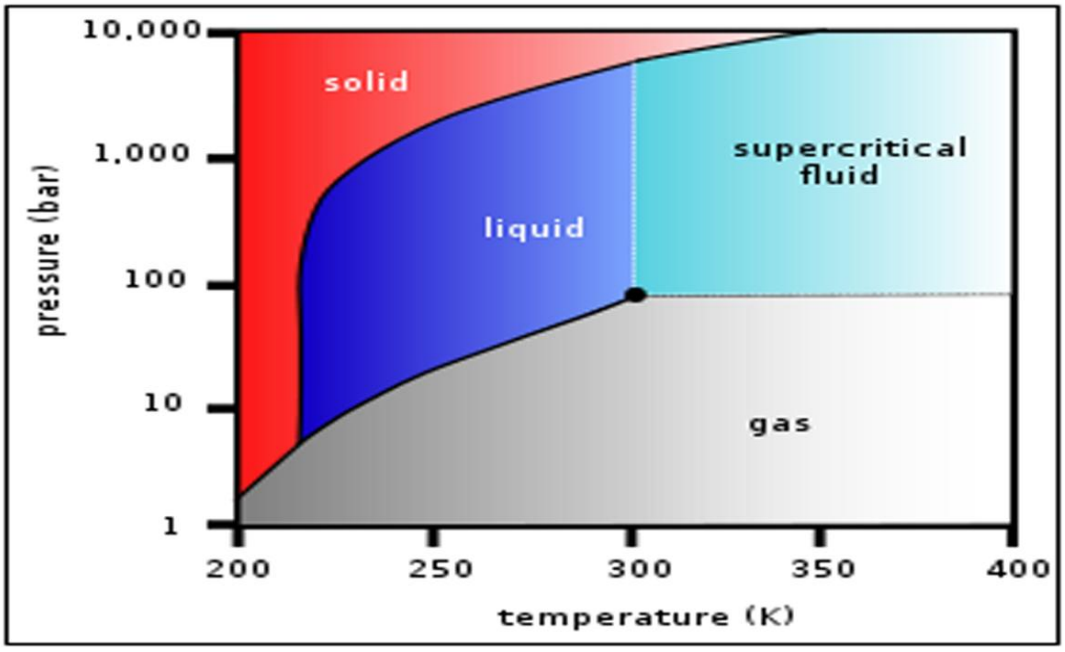

Figure 1.8: Pressure – temperature phase diagram of CO_2 (Pasquali and Bettini, 2008).

SCF's are dense but easily compressible; manipulation of the fluid pressure and temperature in the supercritical region can alter the fluid density and hence solvent power (Brunner, 1994). Another benefit of applying SCF for drug-loading is that the

final product is totally solvent free post fluid evacuation (Bush et al., 2007). Additionally, a great many compounds have been reported to be soluble in SC-CO_2 (Lucien and Foster, 2000). One of the first reports of the application of SCF technology for drug-loading was by Sanganwar and Gupta who loaded fenofibrate onto CAB-O-Sil M-5P® by the application of supercritical CO_2 (SC-CO_2) under processing conditions of (i) 176 bar, 40 ^oC, and (ii) 176 bar, 50 ^oC. By increasing the temperature but maintaining constant pressure, the actual volume of CO_2 used was lowered. The silica was physically separated from the drug as it had been placed in porous Whatman filter paper (11 µm pore size). The supercritical conditions were maintained for 150 min followed by controlled depressurisation over 4 h in a closed system. After SC-CO_2 processing, some of the powder was stored under accelerated storage conditions of 40 ^oC and 75% RH. While the drug was amorphous after processing under SC-CO_2 conditions at 40 ^oC there was drug re-crystallisation after storage. After processing at 50 ^oC, some drug crystallinity was evident which did not increase post storage. The drug release extent was over 90% after 30 min for the samples SC-CO_2 processed with Aerosil® whereas unprocessed fenofibrate did not achieve 100% dissolution until 24 h. Post storage, the release after 30 min of fenofibrate loaded after SC-CO_2 processing at 40 ^oC fell to under 60% from 90% while the release after SC-CO_2 processing at 50 ^oC decreased to 70% (Sanganwar and Gupta, 2008).

Belhadj-Ahmed and co-workers employed a supercritical flow through system where the drug, vitamin E acetate was first dissolved in the SC-CO_2, with the fluid then passed through MCM-41. The processing conditions were 15 MPa, 40 ^oC with a flow rate of 500 g/l. There are more variables to be considered in this system; pressure, temperature, duration time, SCF flow rate, solute concentration the SCF

and its partition coefficient. They found that this system gave similar drug-loading (1.14 g drug/1 g MCM-41) in 1 h compared to solvent loading with hexane in 4 h (Belhadj-Ahmed et al., 2009).

1.4 The influence of silica properties on drug-loading, solid-state form and release

In this section of the thesis, the influence of the silica material properties on drug physicochemical properties such as solid state and release will be discussed. Silica particle properties such as particle size and morphology as well as silica surface functionalisation are pertinent properties that influence drug physicochemical properties and must be discussed. Silica material properties including surface area, mesopore volume, size, shape and arrangement are also considered.

1.4.1 Silica particle properties

Several studies have been reported that silica particle size, shape and morphology did not influence drug-loading and release (Chen et al., 2012, Manzano et al., 2008, Qu et al., 2006). Manzano and co-workers studied the influence of MCM-41 particle morphology on ibuprofen drug delivery. They studied spherical particles which had very defined particle sizes of either 490 nm, 615 nm or 770 nm; for comparative purposes they also included irregular shaped MCM-41 particles that contained particles sized from 300 nm to 10 μm in the sample. The drug load was 25-26% w/w for both the irregular and all spherical shaped MCM-41 particles, regardless of the particle size. The 770 nm sized spheres had a bigger surface area than the 615 and 490 nm sized spheres but the same drug load; it will be shown in the following

section that drug load is influenced by available surface area. In this work, while the surface areas were different, the mean mesopore sizes were very similar at 3.2 nm for 490 nm spheres to 3.6 nm for the 770 nm spheres; this similarity of mesopore sizes may have contributed to the powders recording similar drug loads. They found no difference in drug release between the irregular and spherical shaped MCM-41 particles, or between the different particle sizes of the spherical particles in simulated body fluid (SBF) (Manzano et al., 2008).

Chen and co-workers prepared mesoporous silica nanoparticles (MSN) with varying concentrations of the triblock copolymer pluronic F127. They determined a relationship between increasing F127 concentration with decreasing particle length and diameter size for rod-shaped particles. At the highest level of F127 concentration (0.68 mM) employed in this study, the particles went from rod to spherical shaped. They reported that the particle dimensions and morphology (rod-like or sphere-like) of the MSNs did not have an impact on the amount of drug loaded. However, the impact on drug release was substantial; the spherical-shaped particles had faster drug release compared to the rods in simulated body SBF at 37 ^{o}C. Based on their results, it can be seen that the rods had a particle length of approximately 550 nm and a diameter of 250 nm; the equivalent particle diameter for the spheres was 200 nm. They reported that the difference in particle dimensions (particle length) led to the rods having a slower release than the spheres because of the shorter diffusion distance in the spheres (Chen et al., 2012).

Qu and co-workers published work that also showed that drug release from MCM-41 was faster from silica with a smaller particle size (120 – 250 nm) and spherical morphology compared to silica with a larger particle size of 20 µm and rod-like morphology (Qu et al., 2006). These studies highlighted silica particle size and to a

lesser extent shape (rod or spherical) were important factors to be considered for optimum drug release.

1.4.2 Surface area

Surface area is perhaps the most obvious silica material property to be considered in relation to drug-loading. As mentioned in the previous section, Chen and co-workers prepared mesoporous silica nanoparticles (MSN) using different concentrations of F127, which resulted in a range of MSN differentiated by particle size, morphology and specific surface area. They established a clear relationship between the surface area and drug content that was independent of particle size and morphology (Chen et al., 2012). Qu and co-workers similarly reported that specific surface area was the determinant in terms of drug-loading, similarly independent of silica particle size and shape (Qu et al., 2006).

1.4.3 Surface chemistry

Functionalisation of silica with various organic moieties has been reported in many papers. Functionalisation has been undertaken primarily to increase the attraction between drug and silica with the aim of extended release. Izquierdo-Barba and co-workers studied the functionalisation of MCM-48 and large pore *Ia3d* by octyltriethoxysilane (C8) and octade-cyltrimethoxysilane (C18) using toluene and acetronitrile. Both MCM-48 and large pore *Ia3d* possessed a cubic mesopore array. They reported that the amount of functional groups was solvent dependent; there was higher functional group presence on MCM-48 when functionalisation was performed with acetronitrile (28%) than toluene (21.8%). The presence of the functional groups (C8) led to an almost complete reduction of the MCM-48 surface area and mesopore

volume. The large pore *Ia3d* contained less functional group (C8) than MCM-48, which was attributed to affinity differences between the silicas for C8. These affinity differences were suggested to be due to different populations of SiOH groups present in both silicas after calcination. The functionalised large pore *Ia3d* still recorded a large surface area and mesopore volume reduction. The implications for drug-loading were profound; the functionalised large pore *Ia3d* achieved half the drug-loading of non-functionalised large pore *Ia3d* because of the very large reduction in surface area and mesopore volume. The extent of erythromycin release from the functionalised large pore *Ia3d* was 6 times less that of the non-functionalised large pore *Ia3d*, which highlighted the potential benefits of functionalisation in achieving extended drug release from mesoporous silicas (Izquierdo-Barba et al., 2005).

Song and co-workers described interesting results where they functionalised SBA-15 with 3-aminopropyl-triethoxysilane (APTES) by 2 different processes. The first process was called one-pot synthesis where the SBA-15 was manufactured and functionalised in a single step. The APTES was introduced with the TEOS during the SBA-15 synthesis procedure. Due to the nature of the one-pot synthesis approach, at least 30% of the template surfactant was still present in the SBA-15 which lowered the amount of functional group that could be added. The second process involved manufacturing the SBA-15 first and then carrying out the functionalisation post-synthesis, i.e. after calcination. They reported that there was no mesopore size reduction observed after the one-pot synthesis approach, which suggested that the functional groups were mainly in the mesopores and not surface located. After employing the post-synthesis approach, the mesopore size reduced from 86 to 78 Å while the surface area decreased from 860 to 479 m^2/g. The surface area reduction was attributed to the disappearance of the micropores present in the

SBA-15; this was reflected in the typical mesoporous H1 hysteresis observed in the N_2 adsorption/desorption isotherm. This behaviour was not observed in the samples prepared by the one-pot approach where as the amount of functional group increased, the hysteresis loop broadened, which indicated a widening of the mesopore size distribution (Song et al., 2005).

The drug-loading increased as the amount of functional groups increased in the post-synthesis sample, while drug release rates decreased with the increasing amount of functional group. In the one-pot synthesis sample, drug-loading also increased with increasing functional groups, except at the highest functional group level where drug-load decreased. This decrease at the highest level of functional group was considered to be result of the greater level of inaccessible micropores present in this particular sample (Song et al., 2005). This work highlighted that the choice of functionalisation process has an important bearing on drug-loading and release rates.

Manzano and co-workers also reported that ibuprofen release was extended from amine-functionalised MCM-41 compared to standard non-functionalised MCM-41. They also observed a large increase in ibuprofen loaded onto the amine-functionalised MCM-41 compared to standard MCM-41. In this work, the amine-functionalised MCM-41 had maintained its mesoporous characteristics (Manzano et al., 2008). This work highlighted that silica functionalisation could aid increased drug-loading as long as the silica maintained its mesoporous properties post functionalisation.

Moritz and Laniecki also looked at functionalising SBA-15 with APTES as a carrier for ketoprofen. They reported that the functionalisation of SBA-15 with APTES resulted in the silica material acquiring surface basic properties because the aminopropyl groups of the APTES were basic. The drug-loading achieved was 20%

w/w, while drug release rate was slower from the functionalised SBA-15 compared to the non-functionalised SBA-15 (Moritz and Laniecki, 2012b).

Guo and co-workers utilised MCM-41 and SBA-15 to improve the dissolution rate of naproxen; both silicas were functionalised with APTES. They reported that functionalisation decreased the surface areas, mesopore volumes and sizes of both silicas; they achieved slightly higher drug content in the non-functionalised silicas. Controlled release was observed from the functionalised silicas; for the functionalised SBA-15, total release was not achieved until after 900 min while the corresponding time for the functionalised MCM-41 was 1800 min. The drug was in the amorphous state in the functionalised SBA-15 while in the non-functionalised SBA-15 there was still residual crystallinity, which was attributed to the fact that non-functionalised SBA-15 had larger mesopore sizes than functionalised SBA-15 which may have permitted some drug re-crystallisation (Guo et al., 2013).

1.4.4 Mesopore properties

The mesopore properties of silica materials have a very important impact on drug-loading and other properties, namely solid state structure and long term stability. Numerous studies have looked at the impact of mesopore volume (Charnay et al., 2004, Heikkila et al., 2007), mesopore size (Aerts et al., 2007, Andersson et al., 2004, Horcajada et al., 2004, Izquierdo-Barba et al., 2005, Limnell et al., 2011, Qu et al., 2006, Tozuka et al., 2005, Ukmar et al., 2011b), mesopore geometry, whether unidirectional mesopores or 2-D/3-D (Gao et al., 2012, Heikkila et al., 2007) and mesopore morphology (cubic or hexagonal) (Zhu et al., 2005b). Heikkila and co-workers investigated the impact of mesopore volume on drug-loading by loading ibuprofen onto different mesoporous silicas (TUD-1, SBA-15 and MCM-41) by the

solvent method. TUD-1 had a mesopore volume of 0.57 cm^3/g, while SBA-15 had a mesopore volume of 1.067 cm^3/g and MCM-41 a mesopore volume of 0.72 cm^3/g. They reported that the total mesopore volume was the determining factor for drug-loading and that drug in the mesopores was in the amorphous state (Heikkila et al., 2007). Several other studies have reported the ability of mesoporous silica to stabilise amorphous drugs inside the mesopores (Shen et al., 2010, Mellaerts et al., 2010). The importance of the mesopores can also be observed where drug is loaded onto a non-porous silica. Sanganwar and Gupta loaded fenofibrate onto Aerosil® by SC-CO_2 processing; the drug was not completely amorphous and displayed evidence of crystallinity, which was accentuated after 1 month under accelerated storage conditions (Sanganwar and Gupta, 2008).

Mesopore size has an important role to play in long-term drug stability. As mentioned earlier, if a drug is loaded into a confined space it cannot re-crystallise as long as the confinement space diameter does not exceed the drug molecule diameter by a factor of 20 (Rengarajan et al., 2008, Sliwinska-Bartkowiak et al., 2001). Horcajada and co-workers probed the influence that mesopore size had on drug-loading and release using MCM-41 with various mesopore sizes. They reported that as the mesopore size decreased, drug-loading and release rate decreased. The maximum ibuprofen loaded (34% w/w) into MCM-41 occurred at an average mesopore size of 3.6 nm; this also yielded the fastest and highest release rate. They postulated that the ibuprofen deposited into the MCM-41 (3.6 nm) mesopores lined the mesopore walls, leaving space between the drug molecules for the release media to penetrate and liberate the drug molecules. In contrast, when loading ibuprofen into MCM-41 which had an average mesopore size of 2.5 nm, the drug content was 11% w/w while the release was slower compared to MCM-41 (3.6 nm). The authors

hypothesised that the drug molecules loaded into MCM-41 (2.5 nm) were closely packed together. They presented evidence using N_2 adsorption to support the contention that the mesopore volume occupied by ibuprofen loaded in the MCM-41 (2.5 nm) was higher than that loaded in the MCM-41 (3.6 nm) (Horcajada et al., 2004). Limnell and co-workers also reported the important influence that mesopore size has on drug release rate. They loaded indomethacin onto Syloid which had a mean mesopore size of 19 nm and MCM-41 which has a mean mesopore size of 3.4 nm. They reported that the fastest drug release was obtained from the Syloid due to its larger mesopore size (Limnell et al., 2011).

Gao and co-workers looked into mesopore channel length and morphology; in particular they studied bimodal mesoporous silica (BMM) which had short, random mesoporous channels and MCM-41, which had long, ordered mesoporous channels. The BMM had both small mesopores sized 2.71 nm and large mesopores sized 23.8 nm, while the MCM-41 had a mean mesopore size of 2.73 nm. They reported that the BMM achieved greater drug-loading and faster release than MCM-41 (Gao et al., 2012).

Heikkila and co-workers investigated the influence of mesopore morphology in oral drug delivery using MCM-41, SBA-15 and TUD-1 which had pore sizes of 2 – 3 nm, 5 – 12 nm and 2.5 – 20 nm, respectively. They reported that the fastest drug release was obtained from the TUD-1 material due to its highly accessible mesopore network compared to the unidirectional, uniform hexagonal mesopores of SBA-15 and MCM-41 (Heikkila et al., 2007). Zhu and co-workers studied the application of HMS spheres for hosting drug in comparison to MCM-41. They reported that despite the MCM-41 and HMS having similar surface areas, mesopore volumes and mesopore sizes, much greater drug could be loaded into the HMS because this silica

material contained mesopore channels that ran into a hollow core, whereas the MCM-41 had long mesopore channels running throughout (Zhu et al., 2005b).

1.4.5 *In vivo* studies of silica – based drug delivery systems

Although, it is now well established that loading poorly water – soluble drugs onto mesoporous silicas can lead to greatly enhanced *in vitro* drug dissolution rates (Cha et al., 2012, Sanganwar and Gupta, 2008, Vallet-Regi et al., 2001) it is important to investigate how this dissolution rate enhancement affects *in vivo* oral bioavailability. Several studies have been conducted to address the challenge of improving oral bioavailability through the application of silica drug delivery systems. Mellaerts and co-workers compared the *in vivo* performance of crystalline itraconazole, itraconazole loaded by the solvent method onto SBA-15 and the commercial formulation Sporanox® by administering the powders in hard gelatin capsules (Capsugel, Belgium) to both dog and rabbit models. Crystalline itraconazole and its metabolite hydroxyitraconazole did not enter systemic circulation in the dog model. The SBA-15 formulation and Sporanox® showed broadly similar results in terms of itraconazole and hydroxyitraconazole in both animal models. This result showed that the SBA-15 formulation was equivalent to the commercial formulation and highlighted the potential of SBA-15 to improve oral bioavailability (Mellaerts et al., 2008b).

Van Speybroeck and co-workers assessed the *in vivo* performance of glibenclamide – SBA-15 formulation against the commercial product Daonil®. The weakly acidic, drug was loaded onto the SBA-15 using the incipient wetness (solvent impregnation) method. The researchers hypothesised that significant precipitation in the stomach would lower the amount of drug absorbed in the small intestine; however, if the

precipitation was avoided there would be enhanced *in vivo* performance. Dosing was by hard gelatin capsules (Capsugel, Belgium) administered to male wistar rats. They showed that the drug did not dissolve in SGF (pH 1.2), whereas there was rapid release in FaSSIF (pH 6.8). They reported that the glibenclamide – SBA-15 formulation resulted in a much larger plasma concentration compared to Daonil®. The results highlighted the potential of SBA-15 to increase drug oral bioavailability and showed the impact of pH and surface charge on the *in vitro* and *in vivo* release of weakly acidic drugs from SBA-15 (Van Speybroeck et al., 2011).

In another study, Van Speybroeck and co-workers investigated the *in vivo* performance of itraconazole loaded onto SBA-15, which was physically mixed with precipitation inhibitors, either hydroxypropylmethylcellulose (HPMC) or hydroxypropylmethyl acetate succinate (HPMCAS). Hard gelatin capsules (Capsugel, Belgium) containing crystalline itraconazole, drug loaded SBA-15 with precipitation inhibitor and the commercial product Sporanox® were administered to male wistar rats. They reported that HPMC aided the absorption of the drug, the extent was 60% greater compared to drug-loaded SBA-15 only, whereas the HPMCAS did not enhance drug absorption as it did not dissolve in the stomach (Van Speybroeck et al., 2010b).

In an additional study, Van Speybroeck and co-workers evaluated the impact that the rate and extent of fenofibrate release had on its *in vivo* absorption. Mesoporous silicas with different mesopore sizes of 2.7, 4.4 and 7.3 nm were employed to control the *in vitro* drug release. As previously mentioned, decreasing the mesopore size can slow the *in vitro* release rate; this was also observed in this study. In FaSSIF, they reported that the degree and duration of fenofibrate supersaturation increased with decreasing mesopore size. The formulations were administered to male wistar rats

as hard gelatin capsules (Capsugel, Belgium). They reported that slowing the fenofibrate release rate by applying silica with a small mesopore size (2.7 nm), allowed for a greater duration of drug supersaturation and enhanced the *in vivo* absorption (Van Speybroeck et al., 2010a).

Miura and co-workers studied the oral absorption of K-832 loaded onto Sylysia 350 in a beagle dog model. They dosed the dogs with silica-drug formulations prepared by a solvent method and SC-CO_2 loading, where supercritical conditions of 18 MPa and 60 ^{o}C were maintained for 5 h, followed by controlled depressurisation. The drug in these formulations was mainly amorphous, however there was a slight melting endotherm observed in the sample prepared by SC-CO_2. They reported that the SC-CO_2 prepared sample achieved a higher maximum drug plasma concentration (C_{max}) of 0.40 µg/ml, than that prepared by the solvent method which resulted in a C_{max} of 0.25 µg/ml. Both formulations outperformed crystalline K-832 by a factor 13 and 8 respectively in terms of the C_{max} (Miura et al., 2010).

Kiekens and co-workers investigated the potential of ordered mesoporous silica (OMS) to improve the oral bioavailability of ezetimibe using a dog model. Ezetimibe was loaded onto the OMS (COK-12) using the incipient wetness solvent impregnation method and was in a non-crystallise form. They compared the commercial product, Ezetrol® which is available as a tablet containing 10 mg ezetimibe against the OMS tablet formulations containing either 10 or 5 mg ezetimibe and an OMS capsule formulation containing 5 mg ezetimibe. They reported that the 5 mg OMS capsule resulted in a higher plasma profile compared to the Ezetrol® tablet. The 5 mg OMS capsule allowed the drug to enter into systemic circulation more quickly compared to the 10 mg Ezetrol tablet; in fact ezetimibe absorption from the 5 mg OMS capsule was double the amount from the Ezetrol®

tablet (Kiekens et al., 2012). However, it was also reported that the plasma concentrations of drug from the OMS tablet formulations were lower than expected, based on the *in vitro* data. It was seen that *in vitro* the OMS tablet formulations initially released more drug than the Ezetrol® tablet over first 15 min but after 120 min, some of the drug released from the OMS tablets had re-crystallised out of solution. These results showed the great potential of utilising mesoporous silicas for oral bioavailability enhancement, but also that the *in vitro* release performance may not always reflect the *in vivo* performance.

Cha and co-workers described the effect on fenofibrate oral bioavailability of processing the drug with Neusilin UFL2 using hot-melt, solvent and SC-CO_2 loading in male Sprague Dawley rats. They reported that the drug entered into the mesopores when loaded using SC-CO_2, but was not in the pores after the hot-melt method because of fenofibrate's high molten viscosity. Some of the fenofibrate loaded by the solvent (4.21% (±1.09)) and hot-melt (9.43% (±2.11) methods had retained crystallinity while the fenofibrate loaded by the SC-CO_2 was amorphous. They reported that the drug – silica composite prepared by SC-CO_2 loading achieved faster *in* vitro release kinetics compared to the commercial product Lipidi Supra®, however both formulations recorded similar drug serum concentrations, *in vivo* profiles and C_{max} values, 92.88 (±7.05) µg/ml and 89.60 (±12.02) µg/ml for the SC-CO_2 and commercial formulations, respectively (Cha et al., 2012).

A human trial has also been reported where drug-loaded mesoporous silica was successfully used to significantly increase the rate and extent of absorption of fenofibrate into systemic circulation compared to the commercial product Lipantyl® micro (67 mg). There was a 54% increase in systemic exposure of fenofibrate's metabolite, fenofibric acid and a 77% increase in the dose-normalised fenofibric acid

plasma peak concentration after administration of the mesoporous silica formulation. The subjects were dosed in a random order with 33.5 mg of a fenofibrate – mesoporous silica formulation with 200 ml of water under fasted conditions. After a 7 day washout period the subjects were dosed orally with a 67 mg Lipantyl® micro formulation and 200 ml water, also under fasted conditions (Verheyden et al., 2012). A summary of the *in vivo* research involving mesoporous silica in terms of how the drug is loaded, the *in vivo* model and dosage size and form is shown Table 1.3.

Table 1.3: Summary of the *in vivo* research involving silica materials for enhanced drug dissolution and oral bioavailability.

Mesoporous silica	Drug	Dosage	Loading process	Delivery platform	Animal model	Reference
SBA-15	Itraconazole	~2 mg/kg	Solvent	Hard gelatin capsule	NZ white rabbit	(Mellaerts et al., 2008b)
SBA-15	Itraconazole	~2 mg/kg	Solvent	Hard gelatin capsule	Beagle dog	(Mellaerts et al., 2008b)
SBA-15	Fenofibrate	2.63 mg/kg	Impregnation	Hard gelatin capsule	Male wistar rat	(Van Speybroeck et al., 2010a)
SBA-15	Itraconazole	2.63 mg/kg	Impregnation	Hard gelatin capsule	Male wistar rat	(Van Speybroeck et al., 2010b)
Sylysia	K-832	10 mg/kg	SC-CO_2 flow through	Oral suspension	Dog	(Miura et al., 2010)
SBA-15	Glibenclamide	2.29 mg/kg	Impregnation	Hard gelatin capsule	Male wistar rat	(Van Speybroeck et al., 2011)
COK-12	Ezetimibe	0.5 – 1 mg/kg	Impregnation	Tablet / capsule	Dog	(Kiekens et al., 2012)
Neusilin UFL2	Fenofibrate	50 mg/kg	SC-CO_2	Oral suspension	Male Sprague Dawley rat	(Cha et al., 2012)
Mesoporous silica	Fenofibrate	33mg	Impregnation	Tablet	Human	(Verheyden et al., 2012)

1.4.6 Summary

Silica materials, in particular ordered mesoporous materials have demonstrated excellent properties for the enhancement of drug dissolution and oral bioavailability of a variety poorly water – soluble BCS Class II compounds such as fenofibrate, ibuprofen and itraconazole. The key silica parameters that influence drug-loading and release are the surface area, mesopore volume, size and geometry. It is important to also recognise that the silica particle size and morphology are important factors to be considered. The greater the silica surface area, the more drug that can be hosted by the silica material. If the silica material is porous, the porosity allows stabilisation of the drug in the amorphous or non-crystalline form due to the restricted nature of the drug inside the mesopores, as long as the mesopore diameter is not greater than 20 times the drug molecule width (Sliwinska-Bartkowiak et al., 2001). The mesopore diameter also influences drug release rate; larger mesopore sizes encourage faster drug release compared to smaller mesopore sizes. Silica particle size also influences drug release rate; smaller silica particle sizes allow for faster drug release than larger particle sizes, where there are unidirectional mesopores running through the particle.

The oral bioavailability enhancement of poorly water – soluble drug from loading onto mesoporous silica has been demonstrated in different *in vivo* models, including dog, rat and rabbit. Based on the research, the application of mesoporous silica creates a supersaturation of the drug in the GI tract, leading to enhanced absorption in the upper intestinal region. However, there is evidence that precipitation inhibitors like HPMC would be beneficial to ensure maximum absorption.

Excitingly, a recent human trial involving a fenofibrate – mesoporous silica formulation has shown promising results in comparison to an currently marketed oral formulation, Lipantyl® micro (67 mg) (Verheyden et al., 2012). This report serves to

highlight the strong potential of mesoporous silica for oral drug delivery and rapid strides taken in this field in the last number of years.

1.5 Fenofibrate

The model poorly water-soluble drug chosen for this research was fenofibrate ($C_{20}H_{21}ClO_4$), chemical name isopropyl 2-[4-(4-chlorobenzoyl)-phenoxy]-2-methylpropionate (Kemprotec Ltd, UK). It is a white crystalline powder, has a melting point in the region of 79 – 82 ^{o}C and a molecular weight (MW) of 360.84 kmol/kg. The molecular structure of fenofibrate is shown here (Fig.1.9).

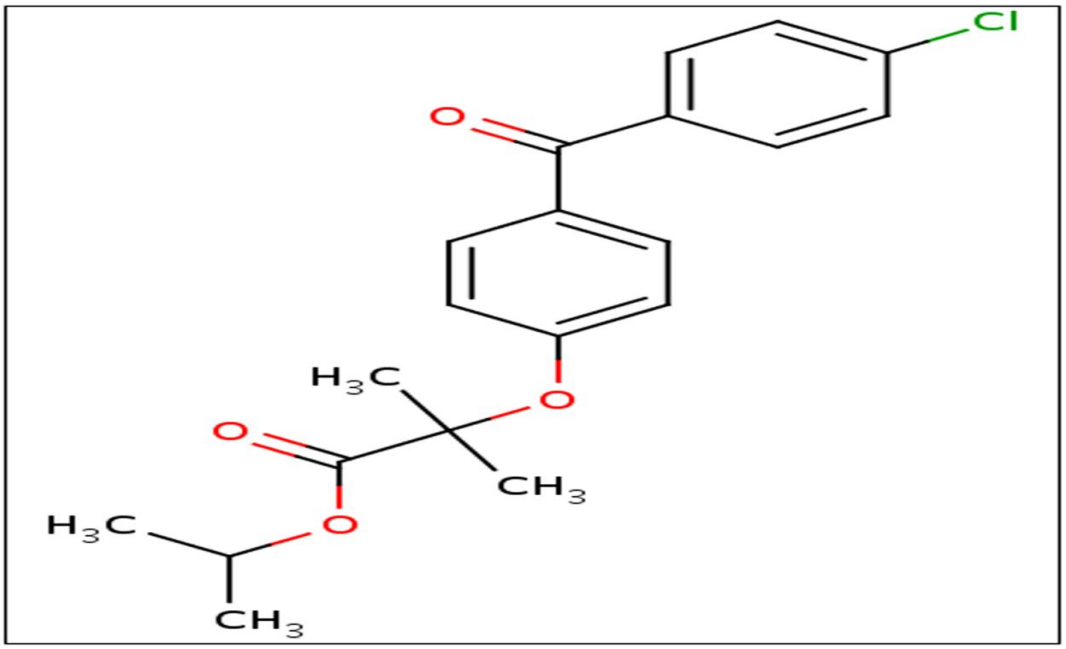

Figure 1.9: Molecular structure of fenofibrate (Knox et al., 2011).

It is a non-ionizable compound, therefore it is not affected by changes in pH (Jamzad and Fassihi, 2006). Fenofibrate does not have strong intermolecular bonds such as hydrogen bonding (Heinz et al., 2009). It does not have hydrogen-donor groups and has only 2 hydrogen-acceptor groups (carbonyl groups) (Van Speybroeck et al.,

2010a). It is practically insoluble in water and is a neutral highly lipophilic drug (log P = 5.3) (Huang et al., 2009, Van Speybroeck et al., 2010a, Jamzad and Fassihi, 2006). Fenofibrate is considered to be a BCS Class II drug; it is very lipophilic but hydrophobic (Amidon et al., 1995). The oral bioavailability of fenofibrate is dependent upon its dissolution rate in the GI tract; therefore increasing its dissolution rate can potentially increase its bioavailability. Historically, fenofibrate has had very low bioavailability of its active metabolic fenofibric acid, when administered on an empty stomach (Guivarc'h et al., 2004). In fact, it has been advised that fenofibrate should be administered with meals (Guivarc'h et al., 2004). Fenofibrate has been the subject of many different processing and formulation approaches to improve its bioavailability, such as micronisation and wet milling (Juenemann et al., 2011), co-grinding and coating onto hydrophilic matrices such PVP (Vogt et al., 2008), loading onto high surface area carriers (silica substrates) (Sanganwar and Gupta, 2008), solid dispersion and emulsions (Huang et al., 2009). An early fenofibrate formulation Lipanthyl$^{(R)}$, was a 200 mg tablet which contained coarse fenofibrate and exhibited high inter-individual variability in its plasma profiles, this formulation was recommended to be taken with food (Juenemann et al., 2011). Some data has been published in literature which showed that 84% of orally administered fenofibrate was recovered in the urine and faeces (Weil et al., 1990). Most of the fenofibrate recovered in the faeces was unchanged fenofibrate while that recovered in the urine was fenofibric acid, the active metabolite of fenofibrate. A new formulation of micronised fenofibrate, Lipidil – Ter$^{(R)}$, was introduced in 2000 which had a dose of 160 mg and less inter-individual variability (Juenemann et al., 2011). Even more recently, nanosized fenofibrate formulations (500 nm) such as Tricor$^{(R)}$ and Lipidil – 145 ONE$^{(R)}$, have been developed that have further increased oral bioavailability as

evidenced by the reduced dosage amount of 145 mg and which removed the effect of food on the bioavailability (Juenemann et al., 2011).

1.6 Objectives of thesis

The objectives of this research were to:

- Enhance fenofibrate release through the application of the high surface area carrier, SBA-15,
- Investigate various processing methods to load fenofibrate onto SBA-15 and determine what impact the loading process had on fenofibrate loading and release from SBA-15 (chapter 4),
- Investigate how SC-CO_2 processing conditions influenced drug-loading and release from fenofibrate – SBA-15 systems,
- Investigate physicochemical factors influencing drug release from fenofibrate – SBA-15 systems.

2 Materials and Methods

In this chapter, the materials used in this thesis, the experiments performed across the various chapters and the subsequent analytical techniques employed will be presented.

2.1 Materials

The materials, suppliers and their application in this thesis are listed in Table 2.1 below.

Table 2.1: List of materials with supplier information and application in this work.

Material	Formula	Supplier	Application
Fenofibrate	$C_{20}H_{21}ClO_4$	Kemprotec Ltd., UK	Drug
Mesoporous silica (SBA-15)	SiO_2	Glantreo Ltd. Ireland	Carrier
Phencyclidine hydrochloride (P123)	$C_{17}H_{25}N.HCl$	Sigma-Aldrich Ltd., Ireland	SBA-15 synthesis
Tetraethyl orthosilicate (TEOS)	$Si(OC_2H_5)_4$	Sigma-Aldrich Ltd., Ireland	SBA-15 synthesis
Carbon dioxide	CO_2	Irish Oxygen Ltd., Ireland	Drug-loading
Methylene chloride (DCM)	CH_2Cl_2	Sigma-Aldrich Ltd., Ireland	Drug-loading
Hydrochloric acid, 37%	HCl	Sigma-Aldrich Ltd., Ireland	Dissolution media
Sodium dodecyl sulphate (SDS)	$C_{12}H_{25}SO_4Na$	Sigma-Aldrich Ltd., Ireland	Dissolution media
Deionised water	H_2O	UCC, Ireland	Dissolution media
HPLC grade acetronitrile	C_2H_3N	Sigma-Aldrich Ltd., Ireland	HPLC mobile phase

HPLC grade water	H_2O	Sigma-Aldrich Ltd., Ireland	HPLC mobile phase
Potassium bromide	KBr	Sigma-Aldrich Ltd., Ireland	FT-IR analysis
Methanol	CH_3OH	Sigma-Aldrich Ltd., Ireland	Solvent

2.2 Preparation of SBA-15

SBA-15 was synthesised according to the method outlined in the literature (Zhao et al., 1998). Briefly, 200 g of tri-block polymer (P123) was dissolved in 1.6 M HCl solution. The solution was heated to 40 ^{o}C to completely dissolve the polymer, after which 607 ml of 98% TEOS was added to the solution. The solution was stirred for 24 h at 40 ^{o}C and dried for a further 96 h at 60 ^{o}C. The SBA-15 was recovered by filtration, washed with deionised water to remove any remaining amounts of ethanol and HCl, prior to calcination in an Ashing furnace (Carbolite Ltd., UK), which was set to 550 ^{o}C for 14 h to remove the polymer template.

2.3 Chapter 4: Preparation of fenofibrate – SBA-15 systems

Drug – silica samples were prepared with a ratio of 1 mg drug per 3 m^2 mesoporous silica surface area. Approximately 400 mg of drug was combined with 2 g mesoporous silica and processed according to the methods detailed below. All samples were prepared in triplicate.

2.3.1 Physical Mixing

Drug – mesoporous silica physical mixes were prepared by placing the fenofibrate and mesoporous silica inside 50 ml capped plastic containers (Sarstedt AG, Germany) and blending for 30 min at 100 revolutions per minute (rpm) using an AR402 Erweka blender (Erweka GmbH, Germany).

2.3.2 Melt method

The melt method involved heating the drug above its melting point (> 80 ^{o}C) and relied on its molten viscosity to distribute the drug on the mesoporous silica surface and into the mesopores. The drug was manually combined with the mesoporous silica to increase the homogeneity of drug distribution. The sample was maintained above 80 ^{o}C for 24 h using an E-series binder oven (Erweka GmbH, Germany) and thereafter cooled to ambient temperature.

2.3.3 Solvent impregnation

Samples were prepared according to the method reported by Mellaerts and co-workers (Mellaerts et al., 2008a). Approximately 8 ml of a concentrated solution of fenofibrate (50 mg/ml) in DCM was added dropwise to the mesoporous silica, after each addition the powder was intensively ground with a pestle. Thereafter, the sample was dried at 40 ^{o}C for 48 h under vacuum (100 Pa).

2.3.4 Liquid CO_2 processing

The drug and mesoporous silica were combined in a high-pressure reactor (BC 316), (High Pressure Equipment Company, USA) and stirred using a magnetic stirrer. The

reactor cell was filled with liquid CO_2 directly from the CO_2 dispensing cylinder up to an initial pressure of 5.5 MPa. The cell was then heated to 25 ^oC using heating tape and maintained at this temperature for the duration of the experiment using a temperature monitor (Horst GmbH, Germany). A high pressure pump (D Series Syringe Pump 260D, Teledyne ISCO, USA) was used to pump additional CO_2 into the cell to reach the final pressure of 27.58 MPa. The pressure was monitored with a pressure gauge. At the end of the experiment the cell was rapidly depressurised by venting the CO_2.

2.3.5 SC-CO_2 processing

The supercritical processing method followed the exact same procedure as the liquid CO_2 process, except that the experimental temperature was 40 ^oC.

2.4 Chapter 5: Preparation of fenofibrate – SBA-15 systems

2.4.1 Investigating SC-CO_2 processing pressures and duration times

A 3^2 factorial design was used to determine the optimum SC-CO_2 processing pressure (13.79, 27.58, 41.37 MPa) and time duration (4, 12, 24 h) for loading of SBA-15 with fenofibrate. In all these experiments, the temperature was maintained at 40 ^oC. For each run, a constant drug to silica ratio of 1 mg of fenofibrate for every 3 m^2 surface area of SBA-15 was maintained. The complete list of the design of experiments is shown in Table 2.2.

Table 2.2: Design of experiments for SC-CO_2 pressure and time optimisation.

Run No.	Pressure (MPa)	Time (h)	Blocks
1	13.79	12	1
2	13.79	4	1
3	41.37	24	1
4	27.58	12	1
5	27.58	24	1
6	41.37	12	1
7	13.79	24	1
8	41.37	4	1
9	27.58	4	1
10	27.58	24	2
11	27.58	4	2
12	41.37	4	2
13	13.79	24	2
14	41.37	24	2
15	13.79	12	2
16	13.79	4	2
17	27.58	12	2
18	41.37	12	2
19	27.58	24	3
20	13.79	24	3
21	41.37	4	3
22	13.79	4	3
23	27.58	12	3
24	27.58	4	3
25	41.37	12	3

26	41.37	24	3
27	13.79	12	3

2.4.2 The effect of drug – silica ratios on drug physicochemical properties

The influence of increasing the amount of fenofibrate to silica surface area was investigated at (i) 1 mg to 3 m^2, (ii) 1 mg to 1.24 m^2 and (iii) 1 mg to 0.82 m^2 to determine what effect this had on drug-loading efficiency, solid state and release. These experiments were conducted at a SC-CO_2 processing pressure of 27.58 MPa, for 12 h time duration with a temperature of 40 ^oC.

2.4.3 Methods of drug – silica combination

Normally, the drug and silica were placed together in the reactor and exposed to SC-CO_2 conditions, under the influence of a magnetic stirring bar (‘mix method’). In an effort to determine the impact of directly combining the drug and silica, an alternative method termed the ‘bag method’ was also investigated The SBA-15 was placed in a porous muslin bag which was placed at the top of the high-pressure cell, this had the effect of physically separating the SBA-15 from the fenofibrate, which was placed at the bottom of the cell. The porous bag allowed the SC-CO_2 and solubilised drug to permeate into the bag during processing. A SC-CO_2 pressure of 27.58 MPa and 12 h duration was employed for both loading methods, also at 40 ^oC.

2.4.4 Effect of SC-CO_2 depressurisation rate

The effect of depressurisation rate was investigated to determine its impact on drug – SBA-15 physicochemical properties. The depressurisation step was controlled by allowing enough CO_2 gas to escape in order to reduce the pressure by 0.69 MPa every minute. SC-CO_2 conditions of 27.58 MPa, 12 h duration time and temperature of 40 ^oC were employed with a drug – silica ratio of 1 mg to 3 m^2 in the 'mix method'.

2.5 Chapter 6: Preparation of fenofibrate – SBA-15 systems

2.5.1 Multiple step drug-loading

It was desired to increase drug-loading efficiency without compromising drug release by loading the drug with a multiple step drug-loading approach. Details of preparation of each of these drug-silica samples are given below. The SC-CO_2 conditions were 27.58 MPa, 12 h and 40 ^oC with rapid depressurisation. The drug and silica were combined with the 'mix method'.

Drug – silica ratio of 1 mg – 1.24 m^2

This drug – silica ratio was prepared in two SC-CO_2 processing steps. Step 1 involved taking 2 g of SBA-15 and the addition of sufficient fenofibrate to produce the initial ratio of 1 mg: 3 m^2. This mixture was then SC-CO_2 processed and the powder recovered. The drug content analysis (% w/w) of recovered powder from step 1 was determined and used to calculate how much extra drug was required for step 2 to achieve a drug – silica ratio of 1 mg – 1.24 m^2. 1.5 g of mixture from step 1

was taken forward for step 2, where the drug – silica ratio of 1 mg: 1.24 m^2 would be prepared.

Drug – silica ratio of 1 mg – 0.82 m^2

This drug – silica ratio was prepared in three SC-CO_2 processing steps. Step 1 involved taking 2 g of SBA-15 and adding sufficient fenofibrate to produce the initial ratio of 1 mg: 3 m^2. This mixture was then SC-CO_2 processed and the powder recovered. 1.5 g of the step 1 mixture was taken forward for step 2, in order to prepare the drug – silica ratio of 1 mg: 1.24 m^2. The rest of the recovered powder from step 1 was used for drug content analysis (% w/w), which was needed to calculate the extra drug required for step 2. After step 2 SC-CO_2 processing, approximately 0.78 g of the step 2 mixture was taken forward for processing in step 3, with enough drug added to produce the theoretical drug – silica ratio of 1 mg: 0.82 m^2 . As with step 1, a portion of the sample processed in step 2 was retained for drug content (% w/w) analysis to determine the extra drug required for step 3. After processing the samples were recovered and analysed. The actual amounts of silica and fenofibrate employed for each of the steps is shown here, Table 2.3.

Table 2.3: Formulations employed at each step of multiple loading approach.

Number of Steps	Drug – silica ratio	Mass of SBA-15 (g)	Mass of fenofibrate (mg)
1	1 mg : 3 m^2	2.00	545.00
2	1 mg : 1.24 m^2	1.22 – 1.27	806.90 – 834.02
3	1 mg : 0.82 m^2	0.49 – 0.5	484.12 – 497.87

2.5.2 Maximum drug-loading based on SBA-15 mesopore volume and drug true density

In chapter 6 it was desired to load as much drug onto the silica as possible without compromising the subsequent drug release rate. To that end, the maximum mass of drug that could be theoretically hosted within the silica mesopores was calculated based on the measurement of SBA-15 mesopore volume and the measured drug density (determined by helium pycnometry section 2.6.3.) according to Eq. 2.1.

Equation 2.1: $\text{Maximum drug in mesopores (g)} = M_{SBA\text{–}15} * PV_{SBA\text{–}15} * \rho_{drug}$

Where $M_{SBA\text{-}15}$ is the mass of SBA-15 (g), $PV_{SBA\text{-}15}$ is the available SBA-15 mesopore volume (cm^3/g) and ρ_{drug} the true density of fenofibrate (g/cm^3).

The % theoretical mesopore fill was then calculated according to Eq. 2.2,

Equation 2.2: $\%\,\text{Mesopore fill} = \left(\frac{\text{Mass of drug to be loaded (g)}}{\text{Maximum drug in mesopores (g)}}\right) * 100\%$

Where the numerator refers to the mass of drug actually loaded and the denominator refers to maximum mass of drug that could be hosted by the SBA-15 mesopores based on Eq.2.1.

Samples were prepared that contained (1) less than, (2) equal to and (3) more than the maximum fenofibrate that could be loaded into the available SBA-15 mesopores.

These samples were termed the standard, maximum and excess samples and further details on each the preparation of each are provided below.

'Standard sample'

The 'standard sample' was based on the drug – silica ratio of 1 mg fenofibrate to 3 m^2 SBA-15 surface area; this ratio was the drug – silica ratio used throughout this thesis. The 'standard sample' was processed with SC-CO_2 conditions of processing pressure, 27.58 MPa, with 12 h time duration and temperature of 40 ^oC.

'Maximum sample'

Based on Eq. 2.1, the 'maximum sample' contained enough drug to theoretically fill 99% of the available SBA-15 mesopore volume. The 'maximum sample' was processed with SC-CO_2 conditions at a pressure of 27.58 MPa, for 12 h duration and at a temperature of 40 ^oC.

'Excess sample'

The 'excess sample' contained enough fenofibrate to theoretically fill the available SBA-15 mesopore volume 2.86 times. This sample was prepared by taking 2.00 g of the 'maximum sample' and carrying out a second SC-CO_2 processing step to load extra drug on to the sample, per the multiple step drug-loading procedure outlined above. The 'excess sample' was processed under the SC-CO_2 conditions at a pressure of 27.58 MPa, for 12 h duration and at a temperature of 40 ^oC. The % mesopore fill, actual amounts of silica and fenofibrate and % drug (w/w) for each of the samples is shown here, Table 2.4.

Table 2.4: % mesopore fill, mass of SBA-15 and fenofibrate and % drug (w/w) of the standard, maximum and excess samples.

Sample	% Mesopore fill	SBA-15 (g)	Fenofibrate (mg)	% Drug (w/w)
Standard	32.50	2.00	545.00	21.41
Maximum	99.00	2.00	1700	45.95
Excess	286.00	1.08	2619	70.78

2.6 Characterisation techniques

2.6.1 Scanning electron microscopy / energy dispersive X-ray spectroscopy

Scanning electron microscopy (SEM) was used to obtain images of the mesoporous silica and fenofibrate. Using a JSM-5510 SEM, (Jeol, UK), with heated tungsten as the electron beam source, the morphology and particle size of the samples was acquired. The voltage was constant at 5 kV. Samples were gold coated in SEM gold coater (Jeol, UK) prior to analysis to prevent charging of the samples by the SEM electron beam. A coating time of approximately 45 seconds was used to deposit a thin layer onto the samples.

Environmental scanning electron microscopy (SEM) and energy dispersive X-ray spectroscopy (EDX) were performed with a Hitachi VP-SEM S-37900N (Hitachi High-Technologies Europe GmbH, Germany) with an Oxford Instruments X –Max 80 mm^2 (Oxford Instruments Ltd., United Kingdom). SBA-15 was probed via its silicon (Si) atom, while fenofibrate was probed via its chlorine (Cl) atom.

2.6.2 Particle size analysis

The particle size distributions of mesoporous silica and fenofibrate were determined using a Retsch AS 200 sieve shaker (Retsch GmbH, Germany). Sieving was performed with the amplitude set at 1.5 mm/g for 15 min.

2.6.3 Density testing

Bulk density was calculated using a SVM 122/222 tapped density tester, (Erweka GmbH., Germany) using the procedure as outlined in Section 2.9.15 of the European Pharmacopoeia (Ph Eur 5.0). A 100 ml cylinder was filled up to the mark with powder of a known mass; it was then possible to calculate the powders bulk density. The cylinder was tapped 10, 500 and 1250 times which compacted the powder by removing air from voids within the sample. The Hausner ratio (H.R.) was calculated according to Eq.2.3 and was used to determine the powder flow characteristics.

Equation 2.3: $\text{Hausner ratio (H.R.)} = \frac{V_{Bulk}\,(ml)}{V_{Tapped}\,(ml)}$

Where $V_{Bulk}\,(ml)$ was the initial bulk volume of the powder and $V_{Tapped}\,(ml)$ was the final tapped volume of the powder.

Absolute or true density was calculated using a gas pycnometer, AccuPyc II 1340, (Micromeritics, USA), with helium, 99.995% purity, supplied in the pressure range 19 – 23 psig. All samples analysed were prepared in an E-Series binder oven (Erweka GmbH., Germany) at 50 ^{o}C for 24 h prior to analysis. During the analyses,

the samples were placed in a sample cup that had a volume of 11.7180 cm^3. The instrument performed 10 cycles with 10 purges each throughout the analysis.

2.6.4 Contact angle

Contact angle measurements were performed using a PG-X Measuring Head under dynamic mode (Fibro System AB, Sweden). Solid discs of the powder were prepared by placing the powder inside a punch and dye apparatus (Specac Ltd., UK) that was subsequently compacted in a press (Specac Ltd., UK) for 5 min under 10 ton compression. Afterward, the solid disc was placed under the PG-X Measuring Head with a drop of water deposited onto the surface of the solid disc. The PG-X measured the contact angle made by this drop of water on the solid surface over 60 s.

2.6.5 Surface area and pore size analysis

Surface area and pore size analyses by N_2 absorption were carried out using a Gemini VI Surface Area and Pore Size Analyser, (Micromeritics, USA) with nitrogen gas utilised as the adsorbate. The operating pressure of the analysis gas was maintained in the range 15 to 18 psig (pounds per square inch gauge). All samples analysed were degassed for 24 h at 50 ^oC in a FlowPrep 060 sample degas system, (Micromeritics USA) prior to analyses. During analysis, liquid nitrogen was used to maintain isothermal conditions (-196 ^oC).The specific surface area was calculated according to the Brunauer-Emmett-Teller (BET) mathematical equation (Brunauer et al., 1938). The pore volume, pore area and pore width were calculated using the Barrett-Joyner-Halenda (BJH) equation (Barrett et al., 1951). All samples were analysed in duplicate. Using the amount of drug present in the sample as calculated in TGA studies, it was possible to predict the specific surface area (S.S.A.) and pore

volume (P.V.) of the processed fenofibrate-silica samples. Eq.2.4 was the equation used to predict the S.S.A:

Equation 2.4: $\text{Predicted S.S.A.} = (S.S.A._{SBA\text{–}15} * F_{SBA\text{–}15}) + (S.S.A._{Drug} * F_{Drug})$

Where F is the fraction of drug and silica in the samples, and S.S.A. is the specific surface area (m^2/g) of each.

Calculation of the predicted P.V. was according to Eq.2.5:

Equation 2.5: $\text{Predicted P.V.} = (P.V_{SBA\text{–}15} * F_{SBA\text{–}15})$

Where F is the fraction of silica in the samples, and P.V. is the SBA-15 pore volume area (cm^3/g).

These equations were based on the assumption that there was no physical or chemical interaction between silica and fenofibrate. The percentage difference between the theoretical and measured pore volumes (% ΔPV) was calculated according to Eq.2.6:

Equation 2.6: $\%\,\Delta PV = ((\text{Predicted P.V.} - \text{measured P.V.})/\ \text{Predicted P.V}) * 100\%$

The % ΔPV expression was used to determine the location of drug within the silica matrix.

2.6.6 Thermogravimetric analysis

Thermogravimetric analysis (TGA) was carried out using a TGA 500, (TA Instruments Ltd., UK). Samples in the range 2 to 10 mg were loaded on tared platinum pans and heated from ambient temperature to 900 ^{o}C at a heating rate of 10 ^{o}C/ min. Nitrogen was used to maintain an inert atmosphere. TGA was used to quantify the presence of moisture in the mesoporous silica, fenofibrate and processed fenofibrate-silica samples. TGA was also used to determine the presence and amount of drug in the processed fenofibrate-silica samples. The amount of moisture present in the samples was calculated from the weight loss between ambient and 100 ^{o}C, while the amount of drug present in the fenofibrate-silica samples was calculated from the weight loss between 100 to 900 ^{o}C, corrected for the weight loss from SBA-15 over the same temperature range, this method has previously been reported (Ambrogi et al., 2008, Hillerström et al., 2009, Li-hong et al., 2013, Van Speybroeck et al., 2009). TGA analysis was conducted using Universal Analysis 2000 software, (TA Instruments Ltd., UK). All samples were analysed in triplicate to determine intra-batch variation.

The % drug load (w/w) was calculated from Eq.2.7:

Equation 2.7: $$\%\,\text{drug load (w/w)} = \left(\frac{M_{Drug}}{(M_{Drug} + M_{SBA\text{–}15}}\right)$$

Where M_{Drug} is the mass of drug (mg) and $M_{SBA\text{-}15}$ was the mass of SBA-15 (mg)

The drug-loading efficiency was calculated according to Eq.2.8:

$$\text{Equation 2.8: Drug-loading efficiency } (\%) = \left(\frac{\%\ \text{actual drug load}_{TGA}\ (\text{w/w})}{\%\ \text{drug load (w/w)}}\right) * 100\%$$

Where the % actual drug load represents the % drug w/w present in the drug – silica sample determined by TGA analysis and the % drug load was the theoretical % in the sample, as calculated from Eq.2.7. Each prepared was analysed in triplicate in TGA to account for intra-batch variation.

2.6.7 Differential scanning calorimetry

Differential scanning calorimetry (DSC) was carried out using a DSC Q1000, (TA Instruments Ltd., UK). DSC was used to measure the glass transition temperature (T_g), melting point (T_m) and enthalpy of melting of fenofibrate and drug-silica samples. Enthalpy of fusion was used to quantify drug crystallinity in the processed fenofibrate-silica samples. Modulated DSC was employed because this mode measures both thermodynamic and kinetic events by superimposing a sinusoidal temperature modulation onto the heat flow (Verdonck et al., 1999). Samples in the range, 3 to 5 mg were prepared in Tzero aluminium pans (TA Instruments Ltd., UK) and weighed on a MX5 microbalance (Mettler Toledo International Inc., USA). The samples were heated from -40 to 120 ^{o}C at a heating rate of 3 ^{o}C/min. Modulation was set at ± 1 ^{o}C/min, while an inert atmosphere was maintained using nitrogen. A refrigerant cooling system (RCS 40), (TA Instruments Ltd., UK) was used to cool samples below ambient temperature. DSC analysis was conducted using Universal Analysis 2000 software, (TA Instruments Ltd., UK). All samples were analysed in triplicate to determine intra-batch variation.

2.6.8 Powder x-ray diffraction

Powder x-ray diffraction (pXRD) was performed at ambient temperature using a Stadi MP diffractometer, (Stoe GmbH., Germany) operating in transmission mode with a linear position-sensitive detector, an anode current of 40 mA, an accelerating voltage of 40 kV and Cu Kα1 X-radiation (λ = 1.5406 Å) typically over a scan range of 3.5 to 60 ° 2θ, scanning in steps of 2 ° for 90 s per step. Samples were held between acetate foils.

2.6.9 Fourier transform infrared spectroscopy

Fourier transform infrared spectroscopy (FT-IR) was used to determine possible chemical interactions or chemical bonding between the fenofibrate and mesoporous silica in the processed fenofibrate-silica samples. This was performed using a Spectrum One FT-IR Spectrometer, (Perkin Elmer Inc., USA). During FT-IR analysis, radiation was passed through a sample where some of it was absorbed and some transmitted; thus generating a molecular "fingerprint". Samples were prepared by grinding in excess potassium bromide (KBr) under infrared light and making solid discs using a punch and dye apparatus (Specac Ltd., UK), that was then placed in a press (10 ton for 5 min) (Specac Ltd., UK). Samples were run over the spectrum range of 450 to 4000 cm^{-1} with a resolution of 4 cm^{-1}. Each sample was scanned 32 times during a run to complete the final spectrum.

2.6.10 Surface tension

The surface tensions of all media employed in this thesis were determined experimentally through application of the KRUSS processor tensiometer K12

(KRUSS GmbH, Germany). The surface tension was measured using a platinum Wilhelmy plate. The plate was washed with deionised water, then ethanol and flamed over a Bunsen burner after each measurement. All measurements were performed at 37 ^{o}C which was maintained with the HAAKE water bath (Thermo Fisher Scientific Inc., USA). Full independent replicates were performed in triplicate.

2.6.11 Solubility studies

Solubility studies were carried out by dissolving excess fenofibrate in each particular media (n=3). The samples were placed in screw capped 50 ml tube plastic tubes, (Sarstedt AG., Germany) sealed with plastic tape and incubated in a shaker water bath (speed 200 rpm) at a temperature of 37 ^{o}C. Samples were withdrawn in triplicate from each tube after 24 and 48 h. Unknown drug concentration was calculated reversed-phase HPLC (See section 2.6.13). In chapters 3, 4 and 5, the solubility of fenofibrate was determined in 0.3% w/v SDS in 0.1M HCl solution. In chapter 6, it was additionally determined in 0.3% w/v SDS in deionised water, 1.5% w/v SDS in deionised water and 1.5% w/v SDS in 0.1M HCl solution.

2.6.12 *In vitro* release testing

The dissolution rate of the unprocessed fenofibrate and release rates of the processed fenofibrate-silica samples were investigated using a 900 ml volume of 0.3% w/v SDS in 0.1M HCl solution at a temperature of 37 ^{o}C in chapters 3, 4 and 5. In chapter 6, fenofibrate *in vitro* release was also evaluated in media composed of 0.3% w/v SDS in deionised water, 1.5% w/v SDS in deionised water and 1.5% w/v SDS in 0.1M HCl solution, all at 37 ^{o}C. The dissolution apparatus used was the USP Type 2

apparatus with paddle speed of 100 rpm. The sink amount of fenofibrate for each dissolution or release experiment was one quarter of the unprocessed fenofibrate solubility in the particular media. In drug – silica samples, the quantity of sample required to ensure sink conditions was normalised based on the mass fraction of fenofibrate in each particular sample. The weighing boats containing the processed fenofibrate – silica samples were fully submerged in the dissolution medium at the start of the study. Samples were withdrawn at defined time points and replaced with fresh media which ensured a constant volume in the dissolution baths. All samples were filtered through a 0.2 µm syringe filter, (Sarstedt AG., Germany) prior to HPLC analysis.

Dissolution and release profiles are presented in this thesis with % dissolution/release on the y-axis and time on the x-axis. The y-axis error bars represent the standard deviation (SD) associated with % dissolution/release at each time point. This standard deviation included both the intra-and-interbatch variation (N = 9).

In chapter 6 during release experiments for the 'standard sample' (1 mg to 3 m^2), the undissolved powder in the release media was recovered after either 15 min or 24 h. The release media was vacuum filtered through 0.45 µm Whatman filter paper. The filtrate was discarded and the solid residue on the filter paper recovered and oven dried at 40 ^oC for 3 days. The residue termed the recovered powder was analysed for drug content and surface and mesopore properties. The % recovery of fenofibrate from the drug – silica release experiment was calculated by Eq.2.9:

Equation 2.9: $$\text{Drug recovery}\ (\%) = \left(\frac{\%\ \text{recovered drug amount}_{\text{TGA}}\ (\text{w/w})}{\%\ \text{actual drug load}_{\text{TGA}}\ (\text{w/w})}\right) * 100\%$$

Where the % recovered drug amount (w/w) was the % of drug in the recovered solid residue calculated by TGA and the % actual drug load was the % drug load in the sample after preparation.

2.6.13 Reversed phase, high performance liquid chromatography

Reversed phase, high performance liquid chromatography (RP-HPLC) analysis was performed using an Agilent 1200 series HPLC system with a UV/VIS detector (Agilent Technologies, USA). A reversed-phase column Kinetex C-18 column (150 mm x 4 mm) with internal pore width 2.6 µm (Phenomenex Ltd., United Kingdom), a mobile phase of acetronitrile and water (70:30) at a flow rate of 1 $ml.min^{-1}$ and an injection volume of 5 µl were employed. The wavelength for fenofibrate detection was set at 286 nm. The retention time for fenofibrate was 4.5 min.

2.6.14 Stability studies

Stability studies were carried according to the ICH (Q1A, R2) guidelines for accelerated storage of pharmaceutical preparations (FDA, 2003). All samples were placed inside 50 ml capped plastic containers (Sarstedt AG, Germany) and stored at 40 ^{o}C and 75% RH in an Erweka (Erweka GmbH., Germany) controlled temperature-humidity oven for various periods of time, e.g. 1 month up to a maximum of 12 months.

2.7 Statistics

2.7.1 Statistical analysis

The data was tested for normality through the Anderson-Darling equation and the equality of variances were analysed with Levene's Equation. When investigating 2 different datasets, either the parametric 2 sample t-test or the non-parametric Mann-Whitney test was employed. When analysing 3 or more datasets with only variable, either the parametric one-way ANOVA or non-parametric Kruskall-Wallis test was carried out. Two-way ANOVA was used to compare 2 independent factors and any interaction between these factors. A p value less 0.05 would indicate that the datasets were significantly different. The Minitab 16 statistical package (Minitab Inc., USA) was the software used to conduct the statistical analysis.

2.7.2 Comparison of dissolution and release profiles

Dissolution and release profiles were also compared by the difference (f_1) and similarity tests (f_2) (Moore and Flanner, 1996). A modified difference factor (f_1^1) was also utilised (Costa and Sousa-Lobo, 2001). The difference and modified difference factors measure the percent error between 2 dissolution or release profiles over all time points. A value of < 15 suggests that the profiles are not different to each other (Costa and Sousa-Lobo, 2001). The difference factor was given by Eq.2.10:

Equation 2.10: The $f_1$equation was: $$f_t = \frac{\sum_{j=1}^{n} |R_j - T_j|}{\sum_{j=1}^{n} R_j} \times 100$$

The Costa modified difference factor was given by Eq.2.11:

Equation 2.11: The modified f_1 was: $$f_1 = \frac{\sum_{j=1}^{n} |R_j - T_j|}{\sum_{j=1}^{n} (R_j + T_j)/2} \times 100$$

The similarity factor measures the logarithmic transformation of the sum-squared error of differences between 2 dissolution or release profiles over all time points. Above a value of 50, the profiles would be considered similar. The equations are reproduced below from the work of Costa and Sousa-Lobo (Costa and Sousa-Lobo, 2001). The similarity factor was given by Eq.2.12:

Equation 2.12: The similarity was $$f_2 = 50 \times \log \left\{ [1 + (1/n) \sum_{j=1}^{n} |R_j - T_j|^2]^{-0.5} \times 100 \right\}$$

Where n is the number of samples (time points), R_j is the percent dissolved of the reference product and T_j is the percent dissolved of the test product.

Concurrently, repeated measures ANOVA was also employed to compare drug dissolution/release over multiple timepoints. The theory behind repeated measures ANOVA can be studied in greater detail in these references (Dunn and Clark, 1987, Jones, 2002).

3 Physicochemical characterisation of SBA-15 and fenofibrate

3.1 Introduction

In this thesis, a range of analytical techniques were employed to study drug – silica systems. It was necessary to thoroughly investigate the properties of fenofibrate and SBA-15 prior to processing in order to understand the subsequent properties of the drug – silica systems.

It has been reported that silica particle size and shape can influence drug physicochemical properties post processing. Chen and co-workers reported that as the silica particle size decreased, the drug release rate increased (Chen et al., 2012). Previously Qu and co-workers reported that spherical particles which had a smaller particle size achieved a faster drug release rate than rod-shaped particles with larger particle sizes (Qu et al., 2006). Therefore, it is important to characterise the silica particle morphology and size with a view to understanding their subsequent effect on drug physicochemical properties, namely drug release rate, post loading.

Bulk density differences between powders can represent potential processing challenges such as achieving blend uniformity when physically mixing powders (Fan et al., 1990, Williams, 1976). Bulk and tapped densities and volumes are also important in terms of understanding powder flowability indicated by the Hausner Ratio (Hausner, 1967) and powder compressibility as defined by Carr's Index (Carr, 1965).

As mentioned previously in section 1.4, the mesoporous silica surface area and pore properties have important ramifications for drug-loading, solid state and release

(Sanganwar and Gupta, 2008, Vallet-Regi et al., 2001). For example, knowledge of the silica surface area and mesopore volume will determine the amount of drug that can be theoretically loaded onto the silica surface (Chen et al., 2012, Heikkila et al., 2007). Therefore, it was important to fully investigate the surface area and porosity properties of SBA-15; also such knowledge of the unprocessed SBA-15 surface area and mesopore volume could be used to deduce the distribution of the drug post processing.

TGA has been applied as a tool to quantify the drug-load on mesoporous silicas (Hillerström et al., 2009, Van Speybroeck et al., 2009). The TGA profiles of fenofibrate and SBA-15 were evaluated with a view to confirming that TGA could be applied in this work for drug-load quantification. Also, TGA facilitated measurement of the moisture content of both SBA-15 and fenofibrate (0 – 100 ^{o}C), which would provide information on their hydrophilicity and hydrophobicity. This information was important because it would shed light on what to expect when the SBA-15 was stored under accelerated storage conditions and how fenofibrate would behave *in vitro.*

The solid state structure of both SBA-15 and fenofibrate was probed with DSC and pXRD. It has been reported that crystalline drugs loaded onto mesoporous silicas can transition to an amorphous (Shen et al., 2010) or non-crystalline form (Mellaerts et al., 2008a). Therefore, it was necessary to understand the solid state characteristics of fenofibrate prior to processing with SBA-15. Thermal events such as glass transition (Tg), melting point (Tm) and recrystallization can be investigated by DSC while pXRD provided a solid state "fingerprint" of crystalline fenofibrate starting material. Therefore, it was necessary to understand the solid state characteristics of fenofibrate prior to processing with SBA-15, in addition to determining if processing led to

changes in the powders. Through the use of FT-IR the presence of hydrogen bonding between the powders as indicated by shifts of existing bonds in the FT-IR spectrum could be probed

Loading poorly water – soluble drug onto mesoporous silicas has been widely reported to increase the dissolution rate and oral bioavailability of drugs such as carbamazepine, (Ambrogi et al., 2008), ibuprofen, (Vallet-Regi et al., 2001) and itraconazole, (Mellaerts et al., 2008b). Therefore before processing fenofibrate with SBA-15 it was important to study unprocessed fenofibrate solubility and dissolution behaviour in a range of dissolution media to determine if processing the drug with SBA-15 had a positive effect on the rate and extent of fenofibrate dissolution.

3.2 Results: Fenofibrate

3.2.1 Particle morphology and size distribution

The SEM image of unprocessed fenofibrate showed crystalline particles with a range of shapes and sizes (Fig.3.1). It can be observed that many of the fenofibrate particles were irregularly shaped and others spherical.

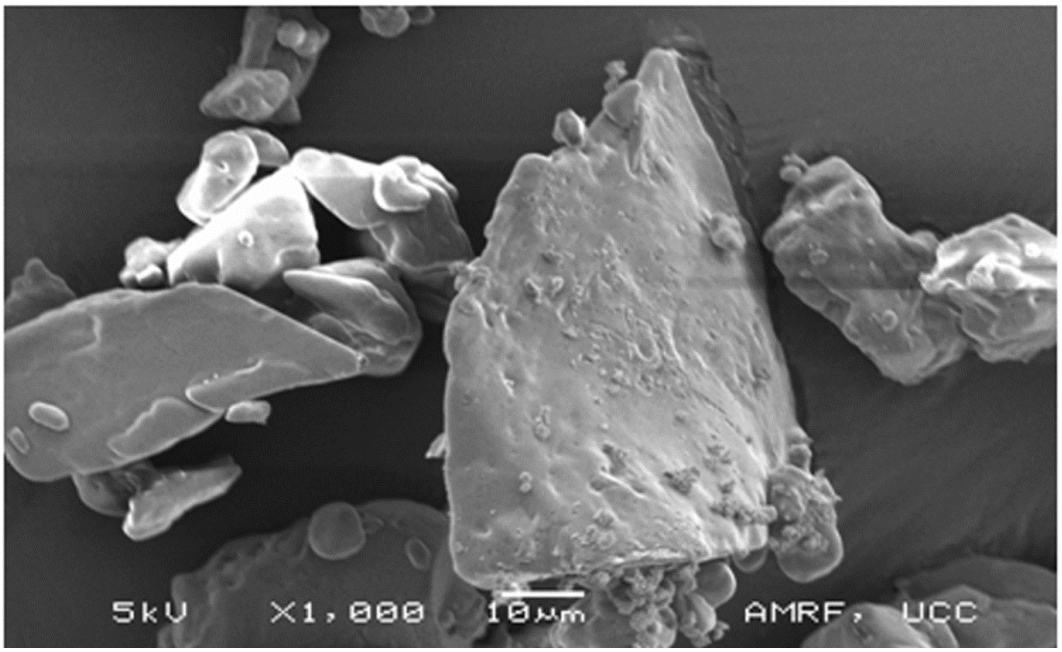

Figure 3.1: SEM image of unprocessed fenofibrate, with magnification X1000.

Sieve analysis showed the majority of the particles were greater than 180 µm (Fig.3.2).

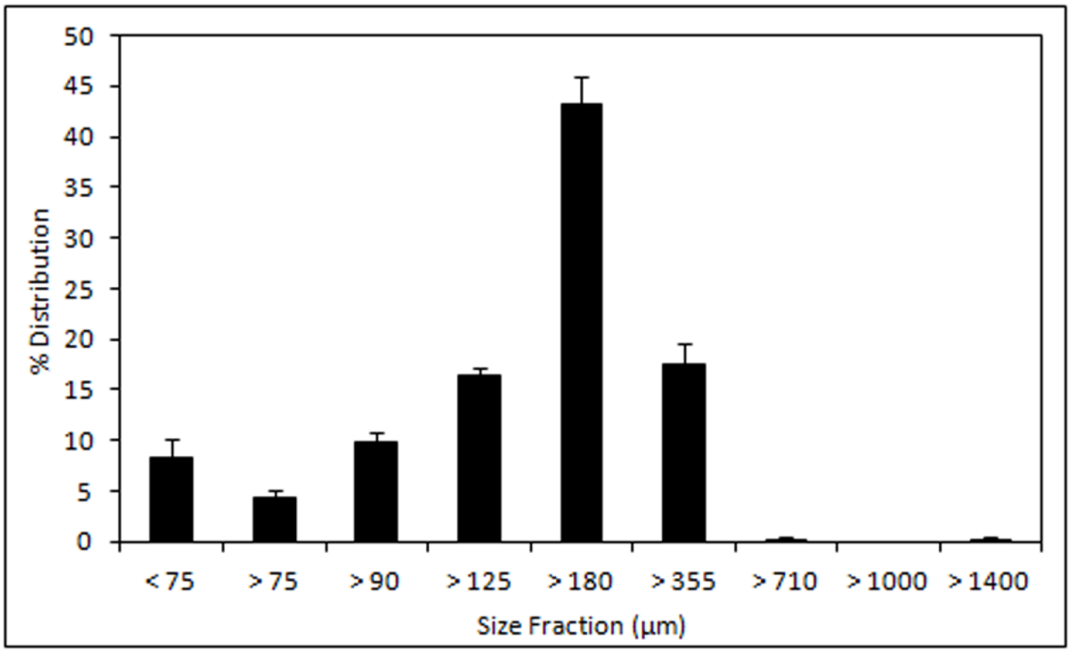

Figure 3.2: Particle size distribution of unprocessed fenofibrate determined using sieve analysis, size distribution standard deviations indicated by y-axis error bars (n = 3).

3.2.2 Derived surface properties: density, surface area and porosity

The bulk density, Hausner ratio, Carr's index and specific surface area of fenofibrate are displayed in Table 3.1 below.

Table 3.1: Bulk density, Hausner ratio, Carr's index and surface area of unprocessed fenofibrate, standard deviation in brackets (n = 3).

Property	Bulk Density	Hausner Ratio	Carr's Index	Surface area
Result	0.64 g/cm^3 (±0.01)	1.13	11.33	0.12 m^2/g (±0.02)

The Carr's Index was 11.33 which was well below the cut-off value of 25. Above a value of 25, the powder would be considered to have poor flowability (Carr, 1965). The Hausner ratio was 1.13 which was below the cut-off point of 1.25, above which indicated poor flowability (Hausner, 1967).

The surface area of fenofibrate was low; therefore, dispersing or loading fenofibrate onto a high surface area, hydrophilic material like mesoporous silica offered the potential to enhance fenofibrate's dissolution by increasing its effective surface area in contact with the dissolution medium (Bruner, 1904, Nernst, 1904).

3.2.3 Thermogravimetric properties

The thermogravimetric profile of unprocessed fenofibrate is shown in Fig.3.3. Fenofibrate possessed very little surface bound water, approximately 0.04% (±0.02), as indicated by the weight loss between ambient and 100 ^{o}C, an indication of both its low surface area and extreme hydrophobicity. Fenofibrate started to decompose at approximately 121.16 ^{o}C ($\pm$ 23.11) and was fully decomposed at approximately 302.82 ^{o}C ($\pm$ 22.84), (Fig.3.3).

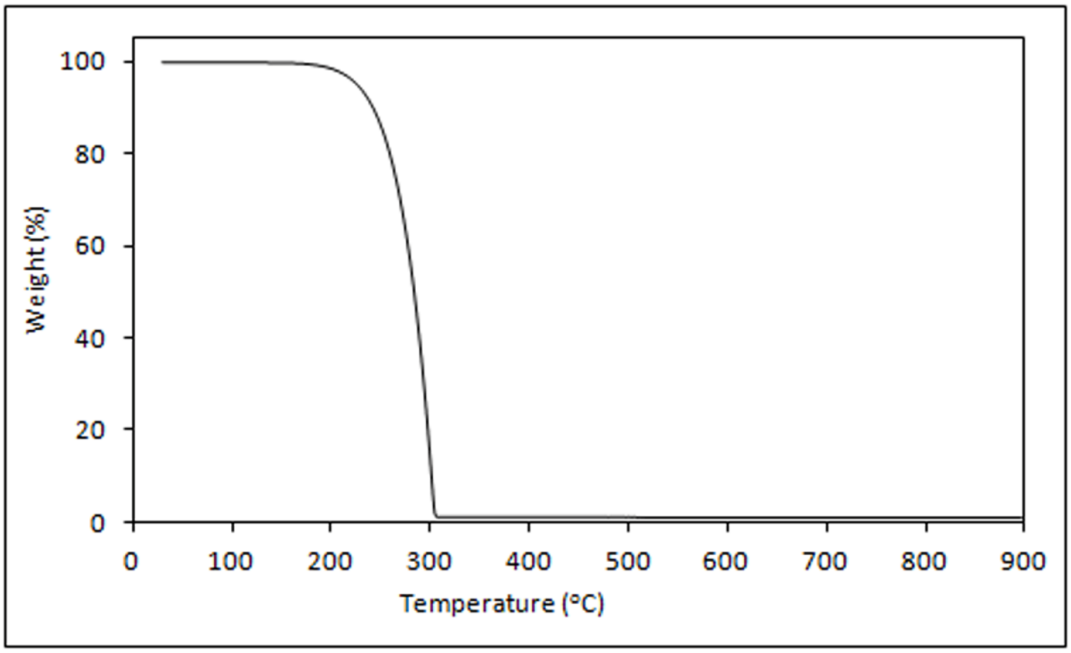

Figure 3.3: TGA profile of unprocessed fenofibrate determined over the temperature range ambient to 900 ^{o}C.

3.2.4 X-ray diffraction analysis

Fenofibrate is a crystalline powder. Its powder X-ray diffractogram shows strong peaks at 14, 16 – 17 and 22 – 23 2 theta, (Fig.3.4).

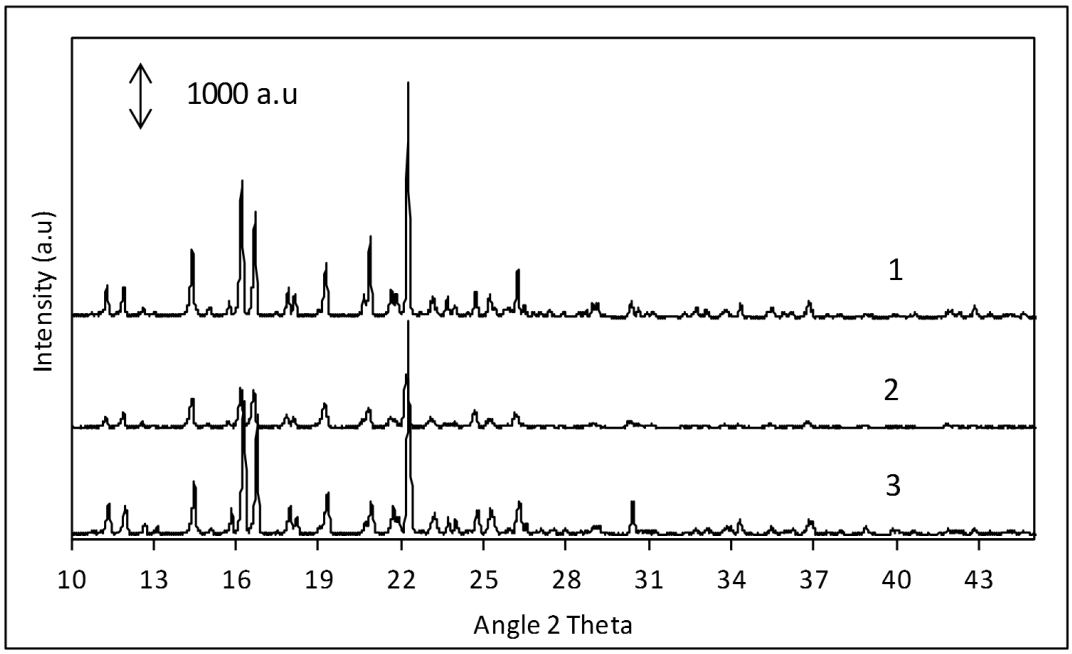

Figure 3.4: pXRD of (1) unprocessed fenofibrate, (2) SC-CO_2 processed fenofibrate and (3) unprocessed fenofibrate post 12 month storage.

These peaks were previously reported for crystalline fenofibrate (Karmarkar et al., 2009). Fenofibrate retained its crystallinity after SC-CO_2 processing and after 12 months storage under 40 ^{o}C and 75% RH which is indicative of its stability in the crystalline form.

3.2.5 Differential Scanning Calorimetry

Thermal analysis of fenofibrate using DSC yielded information about its solid state nature. Fenofibrate's melting endotherm was measured in the DSC thermogram at 80 ^{o}C which corresponded well to literature value (Heinz et al., 2009, Zhou et al., 2002). No glass transition temperature was observed in samples of unprocessed, SC-CO_2 processed or those stored for 12 months under accelerated conditions. Completely amorphous fenofibrate has a reported T_g of -20 ^{o}C and a ΔC_p of 0.72 J/g. ^{o}C (Zhou et al., 2002). In this work, amorphous fenofibrate was prepared by melting the drug

inside a DSC Tzero aluminium pan followed by rapid quench-cooling in liquid nitrogen and immediate DSC analysis. The drug was observed to re-crystallise if left exposed on the bench. It can be seen from the results in Table 3.2, that quench-cooling did not result in completely 100% amorphous fenofibrate.

Table 3.2: Reported and experimentally determined thermal properties of fenofibrate, determined by DSC, standard deviations in brackets (n = 9).

Sample	T_g (°C)	ΔC_p (J/g.°C) at T_g	T_{cr} (°C)	ΔH_{cr} (J/g)	T_m (°C)	ΔH_m (J/g)
Reported values	-20[#]	0.72[#]	30 – 40[#]*	N/R	79 – 81[#]*	91.0[#+]
Unprocessed	N/P	N/P	N/P	N/P	78.87 (±0.81)	90.18 (±3.95)
Processed	N/P	N/P	N/P	N/P	77.00 (±0.28)	94.32 (±1.49)
12 month stored (40 °C, 75% RH)	N/P	N/P	N/P	N/P	78.34 (±0.76)	96.76 (±4.17)
Quench-cool fenofibrate	-22.11 (±0.37)	0.44 (±0.06)	40.62 (±7.39)	64.87 (±8.92)	77.79 (±0.35)	87.16 (±5.43)

Note: N/R not reported, N/P not present

[#] (Zhou et al., 2002)

* (Heinz et al., 2009)

[+] (Srinarong et al., 2009)

The re-crystallisation enthalpy (ΔH_{cr}) was 64.87 (J/g) (±8.92), while the melting enthalpy was 87.17 (J/g) (±5.43). The percentage crystallinity (X_{cr}) is related to the enthalpy of re-crystallisation and enthalpy of melting (Wang et al., 2006). Based on this approach, the percentage of amorphous drug post quench-cooling was about 74%. The DSC thermogram of unprocessed fenofibrate (Fig.3.5) and quench-cooled fenofibrate (Fig3.6) can be seen below.

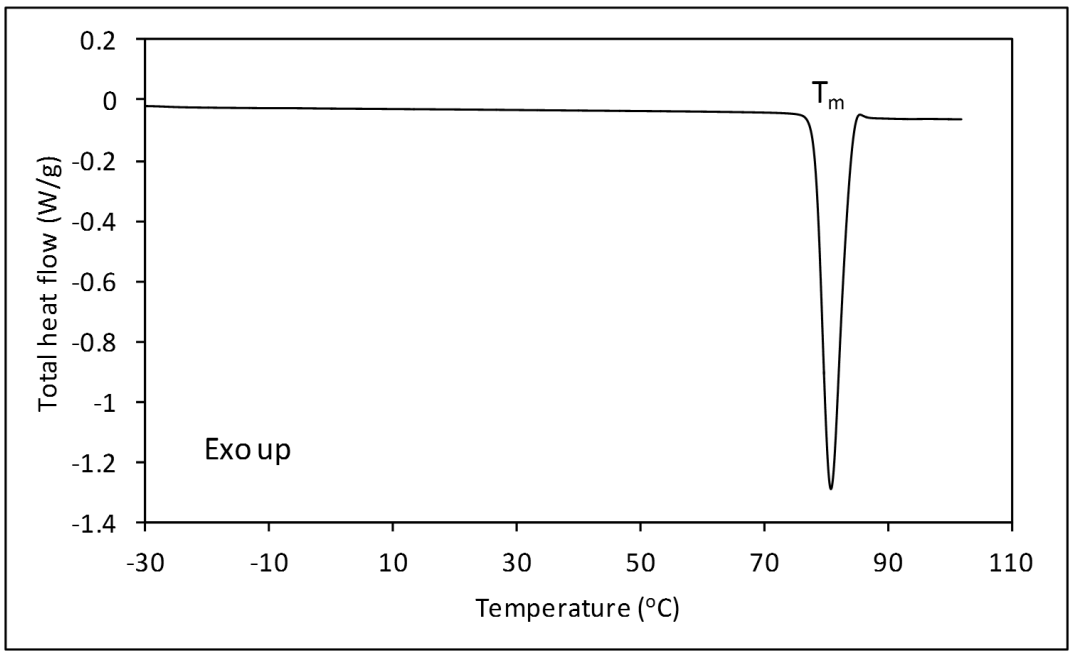

Figure 3.5: DSC thermogram of unprocessed fenofibrate indicating T_m at 80 ^oC.

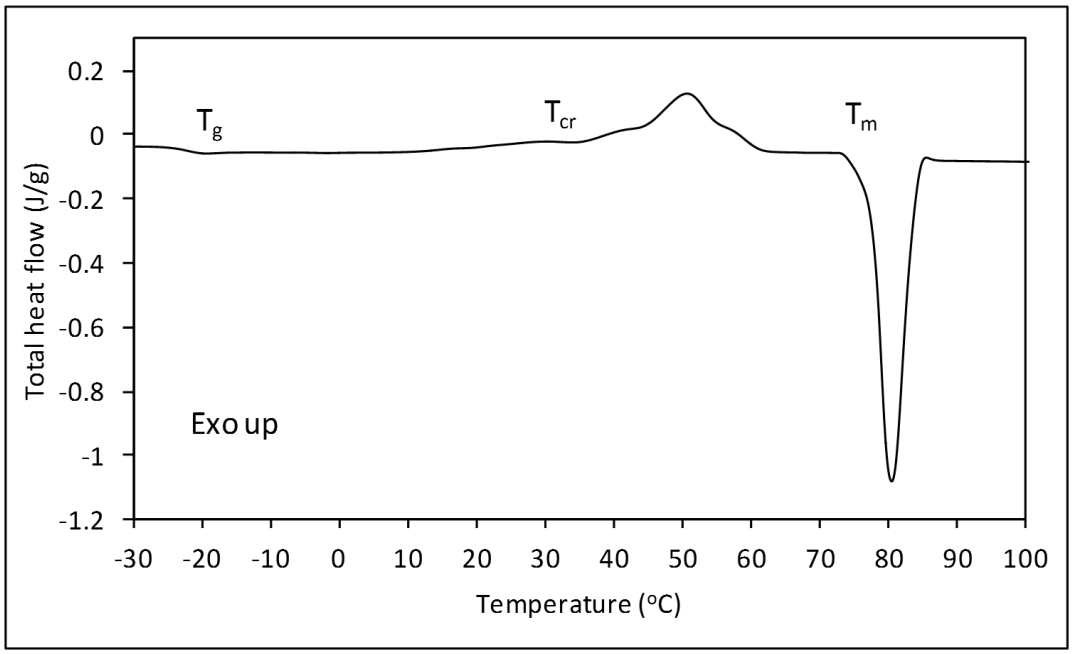

Figure 3.6: DSC thermogram of quench-cooled fenofibrate indicating T_g at -20 ^oC, T_{cr} at approximately 40 ^oC and the T_m a 80 ^oC.

3.2.6 FT-IR spectroscopy

The fenofibrate molecule $C_{20}H_{21}ClO_4$; contains C-H, C-O, C=O, C-CH_3, C-Cl, C-C and C=C bonds (Heinz et al., 2009). The FT-IR spectrum of unprocessed fenofibrate shows a sharp peak at wavenumber 2984 cm^{-1} which was proposed to be alkane stretching. Alkane (C-H) stretching and bending is reported between wavenumbers 2750 – 3300 cm^{-1} (Heinz et al., 2009, Pavia et al., 1979). The sharp peaks at wavenumbers 1651 and 1729 cm^{-1} were assigned to carbonyl (C=O) stretching, as previously reported in the literature (Heinz et al., 2009, Pavia et al., 1979). C-Cl bonds are reported to occur near wavenumber 650 cm^{-1}; there was a sharp peak at 656 cm^{-1} observed in the experimental fenofibrate spectrum which was categorized as the C-Cl bond. The FT-IR spectrum of fenofibrate is displayed below (Fig.3.7).

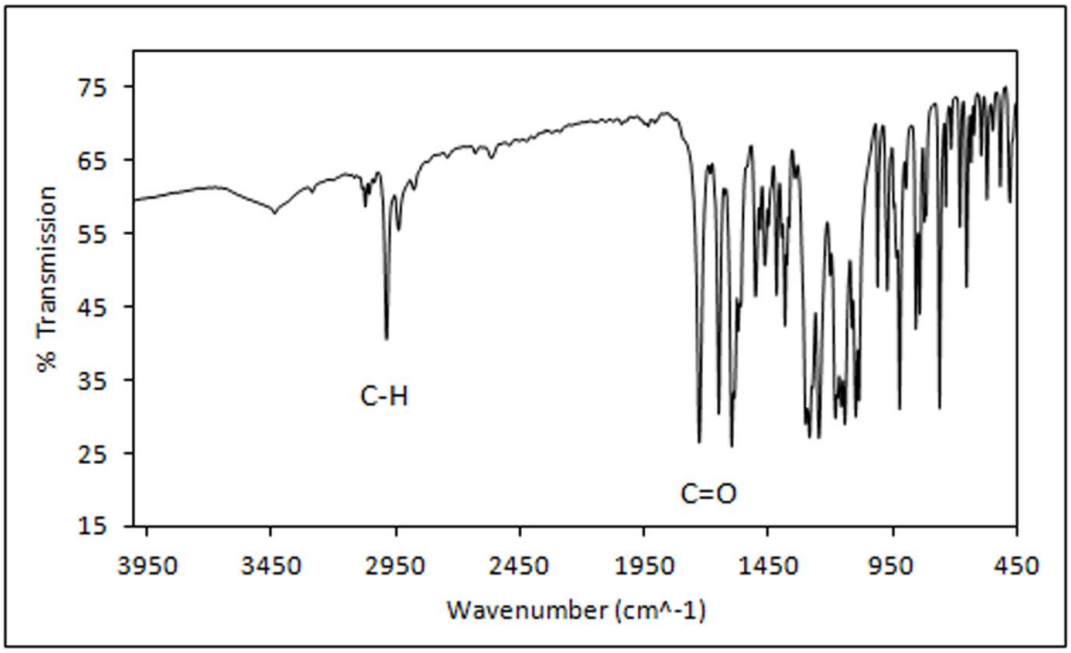

Figure 3.7: FT-IR spectrum of unprocessed fenofibrate.

3.2.7 Fenofibrate solubility in 0.3% w/v SDS in 0.1M HCl solution

The solubility of unprocessed fenofibrate in 0.3% w/v SDS in 0.1M HCl solution was investigated at 37 ^{o}C for 48 h and was found to be 67.21 µg/ml (±4.81).

3.2.8 *In vitro* dissolution studies

Unprocessed fenofibrate displayed a slow rate and low extent of dissolution, achieving 24.25% (±1.14) dissolution after 2 h. This was unaffected by 12 months under accelerated storage conditions. Processing fenofibrate in SC-CO_2 lowered the percentage extent of fenofibrate's dissolution to 6.54% (±1.46) after 2 h. It was observed that when the fenofibrate was recovered from the SC-CO_2 cell, it had visibly larger particles. The *in vitro* release profiles of fenofibrate under sink conditions are shown below (Fig.3.8).

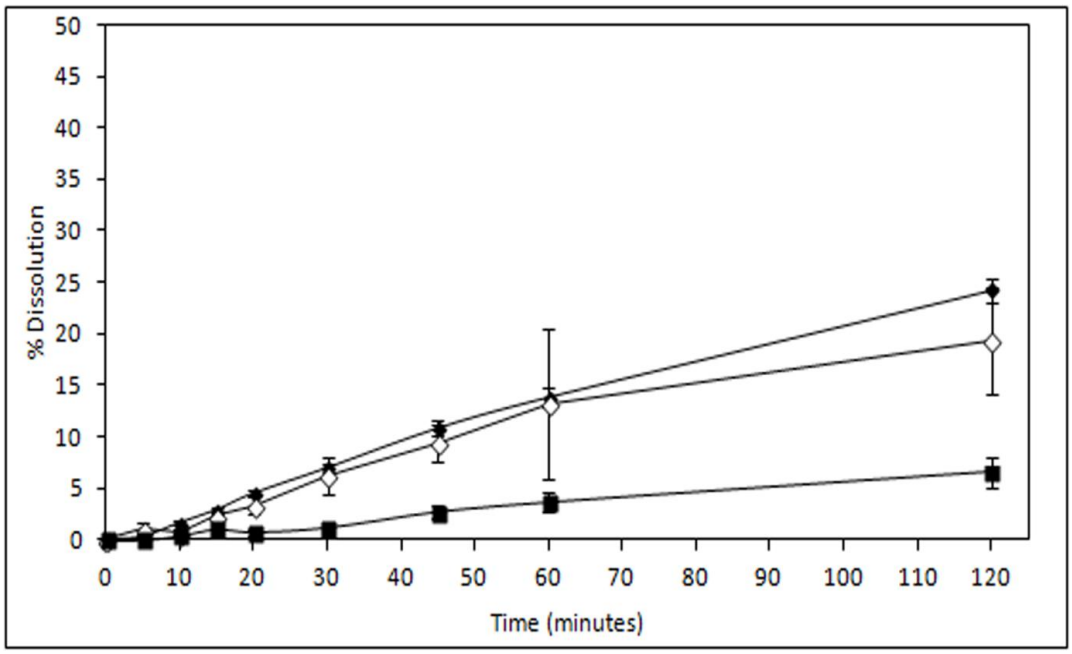

Figure 3.8: Dissolution profiles of fenofibrate (mean ± SD, n = 3), (♦) unprocessed, (■) SC-CO_2 processed and (◊) stored for 12 months under accelerated storage conditions in 0.3% (w/v) SDS in 0.1M HCl media.

3.3 Results: Mesoporous silica

3.3.1 Particle morphology and size distribution

The SEM image shows the SBA-15 submicron particles are present as agglomerates (Fig.3.9). The SEM images appear to show individual particles as small as 4 µm.

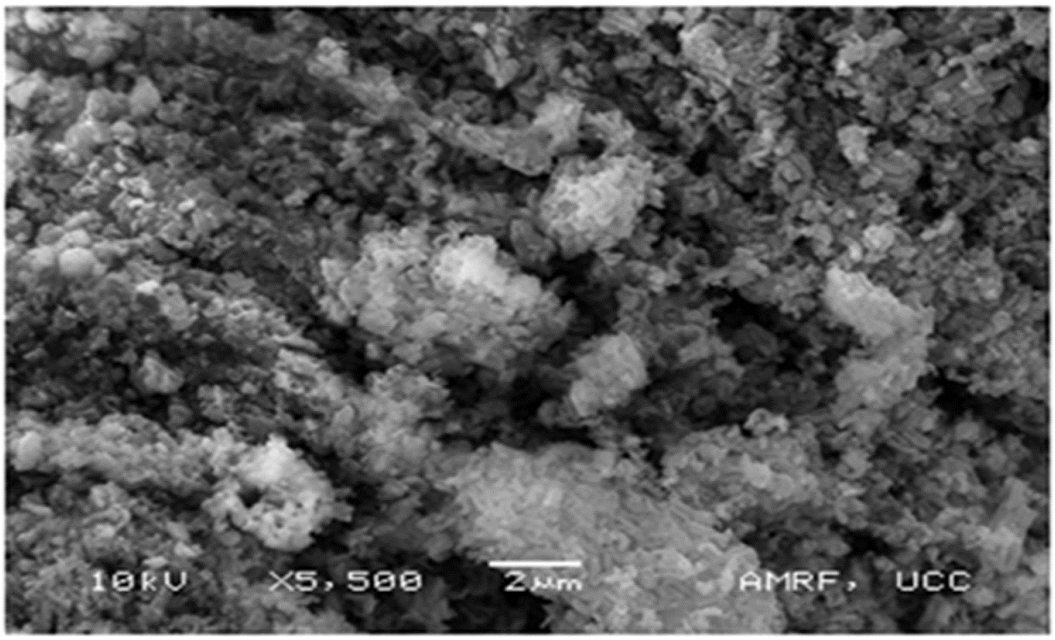

Figure 3.9: SEM image of unprocessed SBA-15, at magnification X5500.

Sieve analysis was employed to determine the particle size distribution of unprocessed SBA-15 and SBA-15 after SCF processing (Fig.3.10).

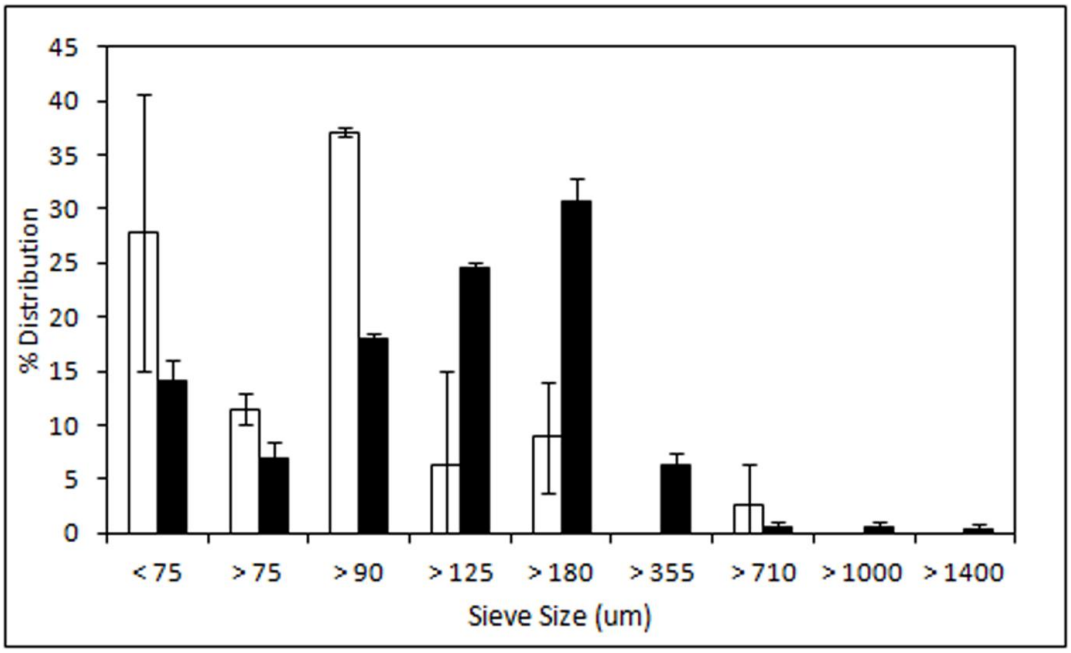

Figure 3.10: Size distribution of (□) unprocessed and (■) processed SBA-15 (MS-6), standard deviation indicated by y-axis error bars (n = 3).

The size distribution recorded for unprocessed SBA-15 indicated that the silica particles were agglomerated together. SC-CO_2 processing of SBA-15 appeared to shift the size distribution, toward smaller sizes. This may be the result of agitation by the magnetic stirrer or the exposure of SC-CO_2 or a combination of both effects during processing resulting in the breaking up of silica agglomerates.

3.3.2 Bulk/true density

The bulk density, Hausner ratio and Carr's index of unprocessed SBA-15 powder are detailed in Table 3.3. Powders with a Hausner ratio less than 1.25 and Carr's index less than 15 are considered to have good flowability characteristics (Carr, 1965, Hausner, 1967), based on these values SBA-15 has poor flowability characteristics.

Table 3.3: Bulk density, Hausner ratio and Carr's index of unprocessed SBA-15, standard deviation in brackets (n = 3).

Property	Bulk Density	Hausner Ratio	Carr's Index
Result	0.09 g/cm^3 (±0.01)	1.33	25

The true density of mesoporous silica was 2.31 g/cm^3 (±0.14).

3.3.3 Surface area and pore properties

The surface area and pore properties of a number of batches of SBA-15 investigated in this study were determined and are detailed in Table 3.4. Major differences existed between batches MS-2 to MS-5B compared to MS-6 and 7. This was the result of variability in the manufacturing process when different equipment was employed.

Table 3.4: Surface area and pore properties of unprocessed SBA-15, standard deviations in brackets (n = 6).

SBA-15 Batch	Surface area (m^2/g)	Mesopore volume (cm^3/g)	Mesopore size (Å)
MS-2	600.47 (±37.02)	0.57 (±0.03)	50.60 (±0.77)
MS-3	496.31 (±4.34)	0.55 (±0.01)	52.57 (±0.06)
MS-5A	637.61 (±42.38)	0.63 (±0.04)	52.16 (±0.01)
MS-5B	666.94 (±17.34)	0.64 (±0.02)	51.85 (±0.05)
MS-6	833.22 (±48.13)	0.68 (±0.02)	50.70 (±0.20)
MS-7	818.97 (±42.28)	0.80 (±0.04)	55.65 (±1.68)

Processing the SBA-15 in SC-CO_2 did not affect the surface are, pore volume and pore size, however after 12 months storage under accelerated conditions (75% RH, 40 ^{o}C), there were significant reductions in the measured surface area and pore volume as shown in Table 3.5. This was caused by the pickup of moisture by the SBA-15.

Table 3.5: Comparison of surface area and pore properties of unprocessed MS-2, SC-CO_2 processed and SBA-15 after 12 months storage under accelerated storage conditions, standard deviations in brackets (n = 3).

SBA-15	Surface area (m^2/g)	Mesopore volume (cm^3/g)	Mesopore size (Å)
Unprocessed	600.47 (±37.02)	0.57 (±0.03)	50.60 (±0.77)
SC-CO_2 processed	590.77 (±6.51)	0.58 (±0.01)	51.27 (±0.24)
12 month storage	324.94 (±30.18)	0.48 (±0.05)	57.97 (±0.06)

The decrease in surface area can be observed clearly in the BET isotherms (Fig.3.11) and pore size distributions (Fig.3.12). The smaller mesopores were closed after 12 months under accelerated storage conditions; this was indicated by the shift of the pore size distribution to the right.

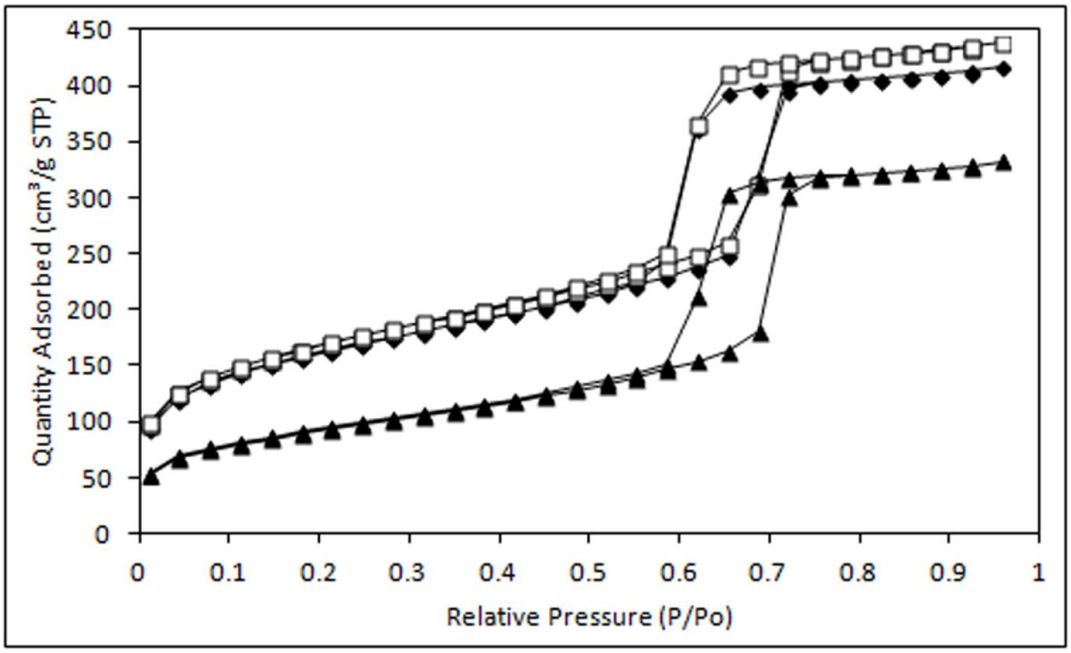

Figure 3.11: BET isotherms of SBA-15 (MS-2) (♦) unprocessed, (□) processed and (▲) processed after 12 months under accelerated storage conditions.

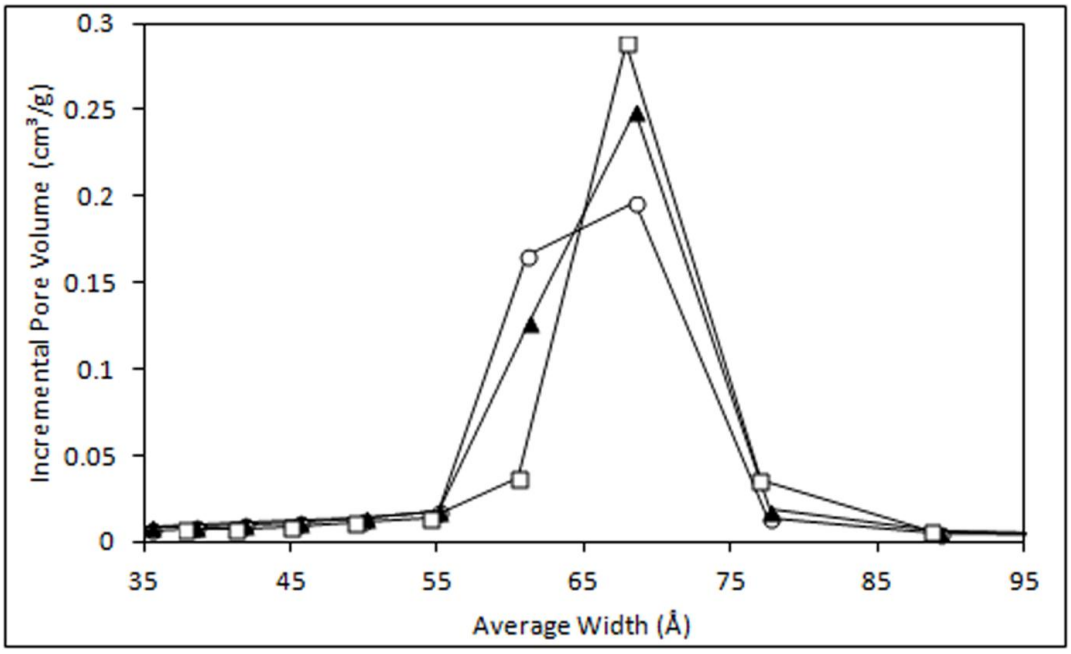

Figure 3.12: Pore size distributions of SBA-15 (○) unprocessed, (▲) processed and (□) processed after 12 months under accelerated storage.

It should be noted that sample degassing prior to analysis was carried out at 50 ^{o}C for 24 h. This degassing regime appears to be insufficient to remove all of the physically bound or molecularly bound/chemisorbed water. Degassing at higher temperatures was considered however as fenofibrate melted at 80 ^{o}C, it would not be possible to degas above 50 ^{o}C in a drug – SBA-15 sample.

3.3.4 Thermogravimetric properties

The TGA profiles of unprocessed, processed and processed SBA-15 post 12 months under accelerated storage are show below (Fig.3.13).

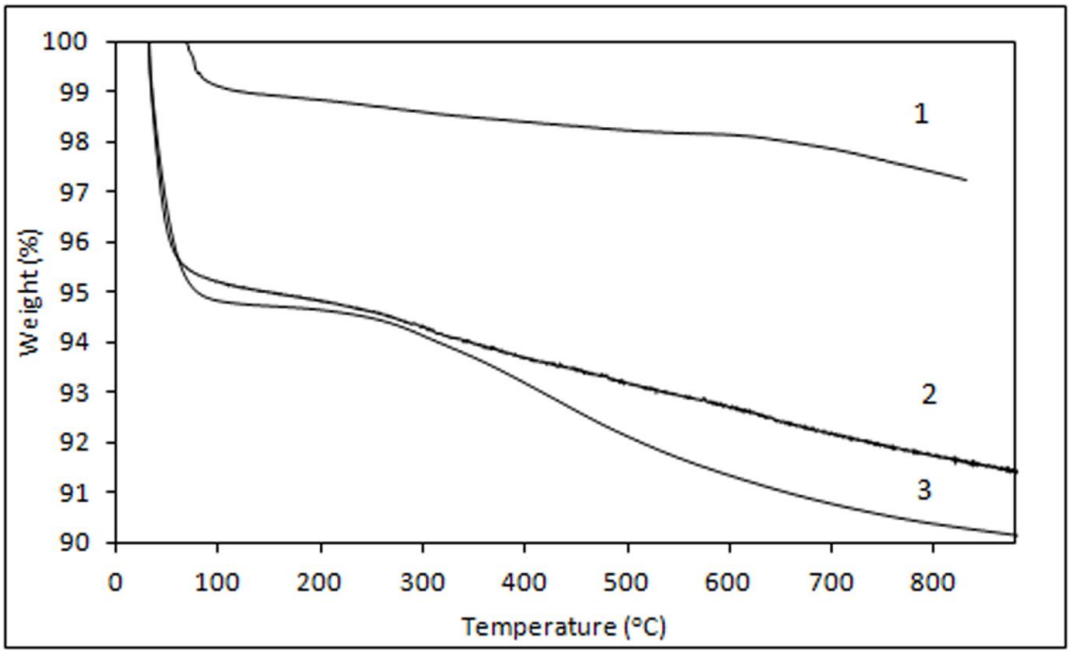

Figure 3.13: TGA profiles of SBA-15 (MS-2), (1) unprocessed, (2) processed and (3) processed, post 12 months under accelerated storage conditions.

SBA-15 does not decompose when heated from 0 – 900 ^{o}C; however there was some weight loss. Coutinho and co-workers employed TGA in the analysis of uncalcined SBA-15; they reported that over 30 – 100 ^{o}C, physically bound moisture evaporated

from the SBA-15, the surfactant template (Pluronic P123) was removed from SBA-15 between 100 – 450 ^{o}C, while over the range 450 – 600 ^{o}C residual decomposition of the template and condensation of water from silanol occurred (Coutinho et al., 2007). As all the mesoporous silicas used in this thesis had been calcined at 550 ^{o}C, i.e. the template had already been removed; any weight loss from 100 – 550 ^{o}C could not be the result of template removal. The weight loss of a number of different mesoporous silica samples is shown below in Table 3.6.

Table 3.6: Comparison of surface moisture and silanol decomposition of SBA-15 unprocessed, SC-CO_2 processed and processed, after 12 months storage under accelerated storage conditions (MS-2), standard deviation in brackets (n = 9).

SBA-15	% Weight Loss, 0 – 100 ^{o}C	% Weight Loss, 100 – 900 ^{o}C
Unprocessed	1.26 (±1.73)	2.24 (±0.45)
SC-CO_2 processed	4.79 (±1.84)	3.85 (±0.37)
Processed, 12 month storage	5.16 (±0.21)	4.72 (±0.02)

Unprocessed MS-2 contained 1.26% (±1.73) physically bound moisture, while after 12 months storage there was 5.16% (±0.21).The SBA-15 molecular moisture content, which was measured over 100 – 900 ^{o}C, increased from 2.24% (±0.45) for unprocessed SBA-15 to 4.72% (±0.02) for processed SBA-15 post 12 months under accelerated storage conditions, which was a significant increase. The act of SC-CO_2 processing did not influence the moisture content of SBA-15; there was no significant change observed between the unprocessed to processed silicas ($p > 0.05$).

3.3.5 Powder X-ray diffraction

SBA-15 is an amorphous powder; no peaks were observed on its pXRD diffractogram, (Fig.3.14). This remained the case after SC-CO_2 processing and when subjected to 12 months storage under accelerated conditions.

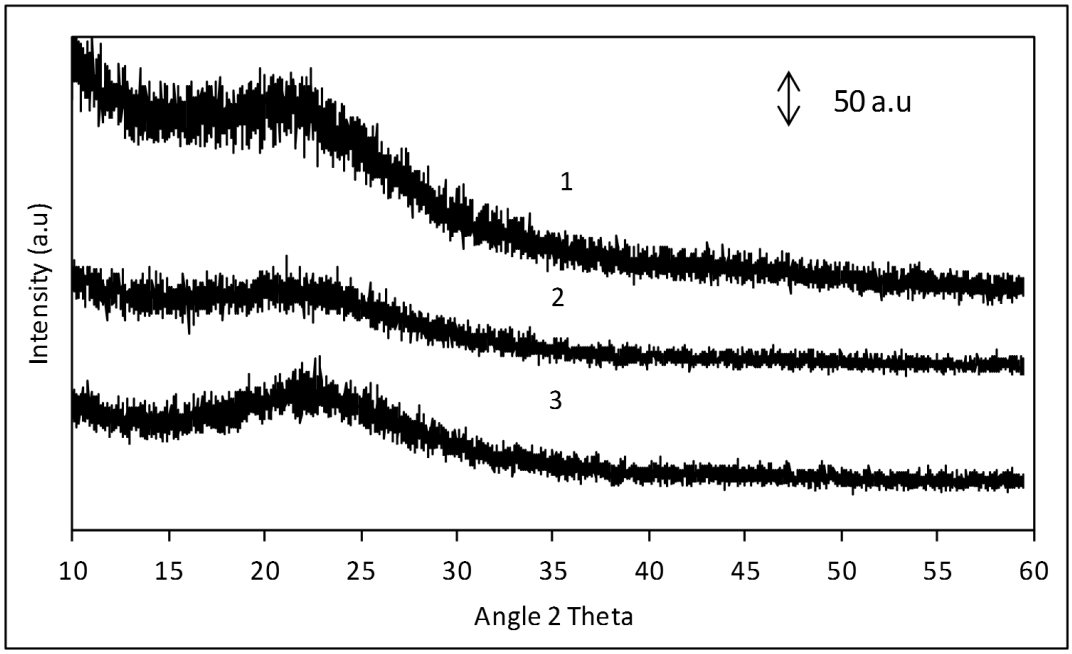

Figure 3.14: pXRD diffractograms of (1) unprocessed SBA-15, (2) after SCF processing SBA-15 and (3) post 1 month storage under accelerated conditions, (75% RH, 40 ^{o}C) using MS-2 batch.

3.3.6 Differential scanning calorimetry

The DSC thermogram of unprocessed SBA-15 (MS-2) is displayed below (Fig.3.15).

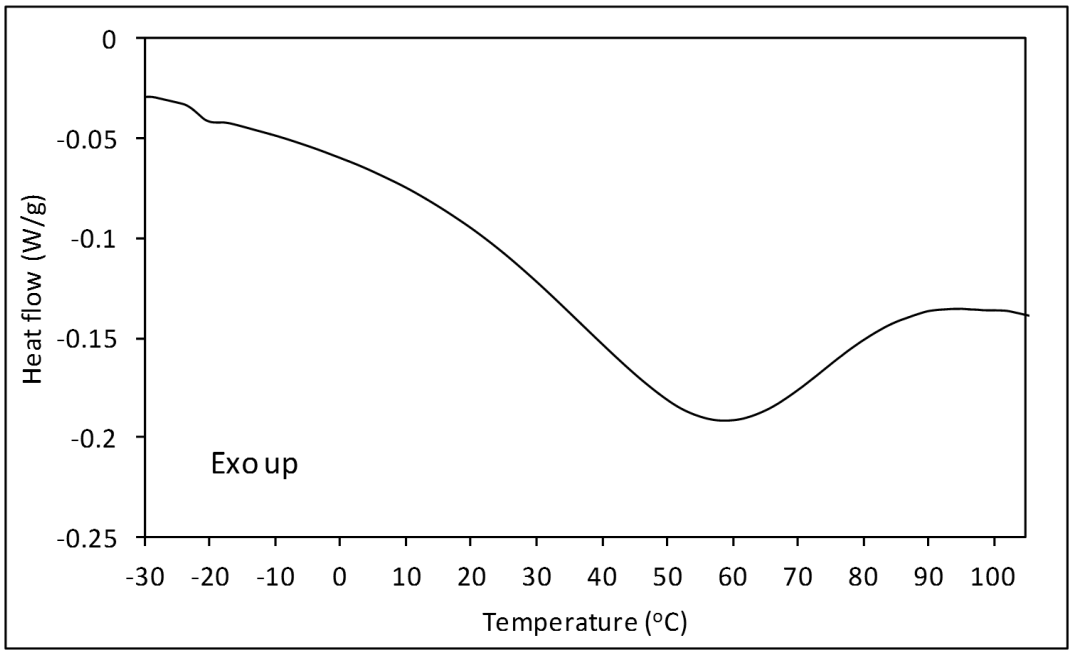

Figure 3.15: Unprocessed SBA-15 (MS-2) total heat flow DSC thermogram over the temperature range -30 – 100 ^{o}C.

The large endotherm from 0 – 100 ^{o}C is the result of evaporation of surface water from the SBA-15. This is a typical DSC thermogram for SBA-15 when studied in standard DSC mode. It is not possible to identify any thermal events from the total heat flow DSC thermogram. The reversing heat flow thermogram of unprocessed SBA-15 (MS-2) shows thermal events around -20 and 80 ^{o}C (Fig.3.16).

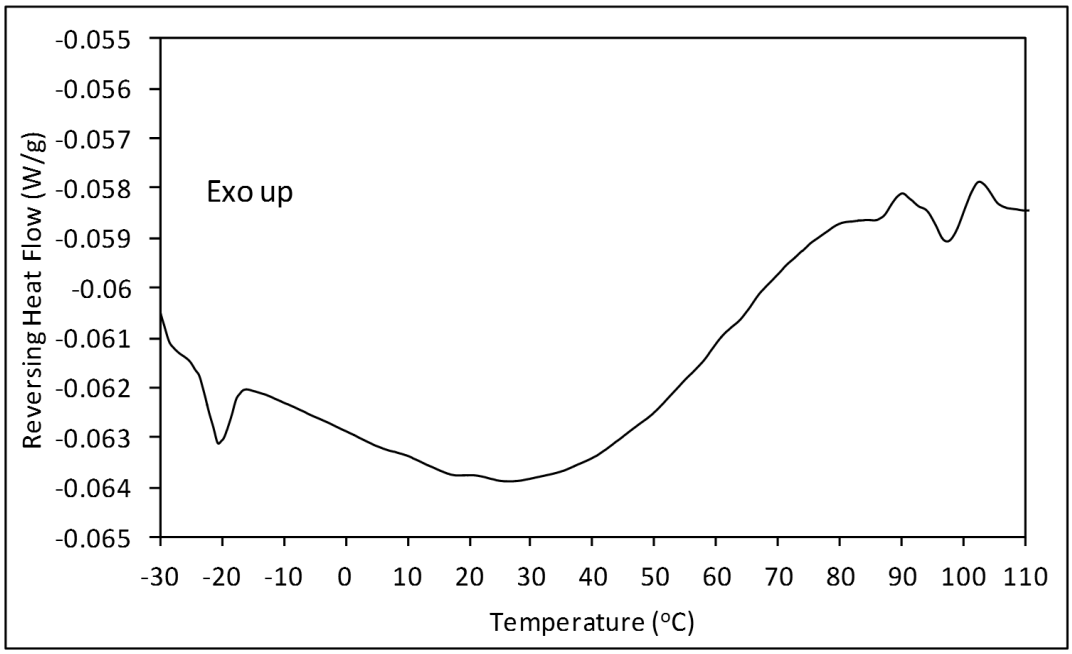

Figure 3.16: Unprocessed SBA-15 (MS-2) reversing heat flow DSC thermogram over the temperature range -30 – 100 ^{o}C.

The reversing heat flow thermograms of SC-CO2 processed SBA-15 and that stored for 12 months under accelerated storage conditions can be seen below (Fig.3.17).

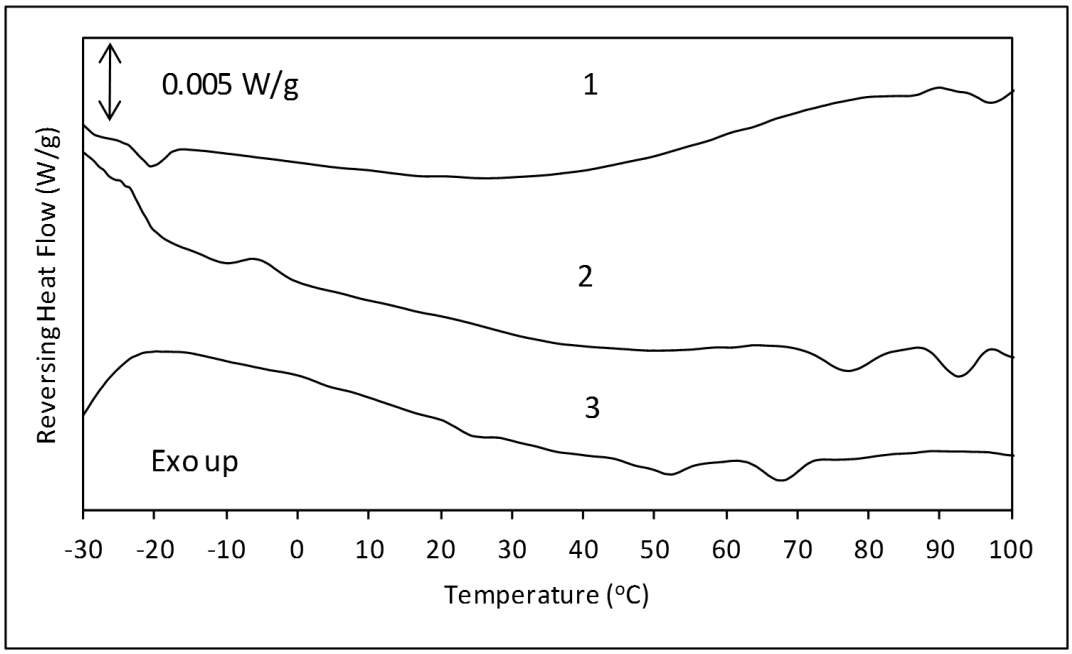

Figure 3.17: Reversing heat flow DSC thermograms of SBA-15 (MS-2) (1) unprocessed, (2) processed and (3) post 12 months storage under accelerated conditions over the temperature range -30 – 100 ^{o}C.

SC-CO_2 processing and storage for 12 months under accelerated conditions did not influence the presence of these events. It was previously reported that the events observed on the SBA-15 DSC profile from -20 to -12 ^{o}C were the melting of frozen water confined in the mesopores (Kittaka et al., 2011). The thermal events observed around 60, 80 and 90 ^{o}C on the reversing heat flow DSC thermograms of all the silicas could be the evaporation of water from the mesopores. It is reasonable to assume that if the melting point of frozen water in the mesopores is depressed, then so would the boiling point. It was previously reported by Sliwinska-Bartkowiak and co-workers that nitrobenzene in controlled pore glass (CPG) had a depressed or lowered melting temperature compared to bulk nitrobenzene (Sliwinska-Bartkowiak et al., 1999).

3.3.7 FT-IR spectroscopy

The molecular formula of SBA-15 is SiO_2. There were several distinct peaks in the FT-IR spectrum of SBA-15, (Fig.3.18).

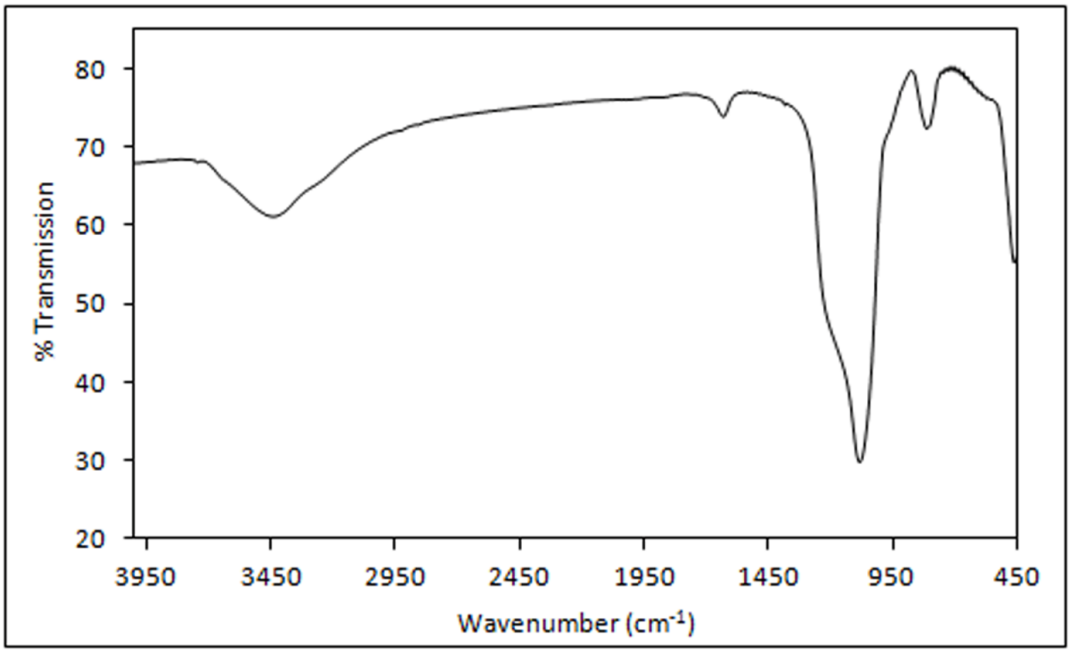

Figure 3.18: FT-IR spectrum of unprocessed SBA-15.

The presence of adsorbed water on SBA-15 was highlighted by the broad peaks present at wavenumbers 3437 and 1630 cm^{-1} (Izquierdo-Barba et al., 2010). In the case of the peak at 3437 cm^{-1}, this was the result of hydroxyl stretching (-OH) in the surface silanol groups (Si-OH) (Izquierdo-Barba et al., 2010, Pavia et al., 1979). The peak at 1630 cm^{-1} was the result of hydroxyl bending (Parida et al., 2006). The other peaks observed in the SBA-15 spectrum were caused by cross-linking of the siloxane (Si-O-Si) bonds (Das et al., 2007, Zheng et al., 2001). The largest peak on the SBA-15 spectrum occurred at wavenumber 1083 cm^{-1}, which was caused by asymmetric stretching of the siloxane bonds, while that at 814 cm^{-1} resulted from symmetric stretching of the siloxane bond. Finally, the peak at wavenumber 450 cm^{-1} was

ascribed to the stretching/rocking motion of the oxygen atom in the siloxane bond (Swann and Patwardhan, 2011).

3.4 Discussion

While the SEM image showed the SBA-15 particles to be small (< 5 μm), particle size analysis showed the silica particles to be agglomerated together, a reflection of the high surface area (Zhao et al., 1998) and surface energy (Masuda et al., 2006). Fenofibrate had a much higher bulk density than SBA-15; this meant that any type of physically processing of these powders would run a high risk of powder segregation.

The determined SBA-15 surface areas and mesopores volumes compared well with previously published data (Mellaerts et al., 2008a, Heikkila et al., 2007). It has been reported that the surface area is a crucial property in terms of how much drug can be loaded onto mesoporous silicas (Chen et al., 2012) and that the porous nature of the SBA-15 allows for the stabilisation of drug in the an amorphous (Shen et al., 2010) or molecularly dispersed form for up to 12 months under accelerated storage conditions (Mellaerts et al., 2010). SC-CO_2 processing did not alter the surface area and porosity of SBA-15; however storage for 12 months under accelerated storage conditions of 40 ^{o}C and 75% RH resulted in a significant decrease in the SBA-15 surface area and porosity. This was caused by the adsorption of moisture by SBA-15. The variations in SBA-15 specific surface area and mesopore volume observed across the batches had important implications; it was necessary to normalise these samples to allow for direct comparisons across the batches. In this work, the drug – silica ratio was based on the amount of drug to silica specific area which removed the influence of different absolute values. The reduction in SBA-15 specific surface area and mesopore volume was caused by the adsorption of moisture; TGA results showed that after storage, there was a significant increase in the amount of molecularly bound water on the SBA-15. The extreme hydrophobicity of fenofibrate was highlighted by the fact that there was practically no moisture present on its

surface; in fact fenofibrate did not pick up moisture after 12 months under accelerated storage conditions. Fenofibrate decomposed between 120 – 300 ^{o}C, while the SBA-15 remained stable apart from some moisture loss over the same temperature range. Therefore, TGA can be applied later in this thesis for the determination of the drug-load on SBA-15, as previously reported (Van Speybroeck et al., 2009).

Fenofibrate is a stable crystalline drug, unaffected by SC-CO_2 processing or long term accelerated storage. The T_g of fenofibrate occurs at -20 C (Zhou et al., 2002), which also coincides with the melting point of water frozen in the SBA-15 mesopores (Kittaka et al., 2011). This draws attention to the fact that the detection of amorphous fenofibrate loaded onto SBA-15 may be confounded when there are drug-loaded samples to be studied.

The FT-IR spectra showed the chemical bonds present in both SBA-15 and fenofibrate. Any hydrogen bonding that may occur between them after processing together can be expected to centre on the silica silanol groups and fenofibrate's carbonyl groups because these are the bonds that contain hydrogen and oxygen.

Fenofibrate dissolution rate and extent was challenged in 0.3% (w/v) SDS + 0.1M HCl; there was approximately 25% dissolution after 2 h. It was seen earlier that fenofibrate was in the crystalline form, extremely hydrophobic with a low specific surface area; processing with SBA-15 should be able to overcome these difficulties and lead to enhanced dissolution.

3.5 Summary

Fenofibrate is a highly stable, crystalline drug; it maintained its crystallinity even after SC-CO_2 processing. It was extremely hydrophobic; it did not adsorb moisture under long term accelerated storage conditions. Its dissolution rate in 0.3% w/v SDS in 0.1M HCl was very limited. Mesoporous silica was characterised as a mesoporous material, with a high surface area and mesopore pore volume, with well defined mesopore sizes. It maintained these characteristics even after SC-CO_2 processing. Mesoporous silica readily adsorbed moisture when under long term accelerated storage conditions.

4 Mesoporous silica for oral drug delivery

4.1 Introduction

It has been long established that increasing the effective surface area of a poorly water-soluble drug in contact with the dissolution medium can enhance drug dissolution (Bruner, 1904, Nernst, 1904). This can be achieved by loading drugs onto silica-based ordered mesoporous materials (OMMs) which are characterised by high surface areas, large mesopore volumes, narrow mesopore size distributions (5 – 8 nm) and ordered unidirectional mesopore networks. These properties allow for homogeneous and reproducible drug-loading and release (Manzano et al., 2009, Vallet-Regi et al., 2007, Vallet-Regi et al., 2001). Many publications have focussed on understanding the key properties of OMMs that influence drug-loading and dissolution rate enhancement. It has been reported that the surface area determines how much drug can be loaded onto OMMs and OMM particle size has an impact on drug release rate, with larger silica particles resulting in slower drug release because of the longer mesopore length (Chen et al., 2012). The mesopore volume influences the amount of drug loaded, especially if the drug is dissolved in a solvent that can carry it into the mesopores (Vallet-Regi et al., 2007). Larger mesopore sizes encourage greater drug release rates (Horcajada et al., 2004), while mesopore geometry has also been shown to affect drug-loading and release (Izquierdo-Barba et al., 2005). Stabilisation of amorphous drug for up to 12 months has been attributed to the mesopores of the OMM (Mellaerts et al., 2010, Shen et al., 2010). The silica surface can be functionalised with organic groups to encourage greater drug-loading by creating stronger bonding between the silica surface and drug (Manzano et al., 2008), and to extend drug release (Vallet-Regi et al., 2007).

Despite the body of literature evaluating the different properties of OMM affecting drug-loading and release, there seems to be a lack of clarity regarding the optimum processing method to load drug onto the OMM and the subsequent implications for drug delivery. Various loading methods have been employed including physical mixing (Ambrogi et al., 2010, Song et al., 2005, Qian and Bogner, 2011), solvent based methods that either involve the suspension of the OMM in a drug-solvent solution (Ambrogi et al., 2012, Andersson et al., 2004, Izquierdo-Barba et al., 2005, Charnay et al., 2004) or impregnation of the OMM by dropwise addition of a concentrated drug solution (Mellaerts et al., 2008a, Van-Speybroeck et al., 2008). Some researchers have mixed the drug and silica and heated the resultant mixture to below (Tozuka et al., 2005) or above the drug's melting point (Aerts et al., 2010, Mellaerts et al., 2008a, Shen et al., 2010). Alternative loading methods such as supercritical CO_2 (SC-CO_2) (Sanganwar and Gupta, 2008) have also been proposed to load drug onto OMMs. The high density of SC-CO_2 should permit a large amount of drug to be solubilised, while its high diffusivity should facilitate ready access to the mesopore network (Fages et al., 2004, Pasquali and Bettini, 2008, York, 1999). This is the first study to directly compare physical mixing, melt, solvent impregnation and CO_2 based drug-loading methods in terms of the subsequent impact on drug – OMM properties; in particular drug distribution throughout the mesoporous silica matrix, solid state properties and drug release. To our knowledge, this is also the first study to enhance drug dissolution by loading drug onto OMM using a liquid (near-critical) CO_2 loading method. The model OMM in this study was SBA-15 and fenofibrate was employed as a representative Class II drug as defined by the biopharmaceutics classification system (BCS) (Amidon et al., 1995). It is

highly lipophilic (log P = 5.3) (Wishart et al., 2008) and practically insoluble in water (< 0.8 µg/ml) (Jamzad and Fassihi, 2006).

4.2 Results

4.2.1 Drug-loading

The drug-loading efficiencies were calculated using Eq.2.8. Similar loading efficiencies of greater than 90% were determined for the impregnation, liquid and SC-CO_2 methods, Table 4.1.

Table 4.1: Comparison of drug-loading efficiency and % ΔPV before and after storage for 1 month for all processed drug – SBA-15 samples, standard deviations in brackets.

Processing Method	Loading Efficiency (%) (n = 9)	% ΔPV (n = 6)	% ΔPV, 1 month storage (n = 6)
Physical Mix	106.26 (±42.83)	1.88 (±5.41)	15.29 (±6.08)
Melt Method	103.90 (±30.22)	36.84 (±5.63)	35.09 (±3.89)
Impregnation	92.55 (±5.14)	33.12 (±2.26)	44.40 (±15.92)
Liquid CO_2	93.25 (±5.35)	32.06 (±1.66)	33.68 (±3.66)
SC-CO_2	91.98 (±6.34)	19.64 (±5.30)	21.27 (±4.16)

Large intra-batch variabilities were evident in physical mix and melt samples that may be attributed to segregation during preparation due to density differences between the mesoporous silica and fenofibrate. In the case of both the physical and melt samples, poor mixing resulted in heterogeneous distribution of drug throughout the silica substrate. The low variability in drug-loading for the impregnation, liquid and SC-CO_2 processed samples was indicative of more homogeneous drug distribution. All loading methods, with the exception of the physical mix, involved

the disruption of the drug solid particles by melting or dissolution. For the melt samples, drug distribution was reliant on the viscosity of molten drug and the degree of drug and silica mixing. The disruption of the drug particulate form that occurred in the impregnation, liquid and SC-CO_2 samples facilitated more uniform drug distribution in these samples.

4.2.2 Porosity analysis

Changes in silica porosity after drug-loading can assist in understanding how the drug is distributed throughout the silica sample. Mesoporous silica starting material had a very large mesopore volume (>0.50 cm^3/g) and displayed the type IV adsorption-desorption isotherm and H1 hysteresis loop (Fig.4.1) characteristic of mesoporous materials (Sing et al., 1985).

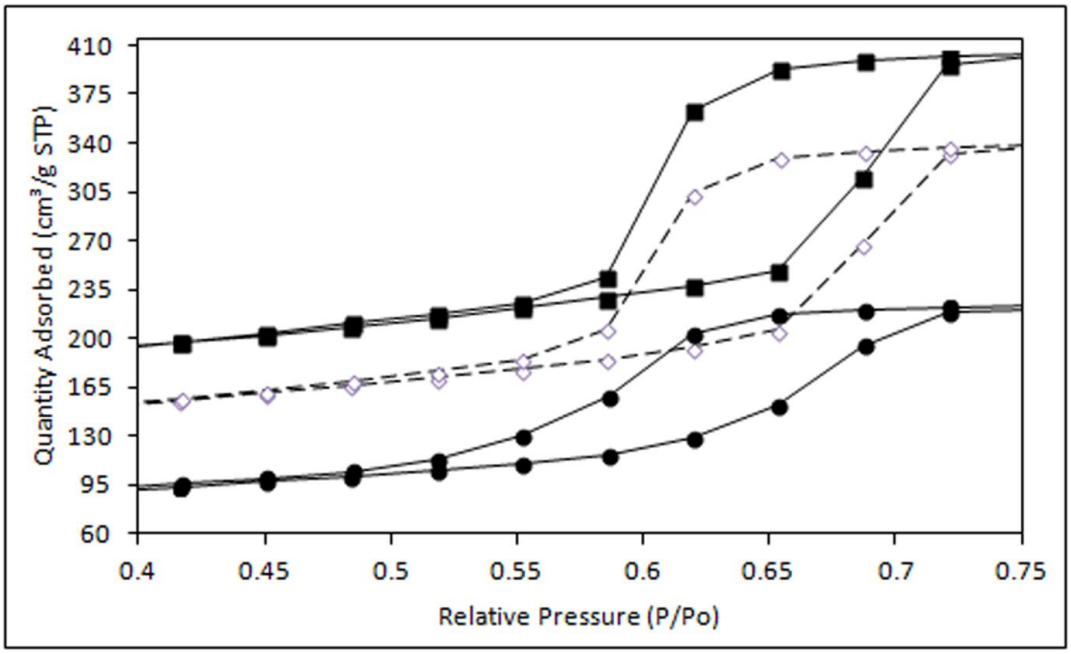

Figure 4.1: N_2 adsorption/desorption isotherms of (■) unprocessed SBA-15, (◊ with dashed line) physical mix and (●) melt method.

These characteristics were retained post drug-loading (Fig.4.2), which indicated that silica was still mesoporous.

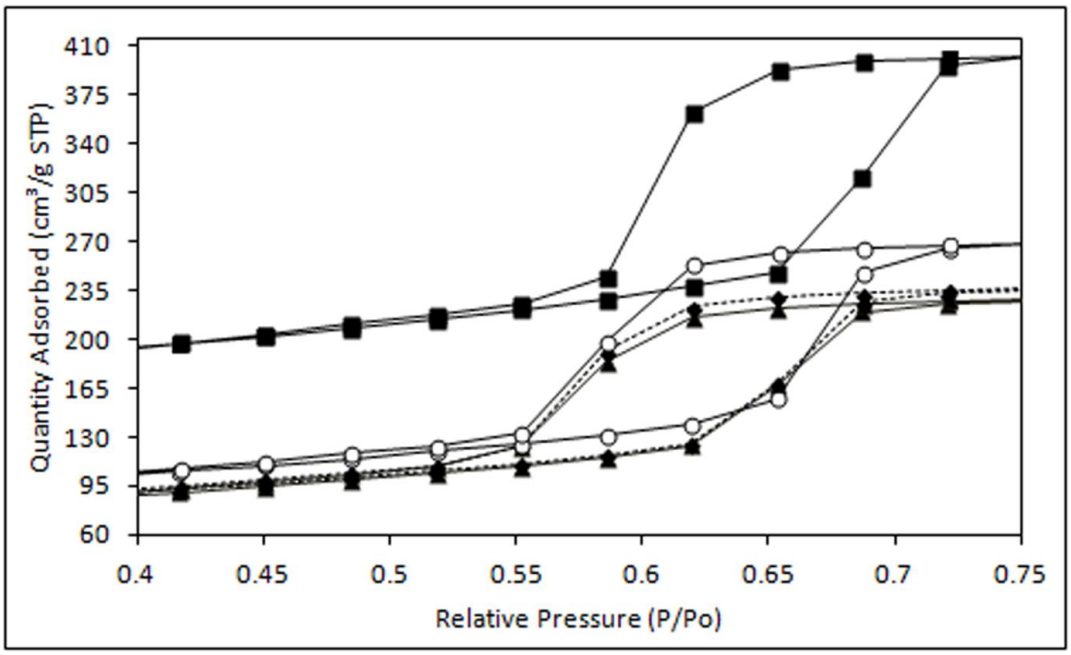

Figure 4.2: N_2 adsorption/desorption isotherms of (■) unprocessed SBA-15, (▲) impregnation, (♦ with dashed line) liquid and (○) SC-CO_2 prepared samples.

With the exception of the physical mix, all drug loaded samples showed marked reductions in the mesoporous silica pore size and volume. The closure point (P/P_o) of the hysteresis loop was reduced for all samples, with the exception of the physical mix (Fig.4.1), indicating a reduction in pore sizes (Izquierdo-Barba et al., 2005). The greatest reduction was observed for the sample prepared by the melt method.

The pore size distribution in relation to the pore volume for the various samples is shown (Fig.4.3).

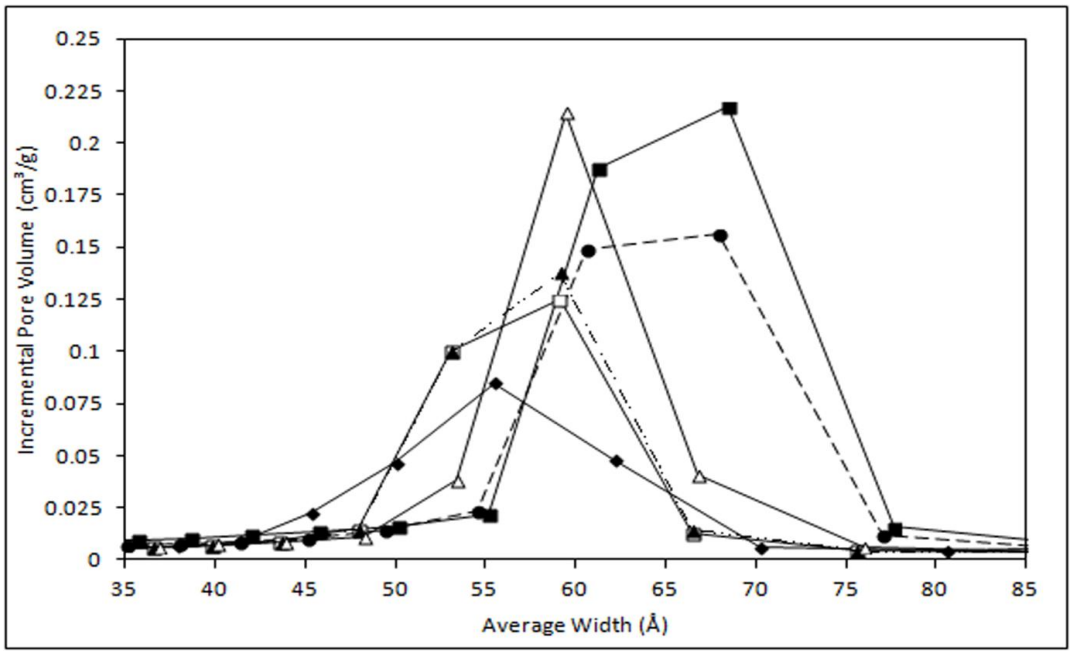

Figure 4.3: Pore size distribution of (■) unprocessed SBA-15, (● with dashed line) physical mix, (♦) melt sample, (□) Impregnation, (▲ with dashed line) liquid CO_2 and (Δ) SC-CO_2.

There appeared to be slight change in the pore size distribution for the physical mix, however this was not quantified. Both impregnation and liquid CO_2 samples show similar reductions in pore size; interestingly the SC-CO_2 sample showed a lower reduction in pore size compared to these samples. The melt sample showed the greatest spread of pore sizes. The % ΔPV values calculated from Eq.2.6 were used to quantitatively compare the reduction in mesopore volumes of the processed samples compared to the theoretical mesopore volume (Table 4.1). The % ΔPV of the physical mix was negligible showing that the presence of the drug had little effect on the silica mesopore volume in these samples. Statistical analysis showed that all the other samples had a significantly greater % ΔPV compared to the physical mix indicating that processing by these methods resulted in a reduction in the silica mesopore volume due to drug deposition into the silica mesopores and blocking of

the mesopores. Despite having similar loading efficiencies, impregnation and liquid CO_2 samples had a significantly higher % ΔPV values compared to the SC-CO_2 samples.

4.2.3 SEM-EDX

Qualitative analysis of the drug, SBA-15 and drug/SBA-15 samples conducted using SEM showed that SBA-15 was composed of agglomerated sub-micron particles and fenofibrate was composed of distinct crystalline particles (Fig.4.4).

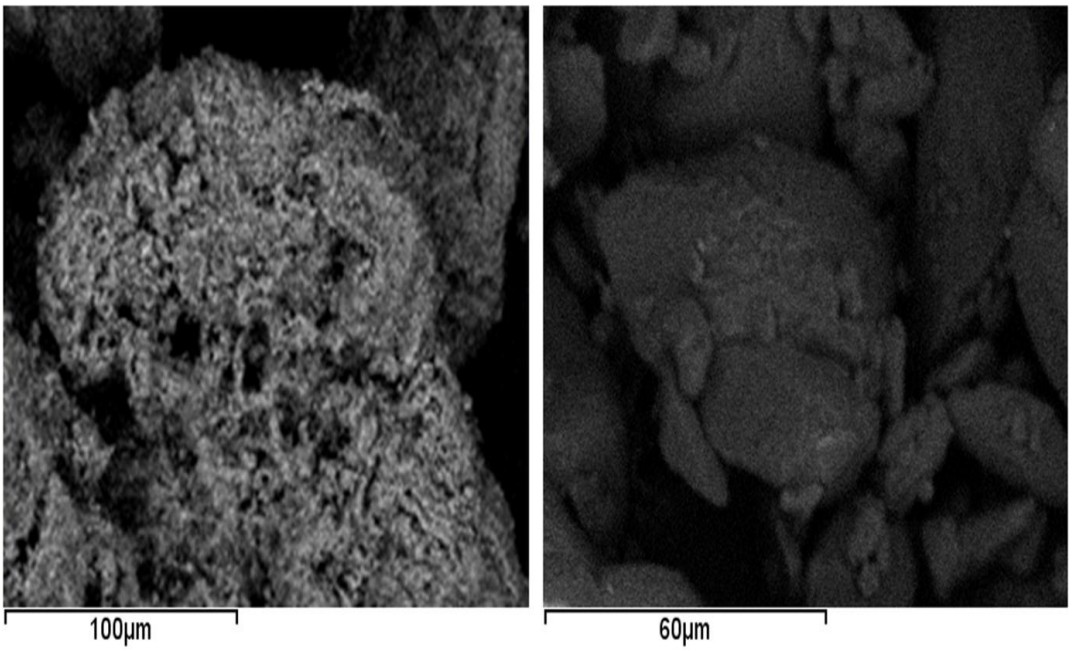

Figure 4.4: SEM images of (left) unprocessed SBA-15 and (right) unprocessed fenofibrate.

EDX analysis was used to probe the distribution of fenofibrate and SBA-15 in these samples. SBA-15 was probed via its silicon (Si) atom and fenofibrate via its chlorine (Cl) atom. The EDX images shown are the Cl atom distribution of the powder under the SEM. Fenofibrate particles were observed in the SEM image of the physical mix

but not in the melt sample. The Cl atom distribution was observed to be more intense in the EDX image of the physical mix but less so in that of the melt sample, (Fig.4.5).

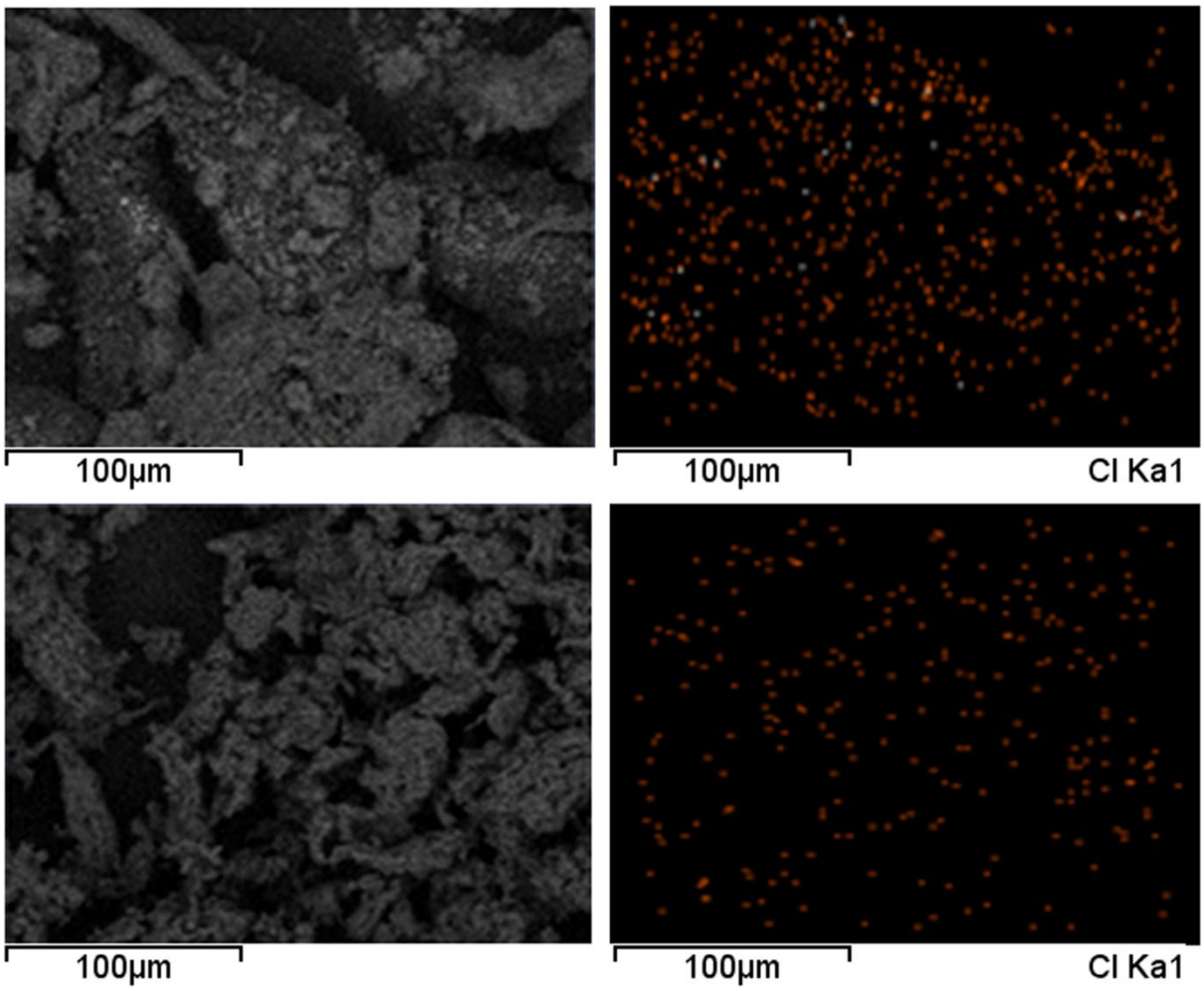

Figure 4.5: SEM/EDX images of (top) physical mix and (bottom) melt sample; the SEM images are on the left while the EDX images are on the right.

The SEM images highlighted that fenofibrate is present as distinct particles in the physical mix whereas in the melt sample the drug was dispersed through the SBA-15 material and there was no evidence of distinct drug particles. This was also the case for the impregnation, liquid and SC-CO_2 samples (Data not shown).

4.2.4 Solid state analysis

Powder XRD and DSC analysis of samples was undertaken to determine whether the loading methods resulted in differences in fenofibrate solid state behaviour. The pXRD diffractogram of the fenofibrate crystalline starting material was in accordance with that previously reported (Heinz et al., 2009). The pXRD diffractograms of drug – silica samples, with the exception of the physical mix, showed no peaks indicating that the drug in these samples was in a non-crystalline state (Fig.4.6).

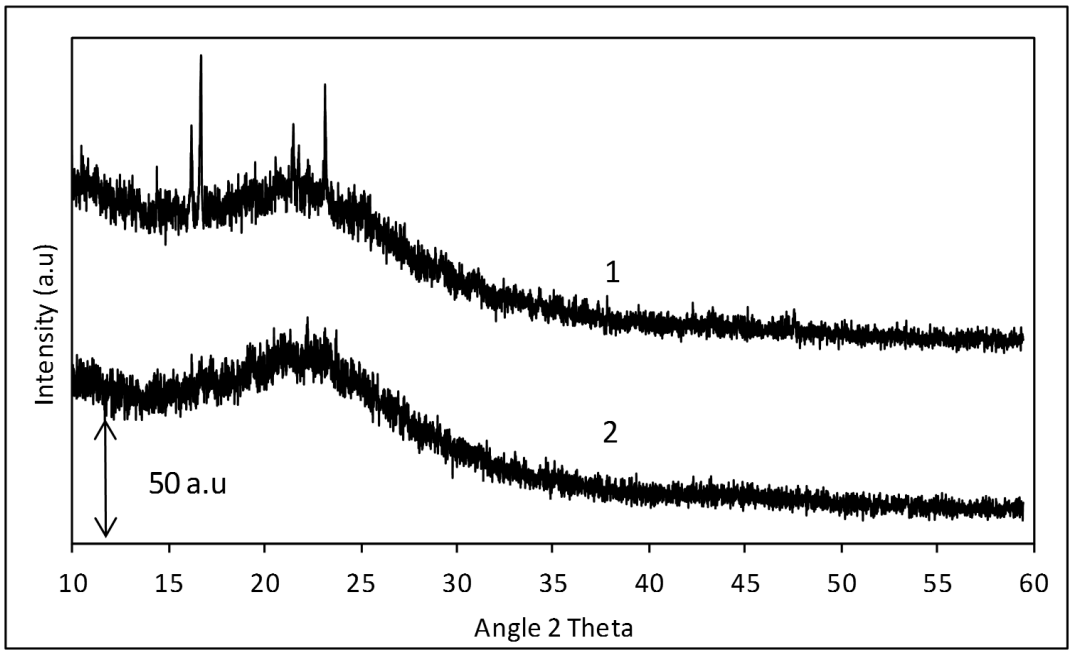

Figure 4.6: pXRD diffractograms of the (1) physical mix and (2) melt sample.

The peaks observed in the pXRD of the physical mix corresponded to the peaks observed earlier for unprocessed crystalline fenofibrate (Fig.3.4). The pXRD diffractograms of drug – silica samples prepared by impregnation, liquid and SC-CO_2 showed no peaks indicating that the drug in these samples was in a non-crystalline state (Fig.4.7).

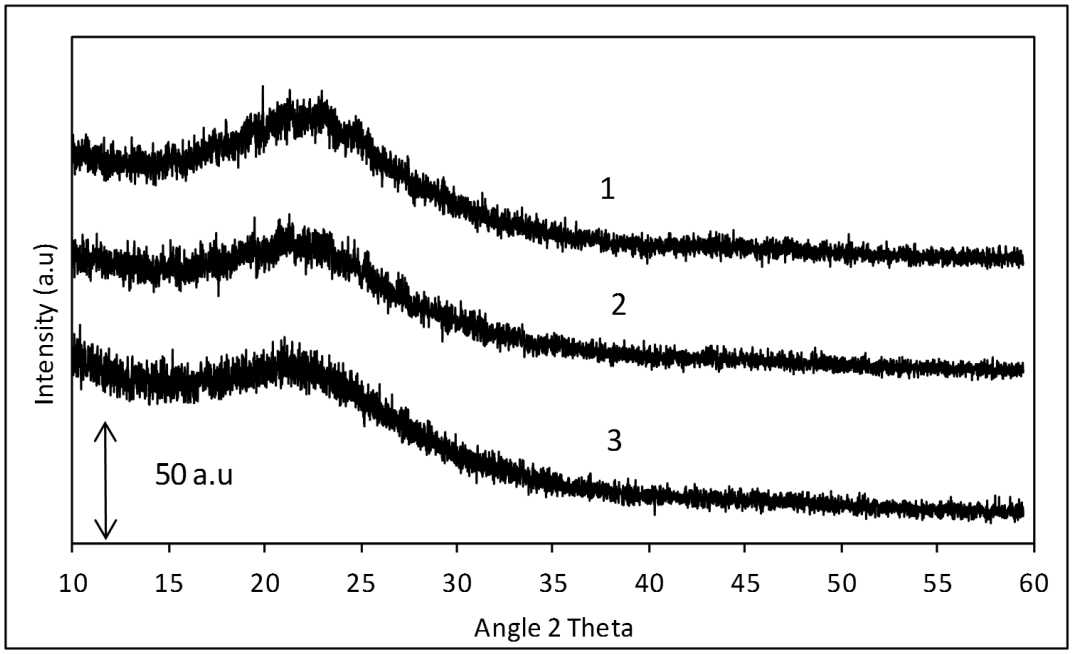

Figure 4.7: pXRD diffractograms of the (1) impregnation, (2) liquid and (3) SC-CO_2 samples.

The melting point for the starting crystalline fenofibrate agreed with the reported T_m of 79 – 81 ^oC (Heinz et al., 2009). Thermal events in the temperature range -20 to -12 ^oC were noted during DSC analysis of the silica starting material (Fig.4.8).

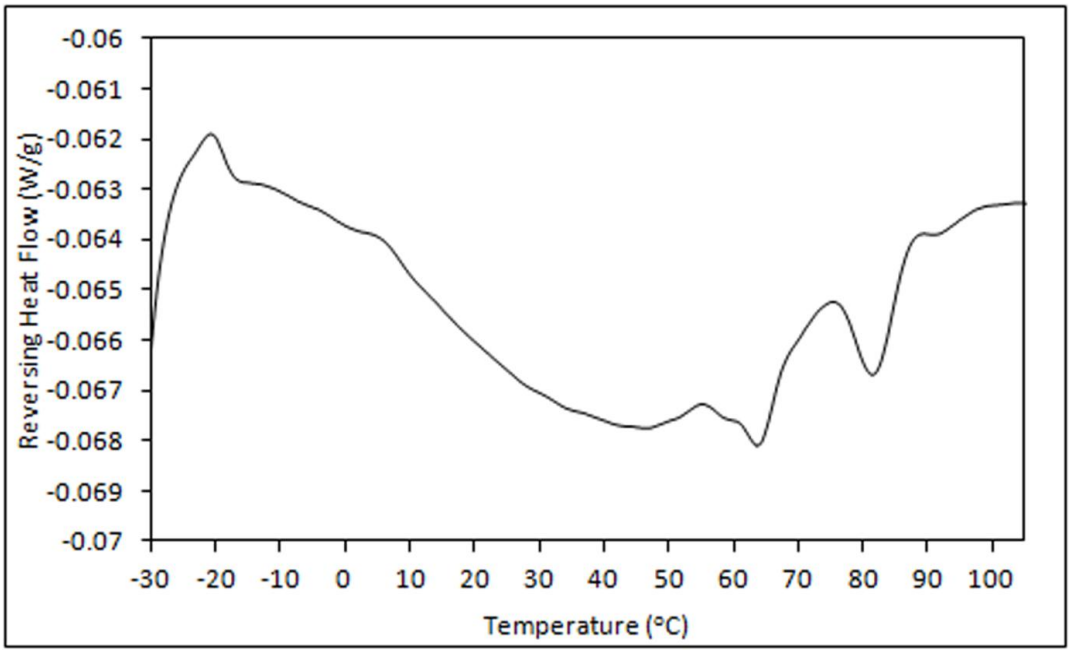

Figure 4.8: Unprocessed SBA-15, MDSC thermogram.

This behaviour was previously reported as the melting point of frozen water confined in the mesopores of mesoporous silica (Kittaka et al., 2011). Endothermic thermal events in the same range -20 to -12 ^{o}C were noted in all drug-silica samples regardless of the method of the loading. As fenofibrate's T_g was reported in this temperature region at -20 ^{o}C, (Heinz et al., 2009) it was not possible to conclusively detect the T_g of amorphous fenofibrate in any of these drug-silica samples. A large melting endotherm with an onset of 78 ^{o}C was visible in DSC thermogram of the physical mix, while there was a slight melting endotherm in the melt sample, indicative of the presence of residual crystalline drug (Fig.4.9).

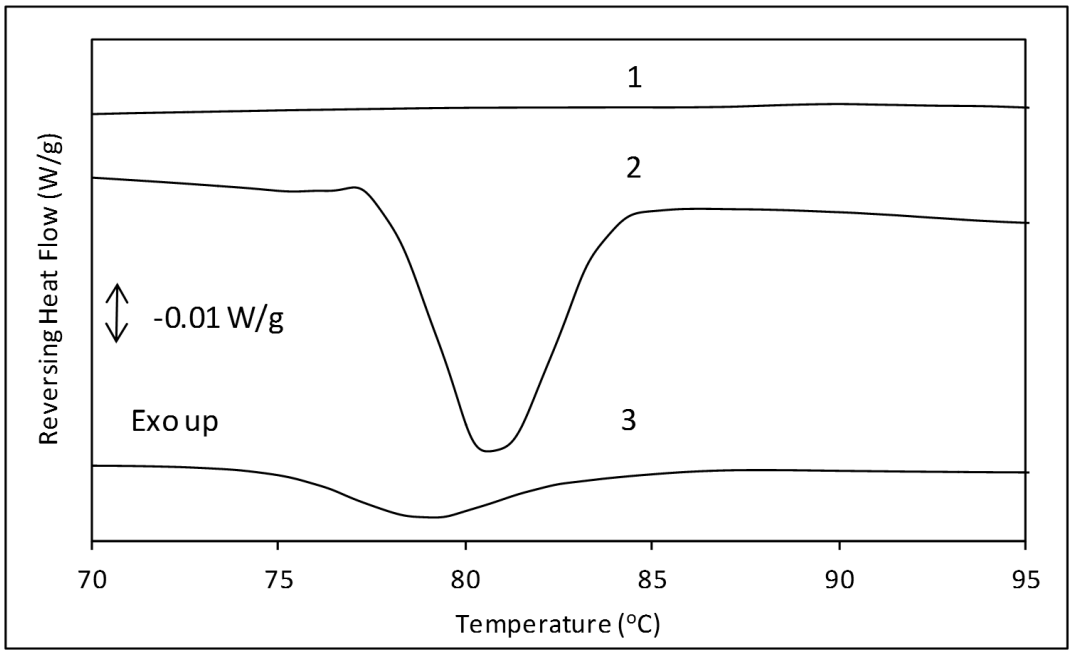

Figure 4.9: (1) Unprocessed SBA-15, (2) physical and (3) melt MDSC thermograms.

The absence of melting endotherms in the impregnation, liquid and SC-CO_2 samples supported the pXRD results that the drug was in a non-crystalline state in these samples (Fig.4.10).

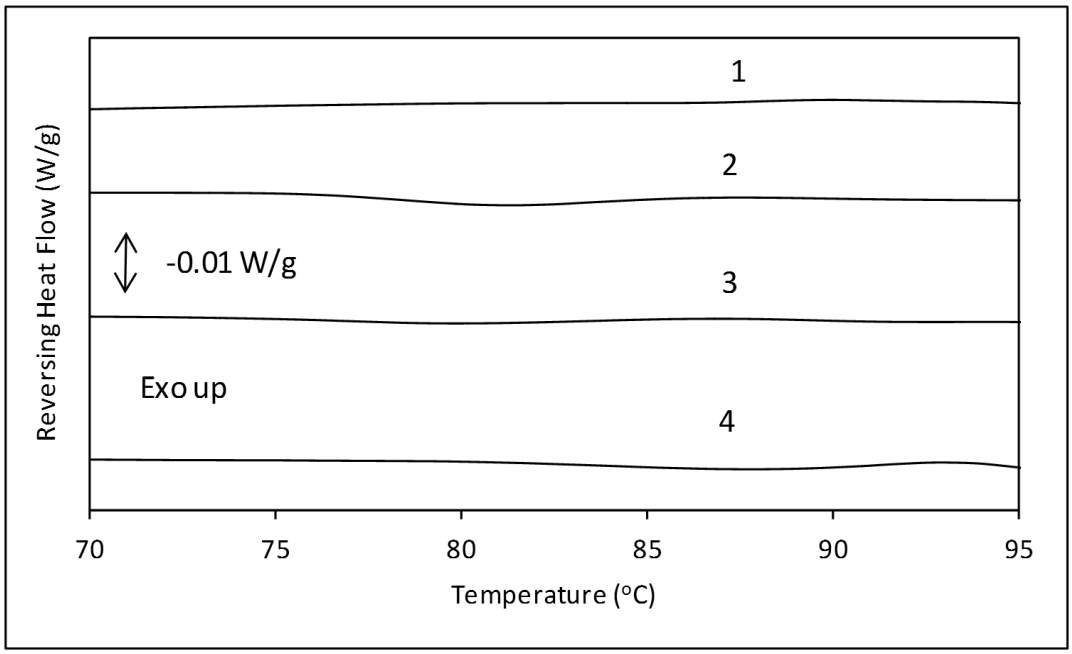

Figure 4.10: (1) Unprocessed SBA-15 thermogram, no evidence of drug melting in (2) impregnation, (3) liquid and (4) SC-CO_2 MDSC thermograms.

4.2.5 *In vitro* drug release

The release of drug from the silica carrier is a key performance indicator to consider when employing OMMs for drug dissolution enhancement. The *in vitro* release of drug from drug – silica samples prepared by physical mixing and melt method compared to the dissolution of the starting fenofibrate are shown (Fig.4.11).

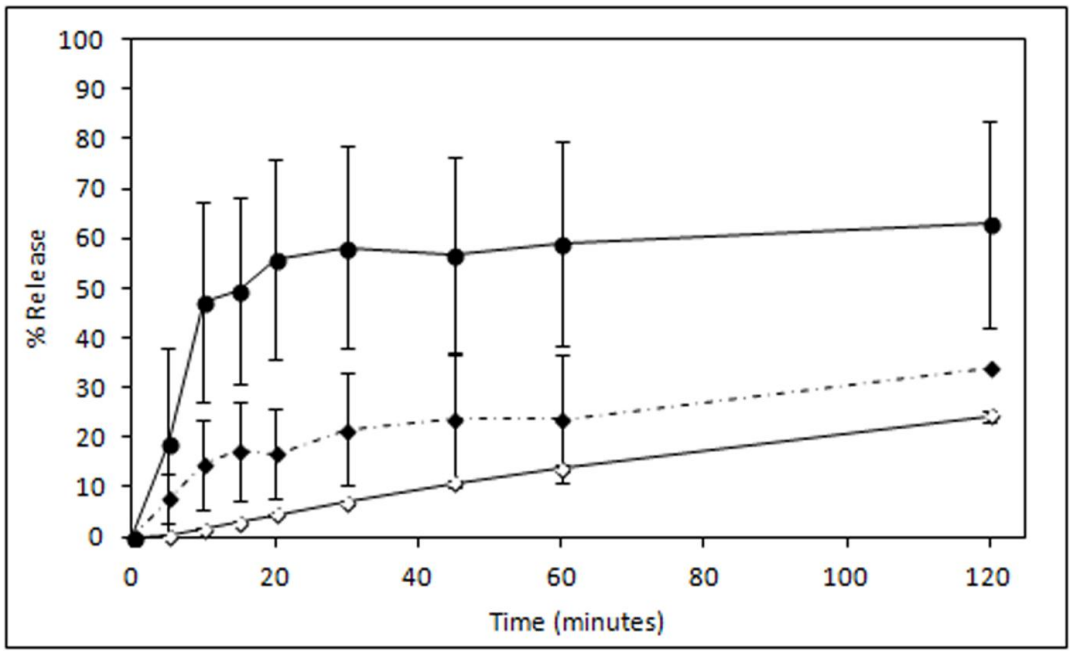

Figure 4.11: Release profiles of (◊) unprocessed fenofibrate, (♦ with dashed line) physical mix and (●) melt sample in 0.3% w/v SDS in 0.1M HCl media (mean ± SD, n = 9).

The *in vitro* release profiles of the impregnation, liquid and SC-CO_2 showed similar results, with very rapid release achieved (Fig.4.12).

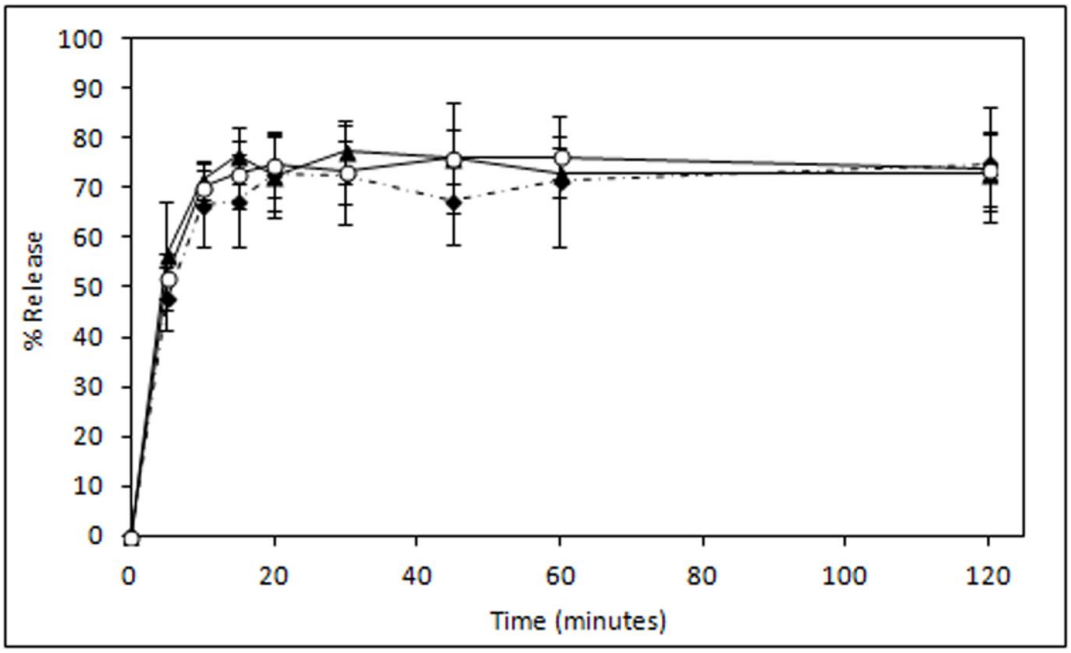

Figure 4.12: Release profiles of (▲) impregnation, (♦ with dashed line) liquid CO_2 and (○) SC-CO_2 sample in 0.3% w/v SDS in 0.1M HCl media (mean ± SD, n = 9).

Utilising mesoporous silica as a carrier material improved the drug dissolution rate for all processed samples. The physical mix showed a slower rate and lower extent of drug release compared to all other loading methods. The release profile of the physical mix was significantly lower that of the melt sample when investigated with repeated measures ANOVA. The release profiles of drug from the impregnation, liquid and SC-CO_2 loaded samples were similar according to the f_1, modified f_1' and f_2 factors. (Moore and Flanner, 1996)Drug was released in a rapid manner in the first 20 min. After 20 min the drug release levelled between 70 – 80 % and did not increase between 20 and 120 min. The release from the melt sample was significantly less that the impregnation, liquid and SC-CO_2 samples according to the f_1, modified f_1', and f_2 values. When the release of the melt sample was compared to the SC-CO_2 sample by repeated measures ANOVA, there was also significant difference observed. In the case of physical mix and melt samples, the variability in

drug release at each time point was high in contrast to the other samples reflecting the heterogeneous drug-loading in these samples referred to previously in Section 3.1. The similarity of the drug release profiles for the melt, impregnation, liquid and SC-CO_2 samples indicated that the deposition behaviour of drug in the mesopores did not adversely affect its release.

4.2.6 Stability analysis

The presence of amorphous drug in the processed samples potentially posed a risk to the drug solid state stability of these formulations. Re-crystallisation of unstable amorphous forms can adversely affect drug properties such as dissolution performance (Hancock and Parks, 2000). While it has been reported that the OMMs can stabilise non-crystalline drug forms (Mellaerts et al., 2010, Shen et al., 2010), the influence of loading method on stability has not been reported. After 12 months accelerated storage at 40 ^{o}C and 75% RH in 50 ml screw-capped plastic containers (Sarstedt AG, Germany), there was no evidence of re-crystallisation in the pXRD diffractograms of the melt, impregnation, liquid and SC-CO_2 samples (Fig.4.13).

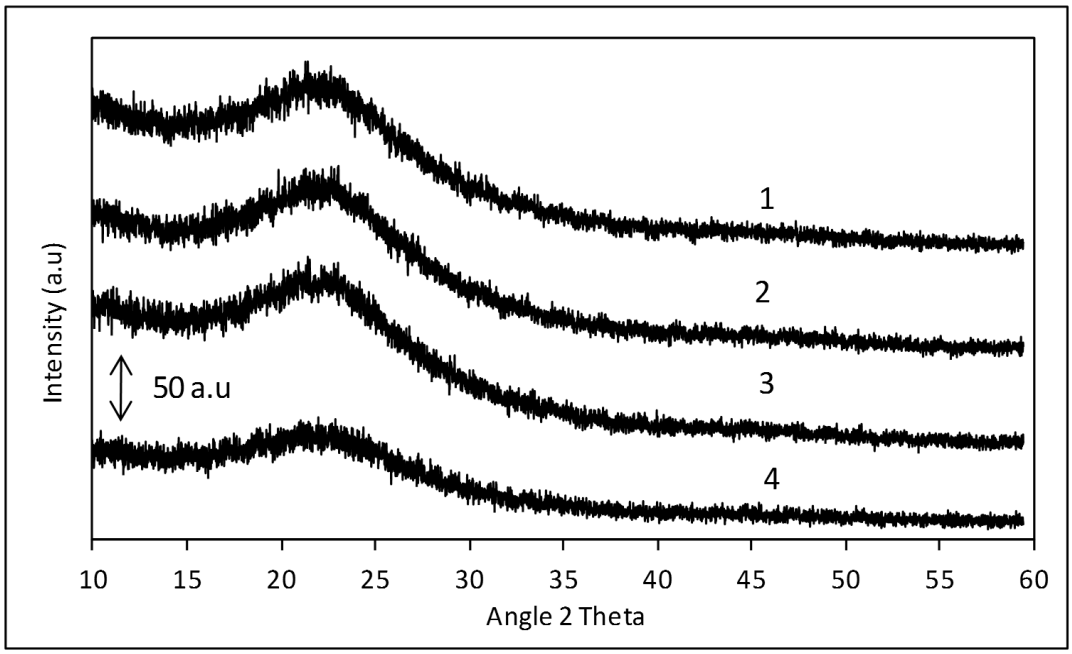

Figure 4.13: pXRD diffractograms of (1) melt, (2) impregnation, (3) liquid and (4) SC-CO_2 post 12 months under accelerated storage conditions.

This was despite the fact the moisture content of these samples increased over time under accelerated storage conditions. For example, the SC-CO_2 processed sample recorded a significant increase in the amount of surface and molecular bound moisture after 12 months compared to its as-prepared state; the surface moisture content increased from 0.72% w/w (±0.14) to 1.82% w/w (±0.42). The surface moisture contents of the impregnation and liquid CO_2 also significantly increased after 12 months under accelerated storage. However no significant increase in moisture was observed for the melt sample. Interestingly, the mesopore volume of the physical mix sample post 1 month storage was significantly reduced compared to the as-prepared sample (Table 4.1). The reduction of the mesopore volume was evident in the decrease in the mesopore size distribution (Fig.4.14). The pore volume and size of the melt, impregnation liquid and SC-CO_2 samples remained unchanged post 1 month storage.

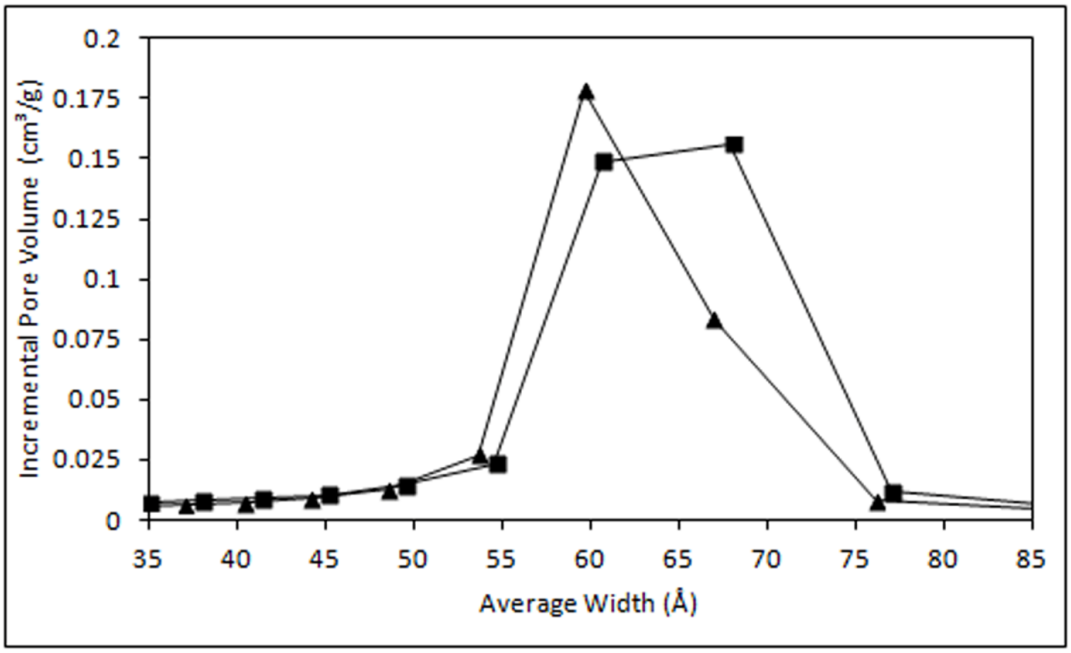

Figure 4.14: Pore size distribution of (■) physical mix as-prepared and (▲) post 1 month storage.

The mesopore volume and size of the melt, impregnation liquid and SC-CO_2 samples remained unchanged post 1 month storage compared to their as-prepared state. This may be explained by the fact that there was no significant increase in the surface moisture content for any of these samples after 1 month. After storage for 1 month, there was some improvement in drug release from the physical mix samples (Fig.4.15).

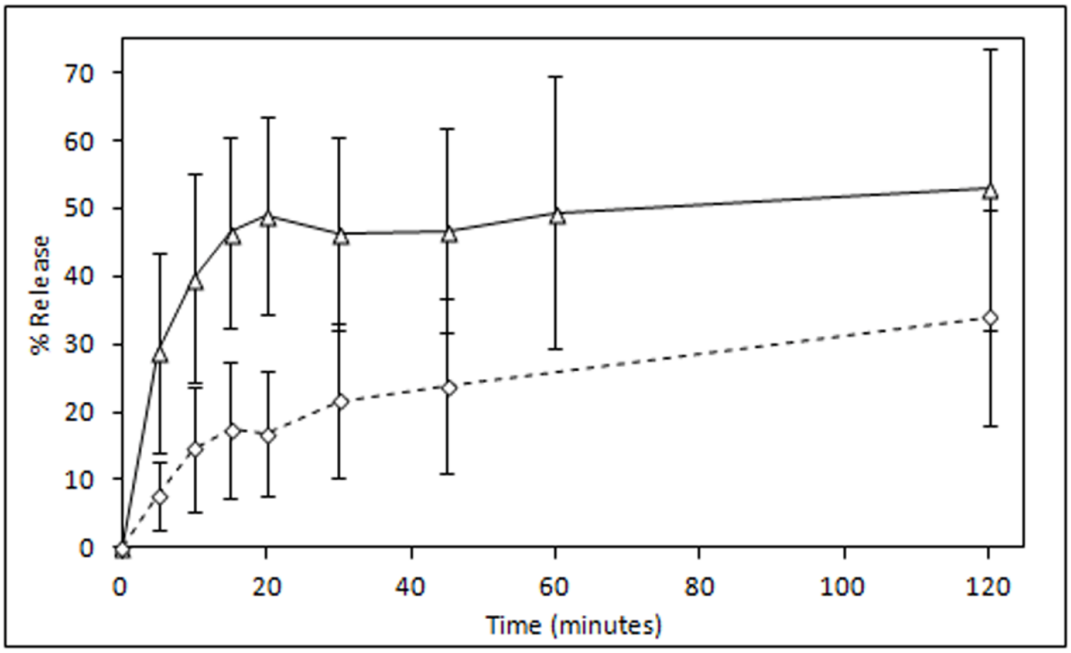

Figure 4.15: Release profiles of (◊ with dashed lines) physical mix as-prepared and (Δ) physical mix post 1 month storage in 0.3% w/v SDS in 0.1M HCl media, sample in 0.3% w/v SDS in 0.1M HCl media (mean ± SD, n = 9).

The f_1, modified $f_1^{'}$, and f_2 values showed a difference between the profiles. A significant increase in the release profile of the physical mix after 1 month under accelerated storage conditions was also observed when the profiles were compard through repeated measures ANOVA. Drug release rate from the impregnation, liquid and SC-O_2 samples was not enhanced even after 12 months accelerated storage (data not shown).

4.3 Discussion

The results of this work highlighted the influence of the drug-loading process on drug distribution within the mesoporous silica structure. The physical mixing and melt methods employed here resulted in heterogeneous distribution of drug throughout the mesoporous silica due to blending difficulties arising from differences in density between the drug and silica. The impregnation, liquid and SC-CO_2 methods obtained samples with drug homogeneously dispersed throughout the mesoporous silica surfaces similar to that reported previously (Van-Speybroeck et al., 2009). This was facilitated by disruption of the drug particulate form.

Changes in the porosity of silica post processing also highlighted differences in drug distribution resulting from different loading methods. For all loading methods examined, the mesoporous silica retained its type IV adsorption isotherm indicative of its mesoporous nature. Similar findings have been reported previously (Mellaerts et al., 2008b, Morere et al., 2012, Moritz and Laniecki, 2012a). The deposition of the drug molecules inside the mesoporous silica mesopores resulted in some of the mesopores being fully or partially filled with drug molecules, which prevented the adsorption and condensation of the N_2 molecules in the mesopores during subsequent mesopore volume measurement. Ukmar and co-workers reported that indomethacin loaded onto MCM-41 and SBA-15 using a solvent impregnation method formed a condensed phase that could block passage of the mesopore channels (Ukmar et al., 2011a). The melt method resulted in the greatest reduction in mesopore size and largest reduction in mesopore volume. This behaviour was attributed to the molten viscosity of drug preventing deep penetration of the mesopores and causing blockage of mesopores. Mellaerts and co-workers utilised a melt method to load itraconazole and ibuprofen onto SBA-15; the subsequent

itraconazole–SBA-15 surface area, mesopore volume and size were similar to the SBA-15, while for ibuprofen-SBA-15 the surface area, mesopore volume and size were reduced (Mellaerts et al., 2008a). Therefore, the distribution of drug in samples prepared using melt methods is strongly dependent on the drug's molten viscosity, while the ability to form a homogeneous mixture of drug and silica prior to the melting step of the process depends on the density difference of the powders. The decrease in mesopore size observed was evidence of the drug coating/lining the inside of the mesopores and was also observed by Mellaerts and co-workers (Mellaerts et al., 2008a). These results were supported by the SEM image of the melt sample which did not show any individual fenofibrate particles in the sample indicating the drug was dispersed on or within the SBA-15 material. EDX images of the melt sample showed a reduced intensity of the Cl atoms which supports the porosity data suggesting some drug is inside the SBA-15 mesopores. This was also the case for the impregnation, liquid and SC-CO_2 but the data was not shown. Due to the greater diffusivity and extremely low surface tension of SC-CO_2 compared to solvents in a liquid state, there appears to be deeper drug penetration of the silica mesopores (Belhadj-Ahmed et al., 2009). This is reflected in the lower reduction of mesopore volume and mesopore size observed for the SC-CO_2 samples compared to the impregnation and liquid CO_2 samples, despite all samples having similar drug-loading. Similar results were also reported by Li-hong and co-workers who loaded ibuprofen onto MCM-41 using both a solvent immersion and SC-CO_2 drug-loading procedure (Li-hong et al., 2013). From these data it appears that although the drug deposition causes a narrowing of the mesopore network, it does not preclude N_2 access during measurement to the same extent as in the melt, impregnation and liquid CO_2 samples. In this work, it was apparent that the processing method has an

important influence on the distribution of drug and subsequent porosity of samples with similar drug-loading.

Loading fenofibrate onto SBA-15 using the impregnation, liquid and SC-CO_2 processes resulted in the drug changing from the crystalline to a non-crystalline state. This is in agreement with previous reports showing the crystalline to non-crystalline transition observed when processing drugs with OMMs (Miura et al., 2010, Nishiwaki et al., 2009, Tozuka et al., 2005, Tozuka et al., 2003). Qian and co-workers demonstrated that crystalline to amorphous transitions occurred in physical mixes of drug and silica via a vapour phase-mediated pathway for compounds with a relatively high vapour pressure in the absence of moisture (Qian and Bogner, 2011). The physical mixing conditions investigated in this study did not result in any detectable amorphization of fenofibrate, perhaps due to the relatively high vapour pressure of fenofibrate and presence of moisture. Azais and co-workers studied the solid state of ibuprofen confined MCM-41 mesopores (35 and 116 Å) using solid state nuclear magnetic resonance (SS-NMR). They reported that the ibuprofen in the mesopores was not in a crystalline or amorphous state at ambient temperature (Azais et al., 2006), and proposed the concept of the drug existing as a molecular dispersion in the silica mesopores. The drug loaded onto SBA-15 by the impregnation, liquid and SC-CO_2 processes appeared to be in a molecularly dispersed state as no T_g or T_m was observed. However as highlighted in Section 3.3.6, frozen water in the mesopores of mesoporous silica may have confounded the detection of the T_g for fenofibrate in these samples. In the melt sample, there was a small endotherm detected in the DSC thermogram around the drug's melting point, which would indicate that some of the drug was still crystalline. It has been previously reported that fenofibrate existed in an amorphous state post loading onto silica. Van-

Speybroeck and co-workers impregnated SBA-15 with fenofibrate and detected the drug T_g at – 20 ^oC, this was ascribed to the higher drug load (higher ratio of drug weight to silica surface area) which promoted drug-drug interactions (Van Speybroeck et al., 2010a). Sanganwar and Gupta reported the presence of residual crystallinity post processing of fenofibrate with aerosil using SC-CO_2 (Sanganwar and Gupta, 2008). However, this may be due to the non-porous nature and hence lower surface area of aerosil and again, a relatively higher drug weight to silica surface area ratio. Other studies of drug-loading SBA-15 using an impregnation process have also reported that the drug was molecularly dispersed as there was no T_g or T_m observed (Mellaerts et al., 2010, Mellaerts et al., 2008a, Van Speybroeck et al., 2010b). Fenofibrate in melt, impregnation, liquid and SC-CO_2 prepared samples was stabilised in the non-crystalline form after 12 month storage under accelerated storage conditions. Given that fenofibrate is very unstable in its amorphous form; it has a T_g of -20 ^oC, its re-crystallisation temperature is 40 ^oC and its reduced temperature scale is 0.6 (Zhou et al., 2002), it was difficult to isolate in the amorphous form due to its rapid re-crystallisation at ambient conditions. Therefore the prolonged stability at accelerated storage conditions must be attributed to its co-processing with SBA-15. These results corresponded with those published by Mellaerts and co-workers who reported that itraconazole was maintained in the amorphous form for up to 12 months after processing with SBA-15 (Mellaerts et al., 2010). Shen and co-workers published similar findings with respect to ibuprofen co-spray-dried with SBA-15 (Shen et al., 2010). Another important factor for the stabilisation of the amorphous form is the effect of nanoconfinement on drug re-crystallisation. A drug cannot re-crystallise when the space in which it is confined

does not exceed the drug molecule width by at least a factor of 10 (Rengarajan et al., 2008, Sliwinska-Bartkowiak et al., 2001).

There was a limited improvement in drug release rate in the physical mix sample, a result which was previously reported by Miura and co-workers, when they physically loaded the drug K-832 onto the silica material sylysia 350 (Miura et al., 2010). Interesting results were also obtained by Ambrogi and co-workers who also observed an improvement in drug dissolution of carbamazepine physically mixed with SBA-15 which they attributed to partial amorphization of the drug (Ambrogi et al., 2013). In this work, the drug – silica prepared by both the physical mix and melt methods yielded a significantly lower release rate compared to the other processing methods. The drug release from the impregnation, liquid and SC-CO_2 samples was rapid and similar. The enhanced rate of drug release was attributable to the more homogeneous distribution of the drug throughout the silica, which spread the drug throughout all of the available surface area. It has been long established that drug release rate can be enhanced by increasing the effective drug surface area in contact with the dissolution medium (Bruner, 1904, Nernst, 1904). The increased wettability of the drug after drug-loading (Wang et al., 2006) and the non-crystalline nature of the drug which has a higher Gibbs free energy compared to the crystalline form (Craig et al., 1999, Yu, 2001) were also contributing factors. The extent of drug release from the physical sample significantly increased after 1 month storage. It has been proposed that water may react with mesoporous silica during storage increasing the hydroxylation of the silica surface. The increased surface hydroxylation can lead to an increase in the extent of drug release; it has previously been reported that adsorbed water on mesoporous silica is advantageous for drug release (Mellaerts et al., 2011). Itraconazole loaded on mesoporous silica prepared using a solvent

impregnation method and stored at 25°C and 97 % RH showed an increase in the extent of drug dissolution post storage (Mellaerts et al., 2010). However, moisture analysis in this study did not show any significant increase. This may be due to the heterogeneous distribution of drug and SBA-15 in these samples which was noted in drug-loading measurements. The extent of drug release did not increase post 1 and 12 month storage for the solvent impregnation, liquid and SC-CO_2 samples. Similar findings were presented by Shen and co-workers who subjected a co-spray dried ibuprofen / SBA-15 sample to 12 month, storage at 40 ^{o}C and 75% RH (Shen et al., 2010). The influence of moisture uptake on the release of drugs loaded on mesoporous silica appears to vary with the loading method and warrants further investigations.

4.4 Summary

The method of loading drug onto SBA-15 was shown to influence drug distribution which is evident by the differences in mesopore size and volume observed for the samples prepared. With the exception of the physical mix and melt samples, solid state and release properties were similar for all processed samples. All processing methods except the physical mix sample, loaded fenofibrate into the SBA-15 mesopores where it was stabilised in a non-crystalline state for 12 month at 75% RH and 40 ^{o}C. Drug release rates were increased for all samples, but depended on loading method. While different loading methods may result in differences in drug distribution, these were not shown to affect solid state stability or drug release in the case of the impregnation, liquid and SC-CO_2 processed samples. This was the first report of liquid CO_2 being utilised to load silica with drug.

5 Optimising SC-CO2 processing paramters

5.1 Introduction

In this chapter, the influence of SC-CO_2 processing conditions on drug-loading efficiency, solid state and release will be further investigated. The employment of supercritical fluids (SCF) like SC-CO_2 for drug-loading offers many advantages compared to traditional organic solvents. An SCF is a fluid that is at or above its critical point and therefore possesses properties of both its liquid and gaseous states, including liquid-like density and gas-like diffusivity (Pasquali and Bettini, 2008). When the supercritical state is reached, properties like density, viscosity and the vapour-liquid equilibrium ratio become dependent on temperature at a certain pressure, which permits the solubility of solutes in the SCF to be controlled (Olson, 1995). Another advantage includes the reduced processing complexity as there is no need for solvent removal steps associated with organic solvent usage (Fages et al., 2004, Pasquali and Bettini, 2008, York, 1999). Carbon dioxide is the most widely used SCF because it has mild critical conditions (7.37 MPa, 31.2 ^{o}C), is inert, non-flammable and inexpensive (Bush et al., 2007, Pasquali and Bettini, 2008). There have been a limited number of studies investigating drug-loading onto silica carriers using SC-CO_2, with each using different parameters for processing in terms of pressurisation, temperature and drug-silica contact. No clear correlation between the processing variables used and the resultant sample properties such as quantity of drug-loaded has been presented. Sanganwar and Gupta investigated a processing pressure of 17.58 MPa and two temperatures, 40 and 50 ^{o}C for 150 min duration to load fenofibrate onto non-porous fumed silica. In the study, the silica material was sealed in a porous filter paper pouch, which was placed inside the pressure vessel

containing excess drug. The CO_2 was pumped in and heat supplied to maintain constant pressure and temperature throughout the duration of the experiment; at the end of the experiment, depressurisation was carried out slowly over 4 h (Sanganwar and Gupta, 2008). Miura and co-workers employed SC-CO_2 processing conditions of 18 MPa and 60 ^{o}C to load a poorly water – soluble drug, K-832 onto mesoporous silica, Sylysia 350. Here the drug and silica were placed together inside the pressure cell, which was then filled with CO_2 and heated to achieve the desired experimental conditions. The cell was maintained under the experimental conditions for a 5 h duration with stirring, before the CO_2 was slowly released from the cell (Miura et al., 2010). Belhadj-Ahmed and co-workers used a flow-through processing method which involved exposing vitamin E acetate to SC-CO_2 and then passing the drug - SC-CO_2 solution through the mesoporous silica carrier at a flowrate of 500 $g.h^{-1}$. The pressure was 15 MPa, while the temperature was 60^{o}C (Belhadj-Ahmed et al., 2009). In this work, the use of SC-CO_2 to load drug onto SBA-15 was investigated at different processing conditions of pressure and duration time. Additionally, the effect of the ratio of drug to SBA-15 was examined to determine if a relationship between drug-loading efficiency and available SBA-15 surface area and pore volume existed. The effect of drug and SBA-15 contact during processing was evaluated in order to understand its impact on drug physicochemical properties and loading. The effect of CO_2 depressurisation rate was investigated; while several studies have been published that employed SC-CO_2 for drug-loading (Belhadj-Ahmed et al., 2009, Sanganwar and Gupta, 2008, Smirnova et al., 2004), there were no studies that explicitly investigated the effect of CO_2 depressurisation rate on drug-loading efficiency, solid state and release rates. There have been some studies involving SC-CO_2 processing where the effect of depressurisation rate was investigated. Arora and

co-workers prepared polystyrene foams where depressurisation rate was reported to influence the size of the microcellular foams when the process temperature was above the glass transition temperature; rapid depressurisation led to larger microcellular foams, (Arora et al., 1998). Aucoin and Legge studied the effect of SC-CO_2 depressurisation rate on the activity of a biocatalyst, Lipozyme IM20. They found the higher the depressurisation rate, the lower the biocatalyst activity (Aucoin and Legge, 2001). In this work, for the first time CO_2 depressurisation rate was investigated to determine its impact on drug – SBA-15 physicochemical properties. The depressurisation was step was controlled by allowing enough CO_2 gas to escape in order to reduce the pressure by 0.69 MPa every minute. The list of process variables investigated in this chapter is presented in the table 5.1 below.

Table 5.1: List of experimental variables investigated in chapter 5, including processing pressure, duration time, CO_2 depressurisation rate, contact method and drug – silica ratio.

Pressure (MPa)	Time (h)	Depressurisation	Contact Method	Ratio
13.79	4	Rapid	Mix	1 mg to 3.00 m^2
27.58	12	Rapid	Mix	1 mg to 3.00 m^2
41.37	24	Rapid	Mix	1 mg to 3.00 m^2
13.79	4	Rapid	Mix	1 mg to 3.00 m^2
27.58	12	Rapid	Mix	1 mg to 3.00 m^2
41.37	24	Rapid	Mix	1 mg to 3.00 m^2
13.79	4	Rapid	Mix	1 mg to 3.00 m^2
27.58	12	Rapid	Mix	1 mg to 3.00 m^2
41.37	24	Rapid	Mix	1 mg to 3.00 m^2
27.58	12	Rapid	Mix	1 mg to 1.24 m^2
27.58	12	Rapid	Mix	1 mg to 0.82 m^2
27.58	12	Rapid	Bag	1 mg to 1.24 m^2
27.58	12	Rapid	Bag	1 mg to 0.82 m^2
27.58	12	Slow, controlled	Mix	1 mg to 3.00 m^2

5.2 Results

5.2.1 Drug-loading

The theoretical amount of drug in each of the SC-CO_2 processed samples prepared for the 3^2 factorial experimental design was 16.67% based on the drug to silica ratio of 1 mg: 3 m^2. However, the actual drug amount varied from 12.62 to 15.62%, which resulted in loading efficiencies ranging from 75.70 to 93.71%, Table 5.2. A statistically significant decrease in drug-loading was observed as processing pressure increased from 13.79 to 41.37 MPa. The duration of processing time had no significant impact on drug-loading ($p > 0.05$). In the case of samples where the drug to silica ratio was increased to 1 mg: 1.24 m^2 and 1 mg: 0.82 m^2 while maintaining constant SC-CO_2 conditions of 27.58 MPa and 12 h, the drug-loading efficiencies for these samples were 74.86% (1 mg: 1.24 m^2) and 69.17% (1 mg: 0.82 m^2) respectively, Table 5.2. There was a significant decrease in drug-loading efficiency with increasing drug – silica ratio. Examination of the impact of physically mixing the drug and silica in the SC-CO_2 environment ('mix method') as opposed to separating drug and silica by means of the porous bag ('bag method'), confirmed that the drug solubilised in SC-CO_2 was loaded onto the silica. The drug-loading efficiencies were reduced when using the 'bag method' compared to the 'mix method', Table 5.2. Comparison of the drug-loading efficiencies achieved with the mix method to the bag method showed that there was a significant decrease in drug-loading efficiency. The drug-loading efficiency of the sample prepared with the standard SC-CO_2 processing conditions with rapid depressurisation was 85.48% (±7.27), while that with controlled depressurisation was 86.25% (±5.92). These loading efficiencies were not significantly different ($p > 0.05$).

Table 5.2: Drug-loading efficiencies and % ΔPV of SC-CO_2 processed samples across all variables, standard deviations in brackets.

SC-CO_2 Conditions	Ratio	Contact	Depressurisation rate	% Drug (w/w), (n = 9)	% Drug-loading efficiency, (n = 9)	ΔPV, (n = 6)
13.79 MPa, 4 h	1 mg to 3.00 m^2	Mix	Rapid	15.62(±0.62)	93.71 (±3.70)	18.4 (±0.51)
13.79 MPa, 12 h	1 mg to 3.00 m^2	Mix	Rapid	13.43 (±4.58)	80.54 (±27.45)	21.33 (±10.39)
13.79 MPa, 24 h	1 mg to 3.00 m^2	Mix	Rapid	15.16 (±0.75)	90.96 (±4.48)	16.68 (±2.14)
27.58 MPa, 4 h	1 mg to 3.00 m^2	Mix	Rapid	14.59 (±1.91)	87.52 (11.46)	16.44 (±1.24)
27.58 MPa, 12 h	1 mg to 3.00 m^2	Mix	Rapid	15.33 (±1.10)	91.98 (±6.59)	19.12 (±4.17)
27.58 MPa, 24 h	1 mg to 3.00 m^2	Mix	Rapid	15.03 (±0.83)	90.17 (±4.98)	18.01 (±1.52)
41.37 MPa, 4 h	1 mg to 3.00 m^2	Mix	Rapid	14.63 (±1.06)	87.74 (±6.37)	17.17 (±2.12)
41.37 MPa, 12 h	1 mg to 3.00 m^2	Mix	Rapid	13.69 (±0.22)	82.12 (±1.30)	16.65 (±1.99)
41.37 MPa, 24 h	1 mg to 3.00 m^2	Mix	Rapid	12.62 (±1.64)	75.70 (±9.84)	19.15 (±8.22)
27.58 MPa, 12 h	1 mg: 1.24m^2	Mix	Rapid	21.39 (±0.15)	74.86 (±0.70)	41.55 (±0.34)
27.58 MPa, 12 h	1 mg: 0.82 m^2	Mix	Rapid	25.94 (±2.84)	69.17 (±10.93)	51.78 (±10.14)
27.58 MPa, 12 h	1 mg: 1.24 m^2	Bag	Rapid	15.07 (±2.34)	52.76 (±15.56)	33.16 (±6.02)
27.58 MPa, 12 h	1 mg: 0.82 m^2	Bag	Rapid	18.84 (±1.54)	50.35 (±8.14)	48.30 (±8.46)
27.58 MPa, 12 h	1 mg to 3.00 m^2	Mix	Rapid	18.57 (±1.58)	85.48 (±7.27)	25.91 (±3.74)
27.58 MPa, 12 h	1 mg to 3.00 m^2	Mix	Slow, controlled	18.73 (±1.29)	86.25 (±5.92)	24.21 (±2.61)

5.2.2 Drug distribution

The SBA-15 had a large pore volume 0.57 cm^3/g (± 0.03), whereas fenofibrate was non-porous. After SC-CO_2 processing fenofibrate with SBA-15, there were marked changes in the SBA-15 pore properties. For all drug – silica SC-CO_2 processed samples, the pore size distribution of SBA-15 shifted to the left after processing, indicating a reduction in the width of SBA-15 mesopores (Fig.5.1).

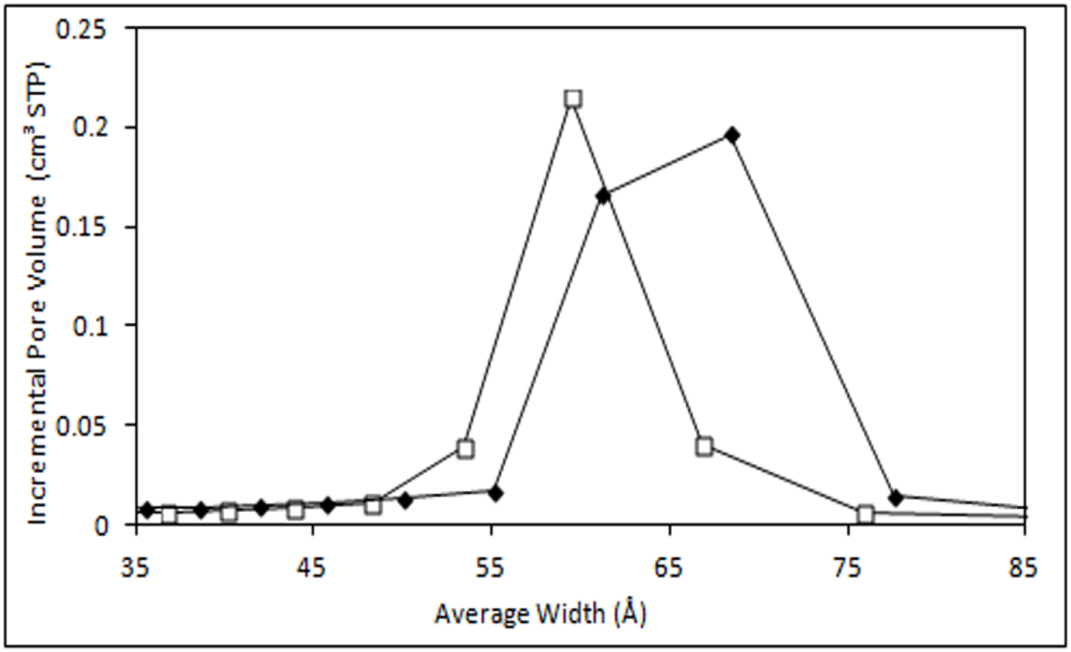

Figure 5.1 Pore size distribution of (♦) unprocessed SBA-15 and (□) representative SC-CO_2 processed fenofibrate-SBA-15 sample, P = 27.58 MPa, T = 12 h.

This reduction may be due to the entrapment of fenofibrate molecules within the mesopores. There were no significant differences observed between the pore size distributions of any of the SC-CO_2 processed samples, when the ratio of drug – silica was maintained at 1 mg: 3 m^2. Increased loading of fenofibrate onto SBA-15 accentuated the shift to a lower pore size distribution (Table 5.2 and Fig.5.2).

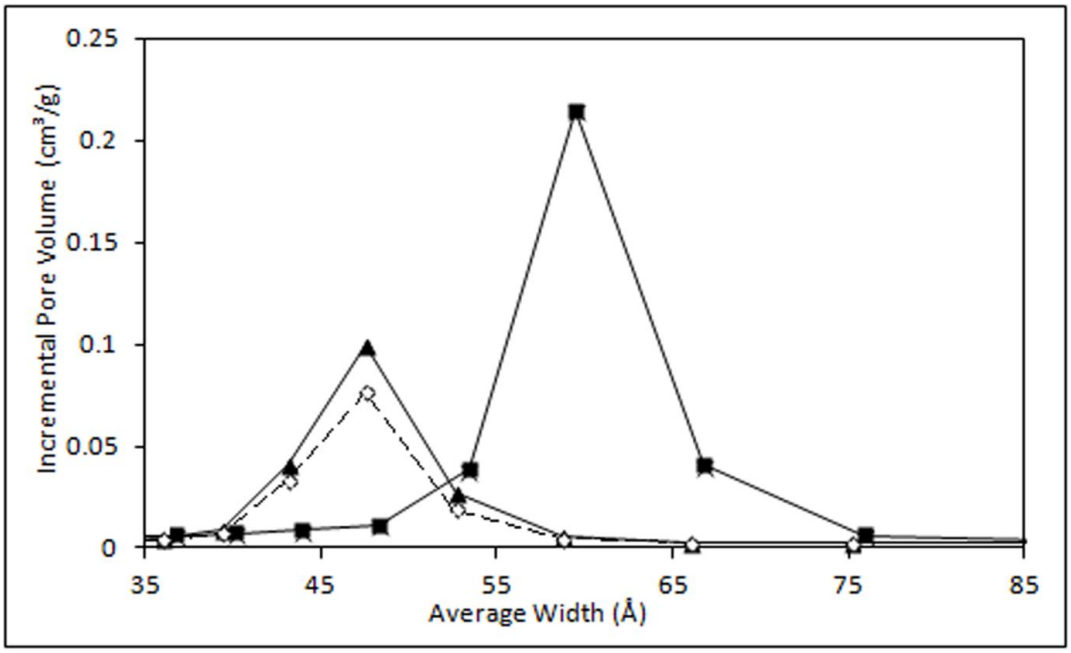

Figure 5.2: SC-CO_2 processed fenofibrate-SBA-15 samples prepared with different ratios of drug: silica by 'mix method', processing conditions P = 27.58 MPa, T = 12 h, (■) 1 mg to 3 m^2, (▲) 1 mg to 1.24 m^2 and (◊) 1 mg to 0.82 m^2.

This reduction in mesopore volume and decrease in mesopore sizes was also seen in the 'bag' samples (Fig.5.3).

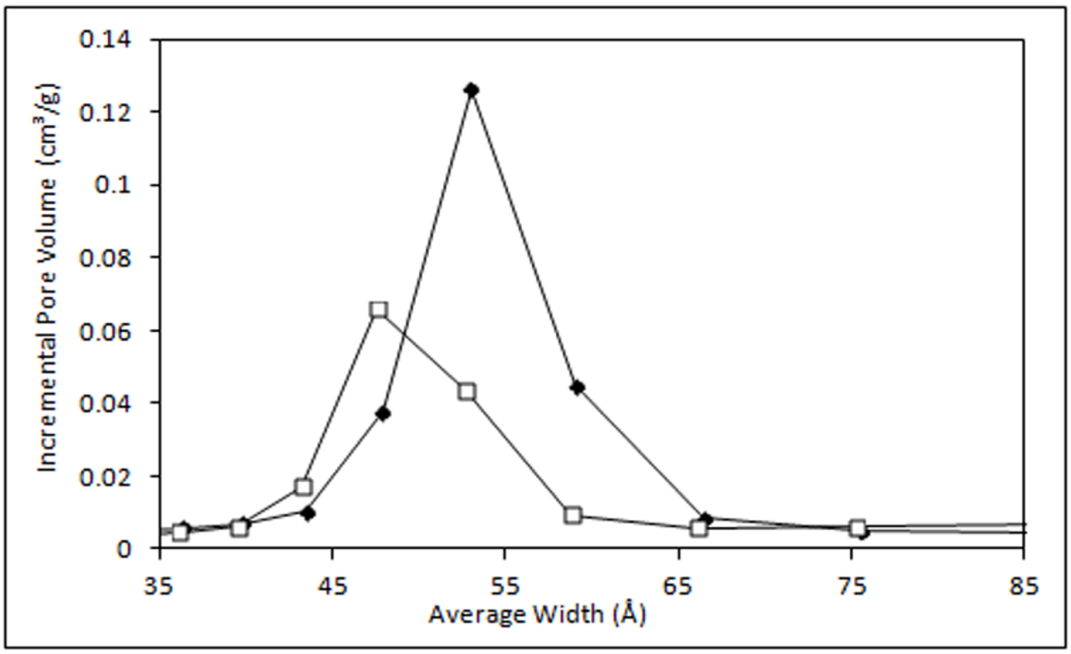

Figure 5.3: SC-CO_2 processed fenofibrate-SBA-15 samples prepared with different ratios of drug: silica by bag method, processing conditions P = 27.58 MPa, T =12 h, (♦) 1 mg to 1.24 m^2 and (□) 1 mg to 0.82 m^2.

Using Eq.2.5, the predicted pore volume of the samples was calculated based on the fraction of SBA-15 and drug present. Large differences between the predicted and measured pore volumes were calculated (Eq.2.6); the percentage difference in pore volume (% ΔPV) ranged from 16.65 – 21.33% (Table 5.2) for the samples prepared under varied SC-CO_2 conditions at a drug mass to silica surface ratio of 1 mg: 3m^2. However, there were no statistically significant differences observed between the measured pore volumes of any of the SC-CO_2 samples, ($p > 0.05$). Increases in drug – silica ratio resulted in a greater % ΔPV. In the case of samples prepared using the 'bag method', while drug-loading efficiency was considerably reduced compared to samples prepared using the 'mix method', the % ΔPV were comparable at the highest drug – silica ratio. There was a strong correlation between the amount of loaded drug and % ΔPV, the Pearson correlation coefficient (r) was calculated to be 0.85. SC-

CO_2 depressurisation rate did not affect the distribution of the drug inside the SBA-15 mesopores; there was no significant difference between the % ΔPV of the rapid depressurisation SC-CO_2 drug-loaded sample, 25.91% (±3.74) and that of the controlled depressurisation SC-CO_2 drug-loaded sample, 24.21% (±2.61).

5.2.3 Drug solid state

There was no T_g or T_m observed in any of the samples and no peaks were observed in any of the diffractograms of the drug – silica SC-CO_2 processed samples, which indicated that the fenofibrate was in the non-crystalline form (Fig.5.4).

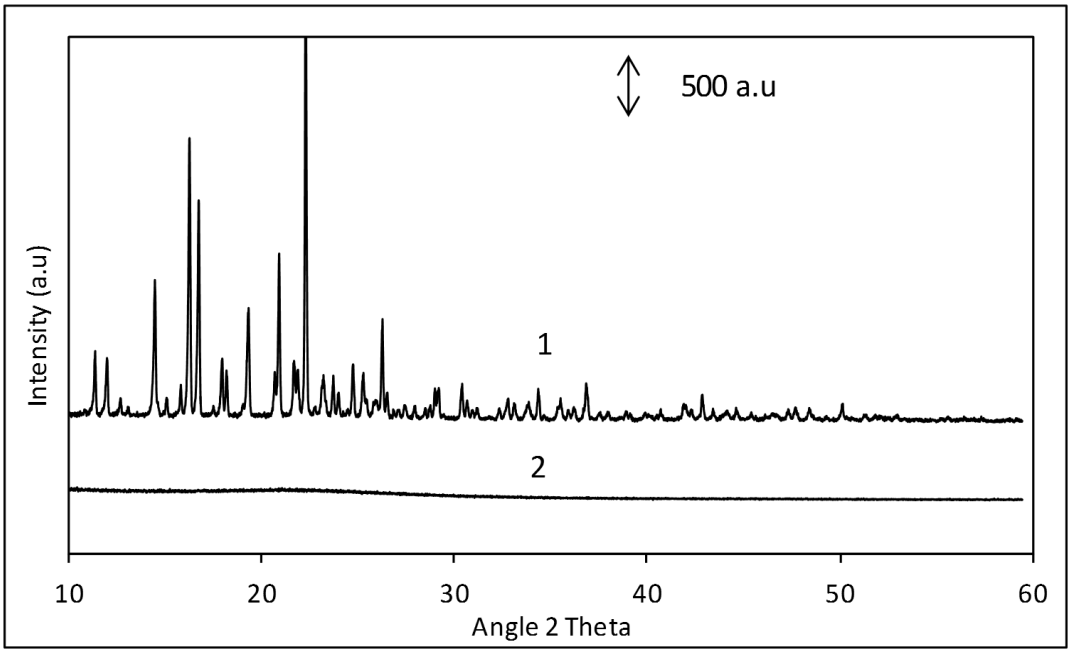

Figure 5.4 pXRD diffractogram of (1) unprocessed fenofibrate and (2) representative SC-CO_2 sample (P = 27.58 MPa, T = 12 h).

When the ratio of drug to SBA-15 was increased, the diffractograms showed the drug to be in a non-crystalline form for both the 'mix' and 'bag methods' (Fig.5.5). It was observed that the fenofibrate remaining outside the porous bag containing SBA-

15 at the end of the experiment, which was not loaded onto the SBA-15, was in the crystalline form (Data not shown).

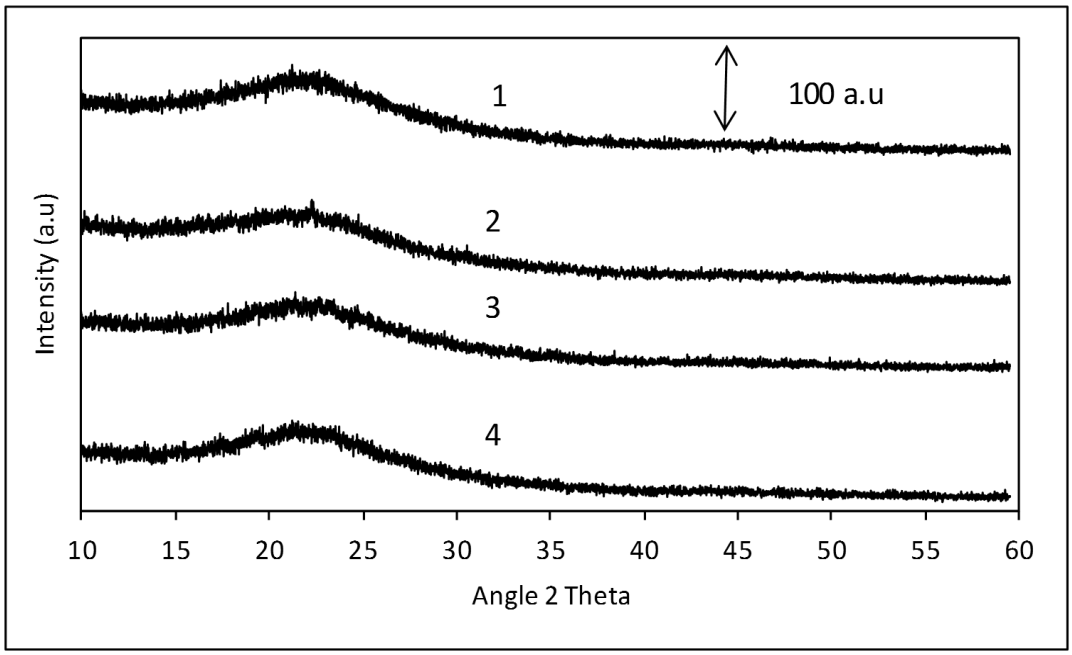

Figure 5.5: pXRD diffractograms of SC-CO_2 processed (1) 'mix sample', 1 mg to 1.24 m^2, (2) 'mix sample', 1 mg to 0.82 m^2, (3) 'bag sample', 1 mg to 1.24 m^2, (4) 'bag sample', 1 mg to 0.82 m^2; processing conditions P = 27.58 MPa, T = 12 h.

5.2.4 Molecular interactions

FT-IR spectrum of SBA-15 shows characteristic peaks for silica; surface silanol (Si-OH) stretching caused by adsorbed water (3000 - 4000 cm^{-1}), asymmetric siloxane (Si–O–Si) stretching (1083 cm^{-1}), Si-O-Si bending (456 cm^{-1}), O-H bending (adsorbed water) (1600 cm^{-1}) and Si-O asymmetric stretching (814 cm^{-1}) which is in agreement with previously reported silica spectra (Coutinho et al., 2007, Das et al., 2007, Izquierdo-Barba et al., 2010, Zheng et al., 2001, Parida et al., 2006). After SC-CO_2 processing fenofibrate with SBA-15, there was some evidence of intermolecular bonding in all samples. The Si-O peak shifted from 814 to 803 cm^{-1} (Fig.5.6),

indicating hydrogen bonding between silica's silanol surface groups and fenofibrate's carbonyl groups. Molecules containing carbonyl functional groups have previously been reported to be adsorbed onto silica surfaces and interactions with the silica surface was proposed to be through hydrogen bonding onto the surface silanol (Diaz et al., 2005). FTIR spectra of fenofibrate-silica samples prepared with increased drug – SBA-15 ratios and using the 'bag method' also showed similar peak shifts (Fig.5.6).

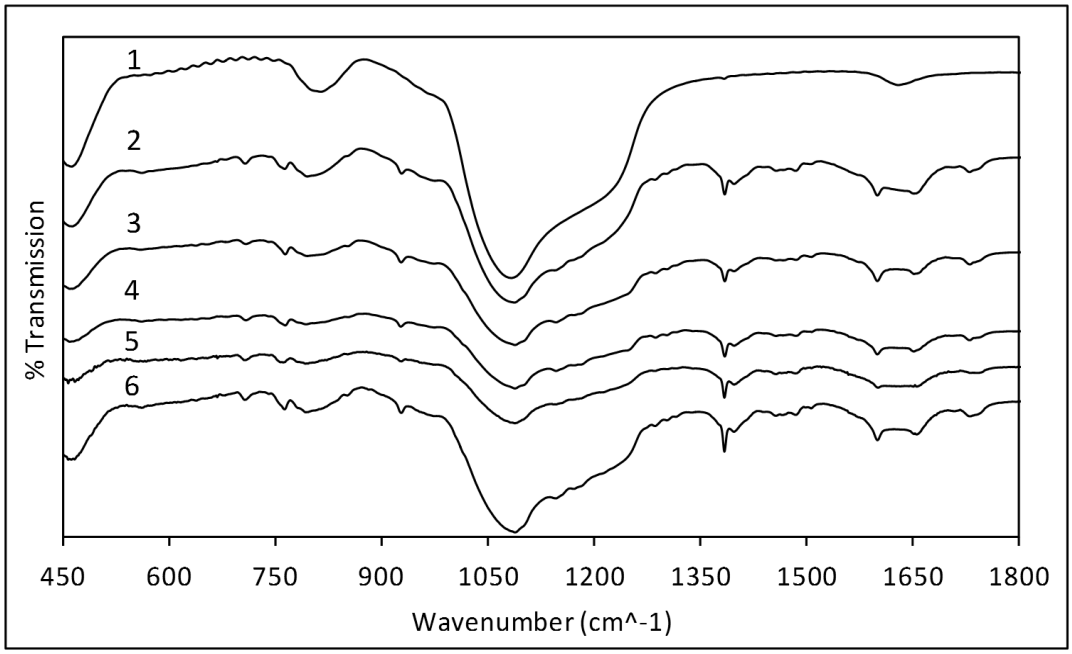

Figure 5.6: FT-IR spectra of (1) unprocessed SBA-15 and selected SCO_2 processsed samples detailed in table 5.2 (2) 1 mg to 3 m^2 mix sample, (3) 1 mg to 1.24 m^2 mix sample, (4) 1 mg to 0.82 m^2 mix sample, (5) 1 mg to 1.24 m^2 bag sample and (6) 1 mg to 0.82 m^2 bag sample (all drug – silica samples processed at P = 27.58 MPa and T = 12).

5.2.5 *In vitro* release

SC-CO_2 processed fenofibrate-SBA-15 samples showed a substantial increase in the release rate of fenofibrate compared to unprocessed fenofibrate (Fig.5.7).

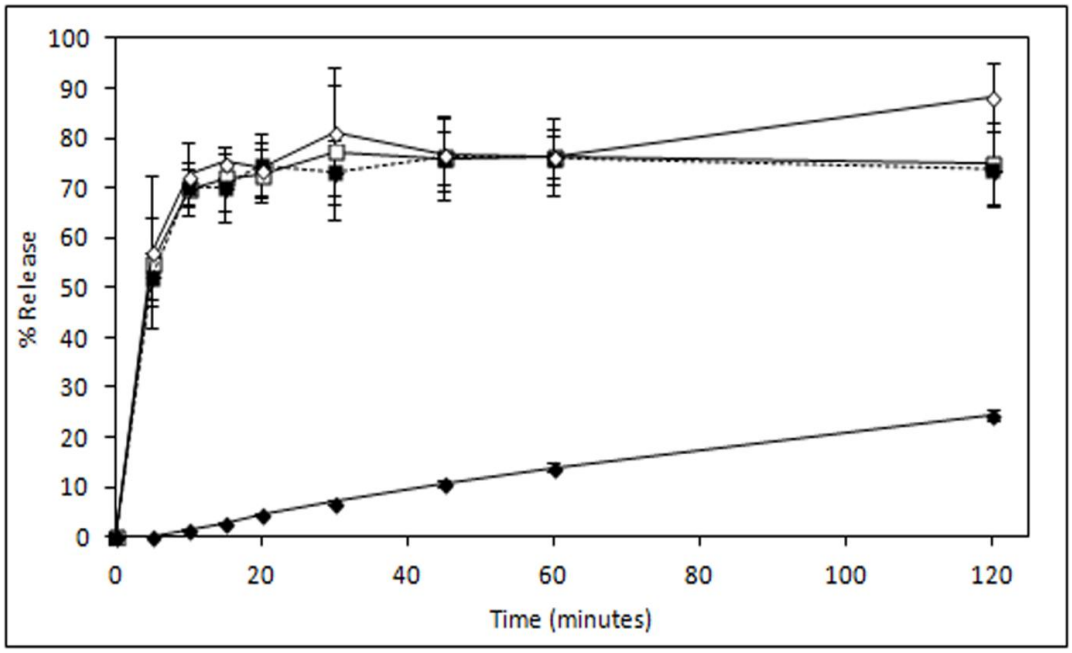

Figure 5.7: Release profiles of (♦) unprocessed fenofibrate and various representative SC-CO_2 samples at a ratio of 1 mg to 3 m^2, (□) P = 13.79 MPa, T = 4 h, (■ with dashed line) P = 27.58 MPa, T = 12 h and (◊) P = 41.37 MPa, T = 24 h in 0.3% (w/v) SDS in 0.1M HCl media, sample in 0.3% w/v SDS in 0.1M HCl media (mean ± SD, n = 9).

There were no significant differences in fenofibrate release profiles for any of the SC-CO_2 processed fenofibrate-SBA-15 (1 mg: 3 m^2) samples irrespective of processing conditions employed according to the f_1, modified f_1' and f_2 tests. The release profiles of the increased drug – silica samples are displayed here (Fig.5.8).

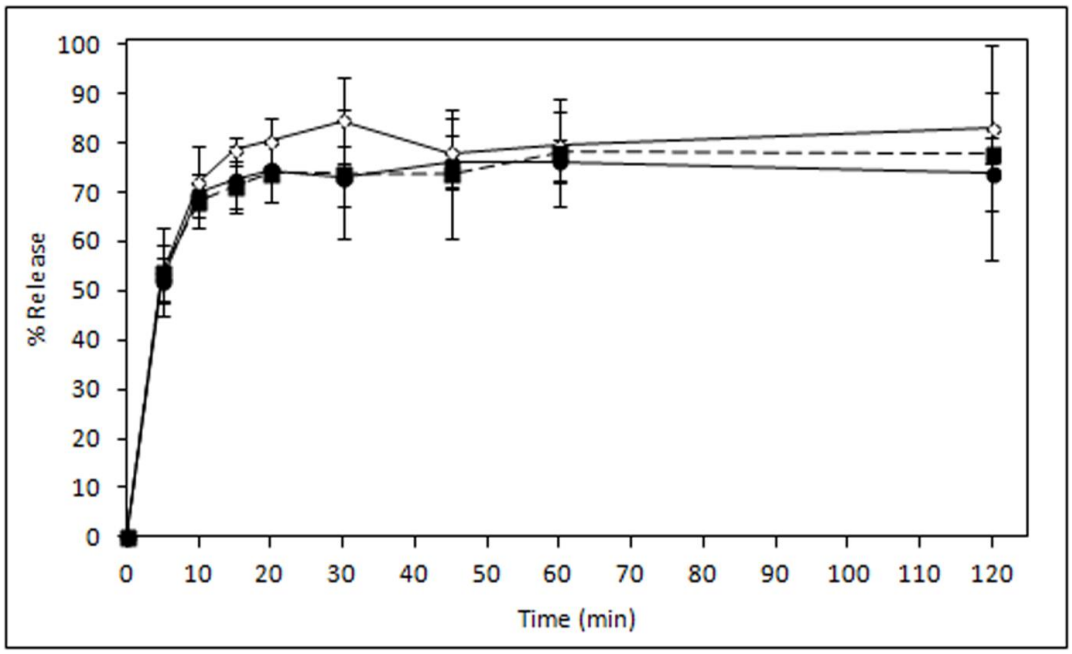

Figure 5.8: Release profiles of 'mix samples' (●) 1mg to 3 m^2, (◊) 1 mg to 1.24 m^2 and (■ with dashed line) 1mg to 0.82 m^2 (P = 27.58 MPa, T = 12 h) in 0.3% (w/v) SDS in 0.1M HCl media, sample in 0.3% w/v SDS in 0.1M HCl media (mean ± SD, n = 9).

There were no significant differences in the release profiles of samples with drug: SBA-15 ratios of 1 mg: 3 m^2, 1 mg: 1.24 m^2 and 1 mg: 0.82 m^2 samples prepared by the 'mix method', according to the according to both the f_1, modified $f_1^{'}$ and f_2 tests and repeated measures ANOVA.

The release profiles of the samples prepared with the 'bag method' are shown in Fig.5.9.

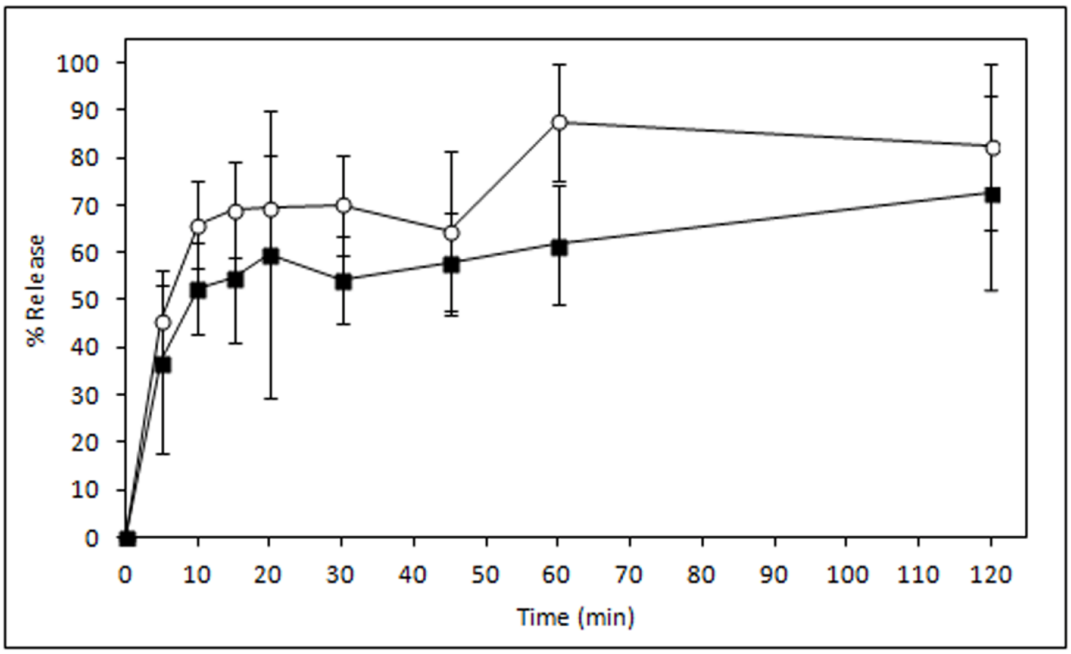

Figure 5.9: Release profile of 'bag samples' at (○) 1 mg to 1.24 m^2 and (■) 1 mg to 0.82 m^2 (P = 27.58 MPa, T = 12 h) in 0.3% (w/v) SDS in 0.1M HCl media sample in 0.3% w/v SDS in 0.1M HCl media (mean ± SD, n = 9).

When samples were prepared using the 'bag method' the release rates appeared to exhibit a greater degree of variability compared to the samples prepared using the 'mix method', which suggested a greater heterogeneity in the dispersion of drug on the SBA-15. It was also seen that there was a significant decrease in drug release from the bag sample with the drug – silica ratio of 1 mg to 0.82 m^2 compared to that with the ratio of 1 mg to 1.24 m^2 according to the repeated measures ANOVA test. The release profiles of the mix and bag samples at the 1 mg to 0.82 m^2 drug – silica ratio are shown here in Fig.5.10.

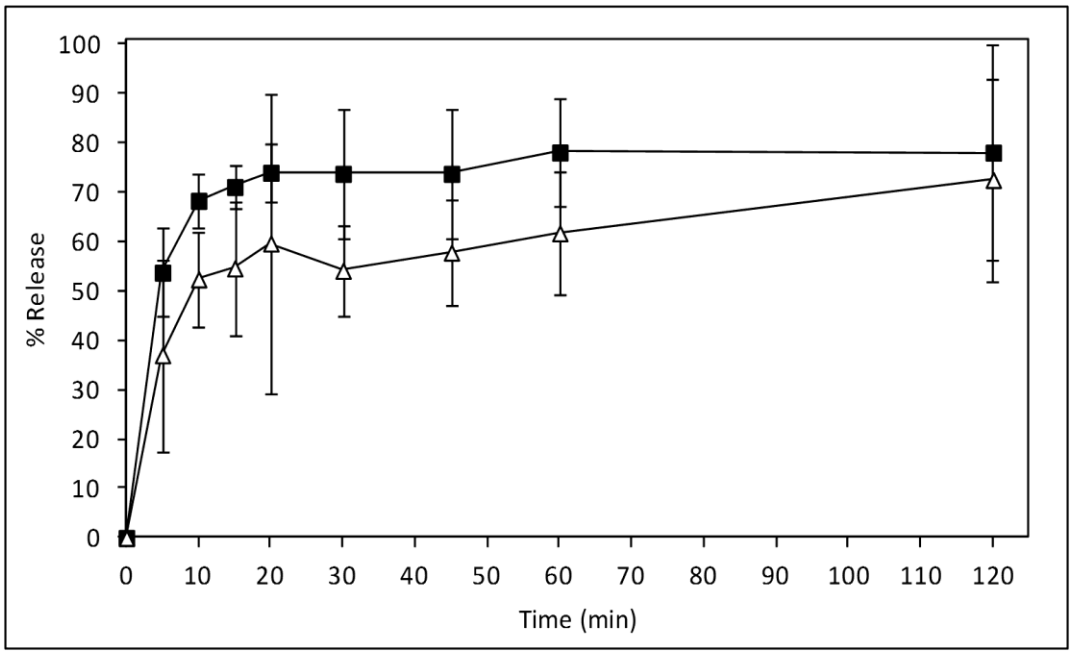

Figure 5.10: Release profiles of (■) mix and (Δ) bag samples at drug – silica ratio of 1 mg to 0.82 m^2 (P = 27.58 MPa, T = 12 h) in 0.3% (w/v) SDS in 0.1M HCl media sample in 0.3% w/v SDS in 0.1M HCl media (mean ± SD, n = 9).

There was a significant difference between the samples prepared by the 'mix method' and the 'bag method' at the 1 mg: 0.82 m^2 drug – silica ratio, according to the f_1, modified f_1 and f_2 tests and repeated measures ANOVA.

The drug release rate from the sample prepared by controlled CO_2 depressurisation was similar to that prepared with rapid CO_2 depressurisation. The drug release reached approximately 80% after 10 min and was maintained at the level thereafter. There was no difference between these release rates according to the f_1, modified f_1 and f_2 tests.

5.3 Discussion

The aim of this research was to understand the impact of supercritical processing conditions on the loading of drug onto SBA-15 and the resulting drug solid state and release properties. In pursuit of this objective, various supercritical processing variables such as pressure (13.79, 27.58, 41.37 MPa) and processing duration (4, 12, 24 h), CO_2 depressurisation rate, ratio of drug to SBA-15 (1 mg: 3 m^2 , 1 mg: 3 m^2 and 1 mg: 0.82 m^2) and methods to combine the SBA-15 with the drug were investigated. It was postulated that at higher pressures, more drug would dissolve in SC-CO_2 as it has been reported that the solubility of solutes in SC-CO_2 increases with increasing pressure (Belhadj-Ahmed et al., 2009, Gordillo et al., 1999, Macnaughton and Foster, 1994, Macnaughton et al., 1996, Crampon et al., 1999) and hence result in greater drug-loading onto SBA-15; the densities of the SC-CO_2 at the experimental pressures of 13.79, 27.58 and 41.37 MPa were found to be 720, 910 and 1001 kg/m^3 respectively, using the Stryjek and Vera modification of the Peng-Robinson equation of state (PRSV) (Stryjek and Vera, 1986). However, decreased drug-loading efficiencies were obtained at the higher pressures. This was attributed to the loss of dissolved drug during the depressurisation step because of faster transfer rates out of the pressure vessel at the higher pressures. The SC-CO_2 drug-loading method employed in this study and also reported by Sanganwar and Gupta, and Miura and co-workers, involved solubilisation of the drug in SC-CO_2 and loading onto the silica carrier within the same pressurised vessel (Miura et al., 2010, Sanganwar and Gupta, 2008). While the loss of solubilised drug during the depressurisation step appeared to adversely impact the drug-loading efficiency using the processing method employed in this study, it is thought that this would not be the case for the impregnation method employed by Belhadj-Ahmed and co-workers in

which the drug was dissolved in SC-CO_2 prior to passage through the silica at a controlled flow rate (Belhadj-Ahmed et al., 2009. Low intra-sample variation, less than 5% RSD, was determined for all SC-CO_2 processed samples, which was indicative of homogeneous drug distribution throughout the SBA-15. As the ratio of fenofibrate to SBA-15 increased under constant SC-CO_2 conditions, the % drug increased but the drug-loading efficiency decreased. These results suggest that fenofibrate drug-loading is limited by its solubility in SC-CO_2 or by the capacity of SBA-15 to accommodate drug. When drug – silica samples were prepared by the 'bag method', the drug-loading efficiencies were lower than fenofibrate-SBA-15 samples prepared by the 'mix method' at the same ratios of drug and SBA-15. The reduced drug-loading observed was attributed to reduced contact between drug and SBA-15 and possibly due to the reduced surface area of SBA-15 exposed during processing. These findings are consistent with those of Chen and co-workers who reported that the amount of ibuprofen loaded by the solvent method was dependent upon the surface area of mesoporous silica (Chen et al., 2012). There has not been any study where the influence of CO_2 depressurisation rate on drug-loading efficiency onto mesoporous silica was reported. There have been studies involving other substrates such as polymers (PLGA) where the depressurisation rate has been found to influence the size of drug-loaded polymer spheres; rapid depressurisation led to macrospheres while controlled depressurisation led to microspheres (Guney and Akgerman, 2002). However, within the limits of this work, CO_2 depressurisation rate did not affect fenofibrate loading, distribution or release from SBA-15.

The large % ΔPV values calculated for all the SC-CO_2 samples were attributed to partial or complete filling of the mesopores by drug molecules as mentioned in chapter 4. Reductions in pore volume reflected both the degree of drug-loading and

the manner of drug molecule deposition within the SBA-15 pores. There were no statistically significant differences in measured pore volumes for any of the samples prepared at a constant drug – silica ratio of 1 mg: 3 m^2 with varying SC-CO_2 conditions. The % ΔPV increased when the drug to SBA-15 ratio increased which correlated with increased drug-loading. Interestingly, the % ΔPV values calculated for the samples prepared by the 'bag method' were relatively high for the amount of drug actually loaded, when compared to samples prepared using the 'mix method'. This was particularly the case for the highest drug – silica ratio sample. This suggests that drug may be obstructing the pore openings or that the drug-loaded by the 'bag method' was deposited in the SBA-15 mesopores in a different manner than in the 'mix method'. There were no differences in drug distribution within the SBA-15 mesopores and % ΔPV as a result of SC-CO_2 depressurisation rate.

Fenofibrate loaded onto SBA-15 was found to be in a non-crystalline state after SC-CO_2 processing in all samples. Retention of the drug in the non-crystalline form was observed after storage conditions of 75% RH and 40 ^oC for 12 months (See chapter 4). None of the processing parameters such as pressure, duration time, drug – silica ratio, method of contact and SC-CO_2 depressurisation rate showed any differences in terms of drug solid state structure. Analysis of unloaded drug recovered at the end of the drug-loading experiments using the 'bag method' showed that the drug retained its crystalline structure. FT-IR spectroscopy indicated the presence of hydrogen bonding between fenofibrate carbonyl groups and SBA-15 silanol groups in all processed samples. It has previously been reported that hydrogen bonding between a silica substrate and drug could be partly attributed to the loss of drug crystallinity (Madieh et al., 2007). Loading the drug onto SBA-15 resulted in a significant improvement in the drug's release rate compared to the dissolution rate of the

unprocessed drug. This was attributed to a combination of (1) the increased effective drug surface area in contact with the dissolution medium after loading onto SBA-15 as mentioned previously (Bruner, 1904, Nernst, 1904); (2) the induction of fenofibrate's non-crystalline form (Yu, 2001) and (3) the increased wettability of fenofibrate after loading onto SBA-15 because of the hydrophilic nature of SBA-15 (Brown et al., 1998). Fenofibrate release from all the fenofibrate-silica SC-CO_2 processed samples (1 mg: 3 m^2) was rapid, with over 50% released by 5 minutes. After approximately 20 min, fenofibrate release reached a plateau and total drug release was not accomplished after 2 h. There was no difference in terms of *in vitro* drug release across the various supercritical conditions investigated; this result has recently been supported in the literature (Li-hong et al., 2013). Incomplete drug release behaviour was attributed to the possible presence of drug deep in the mesopores or in micropores which was potentially inaccessible to the release media due to surface tension effects. There was no significant difference in terms of release profile when the drug – silica ratio was increased in the mix samples. When the samples were prepared using the bag method, the drug release profiles exhibited greater hetereogeneity and at the highest drug – silica ratio of 1 mg to 0.82 m^2, the release was significantly lower for the bag sample compared to the equivalent mix sample at this ratio. This reinforced the hypothesis that the drug-loaded by the 'bag method' was deposited into the SBA-15 mesopores in a different manner compared to the 'mix method'. These results indicated that drug release can be altered with variations in the distribution of deposited drug on the silica substrate and that the drug release profiles can be tailored by altering the method of drug-loading.

5.4 Summary

SC-CO_2 loading of fenofibrate onto SBA-15 using supercritical processing has been demonstrated. Fenofibrate loaded on a SBA-15 carrier was shown to be in a non-crystalline form. A number of variables including processing pressure, the ratio of drug to silica and the contact between drug and silica, prior to and during to SC-CO_2 processing affected the amount of drug-loaded. The percentage drug-loaded increased as the drug – silica ratio increased but was reduced when drug and silica were physically separated during processing. The percentage drug-loaded was shown to be dependent on the silica surface area available for drug deposition. Pore volume measurements indicated differences in drug distribution on the porous silica samples. Both decreased pore volume measurements and fenofibrate release profiles indicated that drug was deposited to a greater degree in the pores when drug and silica were physically separated during processing. Physical mixing of drug and silica powders during SC-CO_2 processing was shown to increase drug release rate and is therefore, more suitable for loading poorly water-soluble drugs. The successful application of SC-CO_2 processing demonstrates its potential for loading poorly water-soluble drugs onto ordered mesoporous materials like SBA-15 to enhance dissolution rate and oral bioavailability.

6 Optimising drug release from drug – silica systems

6.1 Introduction

The objective of this chapter was to optimise the release of drug from drug – silica systems, namely to increase the release rate and extent of fenofibrate from drug - SBA-15 systems. Drug release rates are governed by several factors including wetting and effective surface area of drug in contact with the dissolution media. As stated previously, the Nernst-Bruner equation related drug dissolution rate to surface area with higher surface areas leading to faster dissolution rates (Bruner, 1904, Nernst, 1904). Wetting refers to the ability of a powder to attract a liquid and allow that liquid spread over the powder; the adhesive force between the powder and liquid is stronger than the cohesive force between the liquid. A powder that is easily wetted by water allows for extensive coverage of the solid by water which in turn allows for a greater effective surface area for drug dissolution leading to faster drug release rates. It is well known that the amorphous form of a drug exists in a thermodynamically unstable state and posseses a higher Gibbs free energy (Hancock and Zografi, 1997) and solubility (Hancock and Parks, 2000) compared to its corresponding crystalline form which allows for faster dissolution rates. In drug – silica systems, there are other factors that also need consideration. The extent of drug release from drug – silica systems is dependent on the amount of drug present in the system, the silica mesopore size (Horcajada et al., 2004), specific surface area (Chen et al., 2012) and mesopore volume (Heikkila et al., 2007).

In chapter 5, the application of SC-CO_2 to load fenofibrate onto SBA-15 was investigated and it was established that processing pressure, supercritical processing duration time, CO_2 depressurisation rate and the ratio of drug amount to SBA-15 surface area did not affect drug solid state form or release rate, within the limits of the experiments performed. A relationship between the ratio of drug to SBA-15 and drug-loading efficiency was established; the drug-loading decreased from 91.98 (±6.59) to 69.17 (±10.93) as the drug – silica ratio went from 1 mg: 3 m^2 to 1 mg: 0.82 m^2 when the entire drug amount was loaded in a single processing step. Charnay and co-workers reported previously that successively impregnating silica with ibuprofen solution resulted in increased drug-loads and almost complete mesopore filling (Charnay et al., 2004). It was postulated that successive SC-CO_2 drug-loading steps could increase drug-loading efficiencies compared to a single processing step, without the drug solid state form or release rate being compromised.

While the drug to SBA-15 ratios investigated in chapter 5 did not show any differences in terms of drug solid state form or release rate, it was postulated that there was a limit to the quantity of drug that can be loaded onto silica outside of these ranges, above which there would be a negative impact on these properties. Achieving the maximum drug-load without compromising drug release rate is an important target; increasing the mass of drug loaded onto SBA-15 would for example lower the amount of powder required in an oral dosage form and hence the number of dosage units. In this chapter the maximum drug that could be theoretically hosted within the silica mesopores was calculated based of the measured SBA-15 mesopore volume and the measured drug true density (determined by a gas displacement method). The effect of drug-loading levels at, above and below this level, on subsequent drug physicochemical properties was then evaluated.

In relation to drug release behaviour from drug – silica systems investigated in chapter 4 and 5, it was interesting to note that the maximum percentage drug release was approximately 80% of the total drug, which was reached after 10 minutes and remained steady from 10 – 120 min. A possible explanation for this behaviour was that the release media could not fully access the SBA-15 mesoporous structure. To investigate this phenomenon, drug release experiments were performed and the undissolved drug – SBA-15 powders subsequently recovered by filtration and analysed. The aim was to investigate if any drug remained in the SBA-15 mesopores or was it fully liberated during the release. This is the first study to explicitly investigate the location of drug within the silica matrix during release experiments. The impact of various *in vitro* dissolution media on the extent of fenofibrate release from SBA-15 was also studied. The properties of *in vitro* release media can affect drug release, for example ionizable drugs would be influenced by the media pH while in the case of fenofibrate, it is known that the fenofibrate solubility and hence release is enhanced in media containing increasing amounts of SDS (Jamzad and Fassihi, 2006).

6.2 Results

6.3 Multiple step drug-loading

In chapter 5, three ratios of drug mass (mg) to SBA-15 surface area (m^2) were investigated; these were 1 mg: 3 m^2, 1 mg: 1.24 m^2 and 1 mg: 0.82 m^2. These drug-loading ratios were loaded using a single processing step. In this chapter a theoretical ratio of 1 mg: 1.24 m^2 was loaded over two process steps, while for the 1 mg: 0.82 m^2 sample was loaded over three steps. As stated earlier the rationale behind loading the drug in multiple steps was to increase the drug-loading efficiency. The experimental procedure was described earlier in section 2.5.1.

6.3.1 Drug-loading efficiency

While the % drug load (w/w) increased with each drug-loading step, there were no significant differences in drug-loading efficiencies of the samples prepared by single or multiple steps at equivalent drug – silica ratios (Fig.6.1).

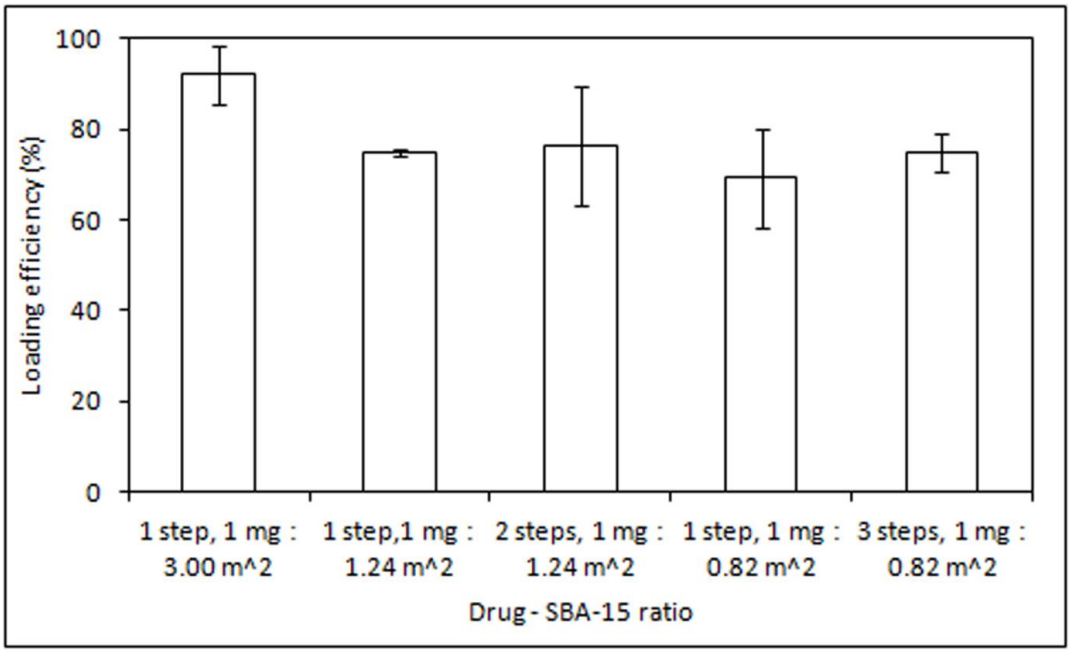

Figure 6.1: Drug-loading efficiency of samples prepared by single versus multiple steps, drug-loading efficiency standard deviations indicated by y-axis error bars (n = 9).

6.3.2 Drug distribution

There was no significant difference between single and multiple drug-loading steps in terms of drug distribution, expressed as % ΔPV for the 1 mg to 1.24 m^2 or 1 mg to 0.82 m^2 samples (Fig.6.2).

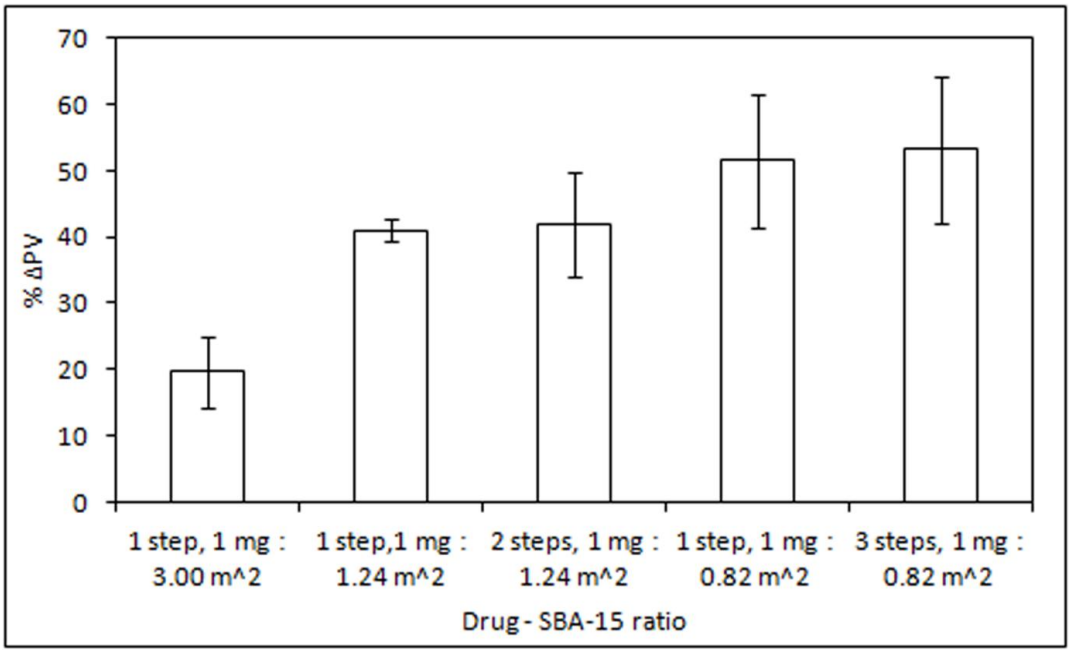

Figure 6.2: Comparison of percentage reduction in pore volume (% ΔPV) of drug – silica samples prepared using single versus multiple loading steps, % ΔPV standard deviations indicated by y-axis error bars (n = 9).

6.3.3 Drug solid state

The solid state of the drug loaded with multiple steps onto the SBA-15 was in a non-crystalline state. No peaks could be observed in the pXRD diffractograms similar to the samples prepared by single step drug-loading (Fig.6.3).

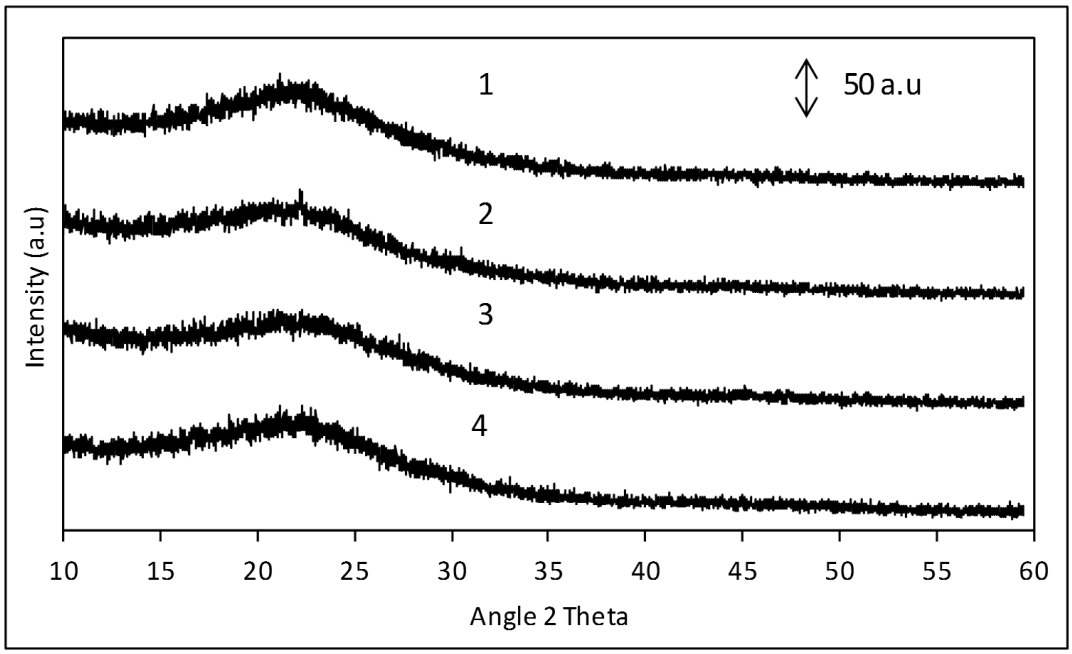

Figure 6.3: pXRD diffractograms of drug – silica samples prepared using: (1) a single step with the 1 mg to 1.24 m^2 ratio, (2) a single step with 1 mg to 0.82 m^2 ratio, (3) 2 steps with 1 mg to 1.24 m^2 ratio and (4) 3 steps with the 1 mg to 0.82 m^2 ratio.

6.3.4 *In vitro* release studies

There were some differences between release profiles when the single and multiple step samples when compared at equivalent drug – silica ratios.

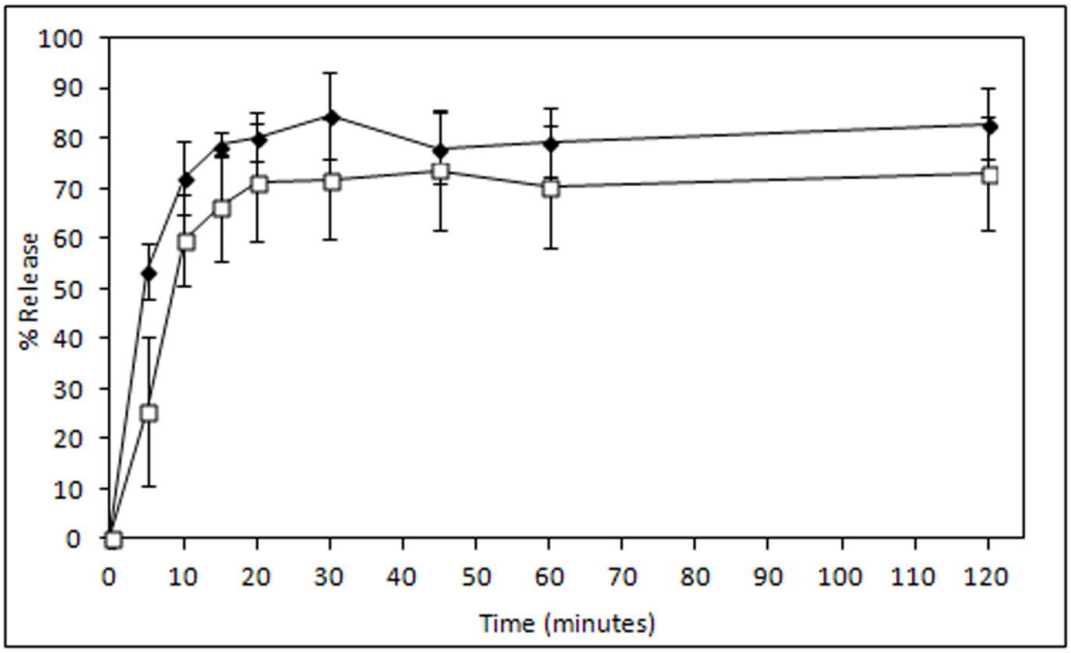

Figure 6.4: Comparison of drug release from (♦) single and (□) multiple step drug-loaded samples at the ratio 1 mg to 1.24 m^2 in 0.3% (w/v) SDS in 0.1M HCl media sample in 0.3% w/v SDS in 0.1M HCl media (mean ± SD, n = 9).

There was a significant difference in drug release between the single and multiple step loaded samples at the 1 mg to 1.24 m^2 drug – silica ratio according to the repeated measures ANOVA.

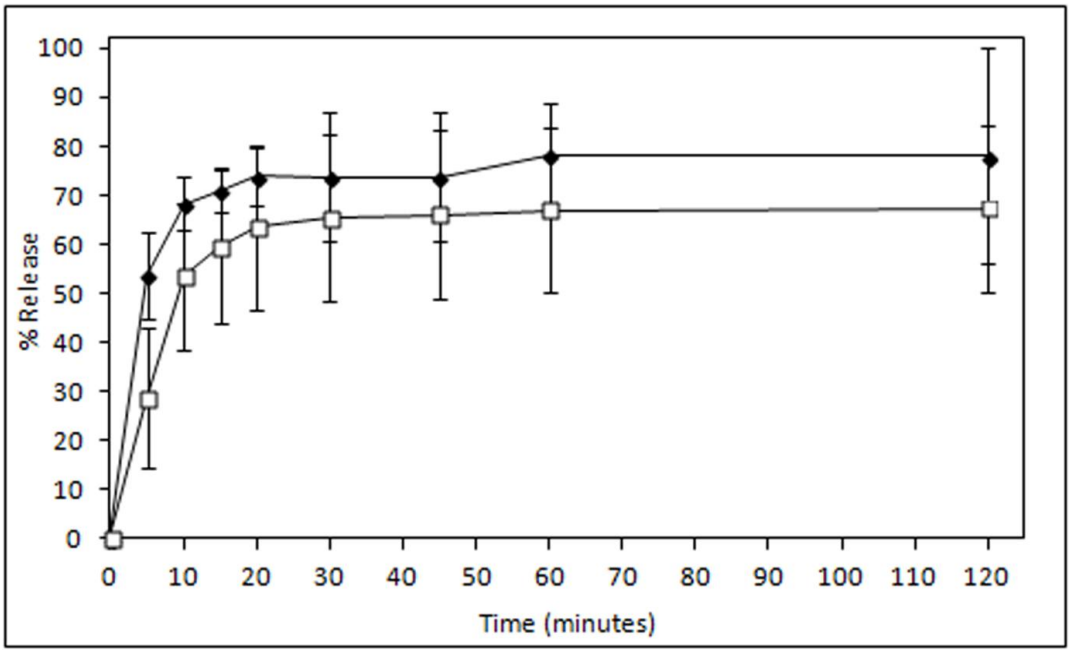

Figure 6.5: Comparison of release profiles of (♦) single and (□) multiple step drug-loaded samples at the ratio 1 mg to 0.82 m^2 in 0.3% (w/v) SDS in 0.1M HCl media sample in 0.3% w/v SDS in 0.1M HCl media (mean ± SD, n = 9).

There was a significant difference in drug release between the single and multiple step loaded samples at the 1 mg to 0.82 m^2 drug – silica ratio according to the repeated measures ANOVA.

6.4 The effect of maximising drug-loading on drug release properties

In this section, the amount of drug that can be loaded onto silica without compromising drug release rate was investigated. The maximum mass of drug that could be theoretically hosted within the silica mesopores was calculated based on the known SBA-15 mesopore volume and the measured drug true density (determined by He pycnometry) using Eq. 2.1 while the % theoretical mesopore fill was

calculated according to Eq. 2.2. The major assumptions of this approach were that (1) the drug will pack into the entire mesopore volume, and there would be no volume lost through voids or blockages due to incomplete drug packing and (2) the true density of powder fenofibrate would be similar to the molecular density of fenofibrate present in the mesopores. The drug – silica system referred to as the 'standard sample' was based on the ratio of 1 mg to 3 m^2 which was investigated in chapters 4 and 5 and contained enough fenofibrate to theoretically occupy 32.50% of the available SBA-15 mesopore volume. The 'maximum sample' contained enough fenofibrate to theoretically fill 99% of the available SBA-15 mesopore volume while the 'excess sample' contained enough fenofibrate to theoretically fill 286% of the available SBA-15 mesopore volume. Section 2.5.2 contains more information on the preparation of these samples and the calculations involved.

6.4.1 Drug-loading

The % drug (w/w), % drug-loading efficiency and moisture content of the standard, maximum and excess samples are displayed below, Table 6.1

Table 6.1: % drug, drug-loading efficiencies and % moisture for standard, maximum and excess samples, standard deviations in brackets (n = 9).

Variable	SBA-15	Standard	Maximum	Excess
% drug (w/w)	N/A	19.31 (±2.22)	38.52 (±4.36)	49.26 (±2.65)
Drug-loading efficiency (%)	N/A	88.89 (±10.21)	83.84 (±9.49)	70.91 (±1.16)
% Moisture (w/w)	10.00 (±2.88)	3.35 (±0.27)	1.54 (±0.41)	1.23 (±0.30)

There was a significant increase in % drug (w/w) as the amount of drug processed with the SBA-15 increased. However there was a significant decrease in the drug-loading efficiency of the excess sample compared to the standard and maximum samples. The presence of drug loaded onto SBA-15 can be detected from the changes of its surface properties, one of which is the lower moisture content after drug-loading. A statistically significant reduction in the moisture content of SBA-15 after loading with fenofibrate was observed in the standard, maximum and excess samples. While the standard sample had significantly higher moisture than the maximum and excess sample, there was no significant difference between the maximum and excess samples in terms of moisture content.

6.4.2 Drug distribution

A representative SEM image of the 'standard sample' is displayed below (Fig.6.6). It was not possible to observe any fenofibrate particles in this sample; it appeared that the fenofibrate had been deposited into the SBA-15 mesopore structure.

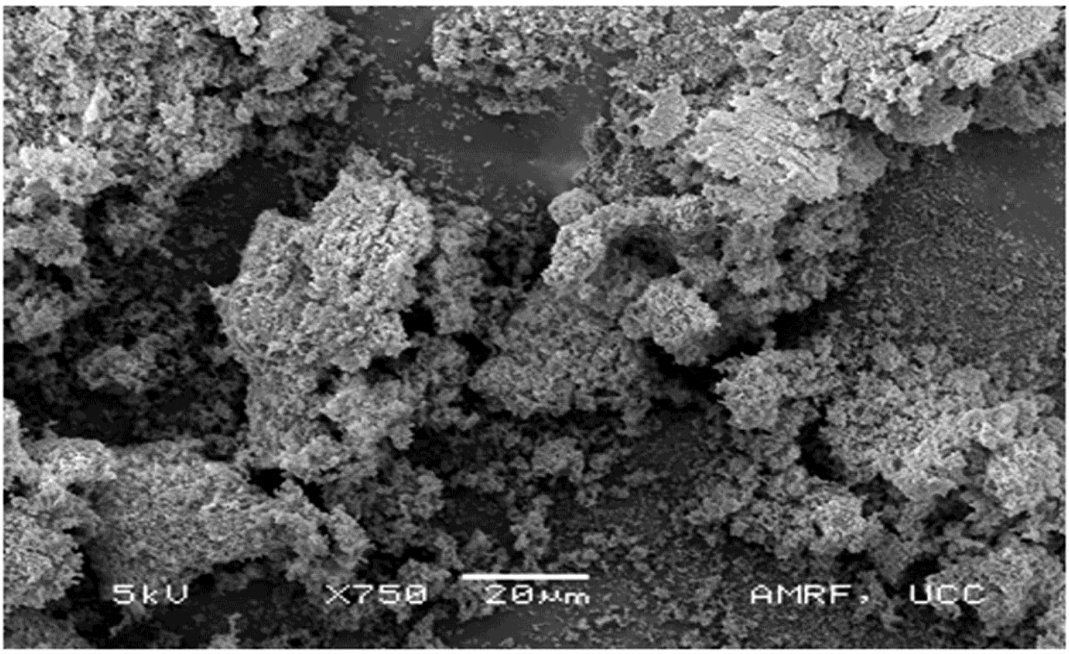

Figure 6.6: SEM image of the 'standard sample' with magnification of X750.

The SEM image of the 'maximum sample' showed fenofibrate particles (Fig.6.7). The visible drug particle appeared to be less than 50 µm in diameter.

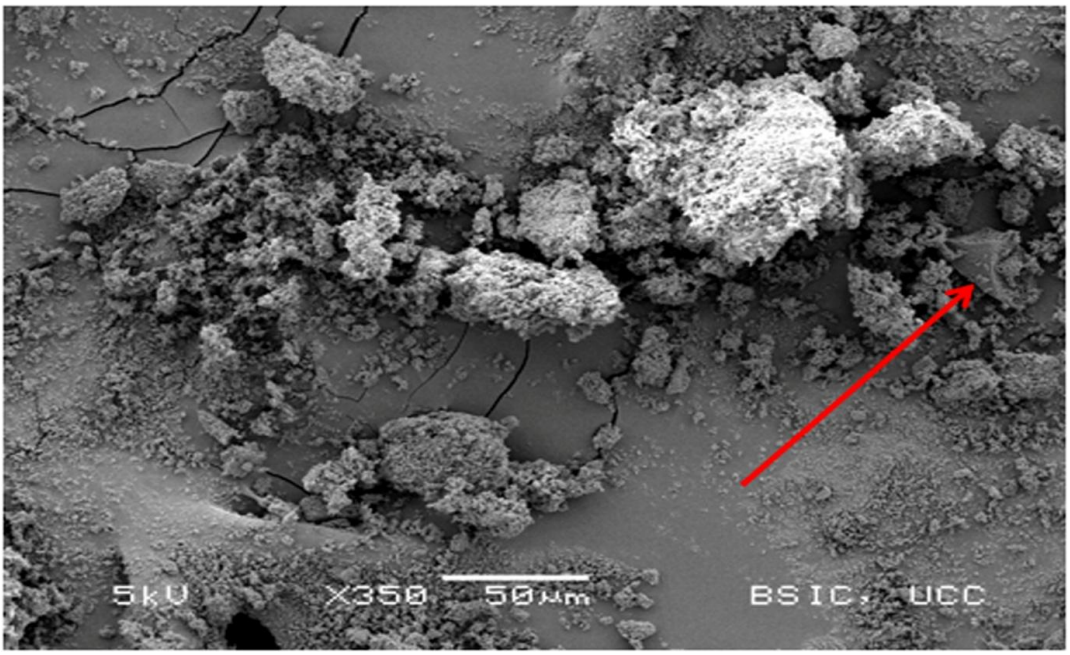

Figure 6.7: SEM image of the 'maximum sample' at X350 magnification.

In the ‘excess sample’, drug particles were also observed throughout the SEM images. A large isolated fenofibrate particle was observed in Fig. 6.8a, while several smaller particles were visible in Fig. 6.8b.

A 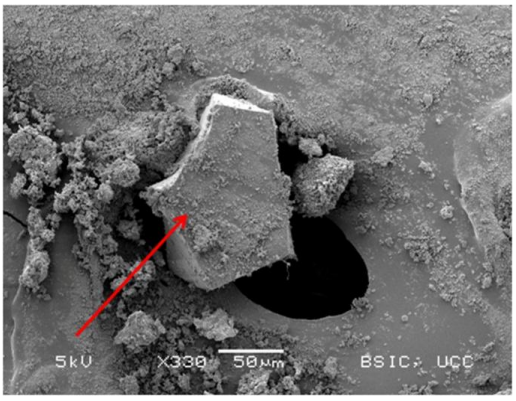

B 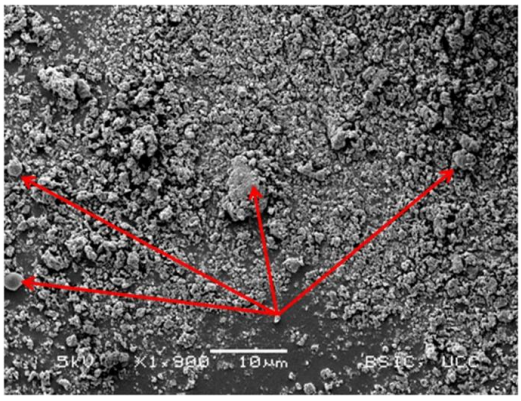

Figure 6.8: SEM images of ‘excess sample’ at a magnification (A) X330 and (B) X1900.

A type IV gas adsorption isotherm indicative of mesoporous materials (Brunauer et al., 1938) was observed in all drug-loaded samples (Fig.6.9).

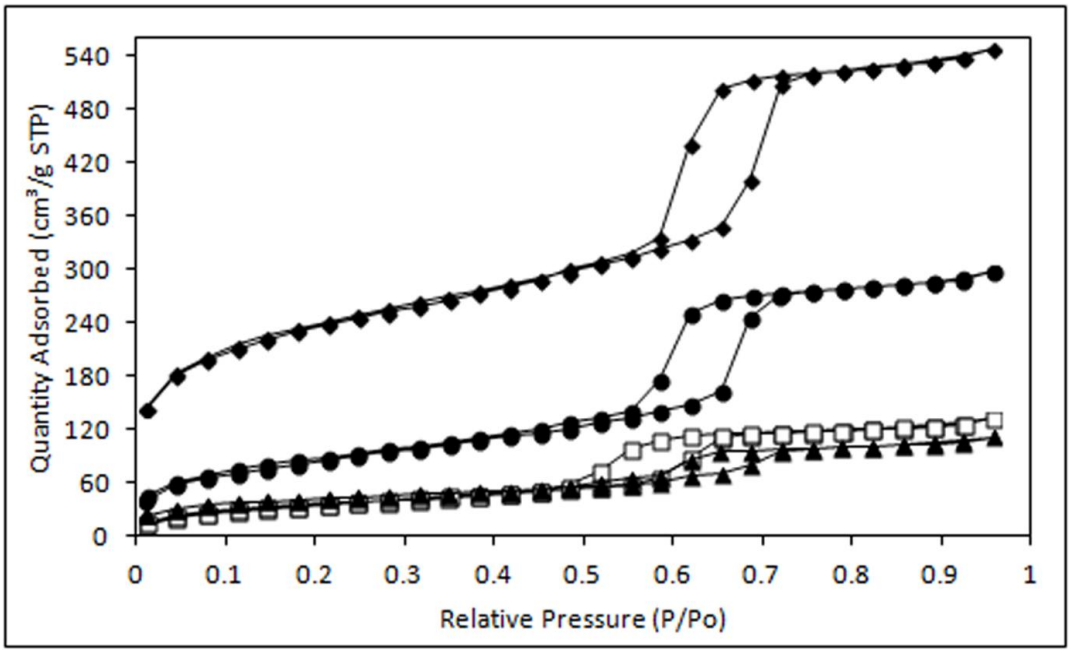

Figure 6.9: BET isotherms of (♦) unprocessed SBA-15, (●) standard, (□) maximum and (▲) excess samples.

The closure point of the hysteresis loop was reduced from 0.5 P/Po to 0.45 P/Po for the standard and maximum samples, an indication that there was a reduction in the mesopore size distribution. The reduction in the amount of N_2 adsorbed highlighted the large reductions of the specific surface area and mesopore volume. The surface and mesopore properties of unprocessed SBA-15, standard, maximum and excess samples are displayed below, Table 6.2.

Table 6.2: Surface area, mesopore volume and % ΔPV for standard, maximum and excess samples, standard deviations in brackets (n = 9).

Variable	SBA-15	Standard	Maximum	Excess
Specific surface area (m^2/g)	833.22 (±48.13)	305.47 (±4.49)	127.96 (±32.99)	33.62 (±13.39)
Mesopore volume (cm^3/g)	0.68 (±0.02)	0.41 (±0.02)	0.19 (±0.05)	0.05 (±0.02)
% ΔPV	N/A	25.91 (±3.74)	55.82 (±8.07)	84.34 (±4.98)

There were significant differences in specific surface area and mesopore volume across all samples. The % ΔPV increased significantly when the amount of drug present increased across all the standard, maximum and excess samples. However, complete mesopore filling was not achieved for either the maximum or excess samples, as evidenced by the fact that there remained a residual mesopore volume, which could also be observed (Fig.6.10).

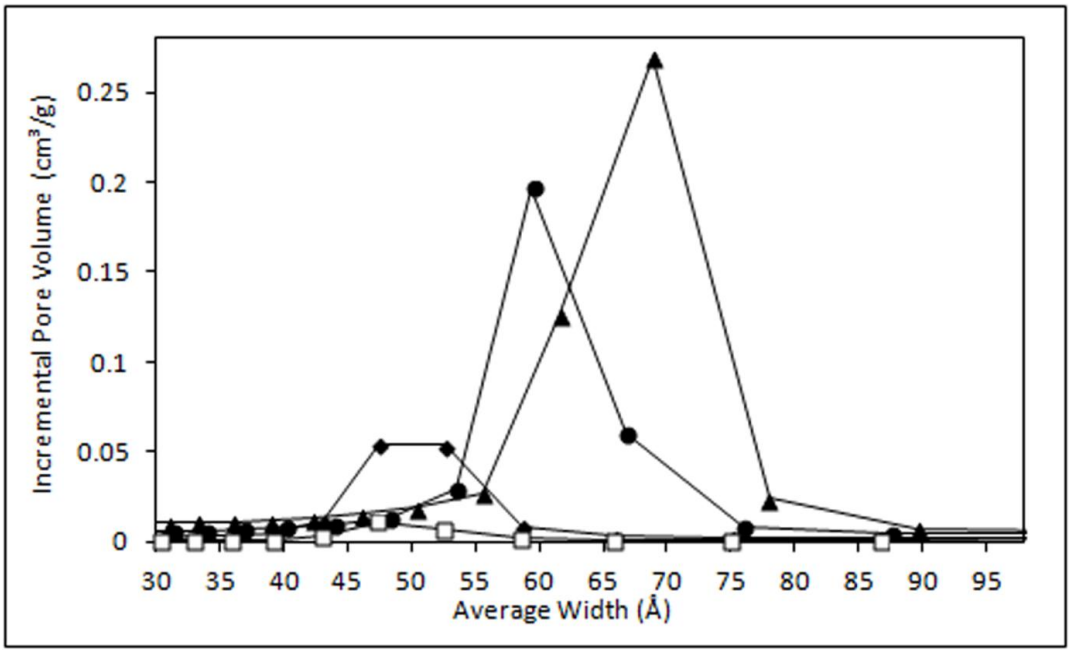

Figure 6.10: Pore size distribution of (▲) unprocessed SBA-15, (●) standard, (♦) maximum and (□) excess samples.

The mean mesopore size of SBA-15 was 50.70 Å (±0.20) while it was 52.39 Å (±1.86) and 49.93 Å (±0.29) for the standard and maximum samples respectively; there was no significant differences between their mean mesopore sizes (Fig.6.11). However in the case of the excess sample, there was a significant increase in mean mesopore size to 61.18 Å (±6.90) compared to unprocessed SBA-15.

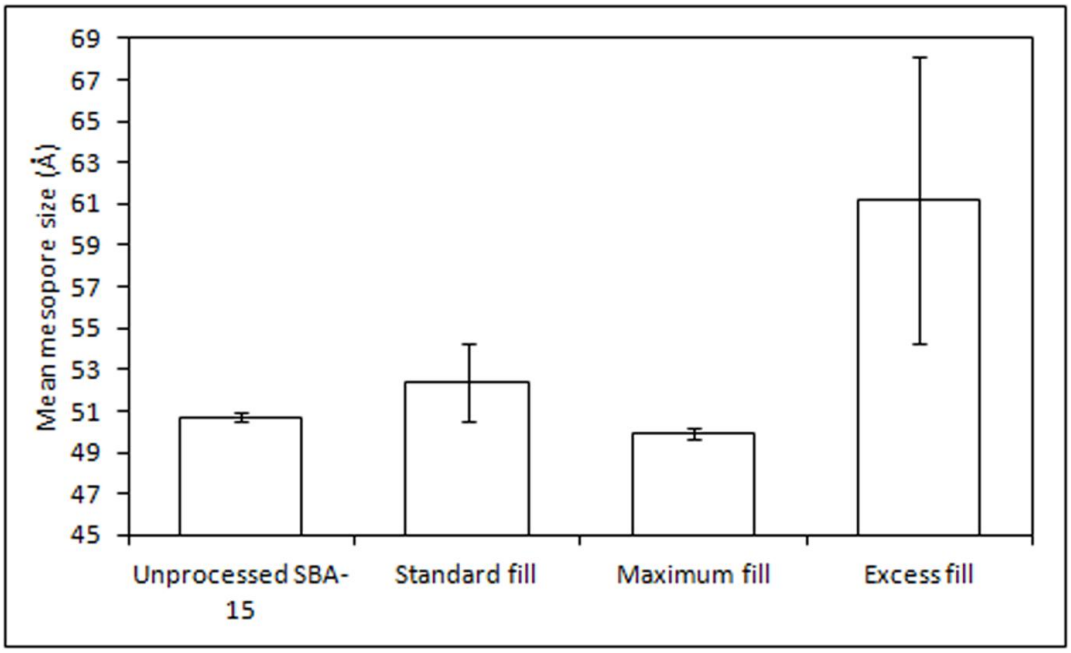

Figure 6.11: Mean mesopore sizes for unprocessed SBA-15, standard, maximum and excess samples; mean mesopore size standard deviations indicated by y-axis error bars (n = 6).

6.4.3 Solid state properties

There was no evidence of drug crystallinity observed in the pXRD diffractogram for the standard sample. There was strong evidence for the presence of crystalline drug in the pXRD diffractograms of the maximum and excess samples (Fig. 6.12). In the excess sample, peaks were present at angles 14, 15, 16 and 23^{o}. These peaks agreed with those observed for unprocessed crystalline fenofibrate in chapter 3.

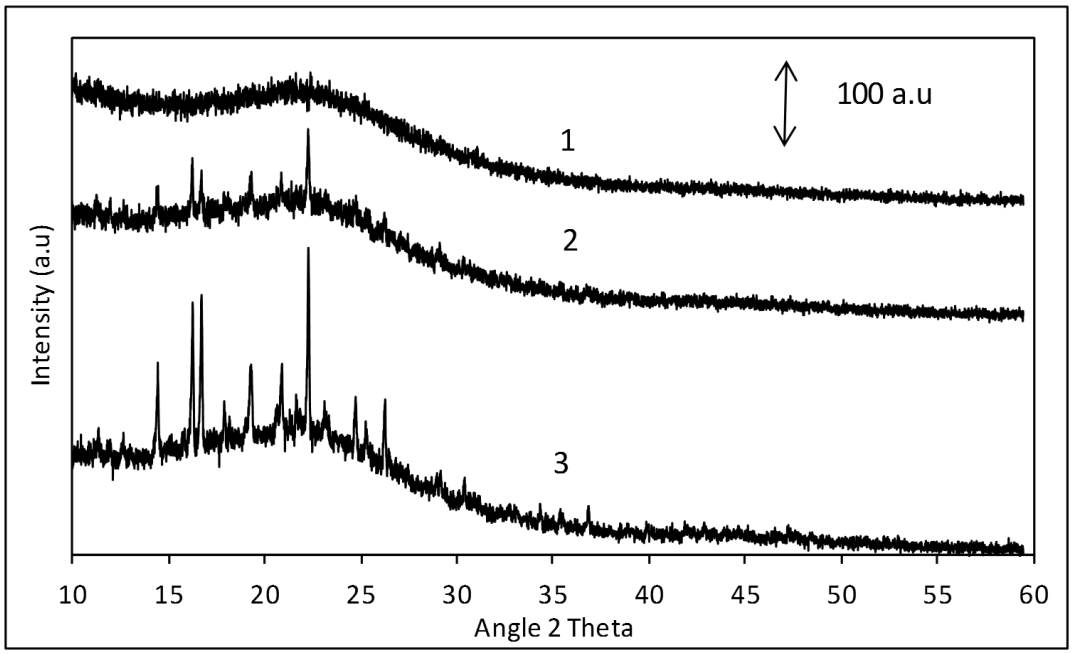

Figure 6.12: pXRD diffractograms of (1) standard, (2) maximum and (3) excess samples.

The DSC thermograms of the maximum and excess samples also displayed evidence of crystallinity. There was a visible endotherm in the thermal region corresponding to fenofibrate's melting point, which was larger in the excess sample, compared to the maximum sample. The standard sample did not display evidence of a melting endotherm. There was no evidence in the form of T_g or T_{cr} to support the presence of an amorphous drug phase in any of the sample DSC thermograms observed (Fig.6.13) However, as previously mentioned the melting of frozen water in the SBA-15 mesopores occurs over the range of -20 – -12 ^oC and may have confounded the detection of the drug T_g in these samples.

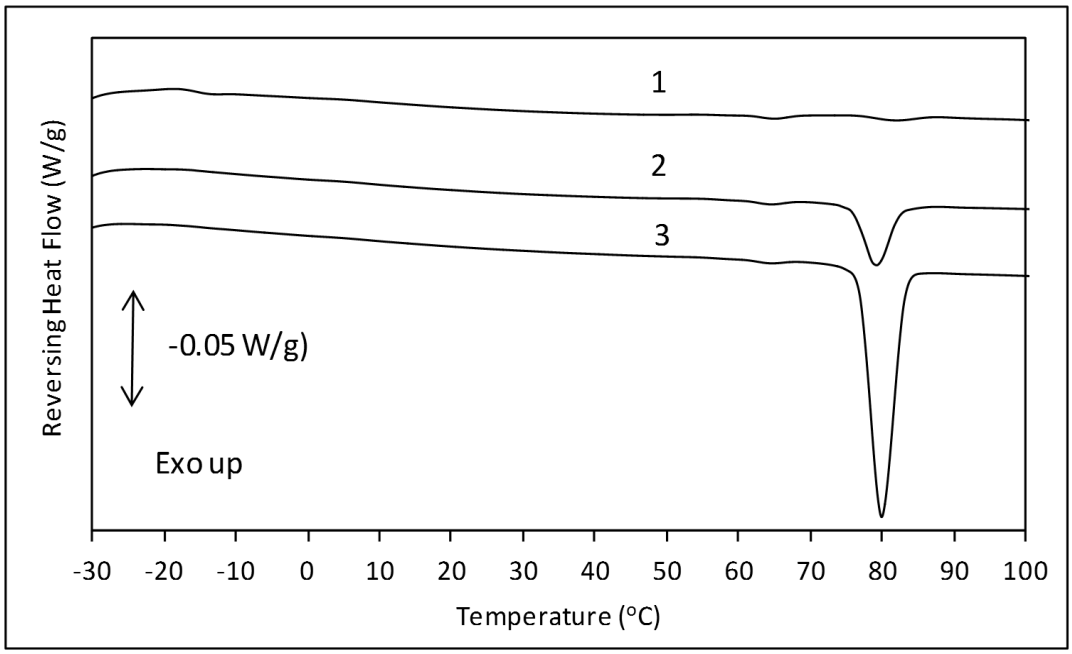

Figure 6.13: DSC thermograms of (1) standard, (2) maximum and (3) excess samples.

6.4.4 *In vitro* release

The maximum and excess samples had a slower release rate and lower amount of drug release after 2 h compared to the standard sample (Fig. 6.14).

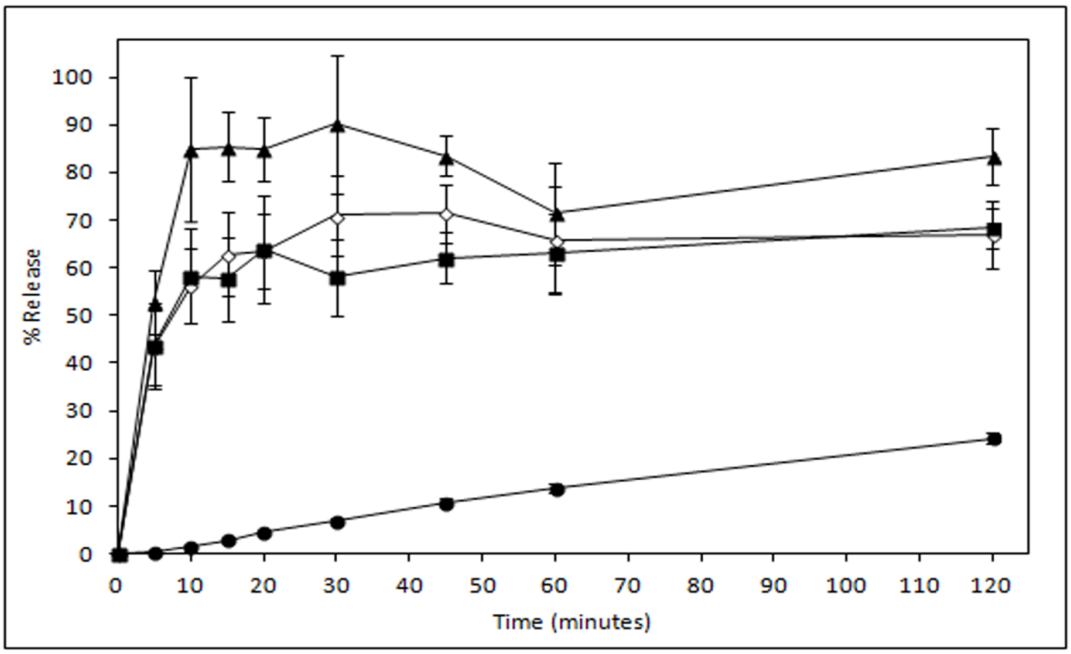

Figure 6.14: Release profiles of (●) unprocessed fenofibrate, (▲) standard, (◊) maximum and (■) excess samples in 0.3% (w/v) SDS in 0.1M HCl media sample in 0.3% w/v SDS in 0.1M HCl media (mean ± SD, n = 9).

The drug release profiles for both the maximum and excess samples were significantly reduced according to the f_1, modified f_1 and f_2 tests, when compared to the standard sample. There was a singficant decrease in drug release from the maximum sample compared to the standard sample according to the repeated measures ANOVA test. This was also the case for the excess sample compared to the standard sample. All samples had significantly higher rate and extent of drug release compared to unprocessed fenofibrate over 2 h.

6.5 Investigating drug release behaviour from drug – SBA-15 systems

As mentioned previously in chapters 4 and 5, the maximum percentage release of fenofibrate from drug – SBA-15 systems in a solution of 0.3% w/v SDS and 0.1M HCl solution (sink conditions) was approximately 80% after 2 h. In an attempt to identify why 80% seemed to be the maximum drug percentage release, release experiments were stopped after 15 min or 24 h and the powders were recovered and characterised after exposure to release media. *In vitro* release experiments were also performed in alternative release media, including 1.5% w/v SDS in deionised water, which was the recommended USP dissolution medium for fenofibrate (USP, 2013), 1.5% w/v SDS in 0.1M HCl solution and 0.3% w/v SDS in deionised water.

6.5.1 Characterisation of powders recovered after release studies

The release media was filtered at 15 min or 24 h, oven dried for 3 days and the recovered solid residue analysed. The sample investigated was SC-CO_2 processed fenofibrate – SBA-15 with the ratio of 1 mg to 3 m^2 (standard sample). The drug content (%), % drug recovered calculated from Eq.2.9 and % drug release of the 'standard sample' prior to release experiments and the powders recovered from the release media after 15 min and 24 h are displayed below, Table 6.3.

Table 6.3: % drug (w/w), % drug recovered (w/w) and % release of powders recovered after 15 min and 24 h in release media, standard deviations in brackets.

Sample	% Drug (w/w) (n = 9)	% recovered (w/w)	% Release(n = 9)
Standard sample	18.57 (±1.58)	N/A	N/A
Recovered after 15 min	6.96 (±0.68)	38.81 (±6.89), (n = 6)	85.42 (±7.24)
Recovered after 24 h	7.45 (±1.96)	40.17 (±8.75), (n = 9)	45.73 (±7.02)

The % drug release was unexpectedly found to decrease from over 80% at 2 h to 45.73% (±7.02) after 24 h. However, this seemed to match with the % drug recovered after filtration, which suggested that the drug was not degraded during the release experiment. The surface and porosity properties of unprocessed SBA-15, the 'standard sample' and the powders recovered from the release media after 15 min and 24 h are shown, Table 6.4.

Table 6.4: Surface and porosity properties of unprocessed SBA-15, standard sample and powders recovered after 15 min and 24 h from release media, standard deviations in brackets.

Sample	S.S.A (m^2/g)	% ΔSSA	P.V. (cm^3/g)	% ΔPV
SBA-15	833.22 (±48.13), (n = 9)	N/A	0.68 (±0.02), (n = 9)	N/A
Standard sample	305.47 (±4.49), (n = 9)	62.39 (±17.86), (n = 9)	0.41 (±0.02), (n = 9)	25.91 (±3.74), (n = 9)
Recovered after 15 min	548.63 (±31.65), (n = 3)	29.22 (±4.41), (n = 3)	0.55 (±0.03), (n = 3)	13.16 (±4.75), (n = 3)
Recovered after 24 h	606.95 (±76.17), (n = 3)	21.29 (±10.52), (n = 3)	0.66 (±0.10), (n = 3)	-5.53 (±16.87), (n = 3)

There was no significant difference between both recovered powders in terms of specific surface area; interestingly the 24 h recovered powder did have a significantly higher mesopore volume than the powder recovered at 15 min. In fact, there was no significant difference between the mesopore volume of unprocessed SBA-15 and the powder recovered after 24 h release. This implied that at 15 min, some of the drug was still in the SBA-15 mesopores, but after 24 h it had been fully liberated. This indicated that the drug inside the SBA-15 mesopores was fully accessible to the release media. The results of the % ΔPV also highlighted this point. It can be seen that the powder recovered after 24 h had a similar pore size distribution to the unprocessed SBA-15, pore size range approximately 4.5 – 8.5 nm (Fig. 6.15).

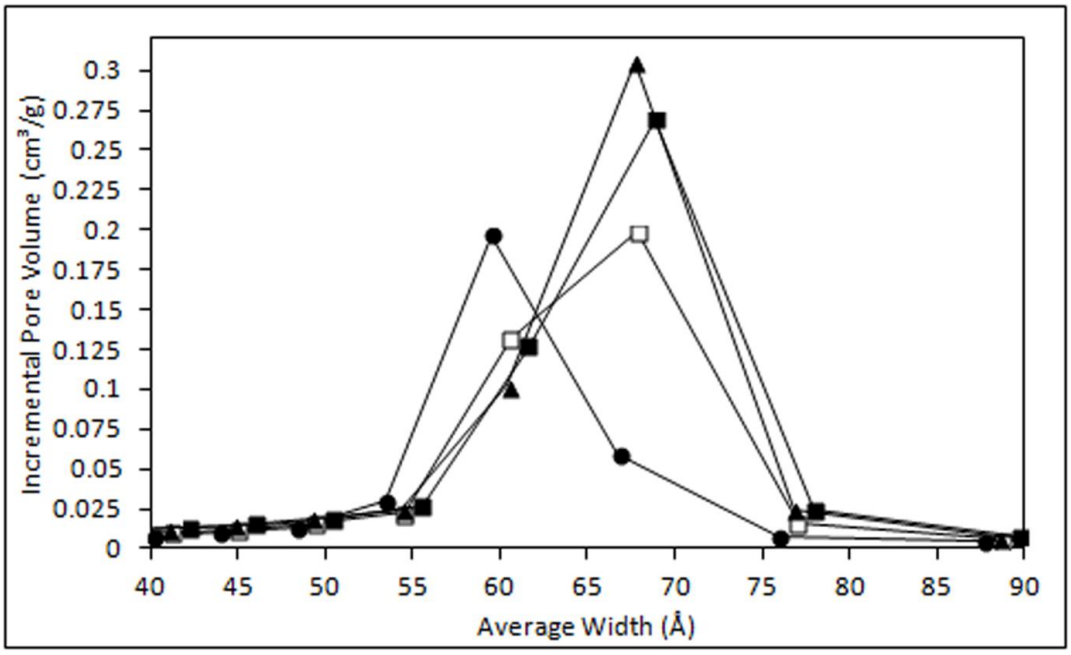

Figure 6.15: Pore size distribution of (■) unprocessed SBA-15, (●) standard sample and powders recovered from release media after (□) 15 min and (▲) 24 h.

The sample recovered after 15 min in release media seemed to have slightly reduced pore size distribution, from 4.5 – 7.5 nm. This is further evidence that some drug was in the mesopores at 15 min.

6.5.2 Effect of *in vitro* media on drug release from SBA-15

The fact that the drug release decreased from over 85.42% (±7.24) at 2 h to 45.73% (±7.02) after 24 h in 0.3% w/v SDS/0.1M HCl solution highlighted that it was possible that the release medium was influencing the release of fenofibrate from SBA-15. In this section, the dissolution/release media investigated were 0.3% w/v SDS and 1.5% SDS in deionised water and 0.3% w/v SDS and 1.5% SDS w/v in 0.1M HCl solution. The solubility of fenofibrate in dissolution media can be altered by the addition of SDS; the greater the amount of SDS in the media, the higher fenofibrate's solubility (Jamzad and Fassihi, 2006). The solubilities of unprocessed fenofibrate in the various media investigated after 48 h at 37 ^{o}C are shown in Table 6.5.

Table 6.5: Solubilities of unprocessed fenofibrate in different media after 48 h at 37 ^{o}C, standard deviations in brackets (n = 9).

Dissolution media	Media pH	Solubility (µg/ml)
SDS 0.3% w/v in deionised water	6.60 – 6.75	20.68 (±3.57)
SDS 1.5% w/v in deionised water	7.84 – 8.83	525.05 (±21.99)
SDS 0.3% w/v in 0.1M HCl solution	1.35 – 1.38	67.21 (±4.81)
SDS 1.5% w/v in 0.1M HCl solution	1.37 – 1.38	256.00 (±30.21)

Interestingly, the effect of HCl on fenofibrate solubility was positive at the lower SDS concentration but negative at the higher SDS concentration. The media containing higher amounts of SDS resulted in higher fenofibrate solubilities. The critical micelle concentration (CMC) refers to the concentration of a surfactant above which micelles form (McNaught and Wilkinson, 1997) and is an important parameter affecting drug solubility in solutions containing SDS. The CMC of SDS in deionised water was previously reported to be 0.24% w/v (8 mM) (Mukerjee and Mysels, 1972). In this work, it was determined that the CMC of SDS in deionised water at 37 ^{o}C was 0.21% w/v SDS while in 0.1M HCl solution at 37 ^{o}C it was 0.023% w/v SDS. This could explain why there was higher fenofibrate solubility in 0.3% w/v SDS/0.1M HCl solution than in 0.3% w/v SDS/deionised water. The dissolution of unprocessed fenofibrate in the various dissolution media up to 2 h is shown below (Fig. 6.16).

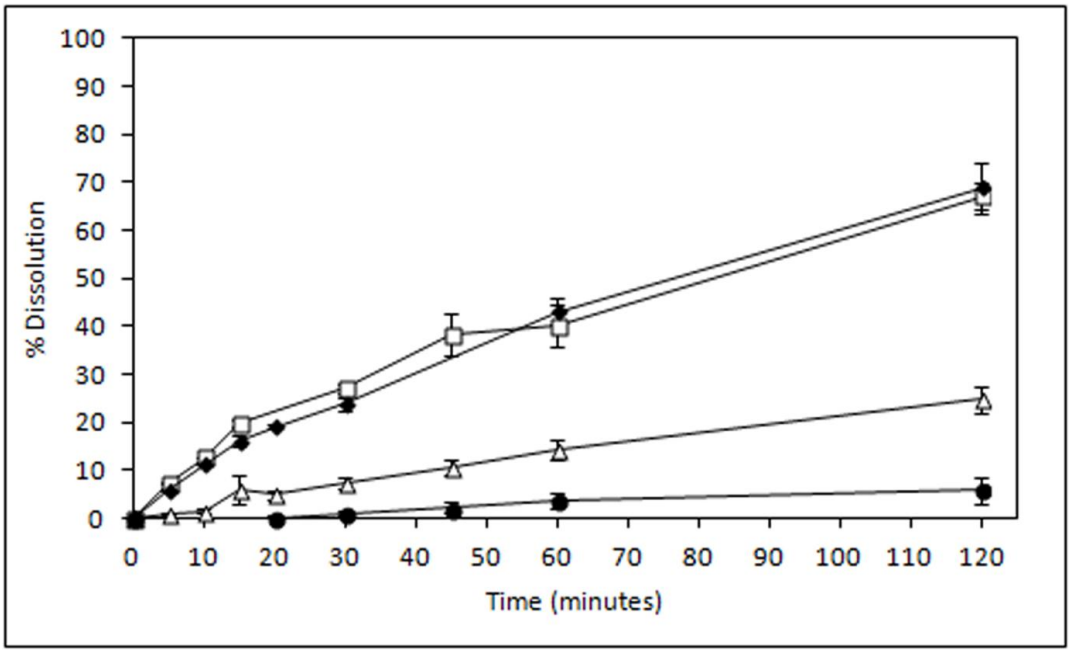

Figure 6.16: Unprocessed fenofibrate dissolution over 120 min in (□) 1.5% w/v SDS/ 0.1M HCl solution, (♦) 1.5% w/v SDS /deionised water, (Δ) 0.3% w/v SDS/ 0.1M HCl solution and (●) 0.3% w/v SDS /deionised water sample (mean ± SD, n = 3).

The lowest drug dissolution was observed in 0.3% w/v SDS/deionised water, with the highest dissolution achieved in 1.5% w/v SDS/deionised water and 1.5% w/v SDS/0.1M HCl solution. The extent of drug dissolution in 0.3% w/v SDS in deionised water was significantly less than that in all other media over 2 h according to the f_1, modified f_1 and f_2 tests. It was also seen in the repeated measures ANOVA test that the dissolution profile of drug in 0.3% w/v SDS/deionised water was singicantly less than that in 0.3% w/v SDS/0.1M HCl solution. There was a significant effect of SDS concentration on drug dissolution rate which was expected. There was no significant difference between the dissolution profiles obtained from 1.5% w/v SDS/deionised water and 1.5% w/v SDS/0.1M HCl solution over 2 h when analysed by the f_1, modified f_1 and f_2 tests. There was a significant increase in

percentage release between 2 to 24 h for unprocessed fenofibrate in all the media except in the 1.5% w/v SDS/0.1M HCl solution (Fig.6.17).

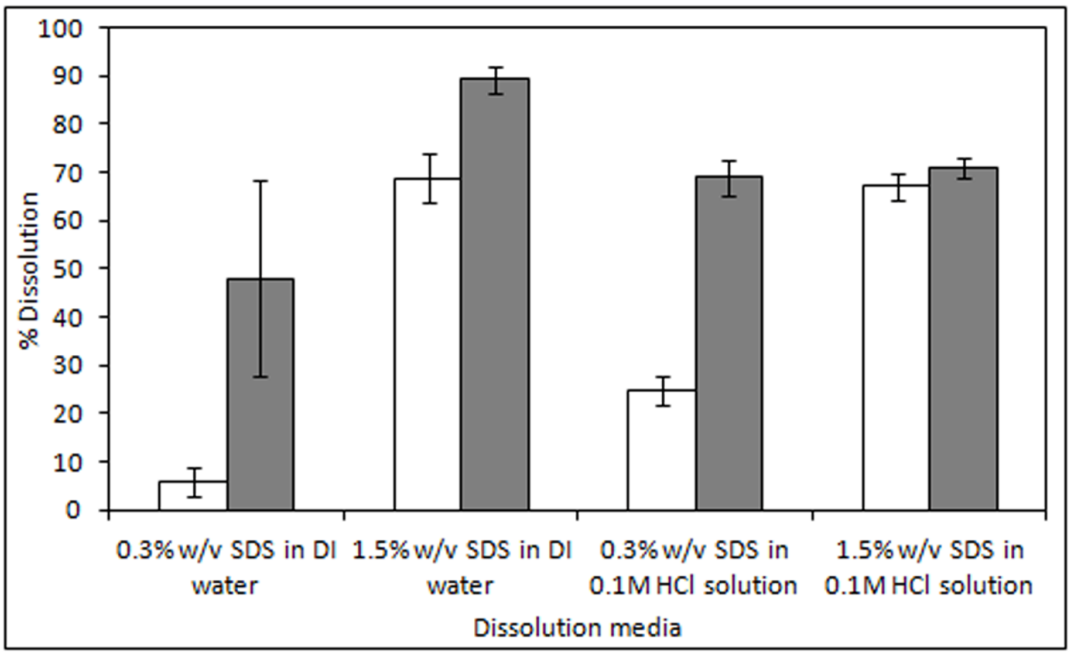

Figure 6.17: Unprocessed fenofibrate % dissolution at 2 h (clear column) and 24 h (dark column) (mean ± SD, n = 3).

While unprocessed fenofibrate was highly susceptible to the properties of the dissolution media; after SC-CO_2 processing fenofibrate with SBA-15 (standard sample), the influence of the release media on the drug release properties was decreased (Fig.6.18).

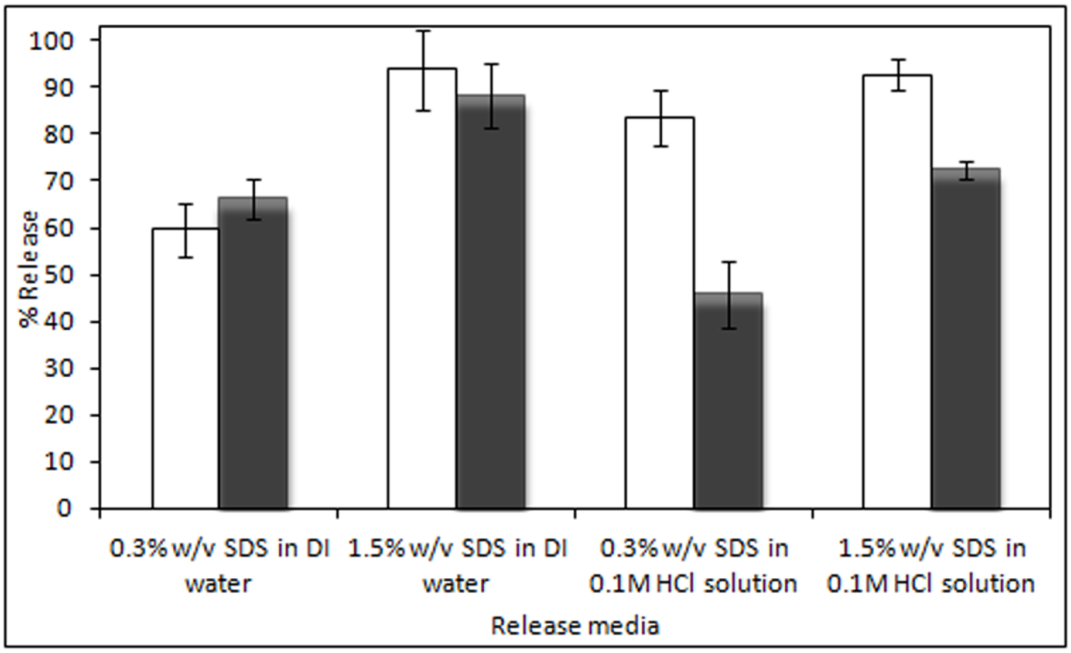

Figure 6.18: Fenofibrate release from SC-CO_2 processed drug – SBA-15 samples (1 mg: 3 m^2) over 120 min in (□) 1.5% w/v SDS / 0.1M HCl solution, (♦) 1.5% w/v SDS /deionised water, (Δ) 0.3% w/v SDS /0.1M HCl solution and (●) 0.3% w/v SDS /deionised water (mean ± SD, n = 9).

The effect of 0.1M HCl in the release media was profound; the percentage release of drug from the SC-CO_2 processed sample decreased from 2 to 24 h, while in media with no 0.1M HCl, there was no significant change from 2 to 24 h.

6.6 Discussion

The aim of this chapter was to optimise the drug-loading and release of SC-CO_2 processed fenofibrate – SBA-15. Multiple step drug-loading was employed in order to achieve an increased drug-loading efficiency in comparison with single step drug-loading. While the drug load increased after each step as expected, the multiple step approach did not yield an increase in drug-loading efficiency compared to loading an equivalent amount of drug in a single step. The drug was stabilised in a non-crystalline form across all loading steps. This result corresponded to previous results obtained where fenofibrate was stabilised in a non-crystalline form, as mentioned in chapters 4 and 5. The significant improvement in drug release compared to unprocessed fenofibrate has already been explained in chapter 4. The drug release from the multiple step drug-loaded samples was significantly less than that of single step samples processed with equivalent drug – silica ratios. It is difficult to understand why this should be so as there was no observable difference in terms of drug solid state or release between the single and multiple step samples. It should be stated that after 20 min, there were no significant differences in drug release between the single and multiple step samples.

To date, there has not been any report of how to calculate how much fenofibrate could be loaded into a known volume of SBA-15 mesopores, while ensuring that the drug is in a non-crystalline state with rapid release. In this chapter, the drug's true density and silica mesopore volume were used to determine the amount of drug that could be accommodated in the mesopores. In the maximum sample, there was enough fenofibrate to completely fill the SBA-15 mesopores; however this did not occur as there was still mesopore volume measured by gas adsorption (BET). There were free drug particles observed on SEM images of both the maximum and excess

samples, which resulted in significant drug crystallinity compared to the 'standard sample'. In chapter 4, it was seen that physically mixing fenofibrate and SBA-15 did not result in amorphous fenofibrate as the fenofibrate was not inside the mesopores. In the physical sample from chapter 4 and the maximum and excess samples in this chapter, the evident drug crystallinity lowered the rate and extent of drug release signifciantly. The moisture content of the maximum and excess samples was also significantly less compared to the standard sample; these samples were less hydrophilic which acted to reduce drug release. This work highlighted that loading drug based on its true density and the available silica mesopore volume was not a promising approach, because of the significant crystallinity and consequent reduction in the rate and extent of drug release. Perhaps, an approach utilising fenofibrate molecular density may offer a possible solution to this problem and could be an object worth pursuing, however this would be assuming that fenofibrate molecular density would not change on mesopore confinement.

The maximum drug release obtained from the SC-CO_2 processed drug – silica samples (standard sample) in the 0.3% w/v SDS/0.1M HCl solution was approximately 80% after 15 min and remained steady up to 2 h. The extent of release reduced to approximately 45% after 24 h. Analysis of the drug – silica powders recovered from the release media suggested that after 15 min, some of the drug was located inside the SBA-15 mesopores, but that by 24 h the majority of drug was outside the mesopores. This was supported by the surface and porosity results of these samples which showed a significant difference between the mesopore volume of unprocessed SBA-15 and the drug – silica powder recovered after 15 min, whereas there was no significant difference between unprocessed SBA-15 and the

drug – silica powder recovered after 24 h. The drug was not degraded during the release experiments as it was recovered with the SBA-15 afterward.

The influence of the *in vitro* release media on drug release was investigated to determine why the drug release was observed to decrease in 0.3% w/v in 0.1M HCl solution. Across all media investigated, the drug release rate from drug – silica samples was more rapid and with a greater extent compared to unprocessed fenofibrate. As expected, fenofibrate solubility and release increased as the SDS concentration increased (Jamzad and Fassihi, 2006). Maximal drug release (100%) was obtained in 1.5% w/v SDS/ deionised water after 10 min and was maintained for 24 h. While 100% drug release was obtained in 1.5% w/v SDS/0.1M HCl solution, the release decreased between 2 and 24 h, interestingly this decrease in the quantity of drug released was only observed in media containing 0.1M HCl, and was more pronounced in the media with lower SDS concentration. While mesoporous silica has been documented as an adsorbent material that could remove pollutants from water (Walcarius and Mercier, 2010), it was felt that the observed decrease of fenofibrate release was not due to SBA-15 re-adsorption of the drug because it only occurred in media containing 0.1M HCl. It has been reported that negatively charged SDS micelles react with hydrogen ions to produce dodecyl sulfonic acid (DSA) and sodium chloride (NaCl) (Bayrak, 2003). This reaction would reduce the number of SDS micelles in solution and could potentially lead to re-crystallisation of the drug out of solution. It was also established that the CMC of SDS in 0.1M HCl solution at 37 ^{o}C was lower than the CMC of SDS in deionised water, which facilitated greater fenofibrate solubility and drug release in 0.3% w/v SDS/ 0.1M HCl compared to 0.3% w/v SDS. Jain and co-workers reported the general equation for micellar concentration,

Equation 6.1: $S_{tot} = S_w + kC_{mic}$

Where S_{tot} is the total molar solubility of the solute, S_w is the water solubility of the solute, k is the molar solubilisation capacity of the surfactant and C_{mic} is the total surfactant concentration minus the CMC (Jain et al., 2004). This equation demonstrated that a higher C_{mic} in the media containing 0.1M HCl compared to the media without 0.1M HCl would prevail because the CMC was lower in the media containing the 0.1M HCl.

Another factor at play is the surface charge of silica across various pH values. The point of zero charge of silica has been reported to lie between pH 1.7 – 3.5 (Kosmulski, 2001). Below a pH of 1.7, the silica surface is positively charged while above pH 3.5 the silica surface is negatively charged. In the media containing 0.1M HCl, the SBA-15 is positively charged and potentially able to attract the negatively charged SDS micelles. These results highlight the many interrelated factors to be considered in determining fenofibrate release from SBA-15 *in vitro*.

6.7 Summary

The application of multiple SC-CO_2 drug-loading steps was investigated and found not to influence drug-loading efficiency or solid state; however it did slow down the release rate compared to single step loading over the first 15 min. Loading the maximum drug theoretically possible based on SBA-15 mesopore volume and fenofibrate true density negatively impacted drug release due to the presence of crystalline drug outside the SBA-15 mesopores, the reduced effective surface area of drug in contact with the release medium and reduced hydrophilic nature of the

these samples. The use of the drug true density to calculate the maximum drug that can be hosted within the SBA-15 mesopores would not be recommended, perhaps, a more appropriate method would be to apply the molecular drug density.

The release medium can profoundly influence drug release behaviour from SBA-15; maximal drug release was only achieved in 1.5% w/v SDS in deionised water and 1.5% w/v SDS in 0.1M HCl solution. In the media containing 0.1M HCl, it was observed that the release declined from 2 to 24 h for the SC-CO_2 processed drug – silica samples which could be due to a number of factors including the reaction of SDS with HCl and interaction between SBA-15 and SDS at low pH.

7 General Discussion

7.1 Introduction to this discussion

The aim of this thesis was to enhance the dissolution rate of the poorly water-soluble drug, fenofibrate by exploiting the high surface area carrier, mesoporous silica (SBA-15). The material properties and advantages of mesoporous silica for oral drug delivery have already been discussed earlier in the introduction to this thesis. As mentioned in the introductory chapter, the objectives of this research were to:

- Enhance fenofibrate release through the application of the high surface area carrier mesoporous silica (SBA-15),
- investigate various processing methods to load fenofibrate onto SBA-15 and determine what impact the loading process had on fenofibrate release from SBA-15,
- investigate how SC-CO_2 processing conditions influenced drug-loading and release from fenofibrate - SBA-15 systems and
- investigate physicochemical factors influencing drug release from fenofibrate – SBA-15 systems.

The objective of this general discussion is to provide an overarching discussion how drug release can be enhanced from SBA-15 in the light of the variables investigated and results presented in this thesis. Therefore, this discussion will aim to consider the results across the all the chapters in terms of how drug release was enhanced after drug-loading into/onto mesoporous silica:

- how the drug solid state affected release properties and

- how drug distribution within the silica matrix affected both drug solid state and release.

7.2 Enhancement of fenofibrate release

In every experiment where fenofibrate and SBA-15 were processed together, there was an enhancement of fenofibrate release from SBA-15 compared to unprocessed drug alone. This was not surprising because dissolution rate can be improved if the drug surface area, or in the case of drug – silica systems the effective drug surface area in contact with the dissolution medium is increased (Bruner, 1904, Nernst, 1904). SBA-15 is also a very hydrophilic material and it readily attracts moisture from its surroundings, whereas fenofibrate is very hydrophobic. After processing fenofibrate with SBA-15, the drug is more easily wetted which improved the release. Wang and co-workers prepared solid dispersions of silica (Aerosil and Sylysia) and nitrendipine and reported that the increased hydrophilicity of the drug as a result of being in the dispersion led to increased wetting which enhanced the drug dissolution (Wang et al., 2006).

7.3 The influence of the *in vitro* media on drug release from SBA-15

The most striking affect on fenofibrate release from SBA-15 was the *in vitro* release media employed for the studies. As shown in chapter 6, the release of fenofibrate from SBA-15 is dependent on both the SDS concentration and the acidic nature of

the media. In 1.5% w/v SDS in deionised water, there was approximately 100% release achieved which was maintained up to 24 h. The effect of reducing SDS concentration was striking; the release after 24 h was approximately 66% in 0.3% w/v SDS in deionised water, in fact the difference was significant between the release profiles of 0.3-and-1.5% w/v SDS. Fenofibrate solubility is known to be sensitive to SDS concentration (Jamzad and Fassihi, 2006). While fenofibrate itself was not ionisable, the acidity of the release media affected fenofibrate release from SBA-15; when 0.1M HCl was in the solution, there was a measurable decrease in % release from 2 to 24 h. This decrease was not evident in the samples without 0.1M HCl (Refer to chapter 6). It has been reported that (a) SDS can react with HCl to form sulfonic acid (Bayrak, 2003) and (b) that SDS monomer and micelles have a negative charge while the surface of SBA-15 is positively charged at pH ~1.2 (Kosmulski, 2001). The decrease was more evident in the media containing 0.3% w/v SDS in 0.1M HCl solution, which would tend to support the supposition that the SDS micelle concentration had been reduced over time. The media containing 1.5% w/v SDS in 0.1M HCl solution should be affected less as there is a higher concentration of SDS micelles in the solution. There are several reports of immediate drug release of various drugs from different silicas in acidic media including simulated gastric fluid with 0.5 wt% SDS with pH 1.2 (Charnay et al., 2004, Mellaerts et al., 2007, Van Speybroeck et al., 2010a, Vialpando et al., 2012, Li-hong et al., 2013). These publications typically reported release over 1 – 2 h and did not observe the impact of HCl on SDS micelle concentration.

7.4 The influence of drug distribution within the silica matrix on release

In this thesis, drug distribution was defined as whether the drug was inside the SBA-15 mesopores or not and was determined using surface area and pore size analysis by N_2 adsorption. It was not possible to directly observe drug in the mesopores due to the resolution of chemical imaging techniques, instead the difference between theoretical and measured mesopore volumes, the % ΔPV term was employed to understand drug distribution within the SBA-15 matrix. The distribution of drug within the silica matrix had the greatest affect on drug release in the context of whether the drug was in the mesopores or not. First of all, the fenofibrate that was not loaded into the SBA-15 mesopores had a slower release rate and lower extent compared to drug within the mesopores, this can be seen with the physical mix sample in chapter 4 and the excess sample in chapter 6. In chapter 4, the impregnation, liquid and SC-CO_2 loading methods were shown to load drug into the mesopores. These methods were very similar in terms of drug-loading efficiency but the SC-CO_2 sample had a much lower % ΔPV of 19.12 (±4.17) compared to the impregnation % ΔPV of 33.12 (±2.08) and liquid CO_2 % ΔPV of 32.06 (±1.55) at the drug – silica ratio of 1 mg to 3 m^2. Based on the % ΔPV, it was thought that the drug was loaded deepest into the SBA-15 mesopores by the SC-CO_2 method. However, there was no observable impact on drug release (Refer to chapter 4). While it has been reported that the length of the mesopores can influence drug release (Chen et al., 2012, Qu et al., 2006), in this work the SBA-15 mesopores should have been of similar length across batches.

While the 'mix' and 'bag sample' prepared at the drug – silica ratio of 1 mg to 3 m^2 with constant SC-CO_2 conditions had similar % ΔPVs, the 'mix sample' had a higher drug-loading efficiency than the 'bag' sample. It was hypothesised that the samples prepared by the 'bag method' were deposited into the SBA-15 mesopores in a different manner compared to the 'mix method' which led to the 'bag samples' having a signficasntly lower release extent than the 'mix sample' according to the f_1, modified f_1 and f_2 factors and repeated measures ANOVA (Fig.7.1).

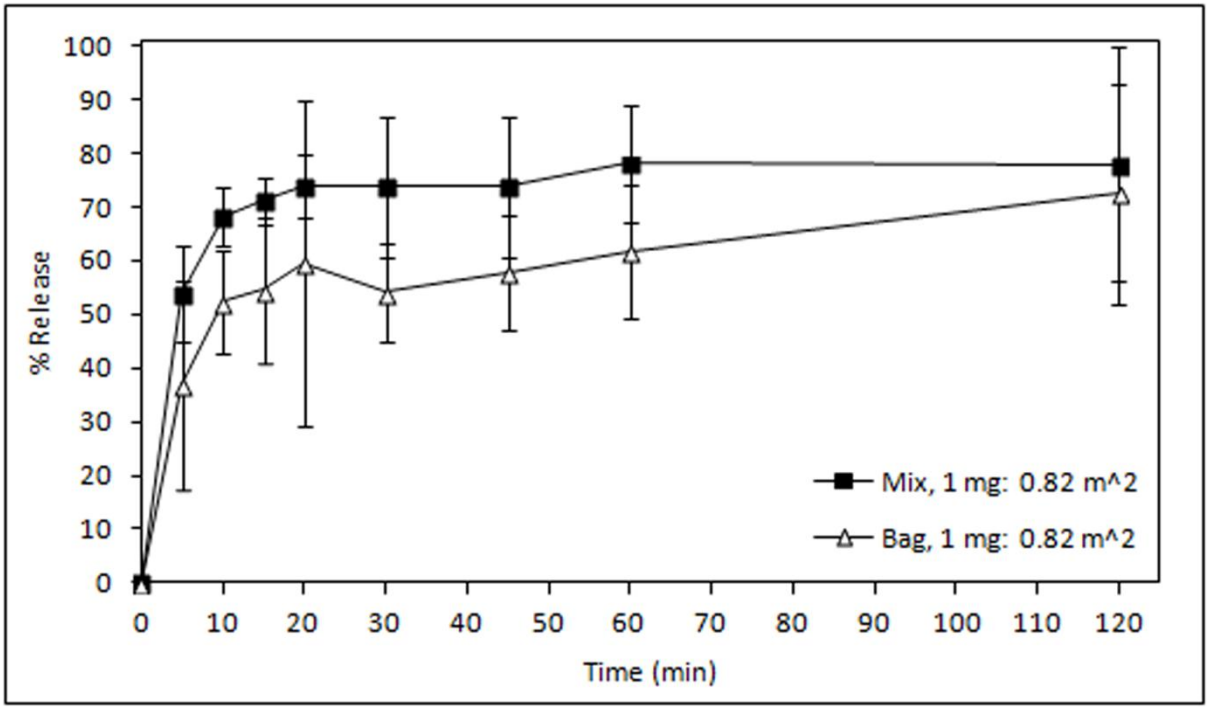

Figure 7.1: Release profiles of 1 mg to 0.82 m^2 samples (■) 'mix method and (Δ) 'bag method' in 0.3% w/v SDS in 0.1M HCl media (mean ± SD, n = 9).

The most obvious effect of drug distribution on drug release was the comparison between drug deposited in the mesopores and drug not in the mesopores. The physical mix had a % ΔPV of 1.88 (±5.37), the melt method a % ΔPV of 37.51 (±5.63) while the SC-CO_2 recorded a % ΔPV of 19.12 (±4.17) at the drug – silica

ratio of 1 mg to 3 m^2. The physical mix did not distribute drug into the mesopores, consequently its release rate was significantly slower and extent lower than the melt and SC-CO_2 samples (Fig.7.2).

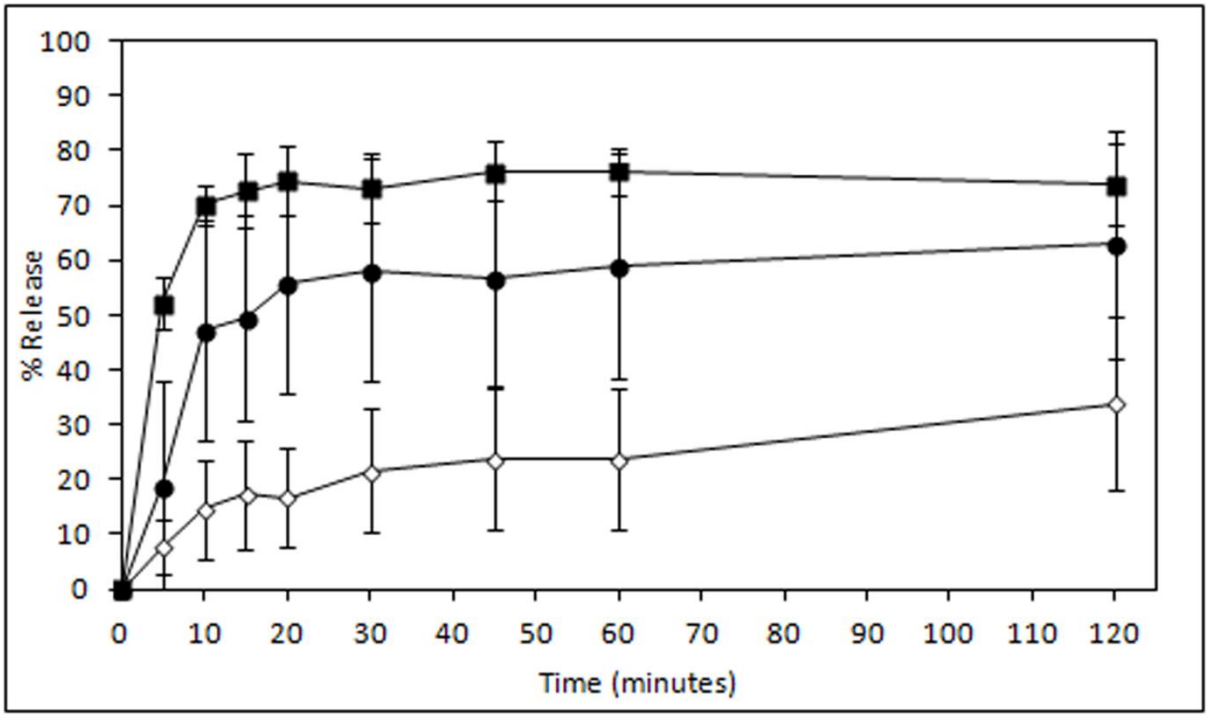

Figure 7.2: Release profiles of 1 mg to 3 m^2 samples, (◊) physical mix, (●) melt method and (■) SC-CO_2 in 0.3% w/v SDS in 0.1M HCl media (mean ± SD, n = 9).

The melt sample had a significantly lower release compared to the SC-CO_2 sample, which could have been due to different distribution of the drug in this compared to the SC-CO_2 or the residual crystallinity it contained (Refer to chapter 4).

7.5 The influence of drug solid state form on release

It is well established that the amorphous form of drugs have higher solubilities than their crystalline forms (Hancock and Parks, 2000). In this thesis, the rate and extent of fenofibrate release from SBA-15 was strongly influenced by the drug solid state

form. The release profiles of samples containing crystallinity are compared against a sample without crystalline drug (Fig.7.3).

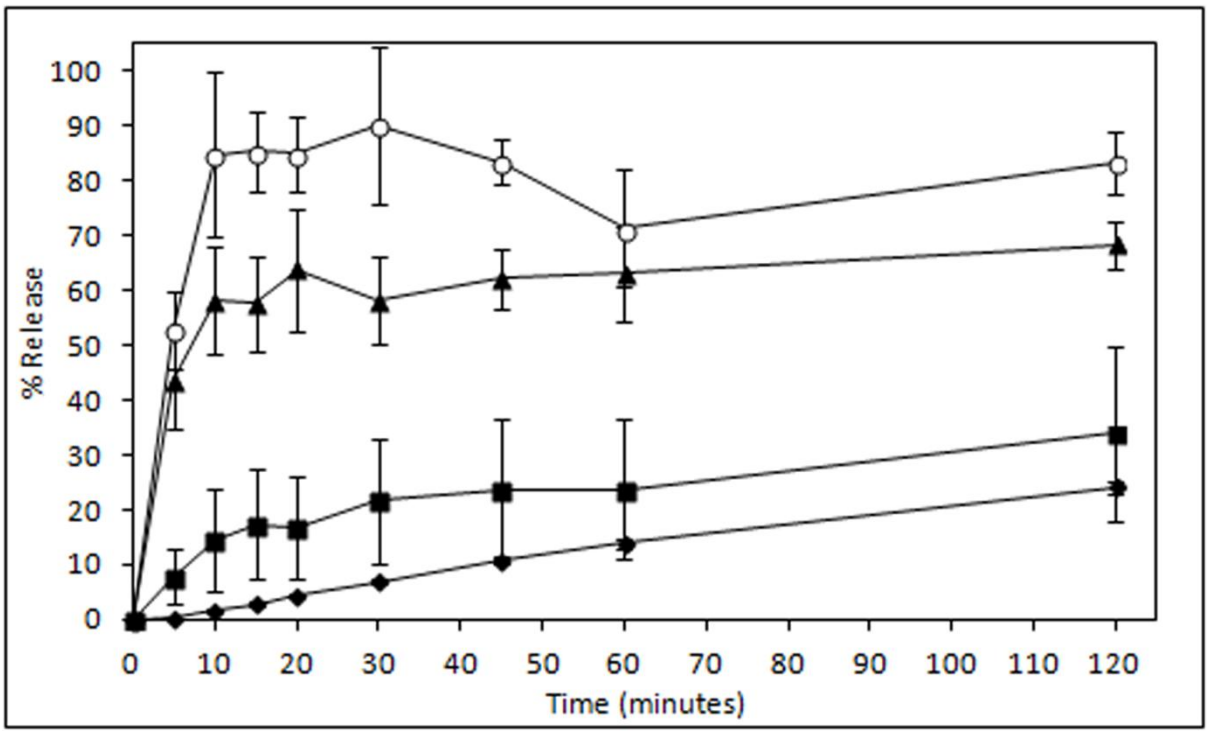

Figure 7.3: Release profiles of samples containing crystalline drug, (●) unprocessed fenofibrate (n = 3), (■) physical mix (n = 9), (▲) 'excess sample' (n = 3) and a sample containing non-crystalline drug (○) "standard sample" (n = 9) in 0.3% w/v SDS in 0.1M HCl media.

All drug – silica samples showed enhanced drug release compared to crystalline, unprocessed fenofibrate only. While both the standard and excess samples were prepared by SC-CO_2 processing, the standard sample contained drug in a non-crystalline state whereas the 'excess sample' contained both crystalline and non-crystalline drug. The physical mix also contained crystalline fenofibrate and displayed a limited enhancement in drug release. The physical mix and the standard

sample were prepared at the drug – silica ratio of 1 mg to 3 m^2. It was quite clear that drug solid state had a significant impact on subsequent release properties. Mellaerts and co-workers showed results where itraconazole loaded onto SBA-15 by a melt method retained some drug crystallinity which led to lower release extent compared to an equivalent sample prepared by impregnation with no crystallinity (Mellaerts et al., 2008a). Cha and co-workers also showed the negative influence of fenofibrate crystallinity where the release from Neusilin UFL2® was suppressed in drug – silica samples containing crystallinity (Cha et al., 2012).

7.6 The influence of drug distribution within the silica matrix on drug solid state form

The meaning of drug distribution within the silica matrix has been explained in section 7.4. The solid state of fenofibrate after processing with SBA-15 was found to be dependent on its distribution within the silica matrix; that is, whether the drug was inside or outside the silica mesopores. Fenofibrate retained its crystalline nature after SC-CO_2 processing when not in contact with silica. Crystalline fenofibrate was recovered from the bottom of the high-pressure cell; this was drug that was not in contact with the SBA-15. This highlighted very clearly that fenofibrate not in contact with the SBA-15 would remain crystalline after SC-CO_2. The physical mix of fenofibrate and SBA-15 displayed several Bragg's peaks typical of crystalline fenofibrate. This agreed with previous work where K-832, prednisolone, flurbiprofen and salicylamide were physically mixed with mesoporous silicas and retained their crystallinity (Miura et al., 2010, Nishiwaki et al., 2009, Tozuka et al., 2005, Tozuka et al., 2003). For the sake of completeness, it should be stated that there have been

reports where physical mixing of high vapour pressure compounds with silica gel led to crystalline compounds becoming amorphous over a period of time; however this process occurred in the absence of moisture and was reversed when moisture was introduced to the system (Qian et al., 2012, Qian et al., 2011, Qian and Bogner, 2011). In the 'excess sample', there was measurable drug crystallinity which was considered to be the result of free fenofibrate particles outside the SBA-15 mesopores; drug particles were observed during SEM analysis (Refer to chapter 6).

Sanganwar and Gupta loaded fenofibrate onto the non-porous silica, Aerosil® with a SC-CO_2 method and found that the drug was not stable in the amorphous form. It is known that drugs confined within spaces that are less than 10 times their molecule diameter cannot re-crystallise (Rengarajan et al., 2008, Sliwinska-Bartkowiak et al., 2001). Azais and co-workers studied the confinement of ibuprofen in MCM-41 mesopores (3.5 and 11.6 nm) with solid state, nuclear magnetic resonance (SS-NMR) and reported that the mesoporous confined ibuprofen was neither crystalline nor amorphous at ambient temperature (Azais et al., 2006). Therefore, if the drug was loaded into the mesopores, it would be in a non-crystalline state. The drug – SBA-15 samples prepared by the impregnation, liquid and SC-CO_2 processes appeared to be in a molecularly dispersed state as there were no observed thermal events like a T_g on the DSC thermogram. There have been several reports where drugs loaded onto SBA-15 using an impregnation process were reported to be molecularly dispersed as there was no T_g or T_m observed (Mellaerts et al., 2010, Mellaerts et al., 2008a, Nishiwaki et al., 2009, Van Speybroeck et al., 2010b).

Fenofibrate, which has a T_g of -20 ^oC, a T_{cr} of 40 ^oC and T_r of 0.6 (Zhou et al., 2002) is very unstable in its amorphous form, yet it was stabilised in the non-crystalline form inside SBA-15 mesopores after 12 months under accelerated storage conditions

in the impregnation, liquid and SC-CO_2 prepared samples. This corresponded to results published by Mellaerts and co-workers who reported that itraconazole was maintained in an amorphous form for up to 12 months after processing with SBA-15 (Mellaerts et al., 2010) and Shen and co-workers who published similar findings with respect to ibuprofen co-spray-dried with SBA-15 (Shen et al., 2010). The fact that it was stabilised in the non-crystalline form was further evidence that the drug was in the mesopores and highlighted that it was critical for the drug to be distributed into the silica mesopores.

7.7 Factors that influence drug distribution within the silica matrix

There are many potential ways which drug is distributed on silica. A schematic of potential drug distribution within the silica matrix is presented below (Fig7.4).

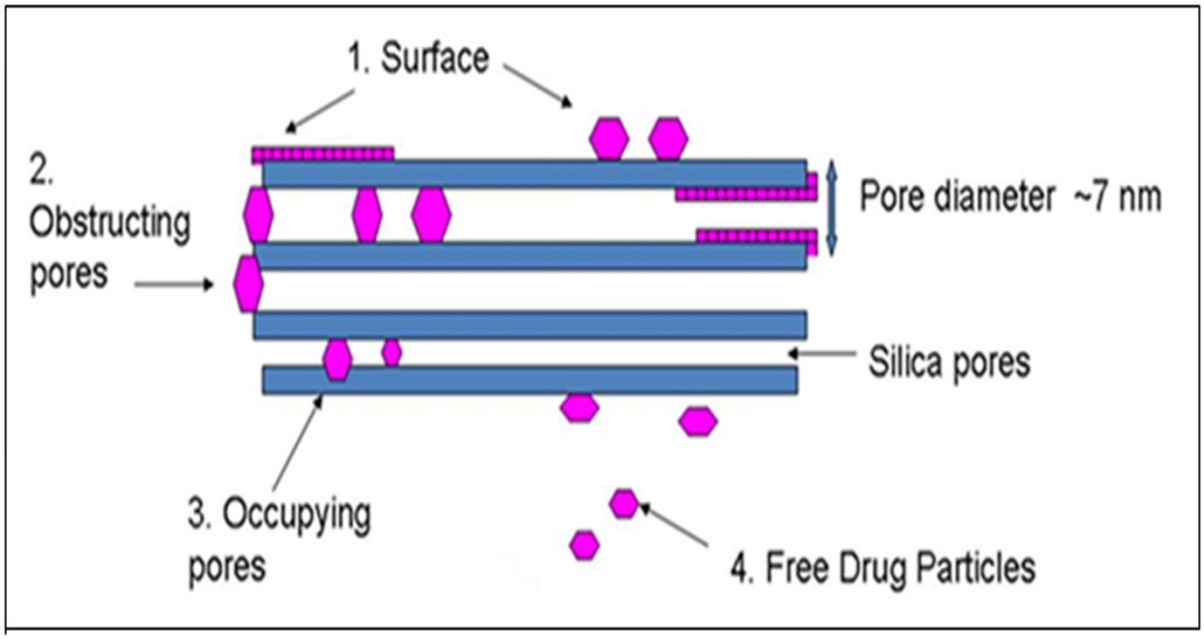

Figure 7.4: Potential drug distribution within silica matrices.

In the first case, it is possible that the drug particles could be on the external surface of the silica. Secondly, there could be drug molecules obstructing mesopore openings or thirdly be obstructing the mesopores further within; this could also include lining or coating the mesopores and causing a reduction in the mesopore size. Fourthly, there could be free drug particles not associated with the silica at all. The factors identified in this thesis that influenced drug distribution within the silica matrix were: (a) the drug-loading process and (b) the drug – silica ratio. The loading method is important because the drug powder must be dissolved in some solvent (e.g. acetronitrile or CO_2) before it can be molecularly dispersed into the silica mesopores. Physically mixing drug and silica particles cannot facilitate drug entry into the mesopores because the drug remained in a particulate state**.** It was found in this work that SC-CO_2 loaded drug somewhat differently into SBA-15 than melt, solvent impregnation and liquid CO_2 methods because a larger mesopore volume was observed for the SC-CO_2 samples after drug-loading. This larger mesopore volume may be due to the fact the drug molecules were deeper within the mesopores after SC-CO2 processing whereas the processing methods like the melt method may have deposited the drug nearer the surface of the mesopores.

The drug – silica ratio heavily influenced drug distribution. No publication has reported a satisfactory manner of calculating the maximum drug that can be accommodated within SBA-15. In a manufacturing process, it would be important to efficiently load the drug into the silica mesopores without exceeding the quantity of drug that can be accommodated within the mesopore volume. In chapter 6, a method of determining the maximum drug mass per SBA-15 mesopore volume was presented. The results highlighted that there were limitations using drug true density and mesopore volume for calculating the mass of drug to be loaded. Possibly one

approach that could be utilised is to apply the drug molecular density and calculate the drug amount from that method.

7.8 Key findings of this thesis

There were several key findings of this thesis. These are listed below:

- For the first time it was shown that the method of processing drug with SBA-15 had important consequences in terms of the drug distribution throughout the SBA-15 matrix, drug solid state form and drug release rate from the SBA-15.

- It was highlighted that drug particles must be dissolved or otherwise disrupted if the drug is to be induced into a non-crystalline molecular dispersion or amorphous form.

- SC-CO_2 processing deposited the drug molecules deepest inside SBA-15, while simple melting of drug ensured that the molecules were comparatively closer to the surface of the mesopores. This is due to the drug molten viscosity; a lower molten viscosity should encourage greater freedom of drug to move inside SBA-15 mesopores.

- It was found that the SBA-15 surface area and mesopore volume have an influence on how much drug could be loaded on to SBA-15. Increasing the amount of drug to SBA-15 surface area lowered the drug-loading efficiency when the drug: silica ratio was increased from 1 mg : 3 m^2 to 1 : 0.82 m^2.

- It was shown that SC-CO_2 processing variables such as processing pressure (13.79 – 41.37 MPa), duration time (4 – 24 h) and depressurisation rate (rapid or controlled) did not influence the drug distribution within the SBA-

15 matrix, drug solid state form or release rate and extent, even after 12 months under accelerated storage conditions. Higher processing pressures (41.37 MPa) did result in reduced drug-loading efficiency which was attributed to the rapid mass transfer rates of CO_2 out of the high-pressure cell.

- It was demonstrated that the rate and extent of fenofibrate release depended on (1) the loading method, (2) distribution of drug on the silica substrate and (3) the composition of the release medium employed.

1

7.9 Future Work

- One potential avenue to be explored is the utilisation of other drug molecules to investigate the robustness of SC-CO_2 to load SBA-15 with different drugs that have a range of chemistries and molecular weights.

- The applicability of higher resolution SEM and TEM may allow drug molecules be visualised inside silica mesopores. Any technique that could identify drug molecules inside silica mesopores should be considered.

- Further studies on the drug supersaturating properties of SBA-15 in biorelevant media such as FaSSIF should be undertaken, especially the effect of drug – silica ratio and crystallinity in drug – silica samples on the extent and duration of fenofibrate supersaturation.

- At present, the mathematical models of drug release do not seem applicable to drug release from silica mesopores. A new equation to describe fenofibrate release from silica mesopores would be a useful addition to knowledge of drug release from silica mesopores. The diffusion of drug from the mesopores and potential adsorptive properties of mesopores silica need to be understood in this context.

- The issues surrounding SBA-15 usage in a pharmaceutical manufacturing environment need also to be addressed. Is it possible to manufacture an oral formulation using large percentages of SBA-15 and could it be possible to simultaneously load the drug onto the SBA-15 and granulate in the SC-CO_2 environment.

1

References

AERTS, C. A., VERRAEDT, E., DEPLA, A., FOLLENS, L., FROYEN, L., VAN HUMBEECK, J., AUGUSTIJNS, P., VAN DEN MOOTER, G., MELLAERTS, R. and MARTENS, J. A. (2010) Potential of amorphous microporous silica for ibuprofen controlled release. *Int. J. Pharm.,* 397**,** 84-91.

AERTS, C. A., VERRAEDT, E., MELLAERTS, R., DEPLA, A., AUGUSTIJNS, P., VAN HUMBEECK, J., VAN DEN MOOTER, G. and MARTENS, J. A. (2007) Tunability of pore diameter and particle size of amorphous microporous silica for diffusive controlled release of drug compounds. *J. Phys. Chem C,* 111**,** 13404-13409.

AMBROGI, V., MARMOTTINI, F. and PAGANO, C. (2013) Amorphous carbamazepine stabilization by the mesoporous silicate SBA-15. *Micropor. Mesopor. Mater.,* 177**,** 1-7.

AMBROGI, V., PERIOLI, L., MARMOTTINI, F., ACCORSI, O., PAGANO, C., RICCI, M. and ROSSI, C. (2008) Role of mesoporous silicates on carbamazepine dissolution rate enhancement. *Micropor. Mesopor. Mater.,* 113**,** 445-452.

AMBROGI, V., PERIOLI, L., PAGANO, C., LATTERINI, L., MARMOTTINI, F., RICCI, M. and ROSSI, C. (2012) MCM-41 for furosemide dissolution improvement. *Micropor. Mesopor. Mater.,* 147**,** 343-349.

AMBROGI, V., PERIOLI, L., PAGANO, C., MARMOTTINI, F., MORETTI, M., MIZZI, F. and ROSSI, C. (2010) Econazole nitrate-loaded MCM-41 for an antifungal topical powder formulation. *J. Pharm. Sci.,* 99**,** 4738-4745.

AMIDON, G. L., LENNERNÄS, H., SHAH, V. P. and CRISON, J. R. (1995) A Theoretical basis for a biopharmaceutic drug classification: The correlation of *in vitro* drug product dissolution and *in vivo* bioavailability. *Pharm. Res.,* 12**,** 413-420.

ANDERSSON, J., ROSENHOLM, J., AREVA, S. and LINDEN, M. (2004) Influences of material characteristics on ibuprofen drug loading and release profiles from ordered micro- and-mesoporous silica matrices. *Chem. Mater.,* 16**,** 4160-4167.

ARORA, K. A., LESSER, A. J. and MCCARTHY, T. J. (1998) Preparation and Characterization of Microcellular Polystyrene Foams Processed in Supercritical Carbon Dioxide. *Macromolecules,* 31**,** 4614-4620.

AUCOIN, M. and LEGGE, R. (2001) Effects of supercritical CO2 exposure and depressurization on immobilized lipase activity. *Biotechnology Letters,* 23**,** 1863-1870.

AZAIS, T., TOURNE-PETEILH, C., AUSSENAC, F., BACCILE, N., COELHO, C., DEVOISSELLE, J.-M. and BABONNEAU, F. (2006) Solid State NMR Study of Ibuprofen Confined in MCM-41 Material. *Chem. Mater.,* 18**,** 6382-6390.

BARRETT, E. P., JOYNER, L. G. and HALENDA, P. P. (1951) The Determination of pore volume and area distributions in porous substances. I. Computations from nitrogen isotherms. *J. Am. Chem. Soc.,* 73**,** 373-380.

BAYRAK, Y. (2003) Micelle formation in sodium dodecyl sulfate and dodecyltrimethylammonium bromide at different temperatures. *Turk. J. Chem.,* 27**,** 487-392.

BELHADJ-AHMED, F., BADENS, E., LLEWELLYN, P., DENOYEL, R. and CHARBIT, G. (2009) Impregnation of vitamin E acetate on silica mesoporous phases using supercritical carbon dioxide. *J. Supercrit. Fluids,* 51**,** 278-286.

BROWN, S., ROWLEY, G. and PEARSON, J. T. (1998) Surface treatment of the hydrophobic drug danazol to improve drug dissolution. *Int. J. Pharm.,* 165**,** 227-237.

BRUNAUER, S., EMMETT, P. H. and TELLER, E. (1938) Adsorption of gases in multimolecular layers. *J. Am. Chem. Soc.,* 60**,** 309-319.

BRUNER, E. (1904) Reaktionsgeschwindigkeit in heterogenen Systemen. *Z. Phys. Chem.,* 43**,** 56–102.

BRUNNER, G. (1994) *Gas Adsorption: An Introduction to Fundamentals of Supercritical Fluids and the Application to Separation Processes* New York, Steinkopff Darmstadt Springer.

BUSH, J. R., AKGERMAN, A. and HALL, K. R. (2007) Synthesis of controlled release device with supercritical carbon dioxide and cosolvent. *J. Supercrit. Fluids,* 41**,** 311-316.

CARR, R. L. (1965) Evaluating flow properties of solids. *Chem. Eng.,* 72**,** 69-72.

CHA, K.-H., CHO, K.-J., KIM, M.-S., KIM, J.-S., PARK, H. J., PARK, J., CHO, W., PARK, J.-S. and HWANG, S.-J. (2012) Enhancement of the dissolution rate and bioavailability of fenofibrate by a melt-adsorption method using supercritical carbon dioxide. *Int. J. Nanomedicine***,** 5565-5575.

CHARNAY, C., BEGU, S., TOURNE-PETEILH, C., NICOLE, L., LERNER, D. A. and DEVOISSELLE, J. M. (2004) Inclusion of ibuprofen in mesoporous templated silica: Drug loading and release property. *Eur. J. Pharm. Biopharm.,* 57**,** 533-540.

CHEN, Z., LI, X., HE, H., REN, Z., LIU, Y., WANG, J., LI, Z., SHEN, G. and HAN, G. (2012) Mesoporous silica nanoparticles with manipulated microstructures for drug delivery. *Colloids Surf. B.,* 95**,** 274-278.

COSTA, P. and SOUSA-LOBO, J. M. (2001) Modelling and comparison of dissolution profiles. *Eur. J. Pharm. Sci.,* 13**,** 123-133.

COUTINHO, A. C. S. L. S., QUINTELLA, S. A., ARAUJO, A. S., BARROS, J. M. F., PEDROSA, A. M. G., JUNIOR, V. J. F. and SOUZA, M. J. B. (2007) Thermogravimetry applied to characterization of SBA-15 nanostructured material. *J. Therm. Anal. Calorim.,* 87**,** 457–461.

CRAIG, D. Q. M., ROYALL, P. G., KETT, V. L. and HOPTON, M. L. (1999) The relevance of the amorphous state to pharmaceutical dosage forms: glassy drugs and freeze dried systems. *Int. J. Pharm.,* 179**,** 179-207.

CRAMPON, C., CHARBIT, G. and NEAU, E. (1999) High-pressure apparatus for phase equilibria studies: Solubility of fatty acid esters in supercritical carbon dioxide. *J. Supercrit. Fluids,* 16**,** 11-20.

DAS, D. P., PARIDA, K. M. and MISHRA, B. K. (2007) A study on the structural properties of mesoporous silica spheres. *Mater. Lett.,* 61**,** 3942-3945.

DAUBERT, T. E. and DANNER, R. P. (1989) *Physical and Thermodynamic Properties of Pure Chemicals: Data Compilation* Washington DC, Talyor and Francis.

DIAZ, L., LIAUWA, C. M., EDGE, M., ALLENA, N. S., MCMAHON, A. and RHODES, N. (2005) Investigation of factors affecting the adsorption of functional molecules onto gel silicas 1. Flow microcalorimetry and infrared spectroscopy. *J. Colloid Interface Sci.,* 287**,** 379–387.

DIMASI, J. A., HANSEN, R. W. and GRABOWSKI, H. G. (2003) The price of innovation: new estimates of drug development costs. *J. Health Econ.,* 22**,** 151-185.

DUNN, O. J. and CLARK, V. (1987) *Applied statistics: Analysis of variance and regression,* New York, Wiley

FAGES, J., LOCHARD, H., LETOURNEAU, J.-J., SAUCEAU, M. and RODIER, E. (2004) Particle generation for pharmaceutical applications using supercritical fluid technology. *Powder Technol.,* 141**,** 219-226.

FAN, L. T., CHEN, Y. M. and LAI, F. S. (1990) Recent developments in solids mixing. *Powder Technol.,* 61**,** 255–287.

FDA (2003) Guidance for Industry Q1A(R2) Stability Testing of New Drug Substances and Products. IN SERVICES, U. S. D. O. H. A. H. (Ed.), U.S. Department of Health and Human Services.

FULVIO, P. F., PIKUS, S. and JARONIEC, M. (2005) Tailoring properties of SBA-15 materials by controlling conditions of hydrothermal synthesis *J. Chem. Mater.,* 15**,** 5049-5053.

GALARNEAU, A., NADER, M., GUENNEAU, F., DI RENZO, F. and GEDEON, A. (2007) Understanding the stability in water of mesoporous SBA-15 and MCM-41. *J. Phys. Chem C,* 111**,** 8268-8277.

GAO, L., SUN, J., ZHANG, L., WANG, J. and REN, B. (2012) Influence of different structured channels of mesoporous silicate on the controlled ibuprofen delivery. *Mater. Chem. Phys.,* 135**,** 786-797.

GORDILLO, M. D., BLANCO, M. A., MOLERO, A. and MARTINEZ-DE-LA-OSSA, E. (1999) Solubility of the antibiotic penicillin G in supercritical carbon dioxide. *J. Supercrit. Fluids,* 15**,** 183-190.

GUIVARC'H, P.-H., VACHON, M. G. and FORDYCE, D. (2004) A new fenofibrate formulation: results of six single-dose, clinical studies of bioavailability under fed and fasting conditions. *Clin. Ther.,* 26**,** 1456-1469.

GUNEY, O. and AKGERMAN, A. (2002) Synthesis of controlled-release products in supercritical medium. *AIChE Journal,* 48**,** 856-866.

GUO, Z., LIU, X.-M., MA, L., LI, J., ZHANG, H., GAO, Y.-P. and YUAN, Y. (2013) Effects of particle morphology, pore size and surface coating of mesoporous silica on Naproxen dissolution rate enhancement. *Colloids Surf. B.,* 101**,** 228-235.

HANCOCK, B. C. and PARKS, M. (2000) What is the true solubility advantage for amorphous pharmaceuticals? *Pharm. Res.,* 17**,** 397-404.

HANCOCK, B. C. and ZOGRAFI, G. (1997) Characteristics and significance of the amorphous state in pharmaceutical systems. *J. Pharm. Sci.,* 86**,** 1-12.

HAUSNER, H. H. (1967) Friction conditions in a mass of metal powder. *Int. J. Powder Metall.,* 3**,** 7-13.

HEIKKILA, T., SALONEN, J., TUURA, J., KUMAR, N., SALMI, T., MURZIN, D. Y., HAMDY, M. S., MUL, G., LAITINEN, L., KAUKONEN, A. M., HIRVONEN, J. and LEHTO, V. P. (2007) Evaluation of mesoporous TCPSi, MCM-41, SBA-15, and TUD-1 materials as API carriers for oral drug delivery. *Drug Deliv.,* 14**,** 337-347.

HEINZ, A., GORDON, K. C., MCGOVERIN, C. M., RADES, T. and STRACHAN, C. J. (2009) Understanding the solid state forms of fenofibrate - A spectroscopic and computational study. *Eur. J. Pharm. Biopharm.,* 71**,** 100-108.

HILLERSTRÖM, A., STAMB, J. V. and ANDERSSONA, M. (2009) Ibuprofen loading into mesostructured silica using liquid carbon dioxide as a solvent. *Green Chem.,* 11**,** 662-667.

HORCAJADA, P., RAMILA, A., PEREZ-PARIENTE, J. and VALLET-REGI, M. (2004) Influence of pore size of MCM-41 matrices on drug delivery rate. *Micropor. Mesopor. Mater.,* 68**,** 105-109.

HUANG, Q.-P., WANG, J.-X., ZHANG, Z.-B., SHEN, Z.-B., CHEN, J.-F. and YUN, J. (2009) Preparation of ultrafine fenofibrate powder by solidification process from emulsion. *Int. J. Pharm.,* 368**,** 160-164.

INAGAKI, S., KOIWAI, A., SUZUKI, N. and KURODA, K. (1996) Syntheses of highly ordered mesoporous materials, FSM-16, derived from kanemite. *Bull. Chem. Soc. Jpn,* 69**,** 1449-1457.

INAKI, Y., YOSHISA, H., KIMURA, K., INAGAKI, S., FUKASHIMA, Y. and HATTORI, T. (2000) Photometathesis activity and thermal stability of two types of mesoporous silica materials, FSM-16 and MCM-41. *Phys. Chem. Chem. Phys.,* 2**,** 5293-5297.

IZQUIERDO-BARBA, I., COLILLA, M., MANZANO, M. and VALLET-REGÍ, M. (2010) *In vitro* stability of SBA-15 under physiological conditions. *Micropor. Mesopor. Mater.,* 132**,** 442-452.

IZQUIERDO-BARBA, I., MARTINEZ, A., DOADRIO, A. L., PEREZ-PARIENTE, J. and VALLET-REGI, M. (2005) Release evaluation of drugs from ordered three-dimensional silica structures. *Eur. J. Pharm. Sci.,* 26**,** 365-373.

JAIN, A., RAN, Y. and YALKOWSKY, S. H. (2004) Effect of pH-Sodium Lauryl Sulfate Combination on Solubilization of PG-300995 (an Anti-HIV Agent): A Technical Note. IN AAPS (Ed.) *AAPS PharmSciTech.* Baltimore Convention Center, Baltimore, AAPS.

JAMMAER, J., AERTS, A., D'HAEN, J., SEOB, J. W. and MARTENS, J. A. (2009) Convenient synthesis of ordered mesoporous silica at room temperature and quasi-neutral pH. *J. Mater. Chem.,* 19**,** 8290-8293.

JAMZAD, S. and FASSIHI, R. (2006) Role of surfactant and pH on dissolution properties of fenofibrate and dlipizide — A technical note. *AAPS PharmSciTech,* 7.

JANSEN, J. C., SHAN, Z., MARCHESE, L., ZHOU, W., PUIL, N. V. D. and MASCHMEYER, T. (2001) A new templating method for three-dimensional mesopore networks. *Chem. Commun.***,** 713-714.

JONAT, S., HASENZAHL, S., GRAY, A. and SCHMIDT, P. C. (2005) Influence of Compacted Hydrophobic and Hydrophilic Colloidal Silicon Dioxide on Tableting Properties of Pharmaceutical Excipients. *Drug. Dev. Int. Pharm.,* 31**,** 687-696.

JONES, D. (2002) *Pharmaceutical Statistics,* London, Pharmaceutical Press.

JUENEMANN, D., JANTRATID, E., WAGNER, C., REPPAS, C., VERTZONI, M. and DRESSMAN, J. B. (2011) Biorelevant in vitro dissolution testing of products containing micronized or nanosized fenofibrate with a view to predicting plasma profiles. *Eur. J. Pharm. Biopharm.,* 77**,** 257-264.

KARMARKAR, A. B., GONJARI, I. D., HOSMANI, A., DHABALE, P. N. and BHISE, S. B. (2009) Use of melt solidification technique for preparation of fenofibrate beads: A technical note. *Dig. J. Nanomater. Bios.,* 4**,** 291 – 297.

KATZ, H. S. and MILEWSKI, J. V. (1987) *Handbook of Fillers for Plastics,* New York, Van Nostrand Reinhold

KIEKENS, F., EELEN, S., VERHEYDEN, L., DAEMS, T., MARTENS, J. and DEN MOOTER, G. V. (2012) Use of ordered mesoporous silica to enhance the oral bioavailability of ezetimibe in dogs. *J. Pharm. Sci.,* 101**,** 1136-1144.

KIM, J. M., KIM, S. K. and RYOO, R. (1998) Synthesis of MCM-48 single crystals. *Chem. Commun.***,** 259-260.

KITTAKA, S., UEDA, Y., FUJISAKI, F., IIYAMA, T. and YAMAGUCHI, T. (2011) Mechanism of freezing of water in contact with mesoporous silicas MCM-41, SBA-15 and SBA-16: role of boundary water of pore outlets in freezing. *Phys. Chem. Chem. Phys.,* 13**,** 17222-17233.

KNOX, C., LAW, V., JEWISON, T., LIU, P., LY, S., FROLKIS, A., PON, A., BANCO, K., MAK, C., NEVEU, V., DJOUMBOU, Y., EISNER, R., GUO, A. and WISHART, D. (2011) DrugBank 3.0: a comprehensive resource for 'omics' research on drugs. *Nucleic Acids Res.,* 39.

KOSMULSKI, M. (2001) *Chemical Properties of Material Surfaces,* New York, Marcel Dekker.

KRESGE, C. T., LEONOWICZ, M. E., ROTH, W. J., VARTULI, J. C. and BECK, J. S. (1992) Ordered mesoporous molecular sieves synthesized by a liquid-crystal template mechanism. *Nature,* 359**,** 710-712.

LERK, C. and BOLHUIS, G. (1977) Interaction of lubricants and colloidal silica during mixing with excipients. II. Its effect on wettability and dissolution velocity. *Pharm. Acta Helv.,* 52(3):39-44**.,** 39-44.

LERK, C., BOLHUIS, G. and SMEDEMA, S. (1977) Interaction of lubricants and colloidal silica during mixing with excipients. I. Its effect on tabletting. *Pharm. Acta Helv.,* 52**,** 33-39.

LEWIS, R. J. (2013) *Sax's Dangerous Properties of Industrial Materials,* New York, John Wiley & Sons.

LI-HONG, W., XIN, C., HUI, X., LI-LI, Z., JING, H., MEI-JUAN, Z., JIE, L., YI, L., JIN-WEN, L., WEI, Z. and GANG, C. (2013) A novel strategy to design sustained-release poorly water-soluble drug mesoporous silica microparticles based on supercritical fluid technique. *Int. J. Pharm.,* 454**,** 135-142.

LIMNELL, T., SANTOS, H. A., MÄKILÄ, E., HEIKKILÄ, T., SALONEN, J., MURZIN, D. Y., KUMAR, N., LAAKSONEN, T., PELTONEN, L. and HIRVONEN, J. (2011) Drug delivery formulations of ordered and nonordered mesoporous silica: Comparison of three drug loading methods. *J. Pharm. Sci.,* 100**,** 3294-3306.

LIPINSKI, C. A., LOMBARDO, F., DOMINY, B. W. and FEENEY, P. J. (1997) Experimental and computational approaches to estimate solubility and permeability in drug discovery and development settings. *Adv. Drug Delivery Rev.,* 23**,** 3-25.

LUCIEN, F. P. and FOSTER, N. R. (2000) Solubilities of solid mixtures in supercritical carbon dioxide. *J. Supercrit. Fluids,* 17**,** 111-134.

MACNAUGHTON, S. J. and FOSTER, N. R. (1994) Solubility of DDT and 2,4-D in supercritical carbon dioxide and supercritical carbon dioxide saturated with water. *Industrial Engineering and Chemistry Research,* 33**,** 2757-2763.

MACNAUGHTON, S. J., KIKIC, I., FOSTER, N. R., ALESSI, P., CORTESI, A. and COLUMBO, I. (1996) Solubility of anti-inflammatory drugs in supercritical carbon dioxide. *J. Chem. Eng. Data,* 41**,** 1083-1086.

MADIEH, I., SIMONE, M., WILSON, W., MEHRA, D. and AUGSBURGER, L. (2007) Investigation of drug–porous adsorbent interactions in drug mixtures with selected porous adsorbents. *J. Pharm. Sci.,* 96.

MANZANO, M., AINA, V., AREÁN, C. O., BALAS, F., CAUDA, V., COLILLA, M., DELGADO, M. R. and VALLET-REGÍ, M. (2008) Studies on MCM-41 mesoporous silica for drug delivery: Effect of particle morphology and amine functionalization. *Chem. Eng. J.*, 137**,** 30-37.

MANZANO, M., COLILLA, M. and VALLET-REGI, M. (2009) Drug delivery from ordered mesoporous matrices. *Expert Opin. Drug Deliv.*, 6**,** 1383-1400.

MASUDA, H., HIGASHITANI, K. and YOSHIDA, H. (2006) *Powder Technology Handbook,* Boca Raton, Taylor and Francis.

MCNAUGHT, A. D. and WILKINSON, A. (1997) *IUPAC: Compendium of Chemical Terminology (Gold Book),* Oxford, Blackwell Scientific Publications.

MELLAERTS, R., AERTS, C. A., HUMBEECK, J. V., AUGUSTIJNS, P., MOOTER, G. V. D. and MARTENS, J. A. (2007) Enhanced release of itraconazole from ordered mesoporous SBA-15 silica materials. *Chem. Commun.***,** 1375-1377.

MELLAERTS, R., HOUTHOOFD, K., ELEN, K., CHEN, H., VAN SPEYBROECK, M., VAN HUMBEECK, J., AUGUSTIJNS, P., MULLENS, J., VAN DEN MOOTER, G. and MARTENS, J. A. (2010) Aging behaviour of pharmaceutical formulations of itraconazole on SBA-15 ordered mesoporous silica carrier material. *Micropor. Mesopor. Mater.*, 130**,** 154-161.

MELLAERTS, R., JAMMAER, J. A. G., VAN SPEYBROECK, M., CHEN, H., HUMBEECK, J. V., AUGUSTIJNS, P., VAN DEN MOOTER, G. and MARTENS, J. A. (2008a) Physical state of poorly water-soluble therapeutic molecules, loaded into SBA-15 ordered mesoporous silica carriers: A case study with itraconazole and ibuprofen. *Langmuir,* 24**,** 8651-8659.

MELLAERTS, R., MOLS, R., JAMMAER, J. A. G., AERTS, C. A., ANNAERT, P., VAN HUMBEECK, J., VAN DEN MOOTER, G., AUGUSTIJNS, P. and MARTENS, J. A. (2008b) Increasing the oral bioavailability of the poorly water soluble drug itraconazole with ordered mesoporous silica. *Eur. J. Pharm. Biopharm.*, 69**,** 223-230.

MELLAERTS, R., ROEFFAERS, M. B. J., HOUTHOOFD, K., VAN SPEYBROECK, M., DE CREMER, G., JAMMAER, J. A. G., VAN DEN MOOTER, G., AUGUSTIJNS, P., HOFKENS, J. and MARTENS, J. A. (2011) Molecular organization of hydrophobic molecules and co-adsorbed water in SBA-15 ordered mesoporous silica material. *Phys. Chem. Chem. Phys.*, 13**,** 2706-2713.

MERISKO-LIVERSIDGE, E. M. and LIVERSIDGE, G. G. (2008) Drug nanoparticles: Formulating poorly water-soluble compounds. *J. Toxicol. Pathol,*, 36**,** 43-48.

MIURA, H., KANEBAKO, M., SHIRAI, H., NAKAO, H., INAGI, T. and TERADA, K. (2010) Enhancement of dissolution rate and oral absorption of a poorly water-soluble drug, K-832, by adsorption onto porous silica using supercritical carbon dioxide. *Eur. J. Pharm. Biopharm.,* 76**,** 215-221.

MOORE, J. W. and FLANNER, H. H. (1996) Mathematical comparison of dissolution profiles. *Pharm Tech,* 20**,** 64-74.

MORERE, J., TENORIO, M. J., TORRALVO, M. J., PANDO, C., RENUNCIO, J. A. R. and CABANAS, A. (2012) Deposition of Pd into mesoporous silica SBA-15 using supercritical carbon dioxide. *J. Supercrit. Fluids,* 56**,** 213-222.

MORITZ, M. and LANIECKI, M. (2012a) Application of SBA-15 mesoporous material as the carrier for drug formulation systems. Papaverine hydrochloride adsorption and release study. *Powder Technol.,* 230**,** 106-111.

MORITZ, M. and LANIECKI, M. (2012b) SBA-15 mesoporous material modified with APTES as the carrier for 2-(3-benzoylphenyl)propionic acid. *App. Surf. Sci.,* 258**,** 7523-7529.

MUKERJEE, P. and MYSELS, K. J. (1972) Critical micelle concentrations of aqueous surfactant systems. *J. Pharm. Sci.,* 61.

NERNST, W. (1904) Theorie der Reaktionsgeschwindigkeit in heterogenen Systemen. *Z. Phys. Chem.,* 47**,** 52–55.

NISHIWAKI, A., WATANABE, A., HIGASHI, K., TOZUKA, Y., MORIBE, K. and YAMAMOTO, K. (2009) Molecular states of prednisolone dispersed in folded sheet mesoporous silica (FSM-16). *Int. J. Pharm.,* 378**,** 17-22.

OJOVAN, M. I. (2004) Glass formation in amorphous SiO2 as a percolation phase transition in a system of network defects. *J. Exp. Theor. Phys. Lett.,* 79**,** 632-634.

OLSON, W. P. (1995) *Separations in pharmaceutical manufacturing, in Separations Technology, Pharmaceutical and Biotechnology Applications*, Informa Healthcare.

PARIDA, S. K., DASH, S., PATEL, S. and MISHRA, B. K. (2006) Adsorption of organic molecules on silica surface. *Adv. Coll. Interface Sci.,* 121**,** 77–110.

PASQUALI, I. and BETTINI, R. (2008) Are pharmaceutics really going supercritical? *Int. J. Pharm.,* 364**,** 176-187.

PAUL, S. M., MYTELKA, D. S., DUNWIDDIE, C. T., PERSINGER, C. C., MUNOS, B. H., LINDBORG, S. R. and SCHACHT, A. L. (2010) How to improve R&D productivity: the pharmaceutical industry's grand challenge. *Nat. Rev. Drug. Discov.,* 9**,** 203-214.

PAVIA, D. L., LAMPAN, G. M. and KRIZ, G. S. (1979) *Introduction to Spectroscopy: A Guide for Students of Organic Chemistry*, Saunders College Publishing.

QIAN, K. K. and BOGNER, R. H. (2011) Spontaneous crystalline-to-amorphous phase transformation of organic or medicinal compounds in the presence of porous media, part 1: Thermodynamics of spontaneous amorphization. *J. Pharm. Sci.,* 100**,** 2801-2815.

QIAN, K. K., SUIB, S. L. and BOGNER, R. H. (2011) Spontaneous crystalline-to-amorphous phase transformation of organic or medicinal compounds in the presence of porous media, part 2: Amorphization capacity and mechanisms of interaction. *J. Pharm. Sci.,* 100**,** 4674-4686.

QIAN, K. K., WURSTER, D. E. and BOGNER, R. H. (2012) Spontaneous crystalline-to-amorphous phase transformation of organic or medicinal compounds in the presence of porous media, part 3: Effect of moisture. *Pharm. Res.,* 29**,** 2698-2709.

QU, F., ZHU, G., HUANG, S., LI, S., SUN, J., ZHANG, D. and QIU, S. (2006) Controlled release of captopril by regulating the pore size and morphology of ordered mesoporous silica. *Micropor. Mesopor. Mater.,* 92**,** 1-9.

RENGARAJAN, G. T., ENKE, D., STEINHART, M. and BEINER, M. (2008) Stabilization of the amorphous state of pharmaceuticals in nanopores. *J. Mater. Chem.,* 18**,** 2537-2539.

ROWE, R. C., SHESKEY, P. J., COOK, W. G. and FENTON, M. E. (2012) *Handbook of Pharmaceutical Excipients,* London, Pharmaceutical Press.

RYOO, R., KIM, J. M., KO, C. H. and SHIN, C. H. (1996) Disordered Molecular Sieve with Branched Mesoporous Channel Network. *J. Phys. Chem.,* 100**,** 17718-17721.

SANGANWAR, G. P. and GUPTA, R. B. (2008) Dissolution-rate enhancement of fenofibrate by adsorption onto silica using supercritical carbon dioxide. *Int. J. Pharm.***,** 213-218.

SHEN, S.-C., NG, W. K., CHIA, L., DONG, Y.-C. and TAN, R. B. H. (2010) Stabilized amorphous state of ibuprofen by co-spray drying with mesoporous SBA-15 to enhance dissolution properties. *J. Pharm. Sci.,* 99**,** 1997-2007.

SING, K. S. W., EVERETT, D. H., HAUL, R. A. W., MOSCOU, L., PIEROTTI, R. A., ROUQUEROL, J. and SIEMIENIEWSKA, T. (1985) Reporting physisorption data for gas/solid systems with special reference to the determination of surface area and porosity. *Pure. Appl. Chem.,* 57**,** 603-619.

SLIWINSKA-BARTKOWIAK, M., DUDZIAK, G., GRAS, R., SIKORSKI, R., RADHAKRISHNAN, R. and GUBBINS, K. E. (2001) Freezing behaviour in porous glasses and MCM-41. *Colloids Surf. A,* 187-188**,** 523-529.

SLIWINSKA-BARTKOWIAK, M., GRAS, J., SIKORSKI, R., RADHAKRISHNAN, R., GELB, L. and GUBBINS, K. E. (1999) Phase transitions in pores: Experimental and simulation studies of melting and freezing. *Langmuir,* 15**,** 6060-6069.

SMIRNOVA, I., SUTTIRUENGWONG, S. and ARLT, W. (2004) Feasibility study of hydrophilic and hydrophobic silica aerogels as drug delivery systems. *J. Non-Cryst. Solids,* 350**,** 54-60.

SONG, S.-W., HIDAJUT, K. and KAWI, S. (2005) Functionalized SBA-15 materials as carriers for controlled drug delivery: Influence of surface properties on matrix-drug interactions. *Langmuir,* 21**,** 9568-9575.

SRINARONG, P., FABER, J. H., VISSER, M. R., HINRICHS, W. L. J. and FRIJLINK, H. W. (2009) Strongly enhanced dissolution rate of fenofibrate solid dispersion tablets by incorporation of superdisintegrants. *Eur. J. Pharm. Biopharm.,* 73**,** 154-161.

STRYJEK, R. and VERA, J. H. (1986) PRSV: An improved Peng –Robinson equation of state for pure compounds and mixtures. *Can. J. Chem. Eng.,* 64.

SWANN, G. E. A. and PATWARDHAN, S. V. (2011) Application of Fourier Transform Infrared Spectroscopy (FTIR) for assessing biogenic silica sample purity in geochemical analyses and palaeoenvironmental research. *Clim. Past***,** 65-74.

TOZUKA, Y., OGUCHI, T. and YAMAMOTO, K. (2003) Adsorption and entrapment of salicylamide molecules into the mesoporous structure of folded sheets mesoporous material (FSM-16). *Pharm. Res.,* 20**,** 926-930.

TOZUKA, Y., WONGMEKIAT, A., KIMURA, K., MORIBE, K., YAMAMURA, S. and YAMAMOTO, K. (2005) Effect of pore size of FSM-16 on the entrapment of flurbiprofen in mesoporous structures. *Chem. Pharm. Bull.,* 53**,** 974-977.

UKMAR, T., GODEC, A., PLANINSEK, O., KAUCIC, V., MALI, G. and GABERSCEK, M. (2011a) The phase (trans)formation and physical state of a model drug in mesoscopic confinement. *Phys. Chem. Chem. Phys.,* 13**,** 16046-16054.

UKMAR, T., MAVER, U., PLANINSEK, O., KAUCIC, V., GABERSCEK, M. and GODEC, A. (2011b) Understanding controlled drug release from mesoporous silicates: Theory and experiment. *J Controlled Release,* 155**,** 409-417.

USP (2013) United Sates Pharmacopeia & National Formulary. *United Sates Pharmacopeia & National Formulary.* US Pharmacopei Convention INC, Board of Trustees.

VALLET-REGI, M. (2006) Ordered mesoporous materials in the context of drug delivery systems and bone tissue engineering. *Chemistry – A European Journal,* 12**,** 5934-5943.

VALLET-REGI, M., BALAS, F. and ARCOS, D. (2007) Mesoporous materials for drug delivery. *Drug Delivery Systems,* 46**,** 7548-7558.

VALLET-REGI, M., RAMILA, A., DEL REAL, R. P. and PEREZ-PARIENTE, J. (2001) A new property of MCM-41: Drug delivery system. *Chem. Mater.,* 13**,** 308-311.

VAN-SPEYBROECK, M., BARILLARO, V., THI, T. D., MELLAERTS, R., MARTENS, J., HUMBEECK, J. V., VERMANT, J., ANNAERT, P., MOOTER, G. V. D. and AUGUSTIJNS, P. (2008) Ordered Mesoporous Silica Material SBA-15: A Broad-Spectrum Formulation Platform for Poorly Soluble Drugs. *Journal of Pharmaceutical Sciences,* 98**,** 2648-2658.

VAN-SPEYBROECK, M., BARILLARO, V., THI, T. D., MELLAERTS, R., MARTENS, J., HUMBEECK, J. V., VERMANT, J., ANNAERT, P., MOOTER, G. V. D. and AUGUSTIJNS, P. (2009) Ordered Mesoporous Silica Material SBA-15: A Broad-Spectrum Formulation Platform for Poorly Soluble Drugs. *J. Pharm. Sci.,* 98**,** 2648-2658.

VAN SPEYBROECK, M., BARILLARO, V., DO-THI, T., MELLAERTS, R., MARTENS, J., HUMBEECK, J. V., VERMANT, J., ANNAERT, P., MOOTER, G. V. D. and AUGUSTIJNS, P. (2009) Ordered Mesoporous Silica Material SBA-15: A Broad-Spectrum Formulation Platform for Poorly Soluble Drugs. *J. Pharm. Sci.,* 98**,** 2648-2658.

VAN SPEYBROECK, M., MELLAERTS, R., MOLS, R., THI, T. D., MARTENS, J. A., VAN HUMBEECK, J., ANNAERT, P., VAN DEN MOOTER, G. and AUGUSTIJNS, P. (2010a) Enhanced absorption of the poorly soluble drug fenofibrate by tuning its release rate from ordered mesoporous silica. *Eur. J. Pharm. Sci.,* 41**,** 623-630.

VAN SPEYBROECK, M., MELLAERTS, R., THI, T. D., MARTENS, J. A., VAN HUMBEECK, J., ANNAERT, P., VAN DEN MOOTER, G. and AUGUSTIJNS, P. (2011) Preventing release in the acidic environment of the stomach via occlusion in ordered mesoporous silica enhances the absorption of poorly soluble weakly acidic drugs. *J. Pharm. Sci.,* 100**,** 4864-4876.

VAN SPEYBROECK, M., MOLS, R., MELLAERTS, R., THI, T. D., MARTENS, J. A., HUMBEECK, J. V., ANNAERT, P., MOOTER, G. V. D. and AUGUSTIJNS, P. (2010b) Combined use of ordered mesoporous silica and precipitation inhibitors for improved oral absorption of the poorly soluble weak base itraconazole. *Eur. J. Pharm. Biopharm.,* 75**,** 354-365.

VERDONCK, E., SCHAAP, K. and THOMAS, L. C. (1999) A discussion of the principles and applications of modulated temperature DSC (MTDSC) *Int. J. Pharm.,* 192**,** 3-20.

VERHEYDEN, L., DAEMS, T., EELEN, S., MARTENS, M., ROSIER, J., KIEKENS, F., SCHUELLER, L. and SPEYBROECK, M. V. (2012) A Novel Mesoporous Silica Based Formulation of Fenofibrate Outperforms a Marketed Formulation in a Human Pharmacokinetic Study *AAPS Annual Meeting and Exposition.* Chicago, Illinois, USA, AAPS.

VIALPANDO, M., BACKHUIJS, F., MARTENS, J. A. and VAN DEN MOOTER, G. (2012) Risk assessment of premature drug release during wet granulation of ordered mesoporous silica loaded with poorly soluble compounds itraconazole, fenofibrate, naproxen, and ibuprofen. *Eur. J. Pharm. Biopharm.*

VOGT, M., KUNATH, K. and DRESSMAN, J. B. (2008) Dissolution enhancement of fenofibrate by micronization, co-grinding and spray-drying: Comparison with commercial preparations. *Eur. J. Pharm. Biopharm.*, 68**,** 283-288.

WALCARIUS, A. and MERCIER, L. (2010) Mesoporous organosilica adsorbents: nanoengineered materials for removal of organic and inorganic pollutants. *J. Mater. Chem.*, 20**,** 4478-4511.

WANG, L., CUI, F. D. and SUNADA, H. (2006) Preparation and evaluation of solid dispersions of nitrendipine prepared with fine silica particles using the melt-mixing method. *Chem. Pharm. Bull.*, 54.

WEIL, A., CALDWELL, J. and STROLIN-BENEDETT, M. (1990) The metabolism and disposition of 14C-fenofibrate in human volunteers. *Drug Metab. Dispos.*, 18**,** 115-120.

WILLIAMS, J. C. (1976) The segregation of particulate materials: a review. *Powder Technol.*, 15**,** 246-251.

WISHART, D., KNOX, C., GUO, A., CHENG, D., SHRIVASTAVA, S., TZUR, D., GAUTAM, B. and MHASSANALI (2008) DrugBank: a knowledgebase for drugs, drug actions and drug targets. *Nucleic Acids Res.*, 36.

YORK, P. (1975) Application of powder failure testing equipment in assessing effect on glidants on flowability of cohesive pharmaceutical powders. *J. Pharm. Sci.*, 65**,** 1216-1221.

YORK, P. (1999) Strategies for particle design using supercritical carbon dioxide. *Adv. Drug Delivery Rev.*, 60**,** 388-398.

YU, L. (2001) Amorphous pharmaceutical solids: Preparation, characterization and stabilization. *Adv. Drug Delivery Rev.*, 48**,** 27-42.

ZHAO, D., FENG, J., HUO, Q., MELOSH, N., FREDRICKSON, G. H., CHMELKA, B. F. and STUCKY, G. D. (1998) Triblock copolymer synthesis of mesoporous silica with periodic 50 to 300 angstrom pores. *Science*, 279**,** 548-552.

ZHENG, S., GAO, L. and GUO, J. (2001) Synthesis and characterization of copper(II)-phenanthroline complex grafted organic groups modified MCM-41. *Mater. Chem. Phys.*, 71**,** 174-178.

ZHOU, D., ZHANG, G. G. Z. and LAW, D. (2002) Physical stability of amorphous pharmaceuticals: Importance of configurational thermodynamic quantities and molecular mobility. *J. Pharm. Sci.*, 91.

ZHU, Y., SHI, J., CHEN, H., SHEN, W. and DONG, X. (2005a) A facile method to synthesize novel hollow mesoporous silica spheres and advanced storage property. *Micropor. Mesopor. Mater.*, 84**,** 218-222.

ZHU, Y., SHI, J., LI, Y.-S., CHEN, H., SHEN, W. and DONG, X. (2005b) Hollow mesoporous spheres with cubic pore network as a potential carrier for drug storage and it's in vitro release kinetics. *J. Mater. Res.*, 20**,** 54-61.